mcs# 100632

Delaware River Basin Commission
25 State Police Drive
West Trenton, N.J. 08628

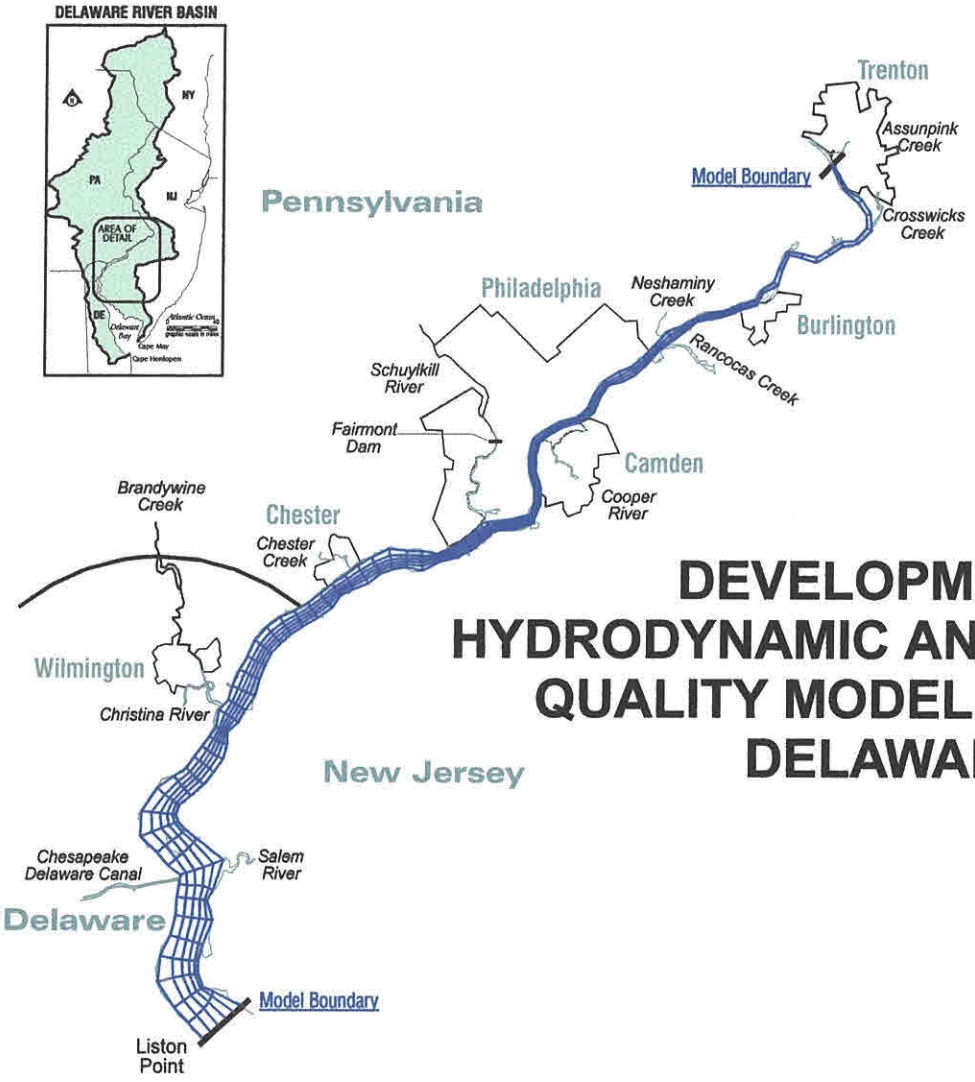

DEVELOPMENT OF A HYDRODYNAMIC AND WATER QUALITY MODEL FOR THE DELAWARE RIVER

May 29, 1998

Project No: DRBC0030

HydroQual, Inc.
Environmental Engineers and Scientists

Delaware River Basin Commission

DEVELOPMENT OF A HYDRODYNAMIC AND WATER QUALITY MODEL FOR THE DELAWARE RIVER

May 29, 1998

Project No: DRBC0030

HydroQual, Inc.
Environmental Engineers and Scientists

CONTENTS

CONTENTS (Cont.)

TABLES

FIGURES

FIGURES (Cont.)

FIGURES (Cont.)

FIGURES (Cont.)

SECTION 1

SUMMARY, CONCLUSIONS AND RECOMMENDATIONS

SUMMARY AND CONCLUSIONS

1. A new model has been developed to replace the existing Dynamic Delaware Estuary Model (DEM). The new modeling framework is more advanced than the DEM model in that it is time variable and three dimensional. It also has a more complex kinetic structure that includes nutrient-algal dynamics in addition to BOD and dissolved oxygen. The spatial domain of the model extends from head tide at Trenton (River Mile 133) to head of Delaware Bay at Liston Point (River Mile 48.5).

2. The hydrodynamic component of the model has been calibrated with tidal stage, tidal velocity data, and salinity data from 1984. Additional hydrodynamic model calibrations were performed with 1991 and 1995 summer salinity data.

3. The water quality model was calibrated with 1991 and 1995 summer data collected by the Delaware River Basin Commission during their normal biweekly sampling surveys of the Delaware River. The water quality model was calibrated against river dissolved oxygen, nitrogen, phosphorus, and chlorophyll-a concentrations.

4. The calibrated model generally reproduces the spatial and temporal trends of the water quality data, although there is considerable variability in the measured data that the model does not represent. Some factors have been identified as sources of variability, but which are not adequately represented in the model due to data limitations. These factors are: 1) variations in river turbidity within the tidal cycle, 2) the effects of aquatic vegetation on river nutrients and dissolved oxygen levels, 3) the effect of Schuylkill River on water quality, and 4) grazing by zooplankton or benthic bivalves.

5. Despite some uncertainty in the modeling calibration analysis, a good tool for assessing the factors affecting the dissolved oxygen balance in the main stem of the Delaware River has been developed. Therefore the model is suitable for immediate use in evaluating

changes in dissolved oxygen levels associated with changes in point and nonpoint source inputs of BOD, ammonia, and nutrients.

6. Based on the summer low flow data collected during 1991 and 1995, the dissolved oxygen concentration at the sag point (RM 85-95) generally ranges between 4 and 5 mg/l with higher values associated with elevated algal levels.

7. Oxidation of ammonia is the principal factor decreasing river dissolved oxygen levels and produces a maximum decrease in dissolved oxygen of approximately 2 mg/l during summer low flow conditions. Point source inputs of ammonia account for about 85% of the total ammonia inputs to the study area.

8. The oxidation of carbonaceous BOD reduces the river dissolved oxygen a maximum of approximately 1 mg/l during the summer. Point source carbonaceous BOD represents about 40% of the total carbonaceous BOD inputs.

9. Sediment oxygen demand decreases river dissolved oxygen an average of 0.6 mg/l during the summer.

10. The net effect of algal photosynthesis and respiration on river dissolved oxygen levels during low flow summer conditions is quite variable spatially and temporally. River dissolved oxygen concentrations are increased in the general range of 0.5 to 2.0 mg/l. Algae can also indirectly effect river dissolved oxygen by contributing to sediment oxygen demand through the settling and decay of algal cells on the river bottom.

11. Based on preliminary estimates, combined sewer overflows (CSOs) result in a maximum dissolved oxygen decrease of a few tenths of a mg/L in the main stem of the Delaware River. This decrease is due primarily to BOD oxidation. CSOs may also, however, exert a larger localized effect around CSO outfalls through SOD.

12. Model calibration of measured chlorophyll-a levels required the assignment of a high loss rate of algae in the upper segments of the study area. When this high loss rate is omitted from the model calibration, higher chlorophyll-a levels, similar to those reported in the 1960's and 1970's, are computed. This may suggest that, with increases in river dissolved

oxygen since the 1970's, benthic bivalves have populated the upstream reach of the study area and now limit algal levels in the upper Delaware River through filter feeding.

13. In the Delaware River Estuary, algal growth is light limited rather than nutrient limited and therefore, point source nutrient control can not be used to control algal growth.

RECOMMENDATIONS

1. Algal effects may be the most important single contribution to variability in river dissolved oxygen levels and additional field studies should be conducted to better understand the factors that control algal levels in the Delaware River. The growth of algae in the Delaware River is light rather than nutrient limited, and, therefore, defining the spatial and temporal changes in light transparency are very important in accurately predicting river algal concentrations. Light extinction, or at the very least secchi depth should be measured at various locations and possibly correlated to a larger database of suspended solids or turbidity measurements.

2. The grazing of algae by benthic bivalves may play a significant role in limiting algal concentrations in certain sections of river. Benthic bivalve density within the study area should be measured to determine what role bivalves play in limiting River algal concentrations.

3. The model occasionally under predicts dissolved oxygen levels near the sag point in the River in the vicinity of the Philadelphia area. Field studies should be performed to determine possible sources of dissolved oxygen including the possibilities of elevated dissolved oxygen and chlorophyll-a levels coming from the Schuylkill River flow or oxygen production by nearby aquatic vegetation.

4. The model occasionally under predicts dissolved oxygen and over predicts nutrients in the upper reaches of the study area, near Trenton. Field studies should be performed to assess the potential impact of the aquatic vegetation on dissolved oxygen and nutrient concentrations in this section of the river.

5. Additional measurements of ultimate carbonaceous BOD (CBODu) and phosphorus on all major point source discharges and tributures should be made to better define the conversion of BOD5 values to CBODu values used in the model.

6. A more comprehensive data set in the Schuylkill River would allow the model to be more rigorously calibrated in the Schuylkill River section of the model. This additional data should be collected in the Schuylkill River as part of the routine DRBC monitoring program.

7. A process for using the model in management decision making should be developed. Specific issues, such as the critical conditions under which the model should be run to evaluate various management alternatives and final criteria by which compliance is measured, need to be finalized.

SECTION 2

INTRODUCTION

The Delaware River Basin Commission (DRBC) currently uses the Dynamic Delaware Estuary Model (DEM) to determine the allocation of the total maximum daily loads (TMDLs) of carbonaceous biochemical oxygen demand (CBOD) for the different management zones of the Delaware River. The DEM model is composed of two interrelated submodels: a hydrodynamic component (DYNHYD) and a water quality component (DYNDEL). In previous work (HydroQual, 1994), the ability of the DEM model to adequately represent water quality conditions in the Delaware River was evaluated. This evaluation was conducted in light of the advances made in water quality modeling since the DEM model was originally developed in 1970's. Compared to current water quality models, the DEM model was found to have four significant limitations:

1) The DYNHYD submodel is unable to represent time varying forcing functions such as tidal stage data, flow inputs and wind. This limits model results to only steady state solutions.

2) The current two dimensional (2D) version of the DEM model is not a fully 2D model, but is rather more empirical in nature and unable to adequately address lateral variability.

3) The DYNDEL submodel has simplified nitrogen kinetics which can lead to inaccurate determination of nitrification rates. Correctly representing nitrification is important because this process has a significant impact on the dissolved oxygen balance in the River.

4) The DEM model is inadequate for analyzing wet weather events. DYNHYD can not handle the time variable nature of combined sewer overflow (CSO) inputs and can not represent lateral variation in water quality conditions during a CSO event.

Based on the four limitations identified above, DRBC has decided to replace the DEM with a more sophisticated model.

As with the DEM model, this new model will be used by DRBC to evaluate pollution control alternatives which will help the Delaware River achieve the fishable and swimmable water quality standards described in the Clean Water Act. The fishable standards are achieved primarily through control measures which maintain the minimum level of DO required to ensure the survival and reproduction of aquatic organisms. The swimmable standards are achieved primarily through control measures which maintain bacteria concentrations below levels posing health risks for swimmers.

Before implementing any control measure, however, DRBC will first use the model to evaluate the effectiveness of that control measure to help improve or maintain water quality in the River. With regard to DO standards, the model will be used to predict the DO concentrations in the Delaware River Estuary for the allocation of the CBOD TMDLs for the different estuary water quality management zones (zones 2-5). The TMDL assigned to each zone is then divided up among the dischargers in that zone to determine each individual permit. The new model will also be used to determine the effectiveness of loading reductions for other pollutants, such as nitrogenous biochemical oxygen demand (NBOD), which also significantly impact DO concentrations. With regard to bacteria standards, the model will be used to determine the fate of CSO bacterial loadings to assess the degree of control required to meet swimmable water quality criteria.

The development of the new model and its calibration is described in detail in the following sections of this report. The use of the model to describe CSO events and to predict bacteria concentrations will be the subject of future work covered under Tasks 3.0 and 4.0 of this project.

SECTION 3

DESCRIPTION OF STUDY AREA

The Delaware River-Estuary System is a drowned river valley located on the eastern seaboard of the United States (Figure 3-1). The River starts in southeastern New York, forms the border between Pennsylvania and New York, Pennsylvania and New Jersey, Delaware and New Jersey and then empties into Delaware Bay. The study area for this project is a subsection of the River extending approximately 80 river miles from Trenton downstream to Liston Point. The DRBC uses a river mile system to help reference different locations on the River. Under this system, the Cape Henlopen-Cape May transect at the mouth of Delaware Bay is designated as River Mile 0.0. River Mile (RM) values then increase going upstream along a transect that runs through the middle of Bay and continues up the River. The DRBC river mile reference system will be used throughout this report.

The study area described above, Trenton (RM 133) to Liston Point (RM 48.2), is a tidal estuary. The tidal section extends up to Trenton where a series of rapids forms a natural barrier preventing the propagation of tides farther upstream. The saline section varies seasonally as a function of the amount of freshwater flow. Typically, the saline waters intrude to Wilmington (RM 70) during periods of high flow and to the southern tip of Philadelphia (RM 90) during the summer low flow period. The upstream dam releases are regulated to maintain a targeted minimum flow of 3000 cfs at Trenton. One of the purposes for maintaining a flow of at least 3000 cfs at Trenton is to prevent saline water from reaching Philadelphia's drinking water plant intake at Baxter (RM 110). This 3000 cfs is, however, just a guideline. The actual minimum flow will depend on a number of other factors affecting river conditions and can at times be lower than 3000 cfs.

The drainage basin of the entire Delaware River encompasses parts of four states: New York, Pennsylvania, New Jersey and Delaware. Including only a subset of this basin, the study area extends from Trenton to Liston Point. At Trenton, the Delaware River drainage area is 6780 square miles and increases to 11,380 at Liston Point. The flow from this additional 4600 square miles enters the River primarily from the tributaries spread out along the 80 mile river stretch of study area.

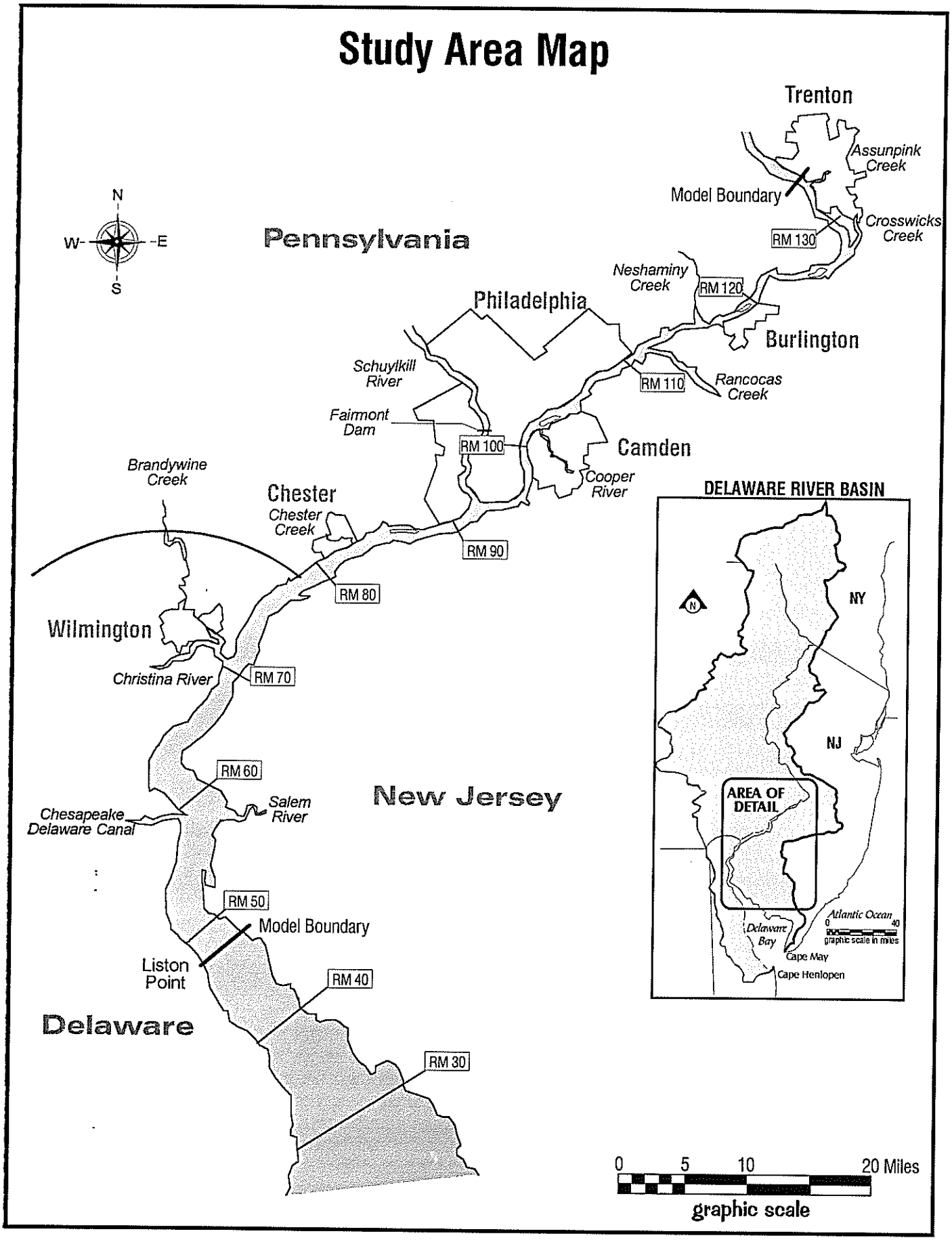

Figure 3-1. Study Area Map.

Nine major tributaries flow into the Delaware within the study area. Listed from upstream to downstream, they are Assunpink Creek, Crosswicks Creek, Rancocas Creek, Neshaminy Creek, Cooper River, Schuylkill River, Chester Creek, Christina River and the Salem River. The largest of these tributaries is the Schuylkill River (RM 91). During the summer period, the Schuylkill River can account for up to one fifth of the flow in the Delaware River. The lower section of the Schuylkill is tidal extending from its mouth at the Delaware to the Fairmount dam located 8 miles upstream. The lower Delaware River is also connected to the Chesapeake Bay via the Chesapeake-Delaware Canal (RM 60). Flow in the canal can vary in magnitude and move in either direction depending on the combination of tidal conditions in both the Delaware and Chesapeake Bays.

The daily flows for the Delaware River at Trenton from 1990 through 1995 are presented in Figure 3-2. The hydrological year can generally be divided into two periods: a higher flow period from November through May and a lower flow period from June through October. During the lower flow period, flows generally remain below 10,000 cfs and may approach or fall below the target minimum flow of 3000 cfs for extended periods. Posted on the top of the plot are the July through September averages for each year to assist in year to year comparisons. The shaded area indicates the two water quality periods modeled in this study: June 11 through October 8, 1991 and July 17 through October 5, 1995. These periods include extended times of low flow conditions and, therefore, represent critical conditions for Delaware River water quality.

The physical characteristics and hydrology of the river are presented in Figure 3-3. Tidal velocity, cross-sectional area, depth, flow, freshwater velocity and travel time are plotted vs river mile, with RM 140 located above Trenton and RM 40 located in upper Delaware Bay. For reference, the tributaries and major point sources are indicated on this Figure using symbols. The tributaries are indicated along the top x axis and the point sources below the bottom x axis. These symbols are interpreted as follows:

Tributaries

cw - Crosswicks Creek
ne - Neshaminy
R - Rancocas Creek
cp - Cooper River

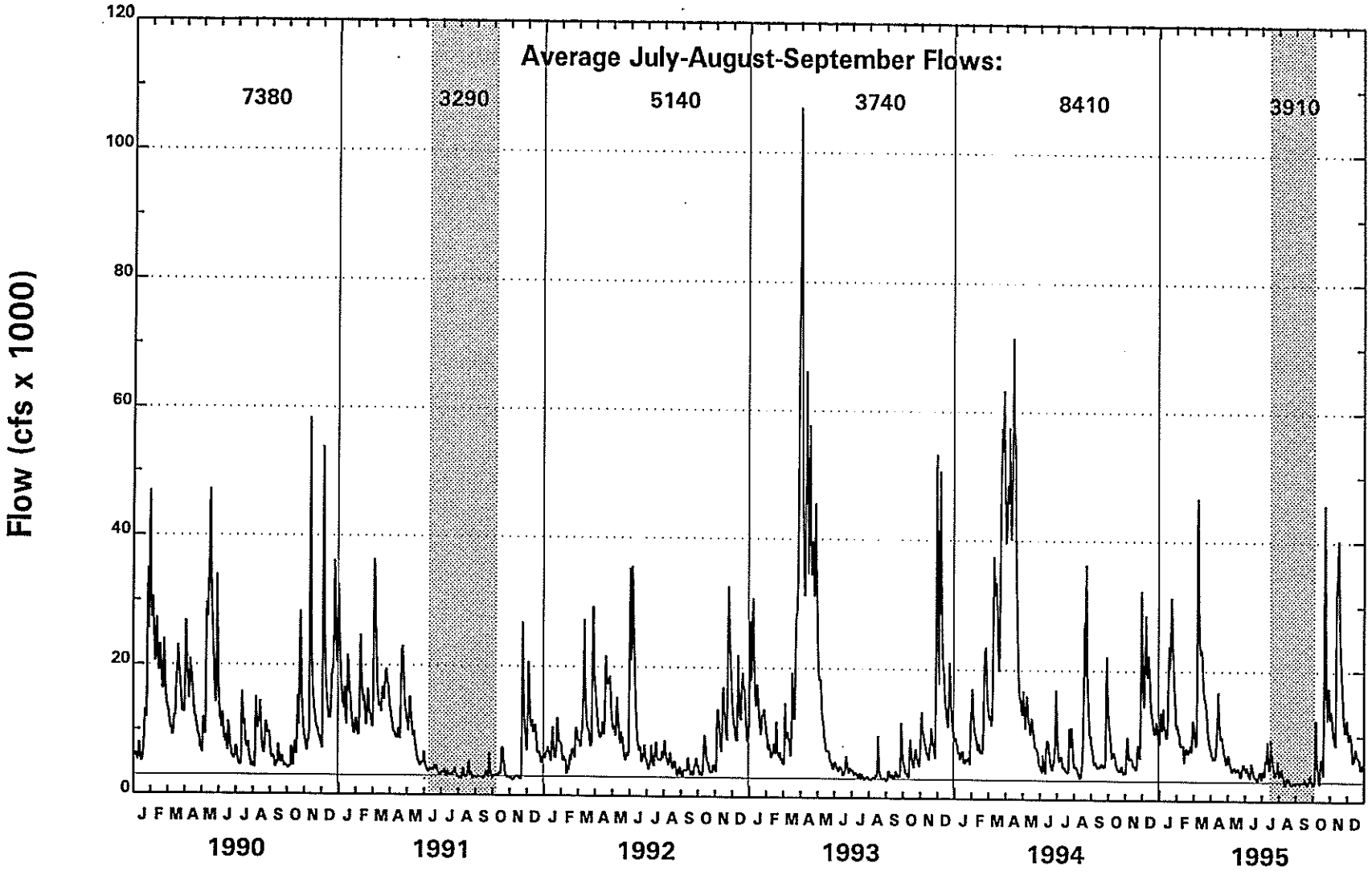

Figure 3-2. Delaware River Flow at Trenton - 1990 through 1995.

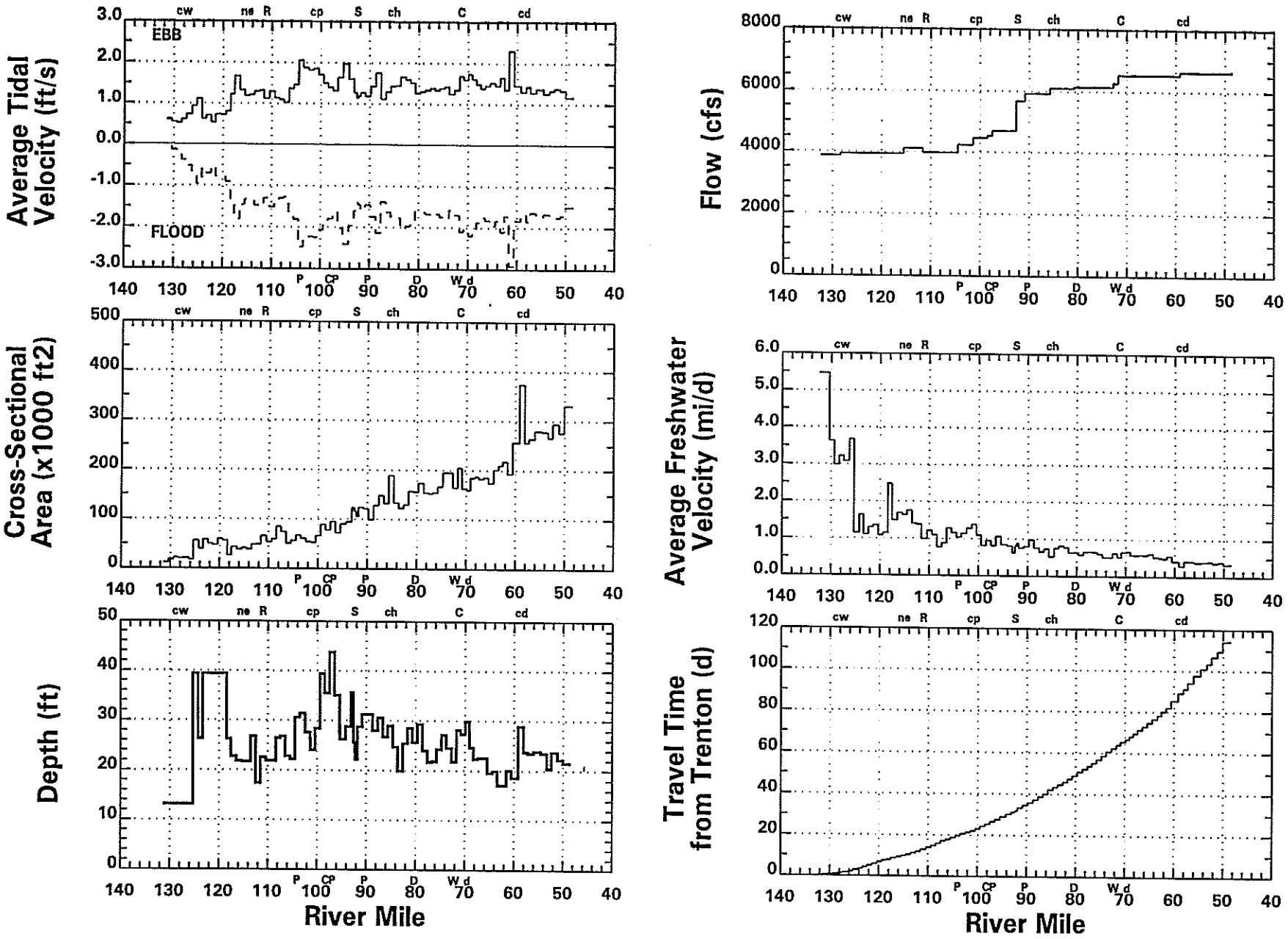

Figure -3-3. Physical Characteristics and 1995 Hydrology for the Delaware River.

S - Schuylkill River
ch - Chester Creek
C - Christina River
cd - Chesapeake-Delaware Canal (also location of Salem River)

Point Sources

P - Philadelphia, Northeast Plant
C - CCMUA (Camden)
P - Philadelphia, Southeast Plant
P - Philadelphia, Southwest Plant
D - DELCORA(Chester)
W- Wilmington
d - DuPont, Chamber Works

These reference symbols are used on Figures throughout the report.

The average tidal velocity for the July 17 through October 5, 1995 period is presented in panel 1. For 1995, the maximum ebb velocity approaches 2.5 ft/s while the maximum flood velocity approaches 3.0 ft/s. Although the flood velocities are slightly greater than ebb velocities, the ebb portion of the tidal cycle is longer in duration than the flood. This accounts for the net transport of freshwater from the River to the Bay.

The cross-sectional area, presented in panel 2, steadily increases from 10,000 to 300,000 ft^2 at Liston Point. Shown in panel 3, the depth averages 25 feet over the length of the study area and ranges from 20 to 40 feet. A navigation channel is maintained by the U.S. Army Corps of Engineers from the mouth of Delaware Bay upstream to Trenton. The channel is 40 feet deep up to RM 125 and only 25 feet upstream of RM 125. The width of the channel varies but is typically 800 ft wide to the mouth of the Schuylkill River and then 400 feet wide from the Schuylkill up to Trenton.

The average freshwater flow is shown in panel 4. The largest increase in flow occurs between RM 105 and RM 90 due primarily to the Schuylkill River and the Philadelphia WWTPs. Through this 15 mile stretch of River, the flow increases by over 50 percent. Please note, the

drop in flow at RM 112 is due to the intake of water by the Baxter drinking water facility. Shown in panel 5, the average freshwater velocity drops rapidly from 5.5 to 1.0 mile/day and then steadily decreases to 0.25 mile/day at Liston Point. The travel time in panel 6 shows the long residence of the Delaware River. During low flow condition, a slug of water at Trenton would take almost 120 days to travel from Trenton to Liston Point. The physical characteristic and hydrology for 1991 is not presented. The physical characteristic of the River (cross-sectional area and depth) are the same for 1991 and the hydrology of 1991 and 1995 shows only slight differences.

In general, the drainage basin of the Delaware River is a mix of agricultural, industrial and municipal land use. The particular stretch of river from Trenton to Liston Point has a heavy concentration municipal dischargers. The location of major cities and their discharges are shown in Figure 3-4 and include three Philadelphia discharges (Northeast, Southeast and Southwest Plants), Camden (CCMUA), Chester (DELCORA) and Wilmington. This stretch of river is also one of the most heavily industrialized sections of river in the country. One of the larger industrial dischargers, the DuPont Chamber Works facility, is also shown on Figure 3-4. The discharges mentioned above along with the remaining municipal and industrial point source loads not shown on this map, but included in the model, are listed in Table 3-1. Also shown on Figure 3-4 is the location of the drinking water intake at Baxter, RM 110. Under low flow condition, the Baxter intake is particularly important in the flow balance of the river because there is an average daily withdrawal of 200 MGD.

In order to manage these dischargers effectively, the DRBC has divided the river into the management zones which are shown on Figure 3-4. The study area essentially includes Zones 2 through 5. Zone 1 is the area above Trenton and Zone 6 is the area below Liston Point.

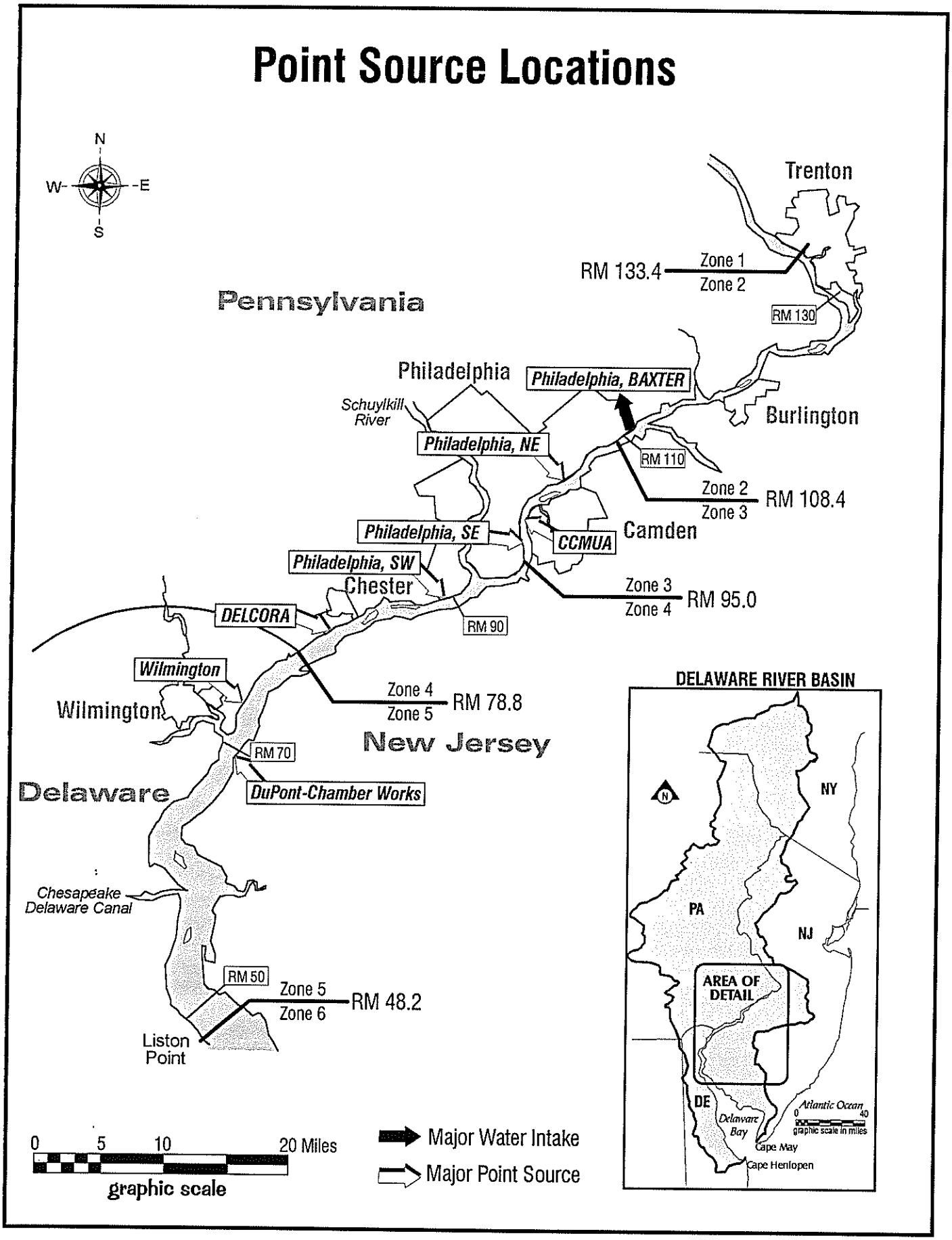

Figure 3-4. Point Source Location and Management Zone Map.

Table 3-1. List of Significant Discharges to the Delaware River Between RM 134 and RM 48.

State	Mile Point	Description
PA	133.00	Morrisville Boro Mun. Auth-STP
NJ	131.80	Trenton Sewer Utility
NJ	128.41	Hamilton Township WPCF
NJ	128.22	Black's Creek WWTP
PA	127.97	United States Steel Group USX
NJ	127.00	Fieldsboro, Borough of
NJ	123.10	Florence Township STP
PA	122.10	Lower Bucks County Joint M.A.
PA	118.87	Bristol Boro Wat. & Sew. Auth.
PA	118.70	Rohm & Haas Company
NJ	117.12	Burlington City STP
NJ	117.10	Colorite Polymers Company
PA	116.91	Bristol TWP
NJ	114.70	Beverly Sewerage Authority
NJ	111.06	Mt. Laurel TWP MUA
NJ	111.06	Riverside STP
NJ	111.06	Willingboro Water PCP
NJ	111.00	Delran Sewerage Authority
NJ	108.82	Cinnaminson STP
NJ	108.76	Riverton Sewage Treatment
NJ	107.66	Palmyra STP
NJ	104.40	Georgia Pacific Corporation
PA	**104.20**	**Philadelphia - Northeast WPCP**
NJ	**97.93**	**CCMUA - Delaware No. 1 (Camden)**
PA	**96.70**	**Philadelphia - Southeast WPCP**
NJ	94.50	Coastal Eagle Point Oil Co.
PA	92.47	Sun Co., Inc., R & M
PA	**90.70**	**Philadelphia - Southwest WPCP**
NJ	89.70	Gloucester Co. Util Auth.
NJ	87.20	Hercules, Inc.
NJ	86.88	Air Products & Chemicals, Inc.

Table 3-1. List of Significant Discharges to the Delaware River Between RM 134 and RM 48.

State	Mile Point	Description
NJ	86.66	Greenwich Township STP
NJ	86.00	E I Dupont De Nemours & Co.
PA	85.28	Tinicum TWP Delaware Co. Sew. Auth.
PA	**80.70**	**DELCORA**
NJ	80.66	Rollins Environmental Services
PA	80.20	BP Oil, Inc.
NJ	79.00	Monsanto Chemical Co.
NJ	79.00	Logan Township MUA
DE	78.20	General Chemical Corp.
NJ	76.97	The Geon Co.
DE	73.40	DuPont Pigments Dept.
DE	73.40	E.I. DuPont De Nemours & Comp.
NJ	72.00	Penns Grove Sewerage Authority
DE	**71.76**	**Wilmington City**
NJ	70.80	Carneys Point Sewage Plant
NJ	**69.75**	**DuPont - Chamber Works**
DE	68.58	ICI America, Inc. Atlas Point
NJ	67.00	Pennsville Sewerage Authority
DE	62.66	Occidental Chemicals
DE	62.66	GeorgiaGulf Corp.
DE	62.65	Std. Chlorine of Delaware
DE	61.70	Star Enterprises
DE	61.70	Formosa Plastics Corp.
DE	60.80	Delaware City Sewage Treatment
NJ	58.37	Salem Wastewater Treatment Plt.
DE	54.59	Port Penn Sewage Treatment Plt.
NJ	54.45	Hancock's Bridge STP
NJ	54.45	Leisure Arms
NJ	51.51	PSE&G Hope Creek Generating St.

SECTION 4

REVIEW OF WATER QUALITY DATA

4.1 SAMPLING PROGRAM

Water quality parameters are measured in the Delaware River-Estuary by the Delaware Department of Natural Resources and Environmental Control (DNREC) under contract to DRBC. Samples are generally collected twice per month from March through November at either low or high water slack tide. High water slack runs are typically made every third survey. All the samples are typically collected at three foot depths, along the center channel and during daylight hours between 6 a.m. - 12 noon. Eighteen stations are sampled per survey.

Starting at RM 31.0 and ending at RM 127.5, two boats follow the slack tide up the river and sample the stations shown on Figure 4-1. Two discontinued stations are also indicated on Figure 4-1. The station at RM 50.8 was switched to RM 48.2 in July of 1995 and the other station at RM 134 was only sampled on a limited basis in 1991. A complete list of the sampling stations and corresponding River Mile is provided in Table 4-1.

The U.S. Geological Survey (USGS) also maintains continuous water quality monitors at four locations on the Delaware River-Estuary; Trenton (RM 134), Philadelphia at Ben Franklin Bridge (RM 100), Chester (RM 82) and Reedy Island (RM 54). These monitors record hourly measurements for dissolved oxygen, temperature, pH and specific conductance. These data were also used in addition to the DRBC data.

4.2 HISTORICAL DISSOLVED OXYGEN TREND

The historical dissolved oxygen levels in the Delaware River are presented in Figure 4-2. This figure shows the average and range of the July through September dissolved oxygen data at RM 84. This DRBC sampling station is located just upstream of Chester, PA and just downstream of the typical dissolved oxygen sag point which occurs between RM 95 and 85. The thirty years of data presented show a dramatic and steady increase in the River's summer dissolved oxygen levels. From the late 1960s to the 1990s, the average dissolved oxygen increased from 1-2 mg/l

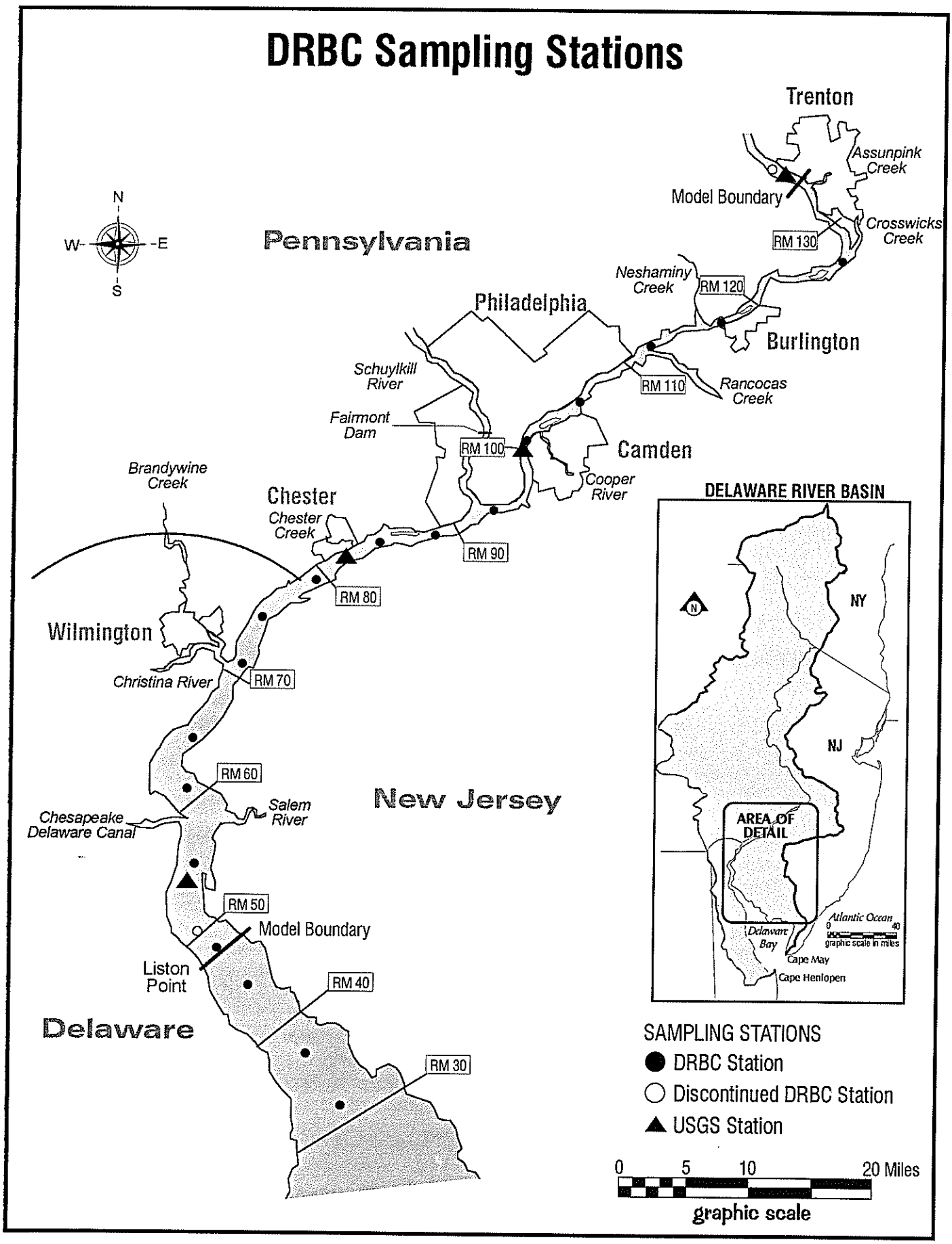

Figure 4-1. Delaware River Basin Commission Sampling Station Map.

Table 4-1. List of Delaware River Basin Commission Sampling Locations

Station	River Mile
Mahon River	31.0
Ship John Light	36.6
Smyrna River	44.0
Liston Point - Buoy 8L	48.2
Appoquinimink (Switched to RM 48.2 July 1995)	50.8
Reedy Island	54.9
Pea Patch Island	60.6
New Castle	66.0
Cherry Island	71.0
Oldmans Point	74.9
Marcus Hook	78.1
Eddystone, PA	84.0
Paulsboro, NJ	87.9
Navy Yard	93.2
Benjamin Franklin Bridge	100.2
Betsy Ross Bridge	104.9
Torresdale	110.7
Burlington Bristol Bridge	117.8
Fieldsboro	127.5
Trenton (Moved)	130.0

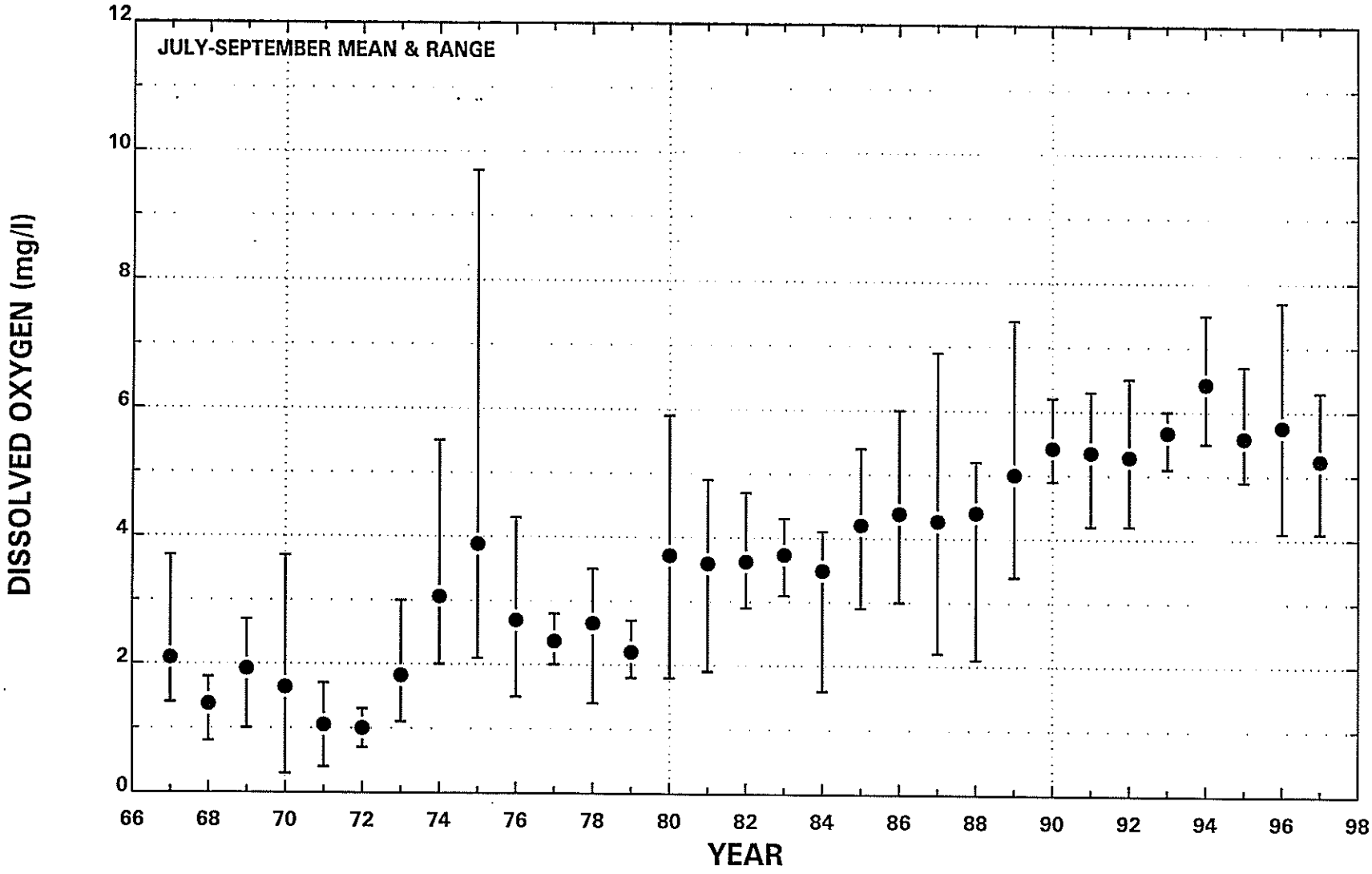

Figure 4-2. Historical July Through September Dissolved Oxygen Data at RM 84 Near Chester, PA.

to over 5 mg/l. Although conditions have greatly improved over the last thirty years, little further improvement has been seen throughout the 1990s. Minimum dissolved oxygen concentrations still occasionally approach 4 mg/l at RM 84 and can sometimes even fall below 4 mg/l at the dissolved oxygen sag point between RM 95 and 85.

4.3 SPATIAL PLOTS

Spatial plots of the water quality data collected during the two modeling periods are presented in Figures 4-3a through 4-4b. Each parameter is plotted vs river mile where RM 140 is upstream above Trenton and RM 40 is downstream in upper Delaware Bay. For each sampling station, the mean and range over the modeled period are shown. As described in Section 3.0, the tributaries and major point source discharges are indicated along the top and bottom x axis, respectively. Figures 4-3a and 4-3b show water quality data for the July 17th through October 5th, 1995 period and Figures 4-4a and 4-4b show data for the June 11th through October 8th, 1991 period.

Figure 4-3a shows DO, temperature, conductivity, TSS, chlorophyll-a, orthophosphate (PO_4), pH and total alkalinity. The DO values range between 4.0 and 8.0 mg/l with lowest DO value of 4.0 mg/l occurring just south of Philadelphia at RM 87.9. Temperature during this period typically ranges between 20°C and 30°C with little spatial variability. Conductivity, which is due primarily to the ions present in seawater, indicates the intrusion of saline water to just south of Chester, RM 80. The total suspended solids (TSS) exhibit the turbidity/solids maximum typical of river-estuary systems. Upstream TSS values average about 10 mg/l and are relatively constant until RM 85, then increase to a peak of 30 mg/l at RM 60 and quickly decrease to almost upstream levels by RM 44. The chlorophyll-a data have upstream values of 10 to 15 μg/l and low downstream values of less than 5 μg/l showing a pattern almost opposite to TSS. Values of pheophytin-a, which is a degradation product of chlorophyll-a, show the same pattern as chlorophyll-a, but at much higher concentrations. Based on TSS, chlorophyll-a and pheophytin-a measurements, the River can be divided roughly into two zones at RM 85; an upstream zone of low solids and high phytoplankton and a downstream zone of high solids and low phytoplankton. Orthophosphate values range between 0.04 and 0.12 mg/l well above concentrations limiting algal growth. The pH ranges between 7.0 and 8.5 slightly decreasing downstream near the Bay as the River becomes more saline. Total alkalinity ranges between 40 and 80 as $CaCO_3$ mg/l, and increases downstream near the Bay.

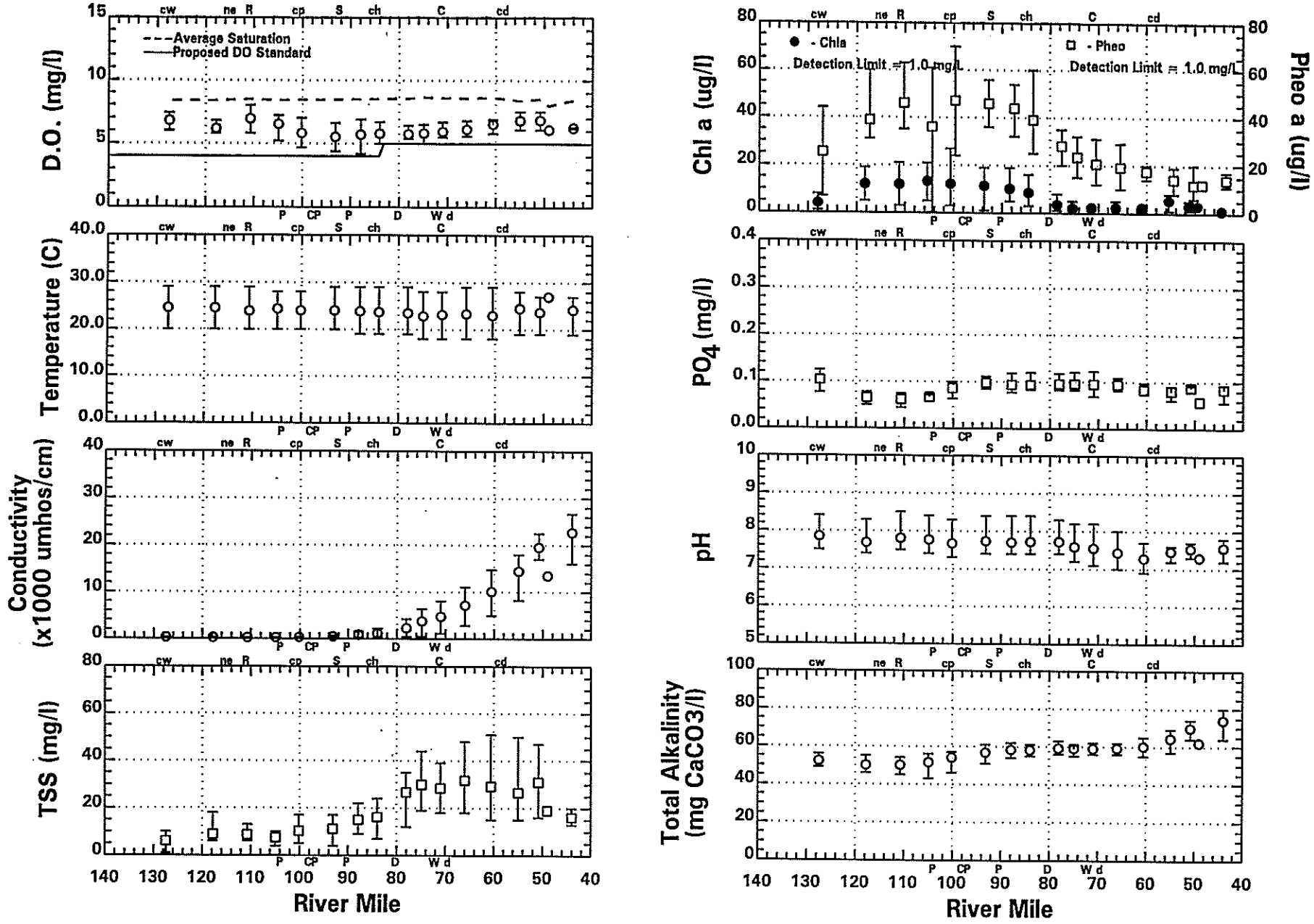

Figure 4-3a. DRBC Delaware River Water Quality Spatial Data - July 17 through October 5, 1995.

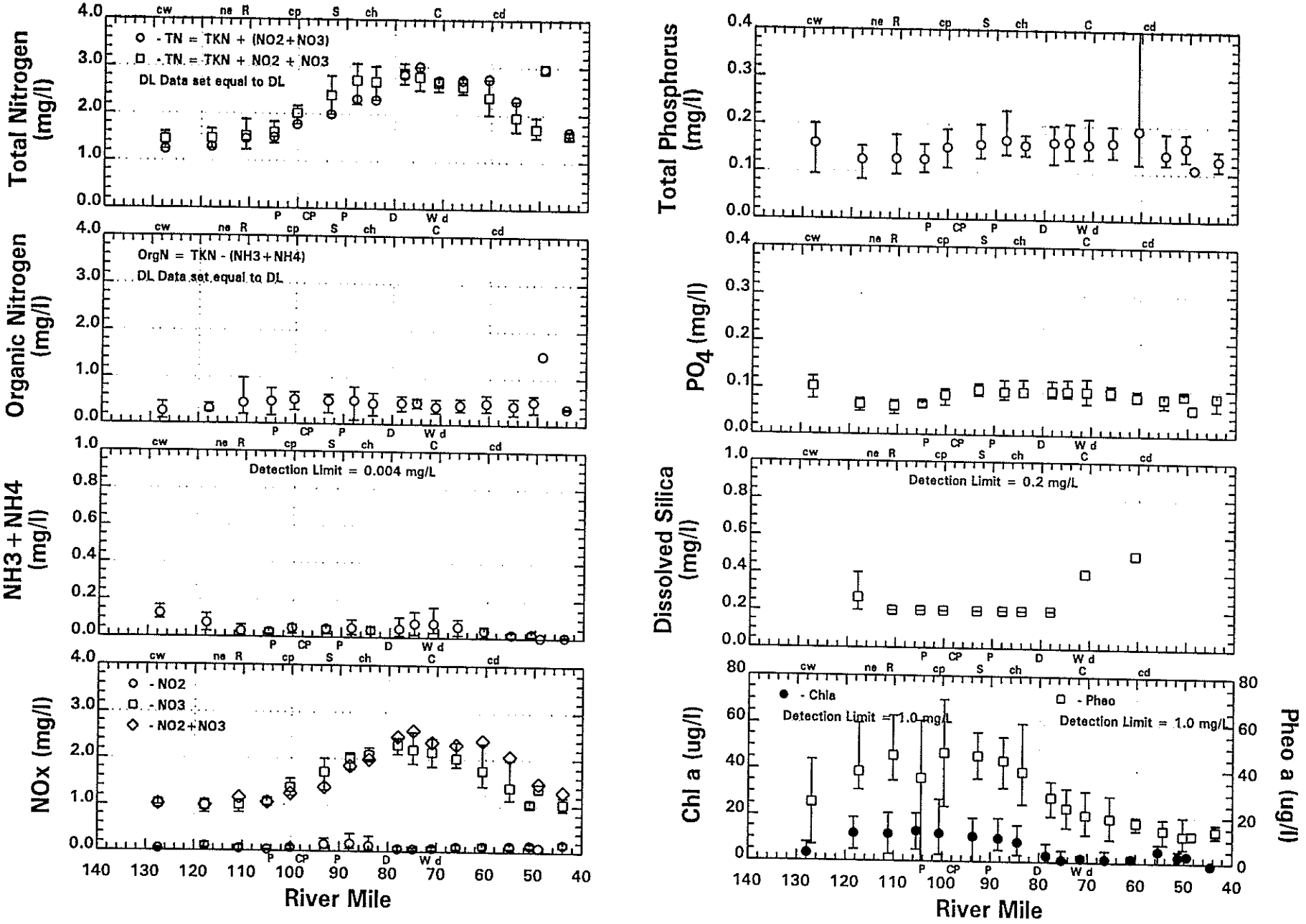

Figure 4-3b. DRBC Delaware River Water Quality Spatial Data - July 17 through October 5, 1995.

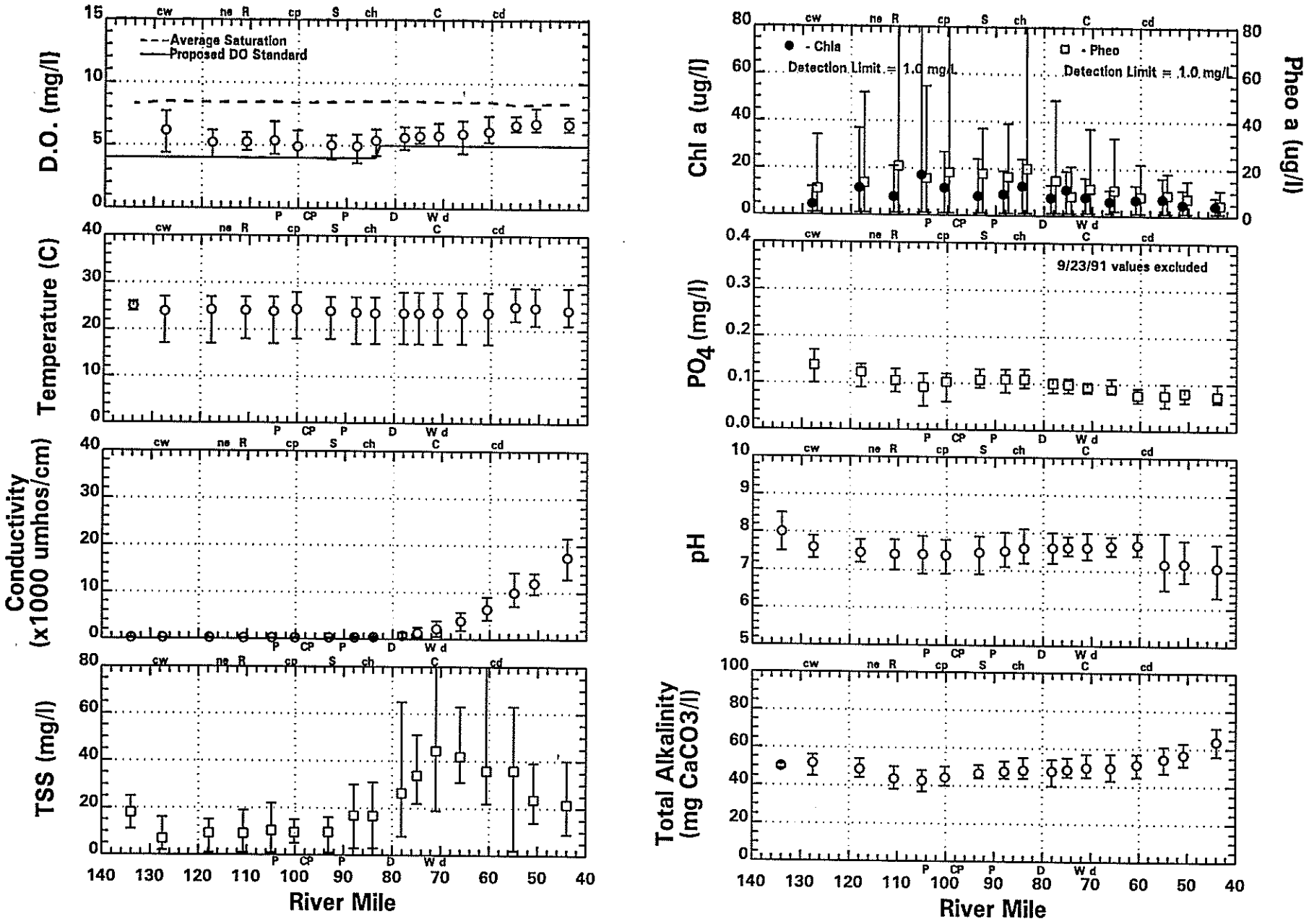

Figure 4-4a. DRBC Delaware River Water Quality Spatial Data - June 11 through October 8, 1991.

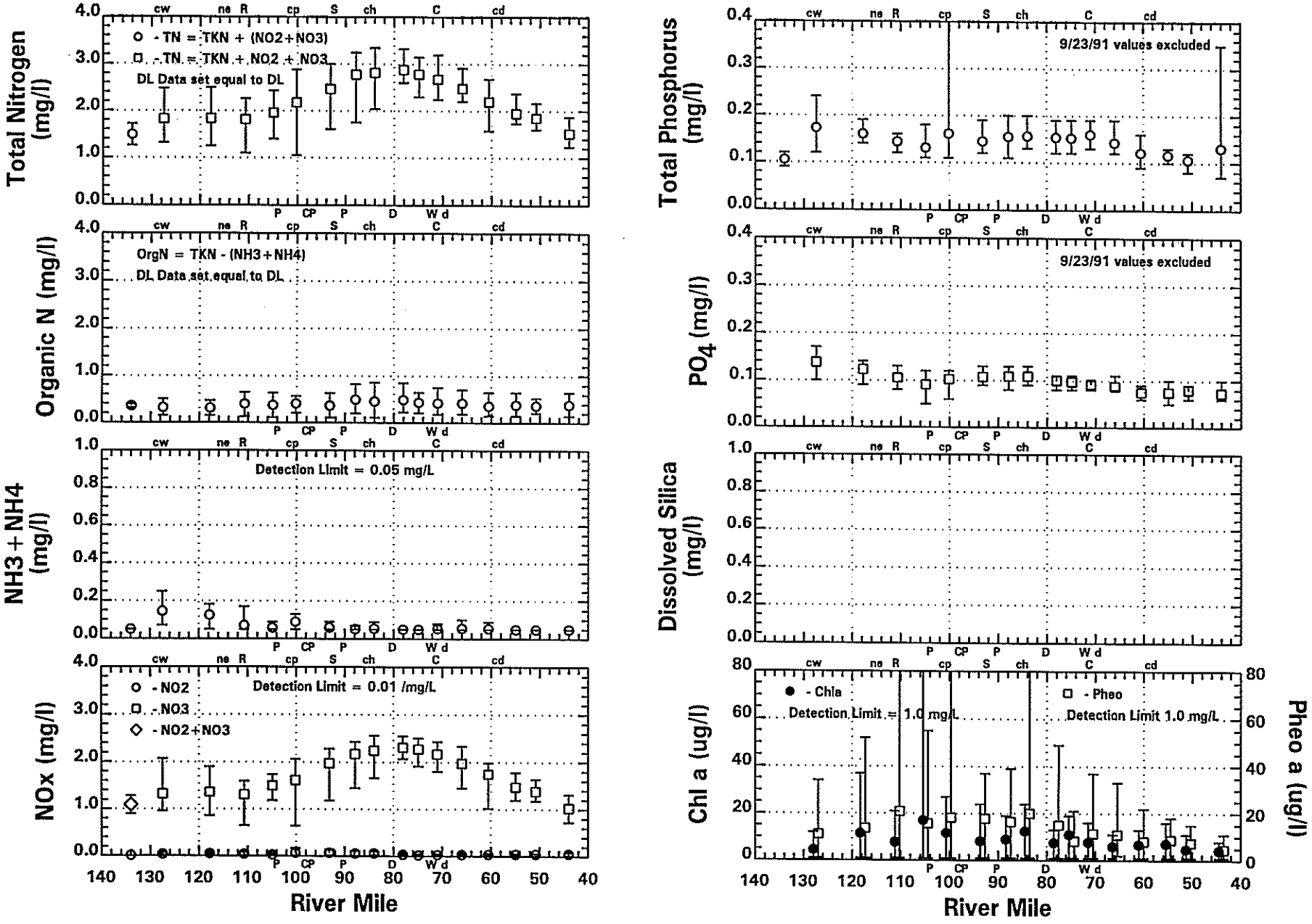

Figure 4-4b. DRBC Delaware River Water Quality Spatial Data - June 11 through October 8, 1991

Figure 4-3b displays the nutrients (nitrogen, phosphorus and silica) and repeats the orthophosphate and chlorophyll-a/pheophytin-a panels from Figure 4-3a for reference. Total nitrogen shows a pattern of increasing from 1.5 mg/l upstream to 3.0 mg/l at RM 75 and decreasing back down to 1.5 mg/l by RM 44. Organic nitrogen, on the other hand, is generally constant over the entire River generally averaging about 0.4 mg/l. Ammonia is also consistently low for the entire River, averaging only about 0.05 mg/l and never measuring above 0.2 mg/l. Showing a similar pattern to ammonia, nitrite is consistently low over the length of the River. Nitrate, however, shows the same pattern as the total nitrogen, indicating that the majority of nitrogen is in the form of nitrate. A high rate of nitrification in the River rapidity converts ammonia to nitrate keeping ammonia levels low and nitrate levels high. Total phosphorus ranges between 0.1 to 0.2 mg/l with approximately half in the form of orthophosphate. Only limited silica data is available and the majority of this data is either at or below detection limit.

The 1991 data, as presented on Figures 4-4a and 4-4b, generally show the same trends as the 1995 data. The 1991 period starts in June, a month earlier than the 1995 period and includes data from three additional surveys. On Figure 4-4a, the DO data show the same trend as in 1995 with the minimum DO of 3.9 mg/l also occurring at RM 87.90. The temperature is slightly colder ranging between 18°C and 28°C. The conductivity indicates that saltwater intrusion only extends to RM 70 approximately 10 miles downstream of the 1995 location. The TSS concentrations show the same pattern as 1995, but the 1991 average peak values of 40 mg/l in the downstream zone are higher and exhibit greater variability. The chlorophyll-a values are noticeably higher downstream than in 1995 and pheophytin-a values exhibit much larger range than 1995 values. These variations may suggest some difference in the dynamics influencing phytoplankton concentrations in 1991 as compared to 1995. Orthophosphate, pH and alkalinity all show very similar data trends and ranges in both 1991 and 1995. The September 23, 1991 orthophosphorus values were much higher than the range of values previously reported. These orthophosphorus values are suspect and, therefore, excluded from this data presentation.

In Figure 4-4b, the different forms of nitrogen (total, organic, ammonia, nitrite and nitrate) have similar magnitudes and ranges and follow the same trends present in the 1995 period. One small difference was a change in the detection limit for ammonia from 0.050 in 1991 to 0.004 mg/l in 1995. Similar to the nitrogen data, the 1991 total phosphorus data have the same magnitude, range and trend as in 1995 period. The orthophosphorus data upstream of RM 95 is,

however, much higher in 1991 than in 1995, but downstream data for both years have similar magnitudes, ranges and trends. No silica measurements were made during this period in 1991.

4.4 TEMPORAL PLOTS

Temporal plots of the 1995 and 1991 data are shown in Figures 4-5 through 4-12. Dissolved oxygen, temperature, conductivity, TSS, chlorophyll-a, and the inorganic forms of phosphorus and nitrogen are shown on these plots. The March through November data are plotted with the period modeled for each year indicated with a shaded area. Four locations for each year are presented: the location of minimum DO (RM 87.9); the midpoint of the upstream zone of low TSS and high phytoplankton (RM 104.9); the midpoint of the downstream zone of high TSS and low phytoplankton (RM 60.6); and the location of the Chester USGS continuous recorder (RM 82.0) plotted with data from the nearest DRBC station (RM 84.0).

Figures 4-5 and 4-6 show the 1995 and 1991 temporal trends at the location of the DO sag point, RM 87.9. While the data show seasonal patterns over the March through November period, the 1995 period being modeled, July 17th through October 5th, is relatively constant. The DO does show some small survey to survey variation, particularly the late August and early September surveys. The higher DO values for these surveys, however, correspond to higher chlorophyll-a values suggesting algal production as the cause. The temperature averages 25°C and varies 3-4 degrees for the both modeling periods. The low temperature reading on August 8, 1995 of 18°C in Figure 4-5 appears to be an outlyers and was excluded from data analysis and modeling. Conductivity and TSS profiles are flat the entire period. Chlorophyll-a shows some survey to survey variation and, in turn, influences DO as mentioned earlier. The inorganic forms of phosphorus (PO_4) and nitrogen (NH_3 and NO_3) available for phytoplankton uptake are relatively constant and sufficient to prevent the system from becoming nutrient limited.

Figures 4-7 and 4-8 show the 1995 temporal trends upstream at RM 104.9 (low TSS and high phytoplankton zone) and downstream at RM 60.6 (high TSS and low phytoplankton zone). The primary differences in these two zones are reflected in the conductivity, TSS and chlorophyll-a values. At RM 60.6, the higher conductivity indicates a much greater influence of the more saline Bay waters than at RM 104.9. Since salinity can inhibit the growth of certain groups of algae, higher salinity may be partly responsible for the low phytoplankton concentrations measured downstream. The downstream zone also has higher TSS concentrations

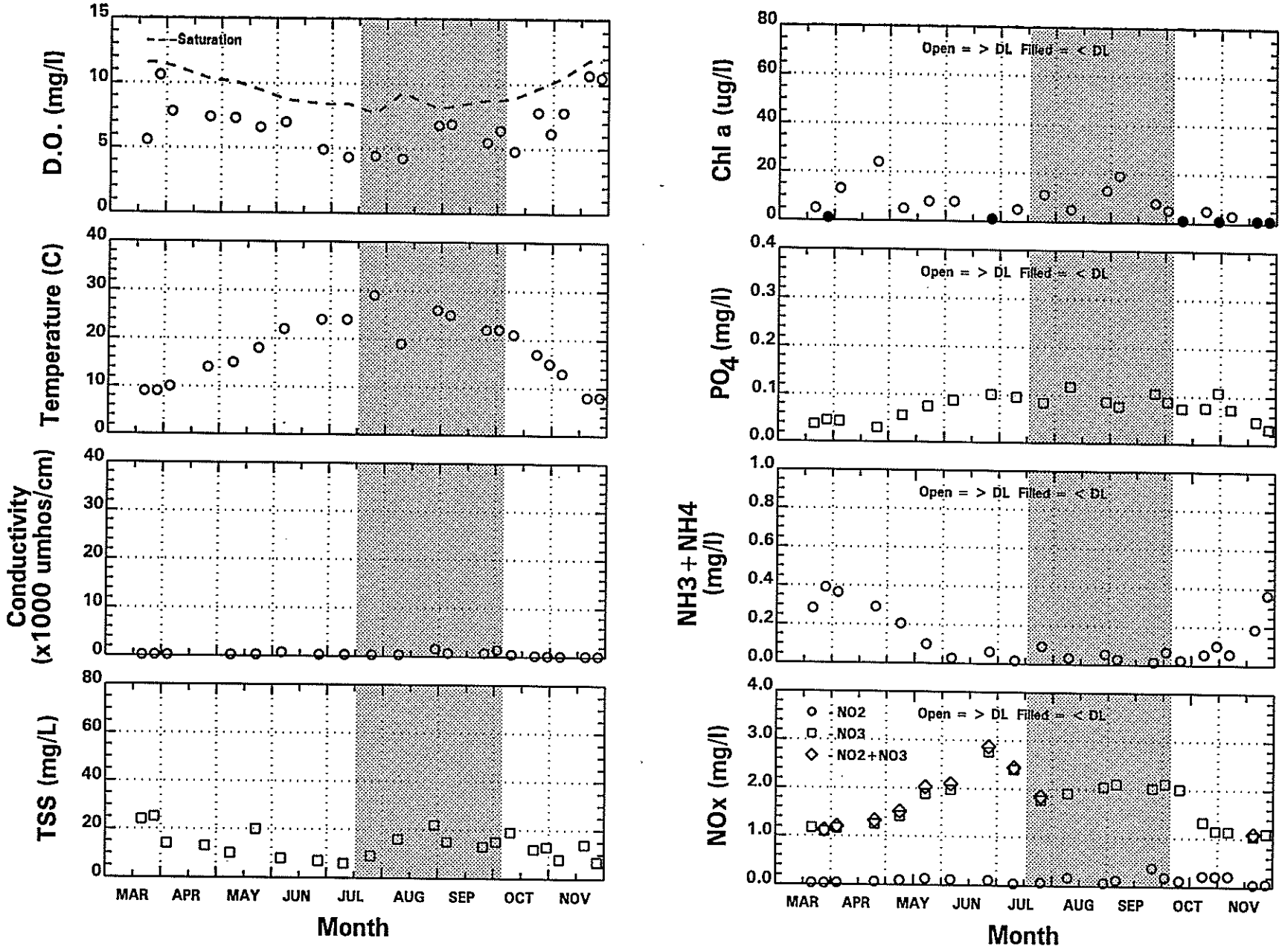

Figure 4-5. 1995 DRBC Delaware River Water Quality Temporal Data at RM 87.9.

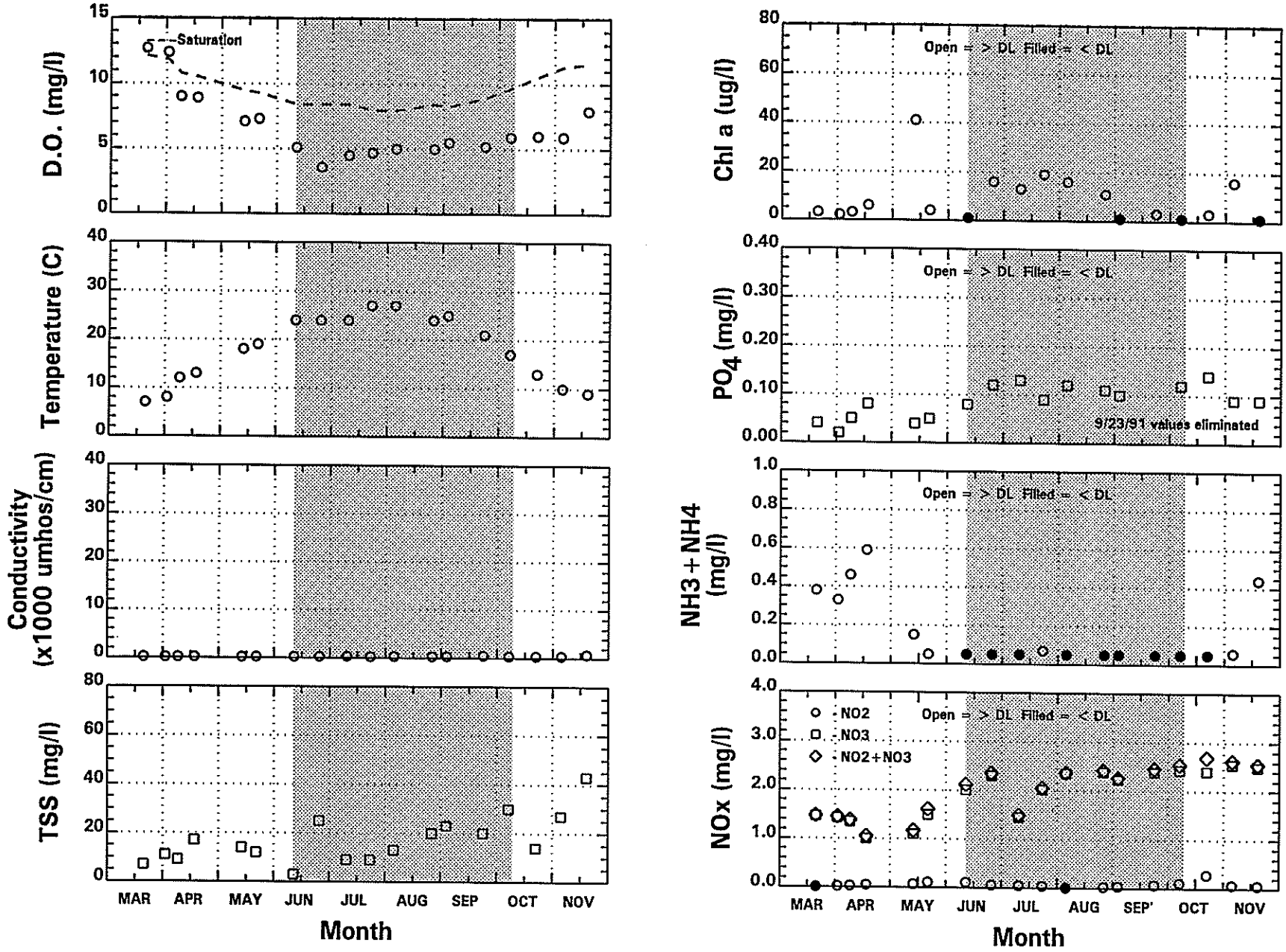

Figure 4-6. 1991 DRBC Delaware River Water Quality Temporal Data at RM 87.9.

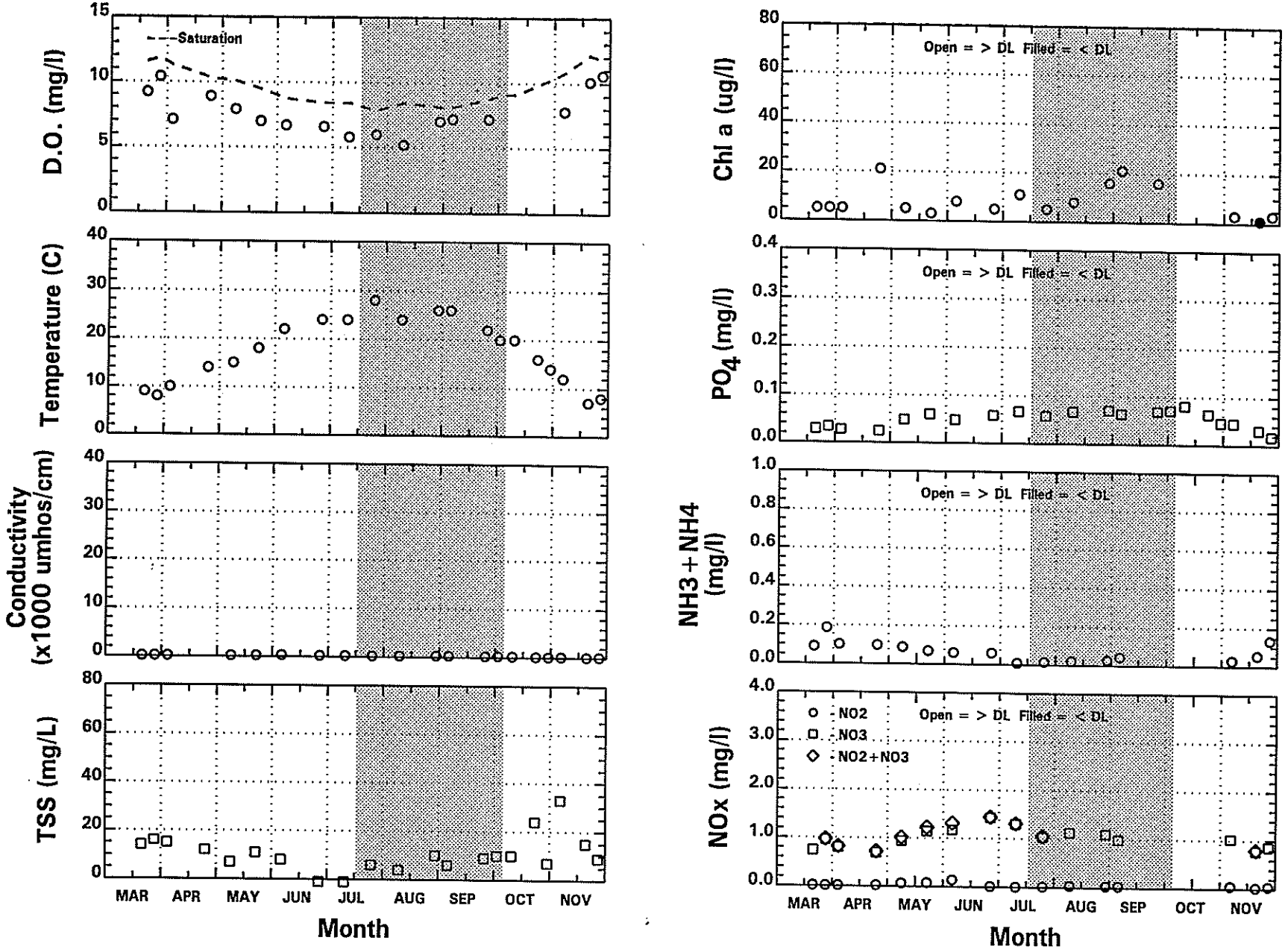

Figure 4-7. 1995 DRBC Delaware River Water Quality Temporal Data at RM 104.9.

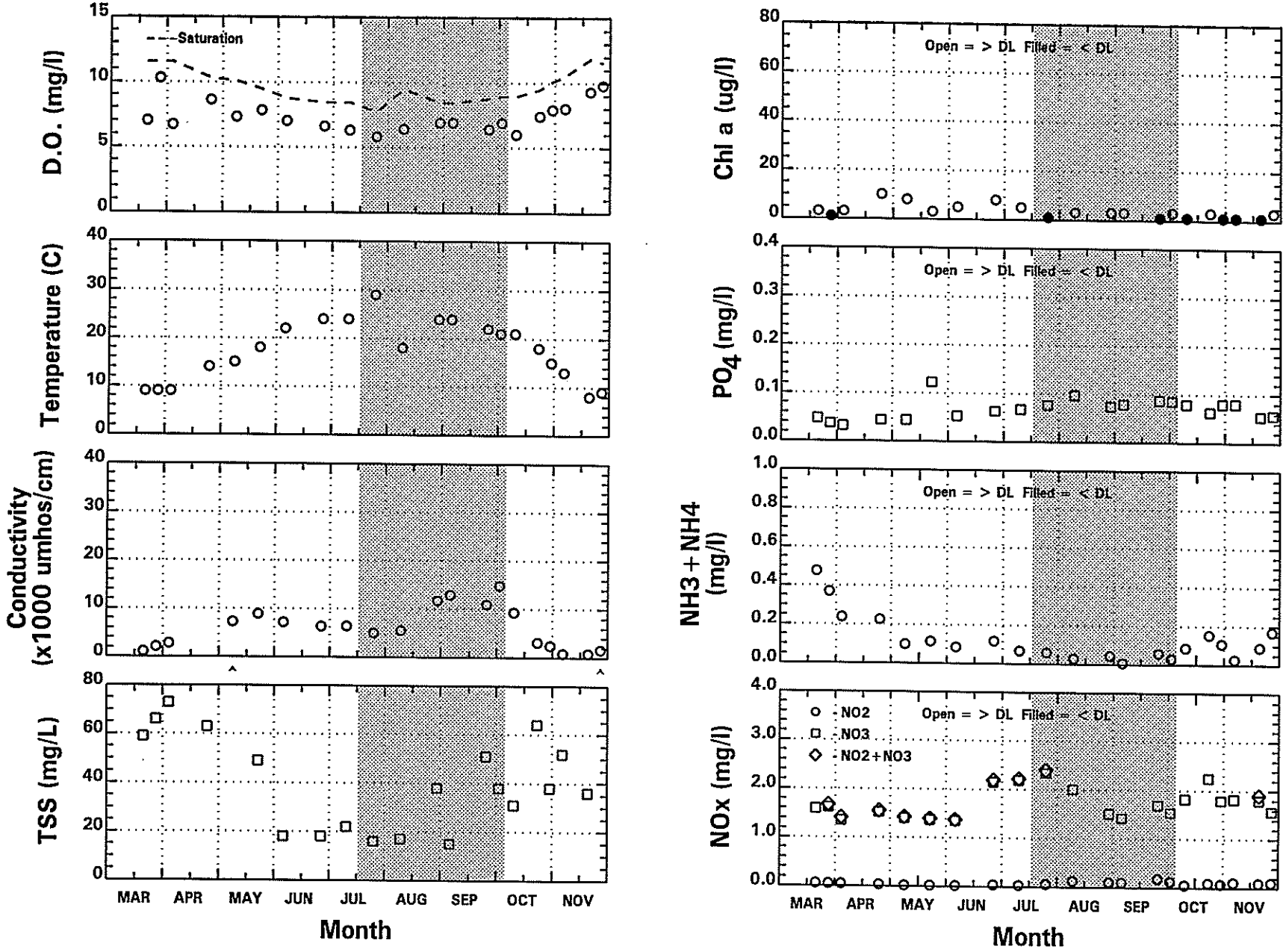

Figure 4-8. 1995 DRBC Delaware River Water Quality Temporal Data at RM 60.6.

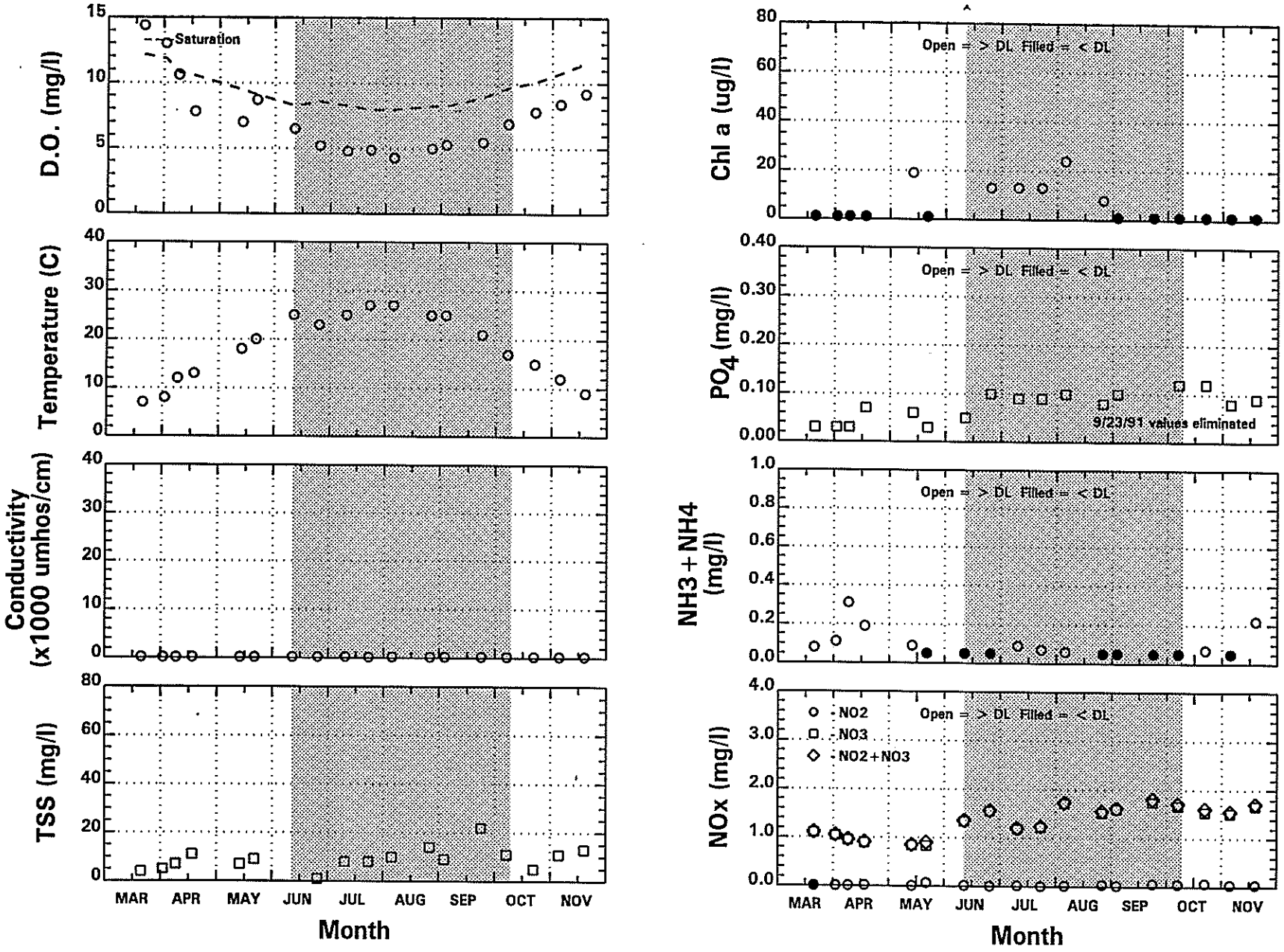

Figure 4-9. 1991 DRBC Delaware River Water Quality Temporal Data at RM 104.9.

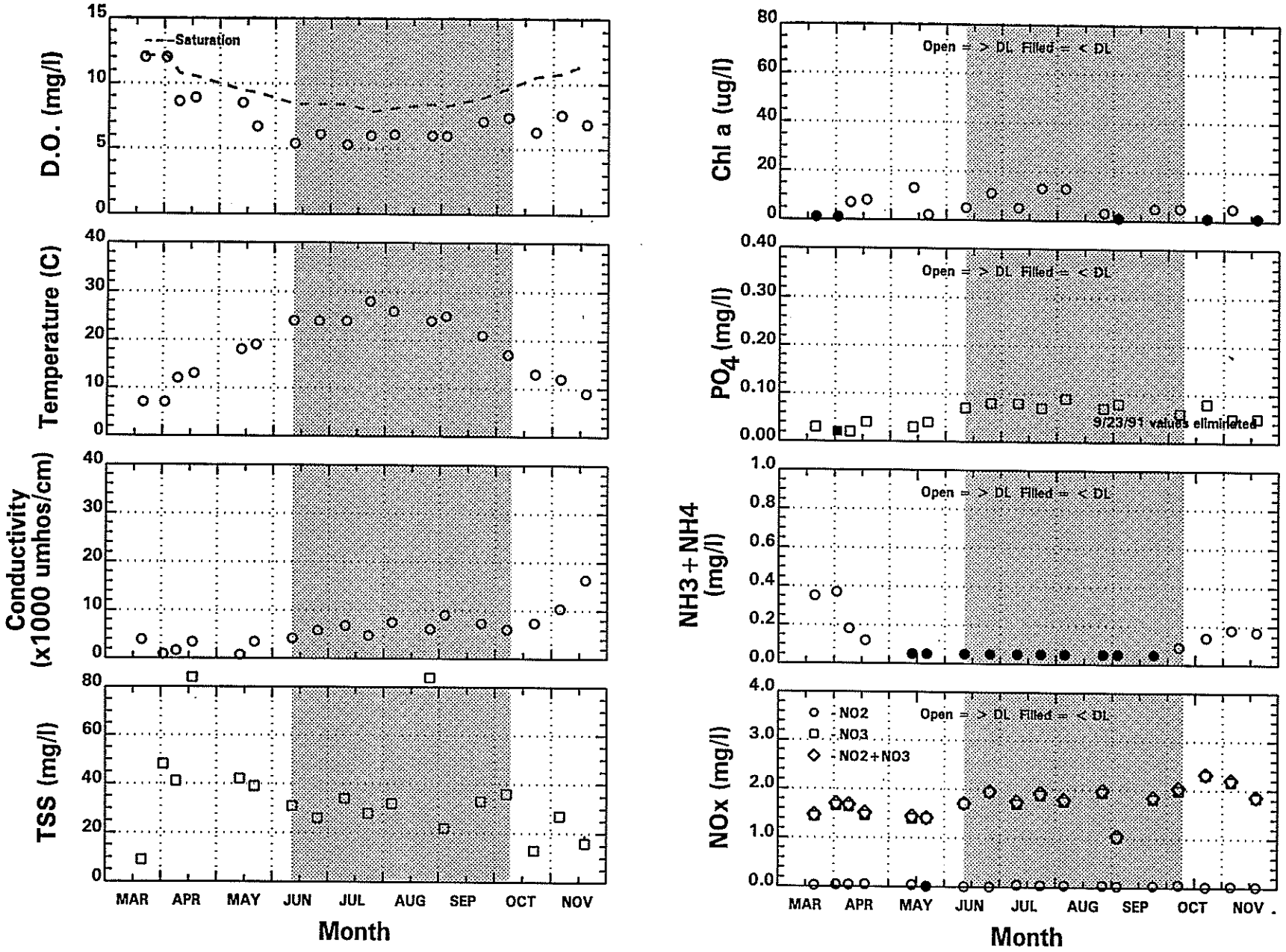

Figure 4-10. 1991 DRBC Delaware River Water Quality Temporal Data at RM 60.6.

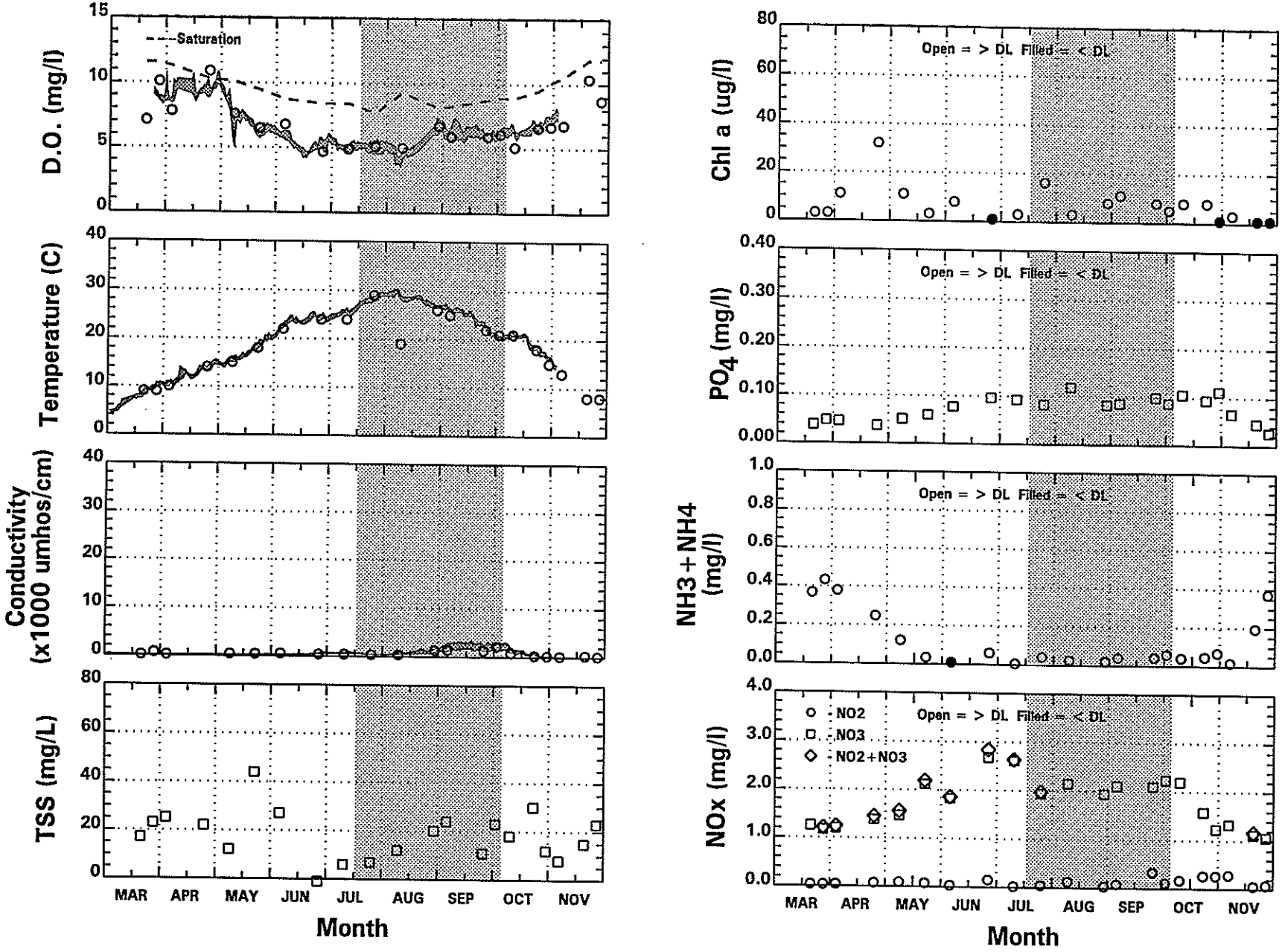

Figure 4-11. 1995 DRBC Delaware River Water Quality Temporal Data at RM 84.0 & USGS Temporal Data at RM 82.

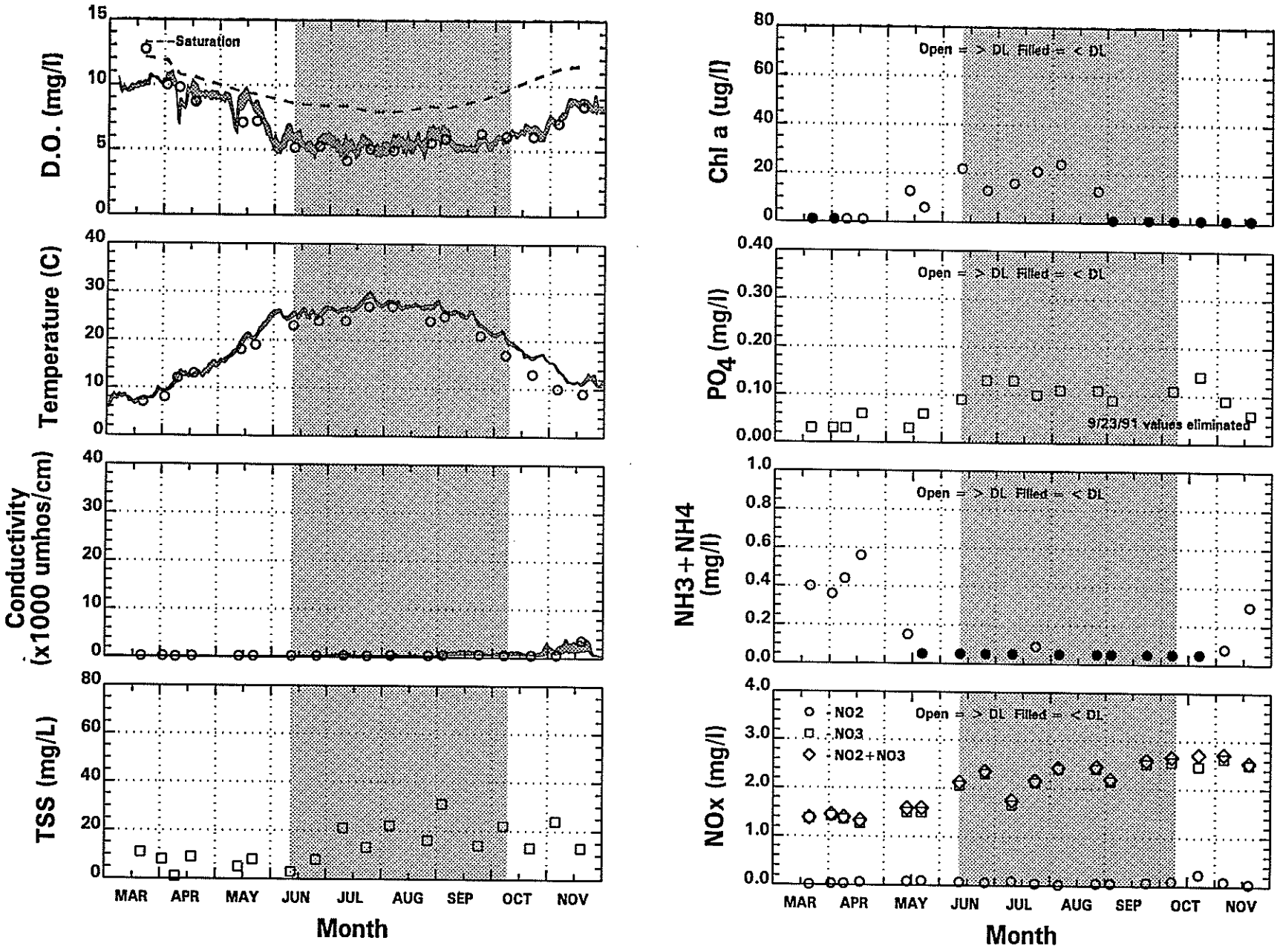

Figure 4-12. 1991 DRBC Delaware River Water Quality Temporal Data at RM 84.0 & USGS Temporal Data at RM 82.

which reduce light penetration into the water column and reduces algal growth. Figures 4-9 and 4-10 show the 1991 temporal trends upstream at RM 104.9 and downstream at RM 60.6. The 1991 data show the same patterns in conductivity, TSS and chlorophyll-a as the 1995 data described above.

Figures 4-11 and 4-12 show the 1995 and 1991 temporal trends at the location of the USGS monitoring station at Chester, RM 82, and the nearest DRBC station, RM 84. The daily range in hourly data recorded at the USGS station is plotted for DO, temperature and conductivity. The USGS and DRBC data generally show good agreement in both the 1995 and 1991 data sets. Also note that there is not a large range in the diurnal DO measurements. The small range of 1.0 mg/l is due to a combination of tidal translation and photosynthetic activity.

SECTION 5

MODELING FRAMEWORK

5.1 HYDRODYNAMIC MODEL

The hydrodynamic modeling framework is based upon the time-dependent, three-dimensional estuarine, coast and ocean circulation model (ECOM) developed by Blumberg and Mellor (1980, 1987) and Blumberg and Herring (1987). ECOM solves prognostic equations for free surface elevation, velocity components, temperature, salinity, turbulence energy and turbulence macroscale. The vertical turbulent mixing processes can be parameterized using either the turbulence closure sub-model of Mellor and Yamada (1982) or simpler empirical formulas that estimate vertical diffusion using a Richardson number approach.

The version of the hydrodynamic model (ECOMsiz) used in the present study has two unique features that should be noted. First, the model was modified such that the barotropic pressure gradient in the momentum equations and the horizontal velocity divergence in the continuity equation are treated implicitly (Casulli, 1990). This improvement provides a significant increase in computational efficiency because the semi-implicit algorithm allows time steps that greatly exceed the limit of the Courant-Friedrich-Lewy (CFL) stability condition. Second, ECOMsiz is a hybrid z-level coordinate model in that the vertical coordinate is discretized using horizontally-constant grid spacing. The last model feature to note is the use of a curvilinear coordinate system in the horizontal plane, which greatly increases model efficiency in treating irregularly shaped coastlines and meeting requirements for high resolution in specific local regions. The model incorporates detailed features of the bathymetry and shoreline and includes: freshwater runoff, surface wind stress, temperature and salinity profiles at the edges of the modeled region as time-dependent forcing boundary conditions, and, therefore, includes the entire spectrum of factors determining the three-dimensional estuarine circulation.

Past applications of ECOM to estuarine systems have generally used a σ-coordinate model with at least ten levels in the vertical. This type of vertical resolution has made it possible to effectively use the Mellor-Yamada turbulence closure sub-model. However, only four z-levels have been used in the present study and this vertical resolution is inadequate to apply the Mellor-Yamada sub-model.

Simulation of vertical diffusion was thus accomplished by using an empirical formula that is a function of the local Richardson number (Ri):

$$Ri = - \frac{g\frac{\partial \rho}{\partial z}}{\rho\left[\left(\frac{\partial u}{\partial z}\right)^2 + \left(\frac{\partial v}{\partial z}\right)^2\right]} \qquad (5\text{-}1)$$

where

R_i	=	Richardson number [unitless],
ρ	=	density [M/L^3]
u, v	=	horizontal current velocities [L/T]
g	=	acceleration due to gravity [L/T^2]

Several empirical turbulence formulas have been proposed and used in earlier hydrodynamic studies in lakes, reservoirs and coastal waters (e.g., Munk and Anderson, 1948). The relationships chosen for use in the Delaware River estuary was developed by Blumberg (1977);

$$K_H = k_1^2 z^2 \left(1 - \frac{z}{h}\right)^2 \left[\left(\frac{\partial U}{\partial z}\right)^2 + \left(\frac{\partial V}{\partial z}\right)^2\right]^{1/2} (1 - \frac{Ri}{Ri_c})^{1/2}, \qquad Ri < Ri_c$$

$$K_H = 0, \qquad Ri \geq Ri_c \qquad (5\text{-}2)$$

$$K_M = (1+Ri)\ K_H \qquad (5\text{-}3)$$

where

K_H	=	vertical eddy diffusivity [L^2/T]
K_M	=	vertical eddy viscosity [L^2/T]
Ri_c	=	10

h	=	total water depth [L]
z	=	local depth [L]
k_1	=	user-specified constant [unitless]

5.2 WATER QUALITY MODEL

5.2.1 Conservation of Mass

The water quality modeling framework used in this study and detailed in this report is based upon the principle of conservation of mass. The conservation of mass accounts for all of a material entering or leaving a body of water, transport of the material within the water body, and physical, chemical and biological transformations of the material. For an infinitesimal volume oriented along the axis of a three-dimensional coordinate system, a mathematical formulation of the conservation of mass may be written:

$$\frac{\partial c}{\partial t} = \underbrace{\frac{\partial}{\partial x}\left(E_x \frac{\partial c}{\partial x}\right) + \frac{\partial}{\partial y}\left(E_y \frac{\partial c}{\partial y}\right) + \frac{\partial}{\partial z}\left(E_z \frac{\partial c}{\partial z}\right)}_{\text{dispersive transport}} \underbrace{- U_x \frac{\partial c}{\partial x} - U_y \frac{\partial c}{\partial y} - U_z \frac{\partial c}{\partial z}}_{\text{advective transport}} \pm \underbrace{S(x, y, z, t)}_{\text{sources or sinks}} + \underbrace{W(x, y, z, t)}_{\text{external inputs}} \quad (5\text{-}4)$$

where

c	=	concentration of water quality variable [M/L^3]
t	=	time [T]
E	=	dispersion (mixing) coefficient due to tides and density and velocity gradients [L^2/T]
U	=	advective velocity [L/T]
S	=	sources and sinks of the water quality variable, representing kinetic interactions [M/L^3-T]
W	=	external inputs of the variable c [M/L^3-T]

x,y,z = longitudinal, lateral and vertical coordinates
M,L,T = units of mass, length and time respectively

The model framework used in this study is comprised of three components:

1) the transport due to advective freshwater flow and density-driven tidal currents and dispersion
2) the kinetics which control physical, chemical and biological reactions being modeled (sources and sinks)
3) the external inputs entering the system.

The transport within the Delaware River-Estuary System is a complex process affected by freshwater inflows, temperatures, wind and offshore forcing from the coastal shelf water via Delaware Bay. This transport is determined by the hydrodynamic model previously described. The hourly average fluxes from this hydrodynamic model were used to drive the transport field for the water quality model.

The kinetics represent the rates of reaction among water quality variables and approximate the physical, chemical and biological processes occurring in the Delaware River-Estuary. This kinetic modeling framework has been used with great success on a number of estuaries (Long Island Sound, Boston Harbor) and is very similar to EUTRO-WASP modeling code supported by the US EPA. The kinetic framework of the water quality model is presented in Figure 5-1 and will be discussed in greater detail below.

External inputs of carbonaceous biochemical oxygen demand (CBOD), nutrients (nitrogen and phosphorus) and other model variables are primarily due to municipal and industrial discharges and model boundary conditions.

The modeling framework used in this study utilizes the 15 state-variables shown below:

1 - Salinity (SAL)
2 - Total Suspended Solids (TSS)
3 - Phytoplankton (PHYT)

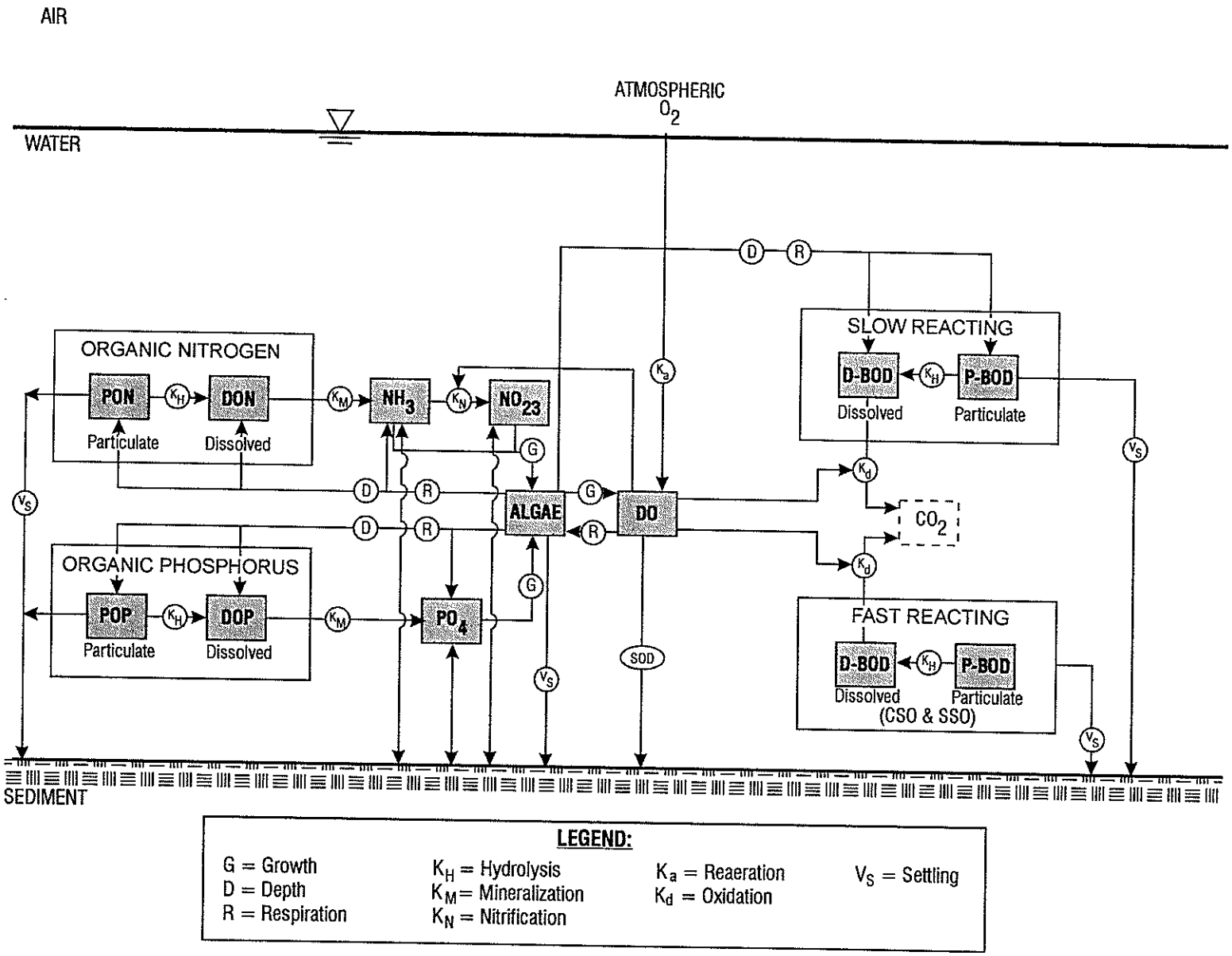

Figure 5-1. Delaware River Water Quality Model Kinetic Framework.

4 - Particulate Organic Phosphorus (POP)
5 - Dissolved Organic Phosphorus (DOP)
6 - Dissolved Inorganic Phosphorus (PO4)
7 - Dissolved Organic Nitrogen (PON)
8 - Particulate Organic Nitrogen (DON)
9 - Ammonia Nitrogen (NH3)
10 - Nitrite + Nitrate (NO23)
11 - Particulate Carbonaceous Biochemical Oxygen Demand - Slow Reacting (PBODS)
12 - Dissolved Carbonaceous Biochemical Oxygen Demand - Slow Reacting (DBODS)
13 - Particulate Carbonaceous Biochemical Oxygen Demand - Fast Reacting (PBODF)
14 - Dissolved Carbonaceous Biochemical Oxygen Demand - Fast Reacting (DBODF)
15 - Dissolved Oxygen (DO)

The state variables described above were picked based on a balance between the importance of the variable in the processes being modeled and the existence of adequate field data for calibration/verification. Adequate data exists either directly or indirectly for all the state variables listed above with the notable exception of BOD. Since BOD values in the Delaware River-Estuary have been historically low, BOD measurements are not part of the Delaware River Basin Commission's (DRBC) monitoring program.

5.3 EUTROPHICATION KINETICS

5.3.1 General Structure

Salinity is included in the water quality modeling framework to verify the proper coupling of the hydrodynamic model to the water quality model. If the water quality model is able to reproduce the salinity fields as computed by the hydrodynamic model, the water quality model is correctly reading the transport field generated by the hydrodynamic model.

Phytoplankton kinetics incorporate almost all the principal processes of the overall eutrophication kinetics. The phytoplankton system interacts with all the other systems modeled with the exception of salinity and TSS. Phytoplankton take up nitrogen and phosphorus for growth and release nitrogen and phosphorus during respiration and death. Phytoplankton also directly affect the dissolved oxygen concentrations through the consumption (respiration) and

production (photosynthesis) of oxygen and indirectly, upon death, by becoming part of the BOD pool.

In the phosphorus kinetics, orthophosphorus is taken up by phytoplankton during growth and incorporated into the phytoplankton biomass. Through endogenous respiration and predatory grazing, phytoplankton phosphorus is converted back to dissolved and particulate organic phosphorus and orthophosphorus. Organic phosphorus can then be converted to orthophosphorus through hydrolysis and mineralization.

The kinetics of nitrogen are fundamentally the same as the phosphorus kinetics. Ammonia and nitrate are taken up by phytoplankton during growth. Ammonia is the preferred form of inorganic nitrogen for algal growth, but phytoplankton can also utilize nitrate-nitrogen as ammonia concentrations become depleted. Through endogenous respiration and predatory grazing, phytoplankton nitrogen is converted to organic nitrogen following pathways similar to those of phosphorus. Organic nitrogen is converted to ammonia through hydrolysis and mineralization. Ammonia is then converted to nitrate through nitrification at a temperature and oxygen-dependent rate. Nitrate may then be converted to nitrogen gas through denitrification in the absence of oxygen at a temperature-dependent rate.

The CBOD kinetics are divided into two main pools: slow reacting CBOD and fast reacting CBOD. The slow reacting pool represents CBOD from well treated effluent and the fast reacting pool represents CBOD from untreated sources such as combined sewer overflows (CSOs) and sanitary sewer overflows (SSOs). Since the slow reacting CBOD is highly treated, this CBOD is more refractory and will have lower oxidation rates than the fast reacting CBOD which is more labile. In both pools, CBOD can exist in either particulate or dissolved form with the particulate being converted to the dissolved form through hydrolysis. This dissolved form of CBOD can then be oxidized by bacteria utilizing dissolved oxygen.

Dissolved oxygen is coupled to the other state variables. The sources of oxygen considered are reaeration and algal photosynthesis. The sinks of oxygen are algal respiration, oxidation of dissolved CBOD, nitrification of ammonia and sediment oxygen demand (SOD).

5.3.2 Phytoplankton

Since this model is calibrated to summer conditions, only one functional phytoplankton group is represented. This algal group represents a mixed population of phytoplankton, including greens, blue-greens, dinoflagellates and some diatoms. The specific growth rate (S_P) for this algal group is first set equal to the maximum growth rate (G_{Pmax}) which occurs at optimum temperature, light, nutrient concentrations and salinity. In order to account for sub-optimum natural conditions, this maximum growth rate is modified by growth reduction factors for temperature, light, available nutrients and salinity, as shown in Equation 5-5:

$$S_P = G_{Pmax}(T_{opt}) \cdot G_T(T) \cdot G_I(I) \cdot G_N(N) \cdot G_S(S) \qquad (5\text{-}5)$$

where

S_P	=	specific growth rate, ([1/T])
G_{Pmax}	=	growth rate at optimal temperature, light, nutrients, and salinity, ([1/T])
$G_T(T)$	=	a factor to adjust G_{Pmax} to ambient temperature
T	=	temperature
$G_I(I)$	=	a factor to account for limited light
I	=	solar radiation (light)
$G_N(N)$	=	a factor to account for limited nutrients
N	=	nutrient concentrations (nitrogen or phosphorus)
$G_S(S)$	=	a factor to account for the inhibition of growth by salinity
S	=	salinity

Initial estimates of G_{Pmax} were based upon previous estuarine modeling studies and were subsequently refined during the calibration process. The selected maximum growth rate was then temperature-corrected using spatially dependent, ambient water column temperature values. The temperature-corrected growth rate is computed using the following equation, which relates $G_T(T)$, the temperature growth reduction factor at ambient temperature, T, to the optimal temperature, T_{opt}:

$$G_T(T) = e^{-\beta_1(T-T_{opt})^2} \qquad T \le T_{opt} \qquad (5\text{-}6)$$

$$G_T(T) = e^{-\beta_2 (T_{opt}-T)^2} \qquad T>T_{opt} \qquad (5\text{-}7)$$

and where β_1 is a coefficient representing the effect of temperature on growth when the ambient temperature is at or below T_{opt} and β_2 is a coefficient representing the effect of temperature on growth when the ambient temperature is above T_{opt}.

Next the temperature-corrected growth rate is then adjusted to reflect attenuation due to ambient light. Under natural conditions, phytoplankton are not uniformly exposed to optimum light intensities. At the water surface and near-surface, photoinhibition can occur due to high light intensities. And at depths below the euphotic zone, light is not available for photosynthesis due to natural (solids) and algal related turbidity. The depth-averaged light attenuated growth rate factor, $G_I(I)$, is presented in Equation 5-8. Equation 5-8 extends from a light curve analysis formulated by Steele (1962), and accounts for both the effects of supersaturating light intensities and light attenuation through the water column. $G_I(I)$ is obtained by integrating the light factor over depth:

$$G_I(I) = \frac{e}{k_e H}\left[\exp\left(\frac{-I_o(t)}{I_s}\, e^{-k_e H}\right) - \exp\left(\frac{-I_o(t)}{I_s}\right)\right] \qquad (5\text{-}8)$$

where

e	=	2.718
H	=	the total water column depth (m), [L]
k_e	=	$k_{ebase} + k_c \bullet P_{chl\text{-}a}$; the total extinction coefficient, computed from the sum of the base, non-algal related, light attenuation, k_{ebase}, and the self-shading attenuation due to the ambient phytoplankton population $k_c P_{chl\text{-}a}$ (m^{-1}), [1/L]
k_c	=	the algal related extinction coefficient per unit of chlorophyll (m^2/mg chl-a), [L^2/M]
$P_{chl\text{-}a}$	=	the ambient phytoplankton population as chlorophyll (mg chl-a/l), [M/L^3], where $P_{chl\text{-}a} = P_c/a_{cchl}$
P_c	=	the ambient phytoplankton population as carbon (mg, (C/l), [M/L^3]

a_{cchl} = the ratio of algal carbon to algal chlorophyll (mg C/mg chl-a), [M/L^3]
I_o = the incident light intensity at the segment surface (ly/day), [E/T]
I_s = the saturating light intensity (ly/day), [E/T]

The value of I_o at the water surface, I_{surf}, may be evaluated at any time within the day, t, using the following formula:

$$I_{surf}(t) = \frac{I_{tot}}{0.635\ f} \sin\left[\frac{\pi\ (t_d - t_{sunrise})}{f}\right] \qquad (5\text{-}9)$$

where

I_{tot} = total daily incident solar radiation, [E]
f = fraction of daylight (daylight hours/24),
t_d = time of day
$t_{sunrise}$ = time or sunrise

To account for the effect of variations of available light as a function of depth, the light intensity, I_o (H), at any depth, H, is related to the incident surface intensity, I_{surf}, via the extinction coefficient, k_e through the formula

$$I_o(H) = I_{surf}\ \exp^{-k_e H} \qquad (5\text{-}10)$$

The effects of various nutrient concentrations on the growth of phytoplankton are quite complex. As a first approximation to the effect of nutrient concentrations on the growth rate, it is assumed that the phytoplankton population follows Monod growth kinetics with respect to nitrogen and phosphorus. Monod growth kinetics predict that at adequate nutrient concentrations, the growth rate will proceed at the maximum rate allowed for the ambient temperature and light conditions. However, at low nutrient concentrations, the growth rate becomes linearly proportional to the nutrient concentration. Thus, for a nutrient concentration N, the factor, for which the saturated growth rate is reduced, is $N/(K_m + N)$. The constant, K_m, which is called the

Michaelis or half-saturation constant, is the nutrient concentration at which the growth rate is half the saturated growth rate. Since there are two nutrients, nitrogen and phosphorus, considered in this framework, the Michaelis-Menton expression is evaluated for each nutrient and the minimum value is chosen to reduce the saturated growth rate,

$$G_N(N) = \text{Min}\left(\frac{DIN}{K_{mN} + DIN}, \frac{DIP}{K_{mP} + DIP}\right) \qquad (5\text{-}11)$$

where

DIN = dissolved inorganic nitrogen (mg N/l), [M/L^3]
DIP = dissolved inorganic phosphorus (mg P/l), [M/L^3]
K_{mN} = half saturation constant for nitrogen (mg N/l), [M/L^3]
K_{mP} = half saturation constant for phosphorus (mg P/l), [M/L^3]

The effect of salinity is determined with the following empirical equation

$$G_s(S) = \frac{0.5}{0.5 + S - 0.1} \qquad (5\text{-}12)$$

where

S = salinity (ppt), [M/L^3]

This term accounts for the adverse effect of salinity on phytoplankton from freshwater sections of the river being transported downstream into more saline waters. The value of 0.1 represents the background salinity in freshwater. The terms in this equation were adjust based on the fit of the model to the phytoplankton data.

Three terms have been included in the modeling framework to account for the loss of phytoplankton biomass: endogenous respiration, sinking or settling from the water column and grazing. The endogenous respiration rate is the rate at which phytoplankton oxidize their organic

carbon to carbon dioxide per unit weight of phytoplankton organic carbon. Respiration is the reverse of the photosynthesis process and contributes to the reduction of the phytoplankton biomass. If the respiration rate of the phytoplankton as a whole is greater than the growth rate, there is a net loss of phytoplankton carbon or biomass.

The endogenous respiration rate equals as a base rate plus a percentage of the specific growth rate (Laws and Bannister, 1980), described below:

$$k_{pr} = 0.04 + 0.38\ S_p \qquad (5\text{-}13)$$

k_{pr} = endogenous respiration rate (1/day), [1/T]
S_P = specific growth rate, (1/day), [1/T]

The base rate of 0.04 represents the energy requirements associated with basic algae cell maintenance necessary for survival. The 38% of growth represents the overhead energy requirement associated with algae cell growth and reproduction.

The sinking of phytoplankton can also be an important contribution to the overall mortality of the phytoplankton population. Algal settling in natural waters is a complex phenomenon, affected by vertical turbulence, density gradients and the physiological state of the different species of phytoplankton. An important factor determining the physiological state of algae is nutrient availability. Although the net effective settling rate under nutrient stressed conditions is greatly reduced in relatively shallow, well-mixed regions of an estuary, sinking can still contribute to the overall mortality of the algal population. For this reason, a term representing phytoplankton settling has been included in the algal mortality expression and is determined by:

$$k_{sP}(T) = \left[\frac{V_{sPb}}{H} + \frac{V_{sPn}}{H} \cdot (1 - G_N(N))\right] \cdot \theta_{sP}^{T-20} \qquad (5\text{-}14)$$

where

$k_{sP}(T)$ = net effective algal loss rate due to settling (1/day), [1/T]

V_{sPb} = base settling velocity of phytoplankton (m/day), [L/T]
V_{sPn} = nutrient dependent settling rate (m/day), [L/T]
$G_N(N)$ = growth reduction factor caused by nutrient limitation
H = depth of the model segment (m), [L]
θ_{sP} = temperature correction factor for algal settling

Grazing is also an important loss rate for phytoplankton depending upon the time of the year and the biomass levels of the grazers. Because the life cycles of grazers such as zooplankton and bivalves are quite complex, they were not included in the model as state variables. Rather, a simple first order loss rate representing the effect of grazing on algal biomass is included. The loss rate due to grazing is temperature corrected:

$$k_{grz}(T) = k_{grz}(20°C) \cdot \theta_{grz}^{T-20} \qquad (5\text{-}15)$$

where

$k_{grz}(T)$ = the temperature corrected loss rate due to grazing (1/day), [1/T]
$k_{grz}(20°C)$ = the loss rate at 20°C (1/day), [1/T]
θ_{grz} = the temperature correction factor for grazing

5.3.3 Algal Stoichiometry and Nutrient Uptake Kinetics

A principal component in the nutrient mass balance equations is the nutrient uptake kinetics associated with algal growth. In order to quantify this nutrient uptake, algal stoichiometry must be specified in units of nutrient uptake per mass of population synthesized. Using carbon as the unit of algal biomass, the relevant ratios are the mass of nitrogen and phosphorus per unit mass of carbon. The Delaware River-Estuary was assumed to follow Redfield stoichiometry with a ratio of approximately 106 Carbon: 16 Nitrogen: 1 Phosphorus (atomic). Since nutrient saturated conditions generally exist in the Delaware River-Estuary, a more complicated variable stoichiometry was unnecessary.

Based on the stoichiometric ratio described above, the nutrient mass balance equations may be written in much the same way as for the phytoplankton biomass. The principal processes determining the distribution of nutrients among the various pools are:

1) the uptake of inorganic nutrients by phytoplankton for cell growth
2) the release of inorganic and organic nutrients due to algal respiration and predation
3) the recycling of organic nutrients to inorganic forms via bacterial hydrolysis and mineralization

Rather than attempt to model bacterial recycling of organic nutrients by including a bacterial system (for which there is little or no data for calibration), a phytoplankton-dependent saturated recycle formulation was used. The bacterial biomass, and hence the recycling rate, is assumed to be proportional to the phytoplankton biomass. A number of field and laboratory studies (Hendry, 1977; Lowe, 1976, Menton et all., 1972; Jewell and McCarty, 1971) support this hypothesis. The saturated recycling relationship may be written

$$k(T) = k'(20°C)\theta^{T-20} \cdot \frac{P_c}{K_{mP_c} + P_c} \qquad (5\text{-}16)$$

where

$k(T)$	=	the temperature corrected recycling rate, [1/T]
$k'(20°C)$	=	the saturated recycling rate at 20°C, [1/T]
K_{mPc}	=	the phytoplankton half-saturation constant for recycling, [M/L^3]
θ	=	the temperature correction coefficient
P_c	=	phytoplankton (mg C/l), [M/L^3]

This mechanism employs a quasi-first-order recycle that slows the recycling rate if the algal population is small, yet does not permit the recycling rate to increase in an unlimited fashion as phytoplankton biomass increases. Instead the mechanism permits zero-order recycling when the phytoplankton greatly exceed the half-saturation constant. The latter assumes that at higher population levels, other factors are limiting recycling rates.

5.3.4 Phosphorus

The model framework includes three forms of phosphorus: dissolved organic (DOP), particulate organic (POP) and dissolved inorganic phosphorus, (PO_4). Inorganic phosphorus is taken up by phytoplankton during growth and is returned to the various organic and inorganic forms via algal respiration and death. A fraction of the phosphorus released during respiration and death is in the inorganic form and is readily available for uptake by other viable algal cells. The remaining fraction released is in the dissolved and particulate organic forms. This particulate organic phosphorus can be hydrolyzed into dissolved organic phosphorus which then must undergo a bacterial decomposition (mineralization) into inorganic phosphorus before it can be used by phytoplankton again.

5.3.5 Nitrogen

The kinetic structure for nitrogen is similar to that of the phosphorus system. During algal respiration and death, a fraction of the cellular nitrogen is returned to the inorganic pool in the form of ammonia (NH_3). The remaining fraction is recycled to the dissolved (DON) and particulate organic nitrogen (PON) pools. The PON is hydrolyzed into DON. Dissolved organic nitrogen undergoes a bacterial decomposition (mineralization), to ammonia. Ammonia, in the presence of nitrifying bacteria and oxygen, can then be converted to nitrite (NO_2) and subsequently nitrate (NO_3) (nitrification). Both ammonia and nitrate are available for uptake and use in cell growth by phytoplankton; however, for physiological reasons, the preferred form is ammonia. The ammonia preference term takes the following form:

$$\alpha_{NH_3} = NH_3 \cdot \frac{NO_2 + NO_3}{(K_{mN}+NH_3)\,(K_{mN}+NO_2+NO_3)} + NH_3 \cdot \frac{K_{mN}}{(NH_3+NO_2+NO_3)\,(K_{mN}+NO_2+NO_3)} \quad (5\text{-}17)$$

The behavior of this equation, for a Michaelis value, K_{mN}, of 10 ugN/l, is illustrated on Figure 5-2. The behavior of Equation 5-17 is most sensitive at low values of ammonia or nitrate. For a given concentration of ammonia, as the available nitrate increases above approximately the Michaelis limitation, the preference for ammonia reaches a plateau. Also, as the concentration of available ammonia increases, the plateau occurs at values closer to unity, that is, total preference for ammonia.

The process of nitrification in natural waters is carried out by aerobic autotrophs, *Nitrosomonas* and *Nitrobacter*, in particular. Nitrification takes place in two steps with *Nitrosomonas* bacteria responsible for the conversion of ammonia to nitrite and *Nitrobacter* subsequently converting nitrite to nitrate. Essential to this reaction process is aerobic conditions. In order to reduce the number of state variables required in the modeling framework, nitrite and nitrate were incorporated together into a single state variable (nitrite+nitrate, NO_{23}). The process of nitrification, therefore, is assumed to be approximated by a first-order reaction rate that is a function of the water column dissolved oxygen concentration and ambient temperature.

Denitrification refers to the reduction of nitrate (or nitrite) to nitrogen gas (N_2) and other gaseous products such as nitrous oxide (N_2O) and nitrogen oxide (NO). This process is carried out by a large number of heterotrophic, facultative anaerobes. Under normal aerobic conditions in the water column, these organisms utilize oxygen to oxidize organic material. Under anaerobic conditions, however, these organisms are able to use nitrate as the electron acceptor. The process of denitrification is included in the modeling framework simply as a sink of nitrate. Denitrification typically occurs in anaerobic sediment. In the water column, however, denitrification should only occur under extremely low dissolved oxygen conditions. This is accomplished computationally by modifying the linear first-order denitrification rate by the expression $K_{no3}/(K_{no3} + DO)$. This expression is similar to the Michaelis-Menton expression controlling the nutrient growth reduction factor. For concentrations of dissolved oxygen greater than 1 mg/L, the expression reduces denitrification to near zero. For dissolved oxygen levels less than 0.1 mg/L, this expression permits denitrification to occur.

5.3.6 Dissolved Oxygen

The photosynthetic carbon fixation by phytoplankton produces dissolved oxygen as a byproduct. The rate of this oxygen production and associated nutrient uptake is proportional to

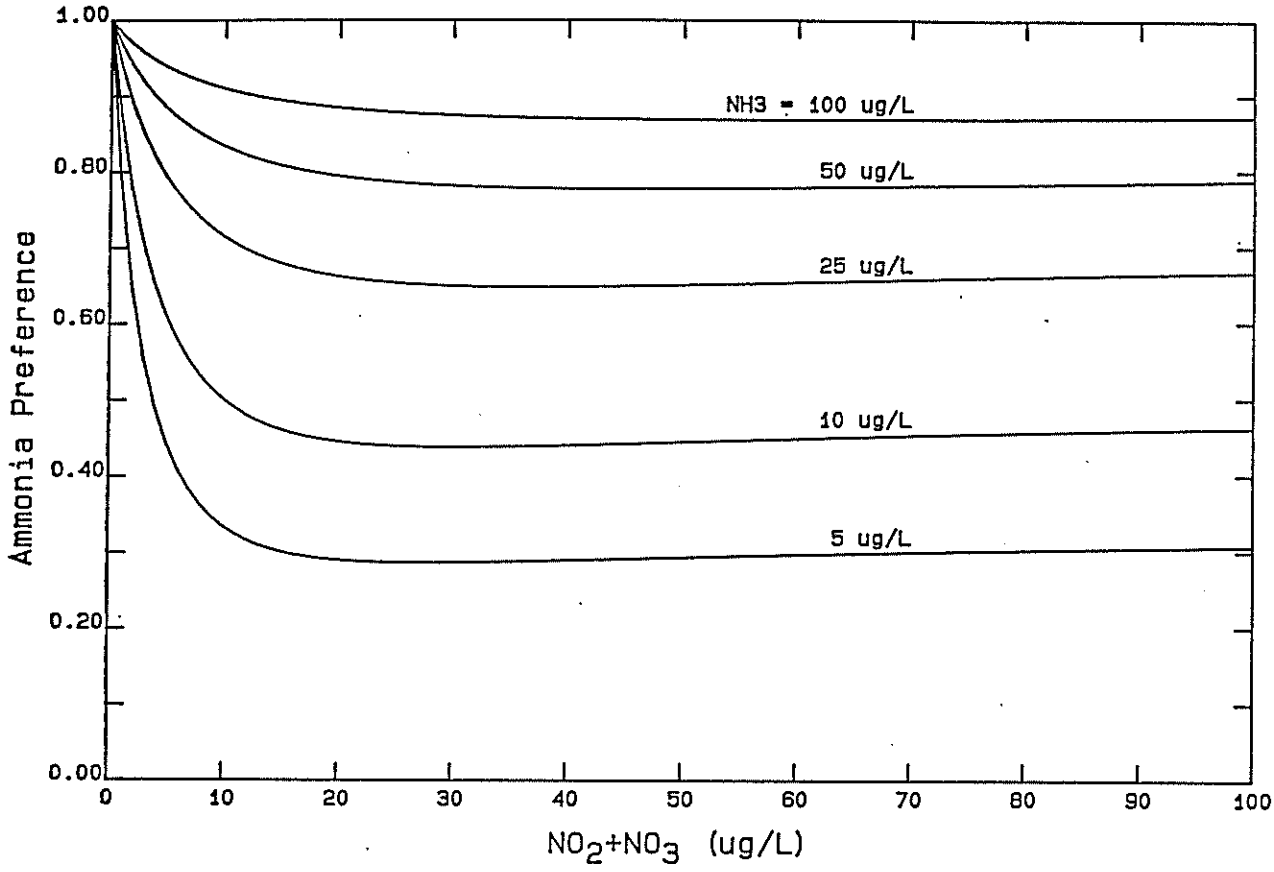

Figure 5-2 Behavior of the Ammonia Preference Structure for Various Concentrations of NH3 and NO2 + NO3.

the phytoplankton growth rate. Typically phytoplankton use ammonia as the primary source of nitrogen. However, if ammonia is not available, the phytoplankton will utilize the available nitrate as described in Section 5.3.5. In the process of fixing nitrogen from nitrate, phytoplankton produce an additional source of oxygen. This additional oxygen source can be seen by comparing equations 5-18 and 5-19 (Morel 1983).

Ammonia as a nitrogen source

$$106\ CO_2 + 16NH_4^+ + H_2PO_4^- + 106H_2O$$

$$\Rightarrow \text{Protoplasm} + 106\ O_2 + 15H^+ \qquad (5\text{-}18)$$

Nitrate as a nitrogen source

$$106\ CO_2 + 16\ NO_3^- + H_2PO_4^- + 122\ H_2O + 17\ H^+$$

$$\Rightarrow \text{Protoplasm} + 138\ O_2 \qquad (5\text{-}19)$$

The above equations present the stoichiometric description of the photosynthetic process assuming ammonia (Equation 5-18) or nitrate (Equation 5-19) as the nitrogen source and assuming algal biomass to have Redfield stoichiometry:

$$\text{Biomass} = C_{106}\ H_{263}\ O_{110}\ N_{16}\ P_1 \qquad (5\text{-}20)$$

Oxygen-deficient or under-saturated waters are replenished via atmospheric reaeration. The reaeration coefficient, k_a, is a function of the average tidal velocity, wind and temperature, and is computed using Equations 5-21 and 5-22

$$k_a\ (20°C) = k_L/H \qquad (5\text{-}21)$$

$$k_a(T) = k_a(20°C)\theta_a^{T-20} \quad (5\text{-}22)$$

where

k_a = reaeration rate (1/day), [1/T]
k_L = the surface mass transfer coefficient (m/day), [L/T]
H = depth (m), [L]
θ_a = temperature coefficient

Dissolved oxygen saturation is a function of both temperature and salinity and is determined via Equation 5-23 (Hyer et al., 1971):

$$DO_{sat} = 14.6244 - 0.367134T + 0.0044972T^2 - 0.0966S$$
$$+ 0.00205ST + 0.0002739S^2 \quad (5\text{-}23)$$

where S is salinity in ppt and T is temperature in °C.

Dissolved oxygen is lost from the water column as a result of algal respiration, nitrification of ammonia, the oxidation of carbonaceous material as BOD (including detrital phytoplankton), and sediment oxygen demand (SOD). Algal respiration and nitrification have been described in preceding sections. The oxidation of carbonaceous material as BOD will be described in the next section. Finally, a spatially varying SOD is assigned as a flux rate in g/m2•d.

5.3.7 Carbonaceous Biochemical Oxygen Demand

Four carbonaceous biochemical oxygen demand (CBOD) state variables are modeled: slow reacting dissolved CBOD (DBODS), slow reacting particulate CBOD (PBODS), fast reacting dissolved CBOD (DBODF), and fast reacting particulate CBOD (PBODF). The principal sources of slow reacting CBOD are wastewater treatment plants and dead algal biomass from grazing. The fast reacting CBOD represents CBOD inputs from combined sewer overflows (CSOs) and

Sanitary Sewer Overflows (SSOs). This CBOD material is relatively untreated and is, therefore, more labile than the treated CBOD inputs.

For both the slow and fast reacting CBOD pools, the particulate form is converted to dissolved form through a temperature dependent hydrolysis process. Only the dissolved form can be oxidized. The rate of oxidation is dependent on both temperature and the concentration of dissolved oxygen through a Michaelis-Menten expression as described in the following equations:

$$\text{Oxidized CBOD} = K_d\, \theta_{kd}^{T-20} * \text{CBOD} * \frac{DO}{K_{DO} + DO} \qquad (5\text{-}24)$$

where

K_d = CBOD oxidation rate (1/day), [1/T]
CBOD = CBOD concentration (mg/l), [M/L^3]
DO = DO concentration (mg/l), [M/L^3]
K_{DO} = half saturation constant (mg/l), [M/L^3]
θ_{kd} = temperature coefficient

SECTION 6

HYDRODYNAMIC MODEL CALIBRATION AND VALIDATION

This section describes the development, calibration and validation of the Delaware River hydrodynamic model. The following sub-section presents the model grid and associated bathymetry that were used to represent the geometry of this estuarine system. A discussion of the forcing functions, e.g., freshwater flows and tidal boundary conditions, used as input to the model is then presented in the next sub-section. The last three sub-sections present calibration and validation results for periods in 1984, 1991 and 1995.

Mean annual flow rates of the Delaware River at Trenton varied considerably between the calibration and validation periods. The average summer (June - September) flow rates at Trenton were 11,000, 3,500 and 4,100 cfs in 1984, 1991 and 1995, respectively. These flow rates can be compared to the long term (1912 to 1995) average flow rate of 7,000 cfs, see Figure 6-1.

6.1 MODEL GEOMETRY AND BATHYMETRY

The portion of the Delaware River estuary being modeled in this study extends from Trenton at the upstream limit to Liston Point at the downstream limit. The model grid has 84 longitudinal elements and five lateral elements in the Delaware River from the Philadelphia region to Liston Point (Figure 6-2). The Delaware River has one or three lateral segments in the reaches that are upstream of Philadelphia. The numerical grid for the approximately 80-mile reach of the Delaware River being modeled also includes the Schuylkill River up to the Fairmount Dam and the Chesapeake and Delaware (C & D) Canal extending to Chesapeake City on its western end. Due to computational restraints, relatively coarse grid resolutional was used in these areas, with the Schuylkill River and C & D Canal both assumed to be laterally-averaged, i.e., only one lateral segment. Longitudinally, the Schuylkill River and C & D Canal were discretized using 4 and 5 segments, respectively.

Bathymetric data were provided by the National Ocean Service (NOS). The NOS Hydrographic Data Base contains over 118,000 digitized depth soundings throughout the study area, including the Schuylkill River. Each horizontal grid element was assigned a depth by averaging the soundings that were located within that element. The grid resolves the shipping

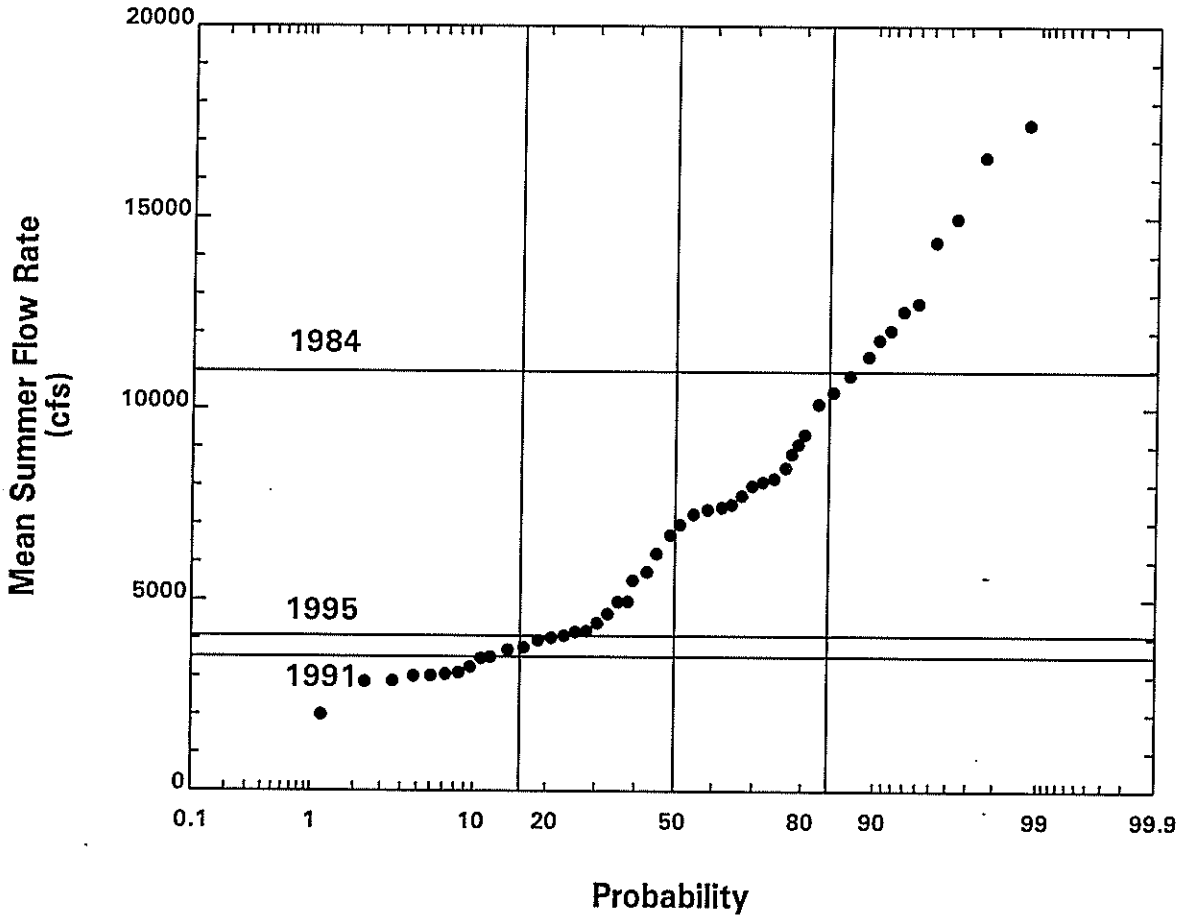

Figure 6-1. Comparison of Mean Annual Flow Rates of the Delaware River at Trenton in 1984, 1991 and 1995 to Distribution of Annual Flows for the Periods 1912 to 1995.

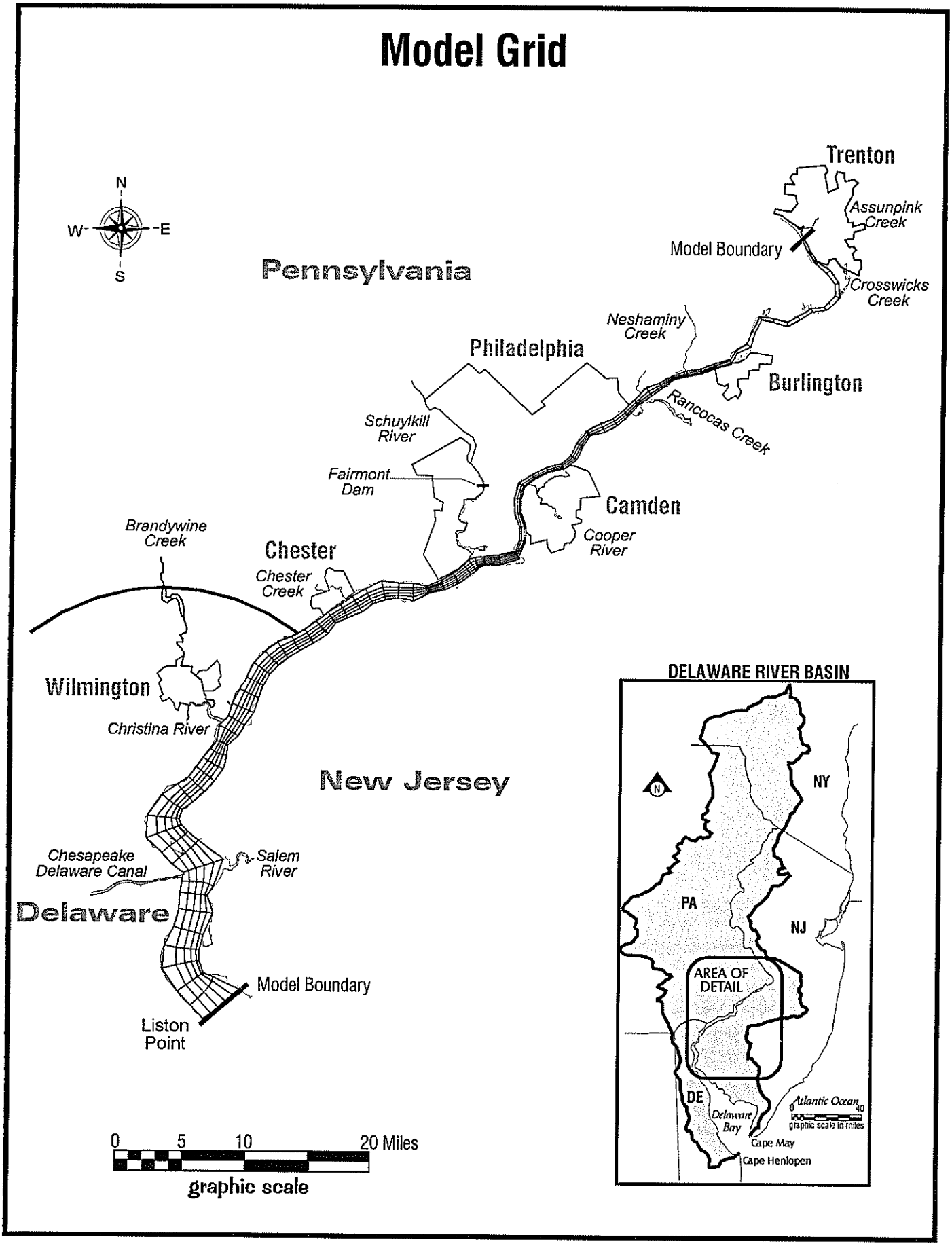

Figure 6-2. Model Grid of the Delaware River from the Philadelphia Region to Liston Point.

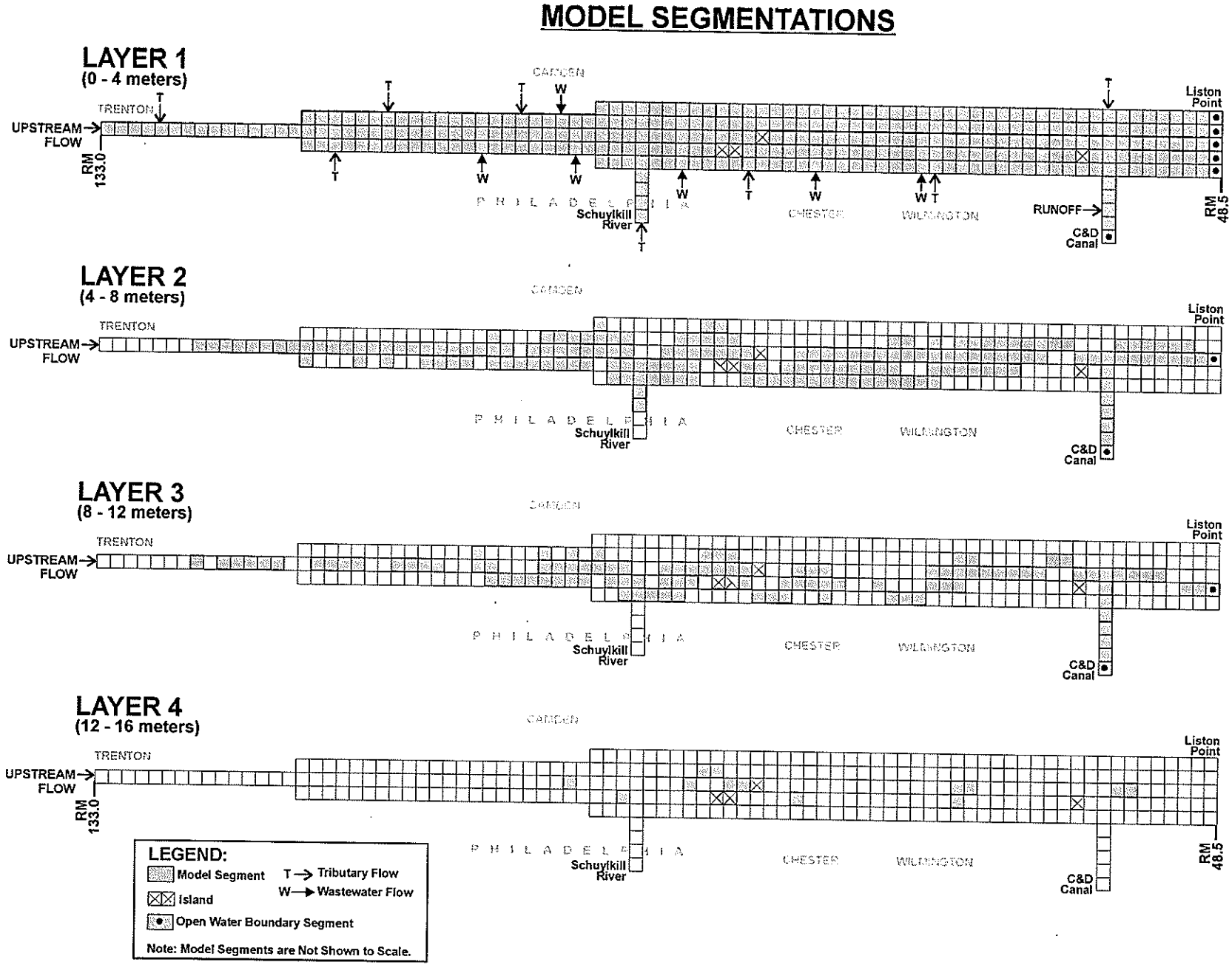

Figure 6-3. Model Grid and Z-Level Layer Segmentation.

channel in the Delaware River and contains depths varying between 1 and 16 meters (3 to 52 ft) throughout the river. The water column was discretized using four z-levels and each layer was 4 m (13 ft) thick.

The model layer segmentation is presented in Figure 6-3 and shows the model segments for each layer of the model. The fresh water input from tributaries (T) and significant wastewater flows (W) are indicated. Open water boundary segments across which tidal exchange takes place are also shown. Please note, the model layer segmentation presented in Figure 6-3 is a schematic and model segments are not drawn to actual dimensions.

6.2 MODEL FORCING DATA

The hydrodynamics of the study area are primarily driven by tides and salinity at the downstream boundaries and freshwater inputs from the Delaware River and other tributaries. The effects of surface heat flux on circulation in this portion of the estuary has not been included because it has been assumed that this forcing function is of second-order importance. Although wind is included as a forcing function, sensitivity runs showed that wind effects had negligible impact on the predicted circulation.

Freshwater flows into the estuary from the Delaware River and various tributaries between Trenton and Liston Point. Flow rates at Trenton are measured at U.S. Geological Survey (USGS) gaging station. The drainage area of the Delaware River at this upstream location is 6,780 mi^2. At Liston Point, the total drainage area is approximately 11,380 mi^2, an increase of ~ 4,600 mi^2. The freshwater flow from nine tributaries between Trenton and Liston Point was determined from USGS flow data that represents ~ 3,900 mi^2, see Table 6-1. Flow from the ungaged drainage area, which represents 6 percent (~ 700 mi^2) of the total drainage area, was estimated by using drainage area proration to increase the effective drainage area of the tributaries (DiLorenzo et al., 1993). Note that Red Clay Creek was used as a surrogate for freshwater runoff flow to the C & D Canal.

Temporal plots of flow rates in the Delaware River at Trenton during the 1984, 1991 and 1995 simulation periods are presented on Figure 6-4. Time histories of freshwater input from the various tributaries to the estuary are shown on Figures 6-5 and 6-7. Another source of freshwater to the system that has been included in the hydrodynamic and water quality model simulations is

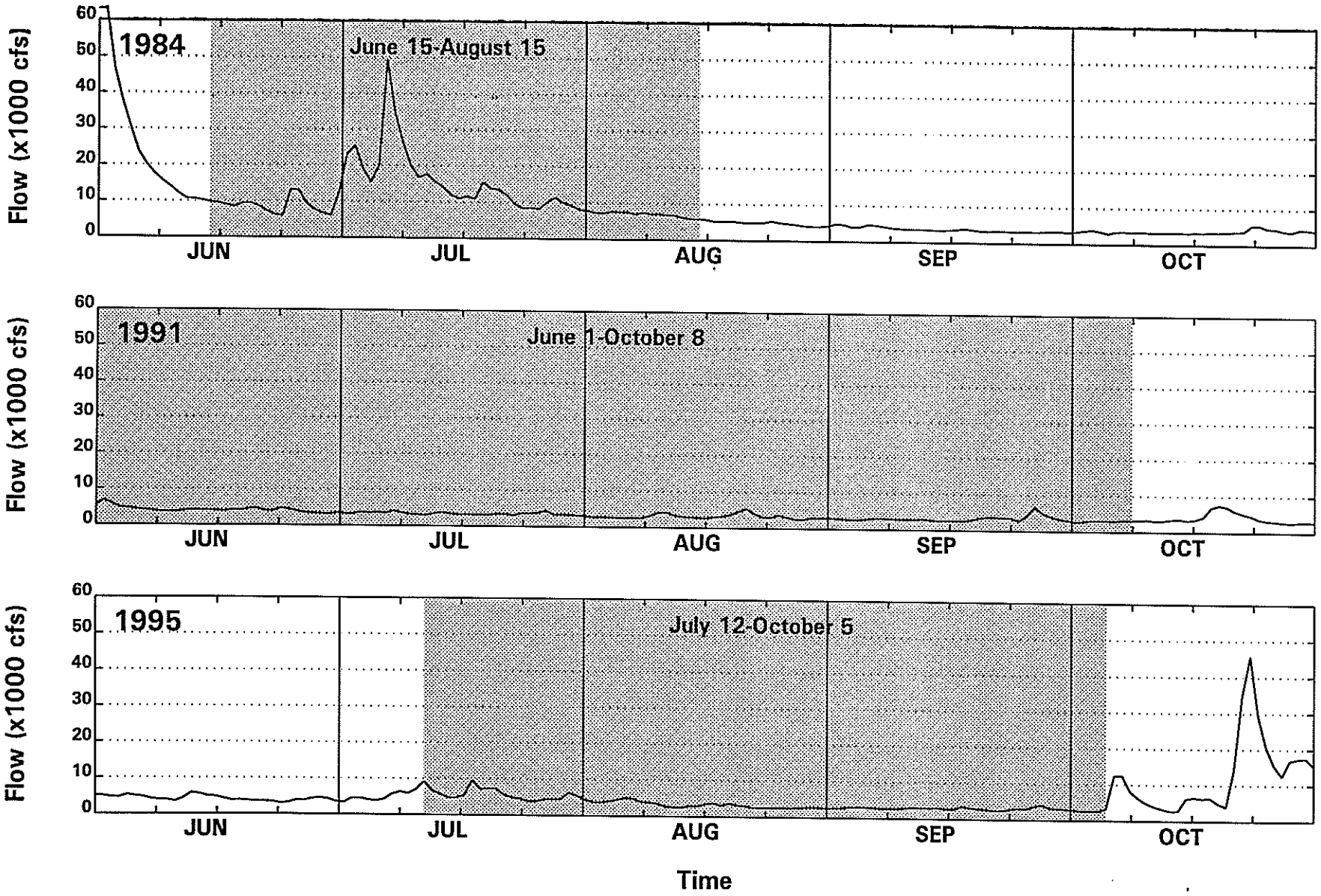

Figure 6-4. Daily Average Flow Rates of the Delaware River at Trenton for June Through October in 1984, 1991 and 1995.

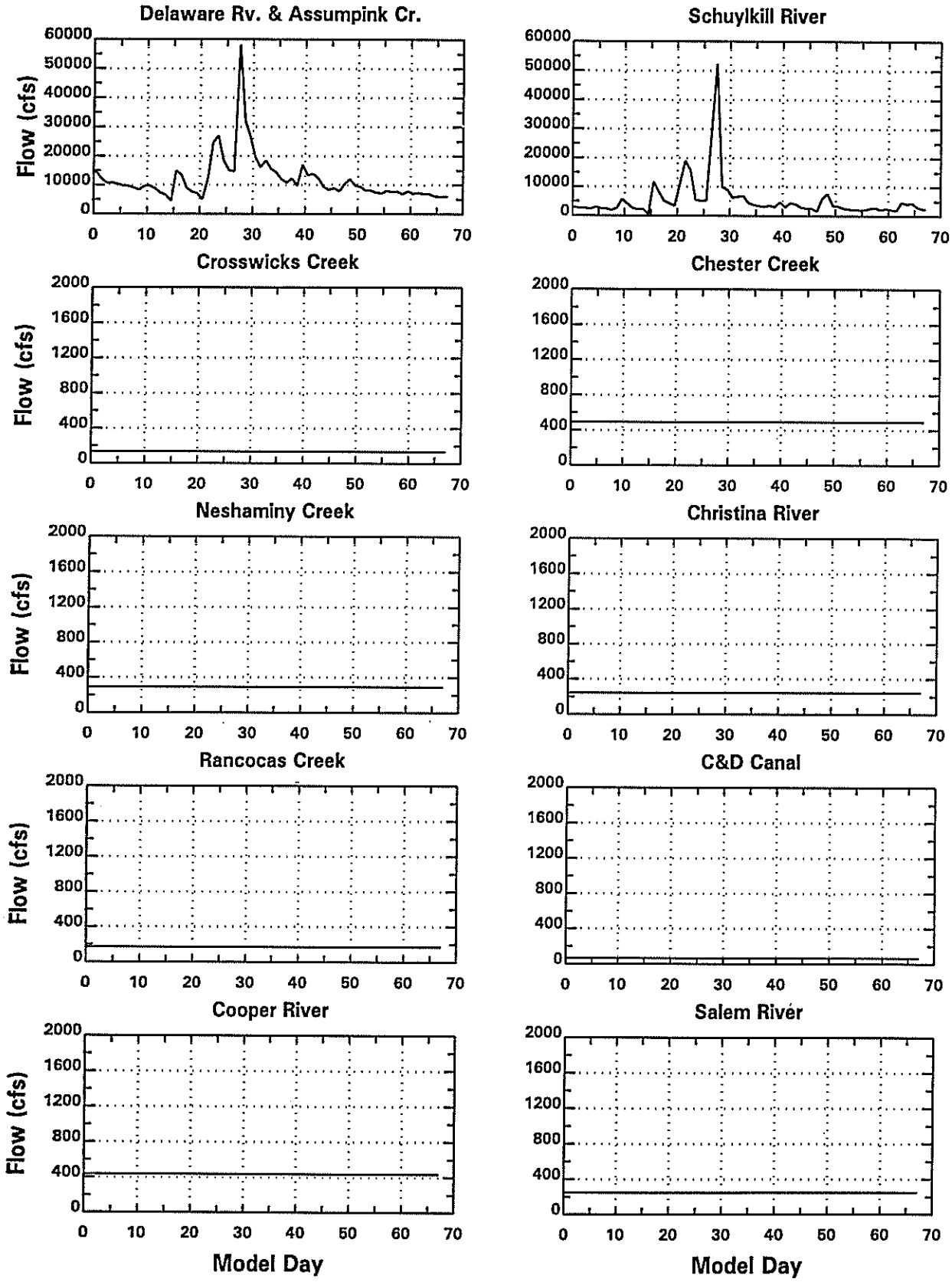

Figure 6-5. Tributary Flow Rates During 1984 Calibration Period.

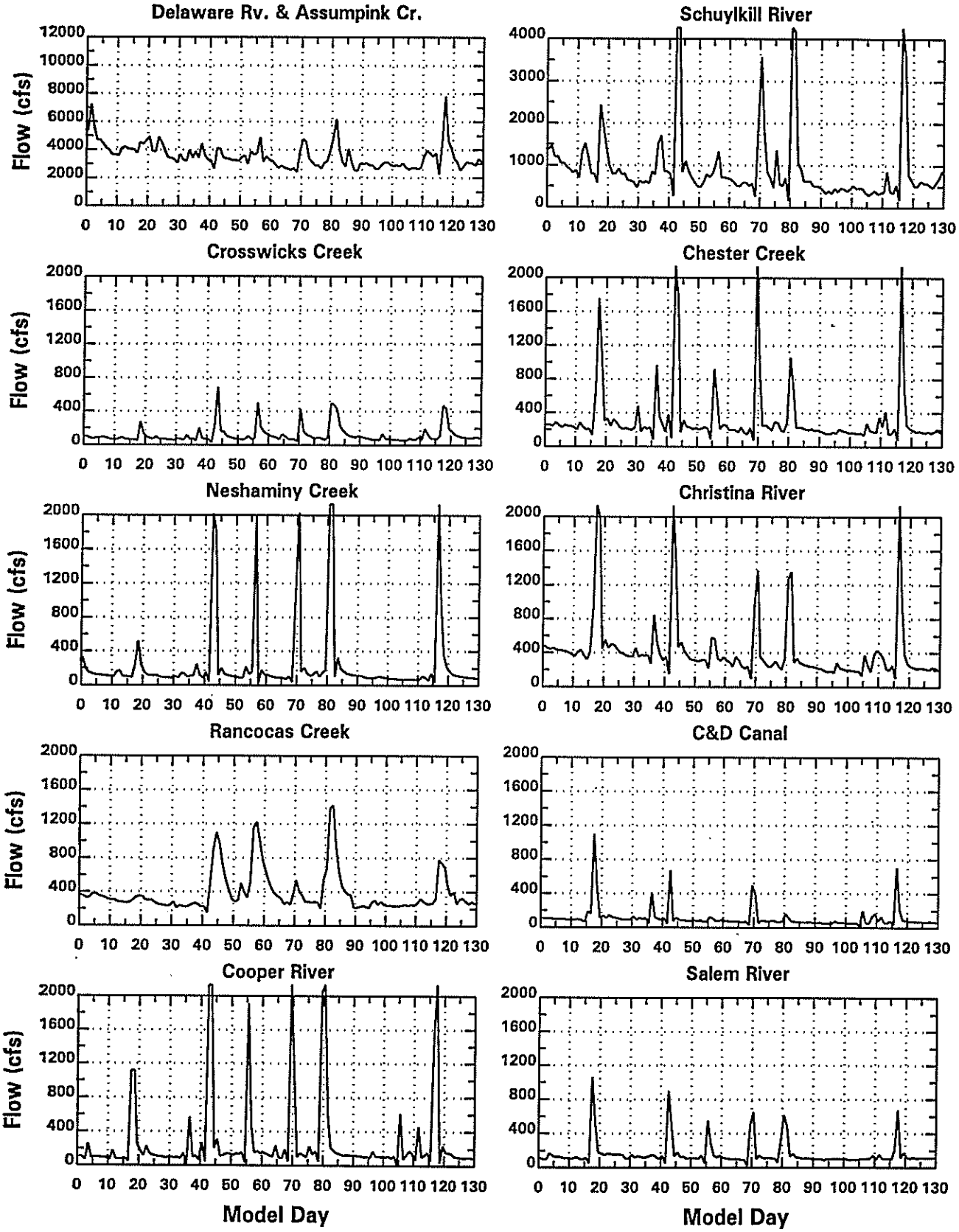

Figure 6-6. Tributary Flow Rates During 1991 Validation Period.

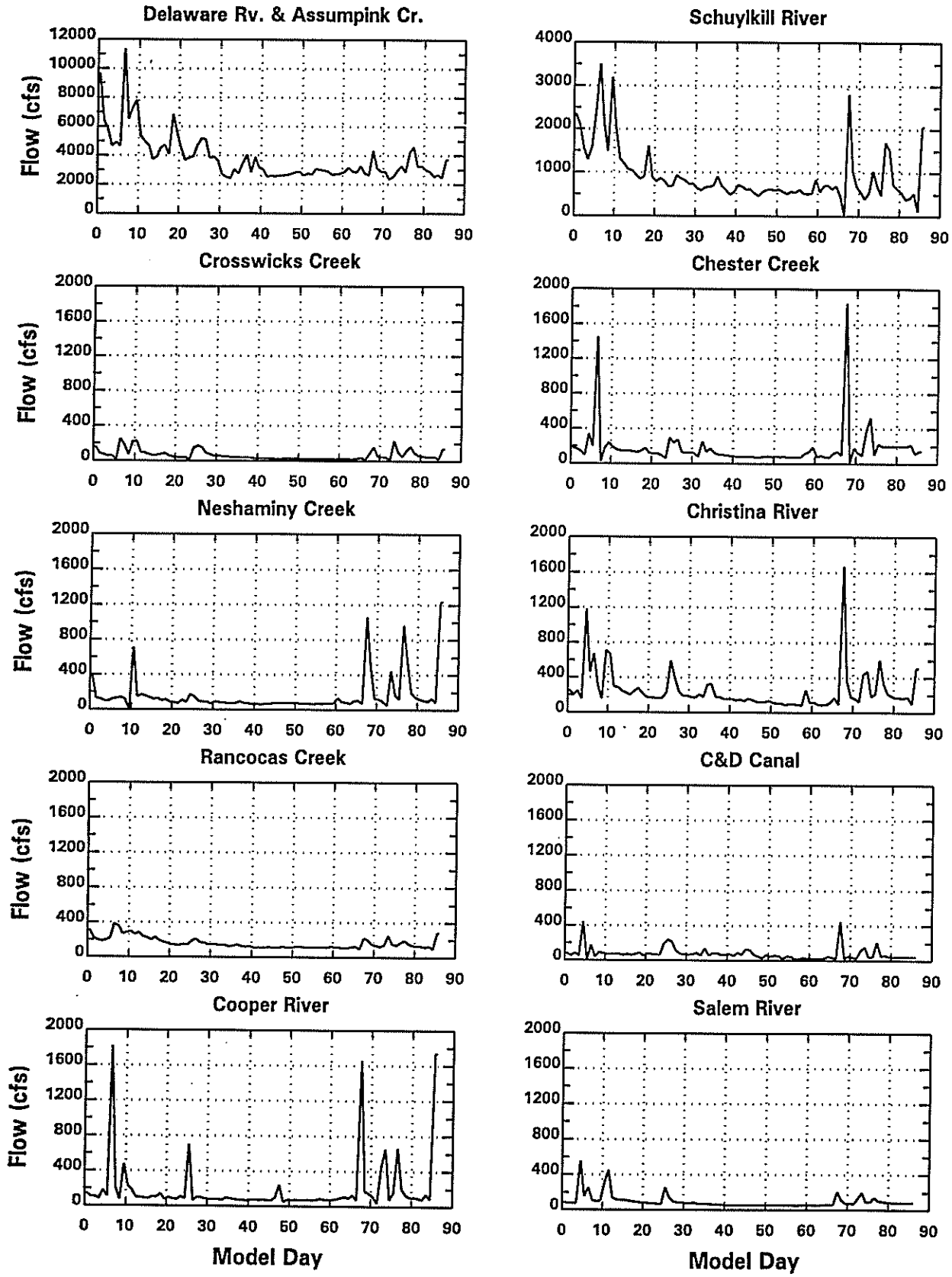

Figure 6-7. Tributary Flow Rates During 1995 Validation Period.

from the various wastewater treatment plants (WWTP) that discharge into the Delaware River estuary. A total of six WWTP discharges have been accounted for in this modeling effort. Their locations were shown in Figure 3-4. Time variable flows from the WWTP discharges were determined from available data and these discharges are illustrated for the different simulation periods on Figures 6-8 and 6-9. Note that WWTP discharges were not included in the 1984 calibration because water quality simulations were not conducted for that period.

Table 6-1. Specification of Tributary Drainage Areas

Tributary	Drainage Area (mi^2)		Proration Ratio
	Gaged	Total	
Delaware River	6780	6780	1.00
Assunpink Creek	89	96	1.07
Crosswicks Creek	84	168	2.01
Neshaminy Creek	210	368	1.75
Rancocas Creek	118	452	3.83
Cooper River	17	215(1)	12.6
Schuylkill River	1893	1987(1)	1.05
Chester Creek	61	342(1)	5.60
Christina River	450	591	1.31
Salem River	27	188(1)	6.98
Freshwater Flow to C&D Canal (Red Clay Creek used as a surrogate))	47	166	3.53

(1) Includes ungaged drainage area in vicinity of tributary

Tidal elevations at Liston Point are specified using either available tide gauge data or NOS tidal harmonics. Water surface elevation data are not collected at Liston Point so measurements made at the Reedy Point tidal gauge have been applied to the downstream boundary of the model. It has been assumed that tidal amplitude is constant between Reedy Point and Liston Point. Initial testing of the hydrodynamic model showed that a phase shift of 40 minutes exists between the two locations, i.e., the tidal wave at Liston Point is 40 minutes earlier than that measured at Reedy Point, and this phase shift has been used in all hydrodynamic simulations.

Tide gauge data at Chesapeake City, which is at the western end of the C & D Canal, do not exist during the periods under consideration in the present study. Thus, NOS tidal harmonics

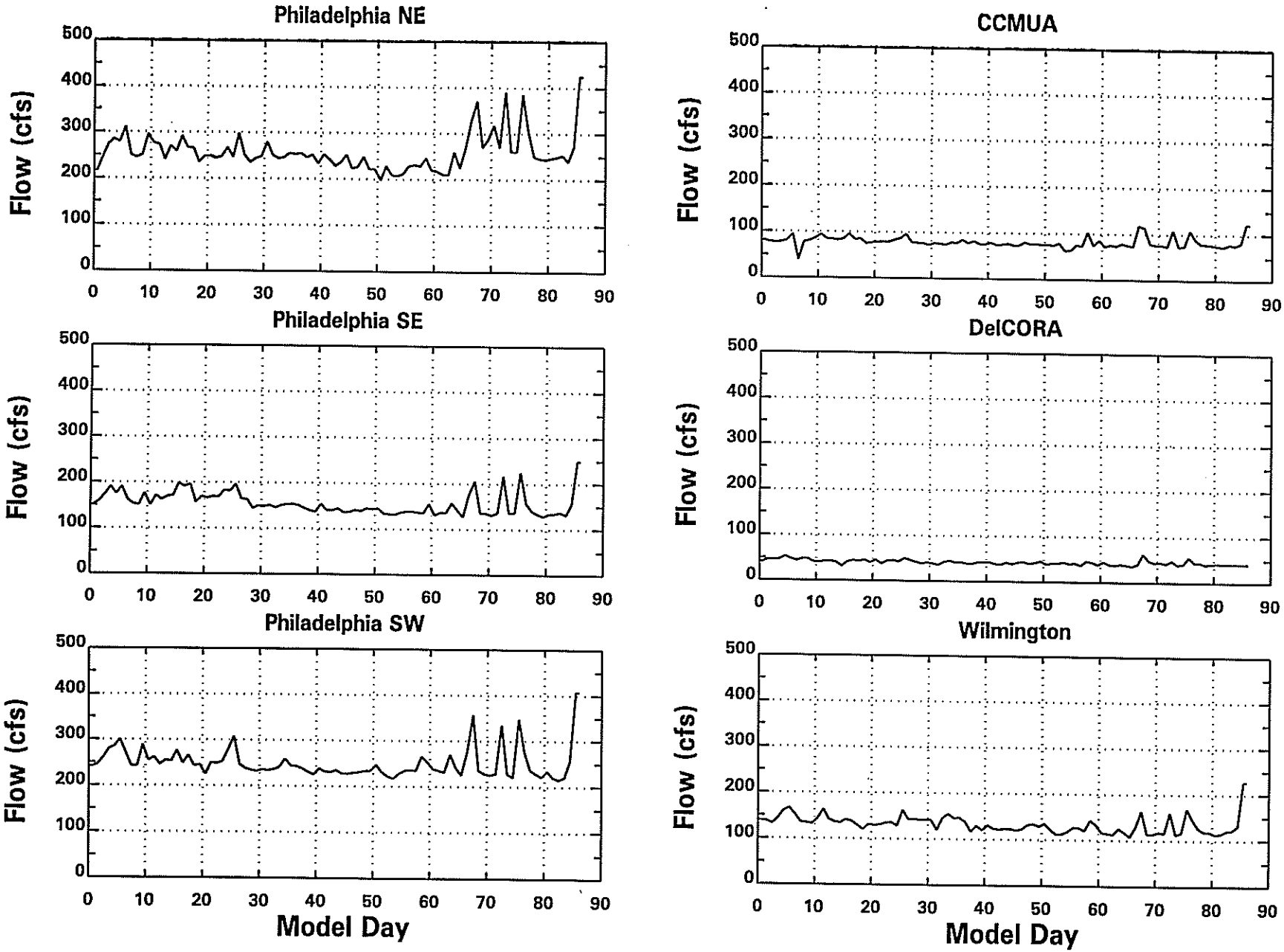

Figure 6-8. Wastewater Treatment Plant Flows During 1995 Validation Period.

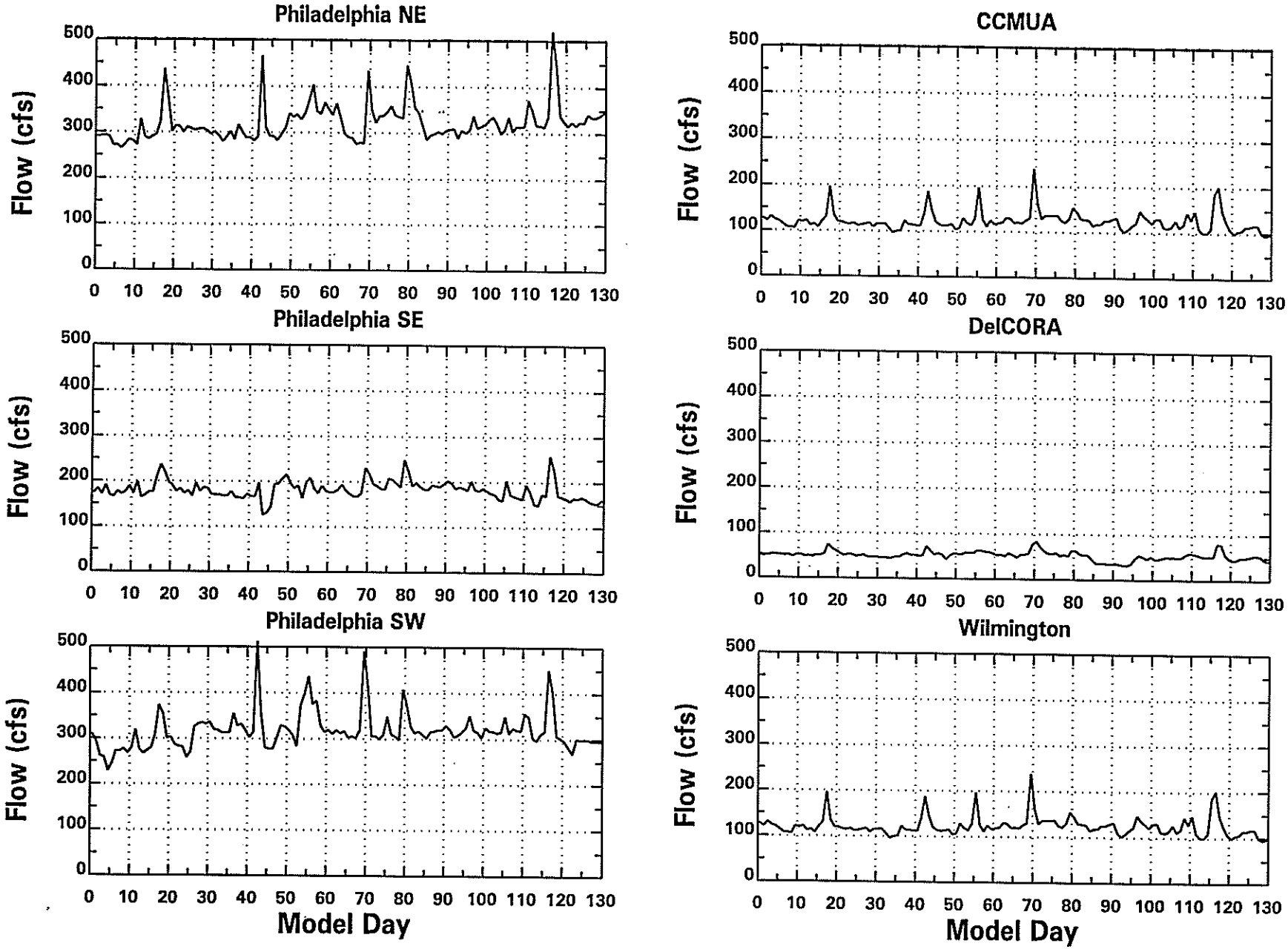

Figure 6-9. Wastewater Treatment Plant Flows During 1991 Validation Period.

have been used to specify tidal elevations at this boundary of the model, see Table 6-2. Net (tidal residual) flow in the C & D Canal is determined by a combination of tidal amplitude/phase and mean water level differences between the eastern and western ends of the canal. Rives and Pritchard (1978) found that for the period they considered in their modeling study of the C & D Canal, a mean water level difference of -1.22 cm (0.04 ft) between the eastern and western ends produced the best results, i.e., mean water level at the western end was lower than at the eastern end. Based upon those results, the mean water level at the Chesapeake City boundary has been set 1.22 cm lower than the mean water level at the Liston Point boundary in all simulations.

Table 6-2. Tidal Harmonics Applied at Chesapeake City

Harmonic Component	Amplitude (m)	Phase (degrees)
M_2	0.300	278
N_2	0.055	251
S_2	0.044	320
K_1	0.062	305
O_1	0.047	321
M_4	0.011	176

The final boundary condition to be applied is salinity at the open boundaries located at Liston Point and Chesapeake City. Limited data were available at these locations during the calibration (1984) and validation (1991 and 1995) periods considered in this study.

The calibration period (1984) salinity at the Liston Point boundary was assigned using salinity data measured by NOS for the Delaware River and Bay Circulation Survey, 1984-1985. Station 33 had measurements taken at a depth of 3.7 m, between June 15 and August 15; station 36 was measured at 4.3 and 8.8 m, between June 15 and June 30; and station 39 was measured at 4.3m, between June 15 and June 30, see Figure 6-10 for station locations. Values were recorded every 10 minutes at all stations. The salinity at Liston Point was estimated by averaging data at stations 36 and 39, which are approximately equal distance downstream and upstream from Liston Point. Since only station 33 had data for the full calibration period, correlations were developed between the three stations to make use of all of the data at station 33. These correlations were used to estimate salinity at stations 36 and 39 when data were not available at those locations. Additionally, the data at both depths for station 33 were used to develop a

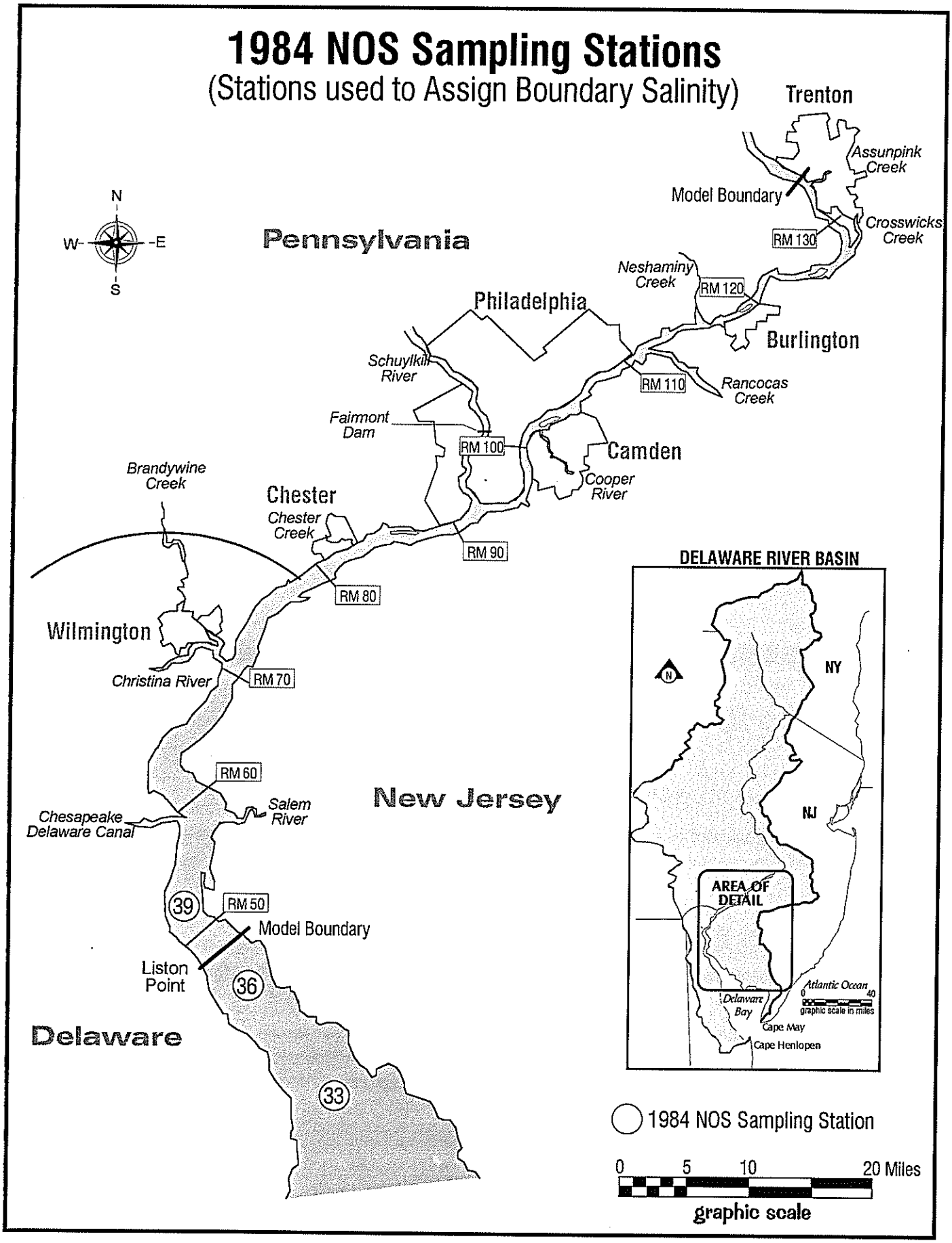

Figure 6-10. Locations of NOS Salinity Sampling Stations in 1984.

vertical distribution of salinity. A surface salinity was assigned to the top two standard levels (0 and 4.3 m depths), and a bottom salinity was assigned to the bottom two standard levels (8.8 and 18 m depths). The 10-minute data were averaged to produce salinity specified on an hourly basis. Figure 6-11 shows the salinity input for all standard levels at the Liston Point boundary for the calibration period.

Salinity at the Liston Point boundary during the 1991 and 1995 validation periods was determined using DRBC conductivity data which were converted to salinities. DRBC collected surface grab samples in the vicinity of Liston Point approximately every two weeks during the validation periods, see Figure 4-1 for sampling locations. In 1991, the data from RM 50.8 and RM 44.0 were linearly interpolated to estimate the surface salinity at Liston Point. In 1995, the sampling location at RM 50.8 was switched to RM 48.2. Since Liston Point is at RM 48.5, data collected at RM 48.2 was assigned at the Liston Point. The vertical distribution of salinity at this location was estimated by examining historical salinity data obtained in the vicinity of Liston Point (Lebo et al., 1990; Kawabe et al., 1990). An analysis of these data indicated that an average salinity gradient of about 0.24 ppt/m, i.e., salinity increases linearly with depth at this rate, exists between the surface and depths between 7 and 12 m. As a first-approximation to the vertical distribution of salinity at Liston Point, surface salinity values specified at the boundary were increased by 0.24 ppt/m to a depth of 8.8 m and then held constant for depths greater than 8.8 m. Hourly values of salinity at the Liston Point boundary were estimated by linearly interpolating the data in time, see Figures 6-12 and 6-13.

Daily salinity data were available at Chesapeake City during the 1984, 1995 and 1991 simulation periods and those data were used to specify salinity at that boundary as daily average values, see Figures 6-12 to 6-14. No salinity data were available for the 1991 validation period so a constant value of 1 ppt was assumed at this boundary. The assumption was made that the water column at this location is well mixed (homogeneous) and a uniform vertical distribution of salinity at the Chesapeake City boundary was used in all calculations.

All freshwater inflows were assumed to have a background salinity value of 0.1 ppt. This assumption had negligible impact on the hydrodynamic results.

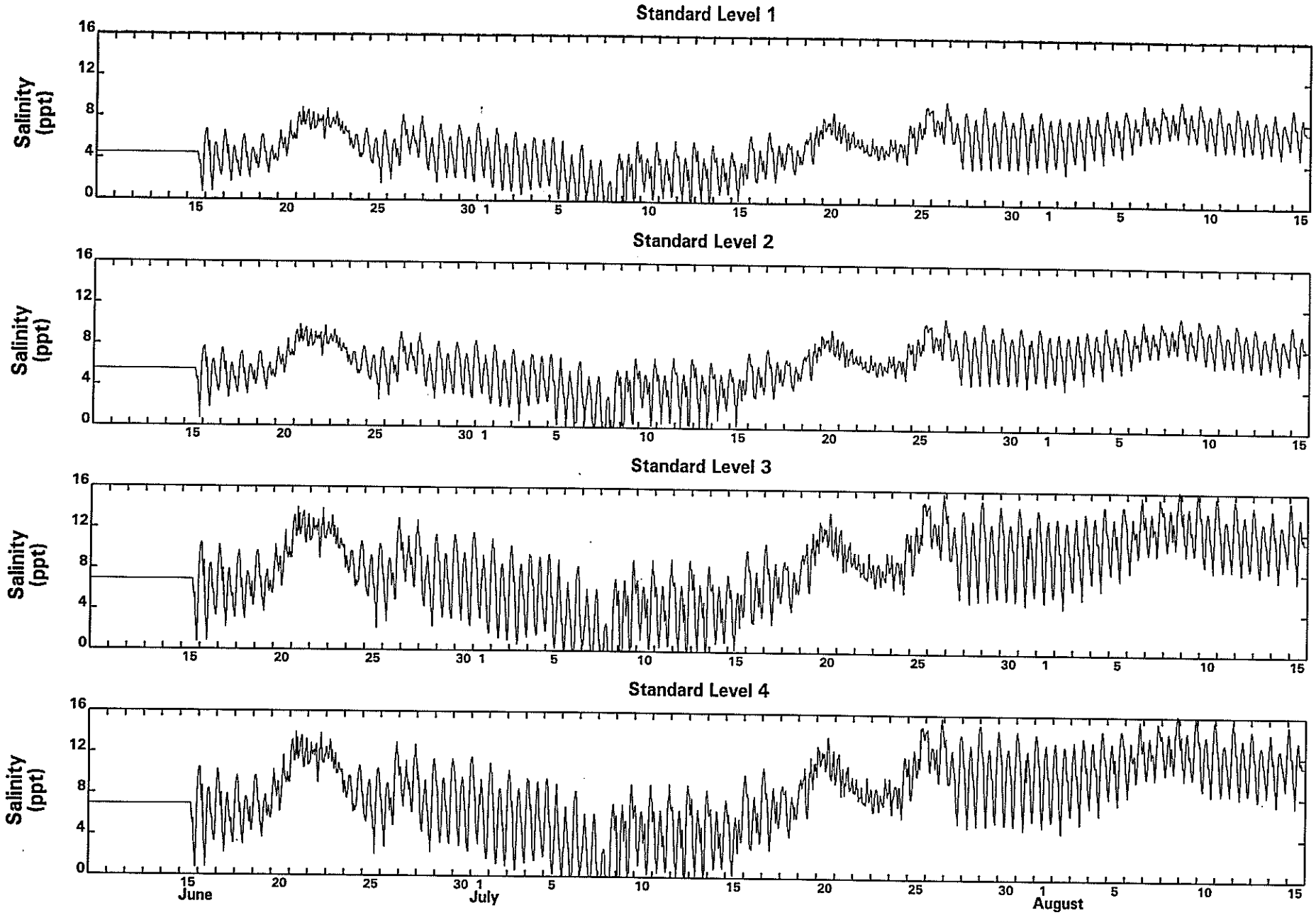

Figure 6-11. Salinity Boundary Conditions at Liston Point During 1984.

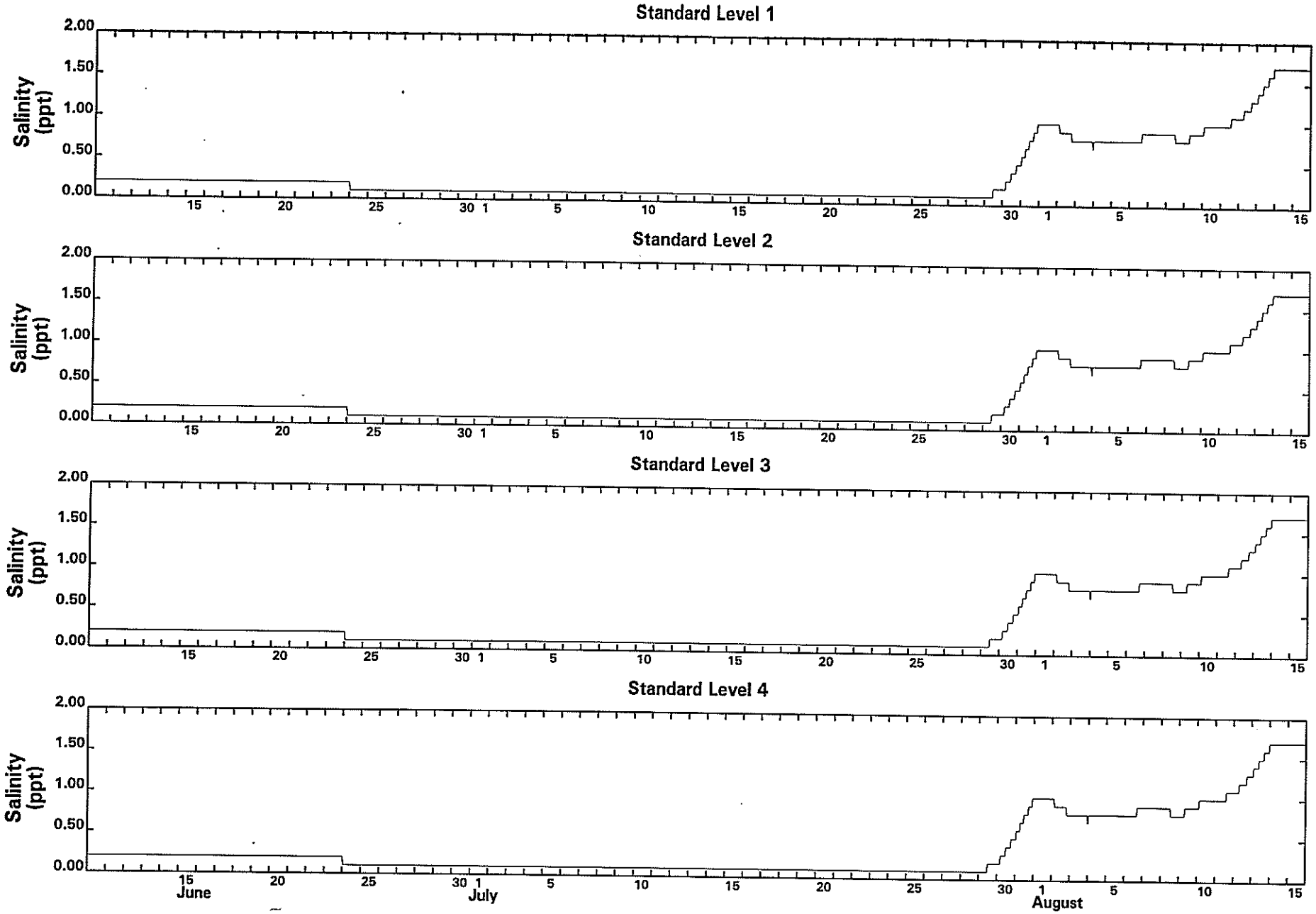

Figure 6-12. Salinity Boundary Conditions at Chesapeake City During 1984.

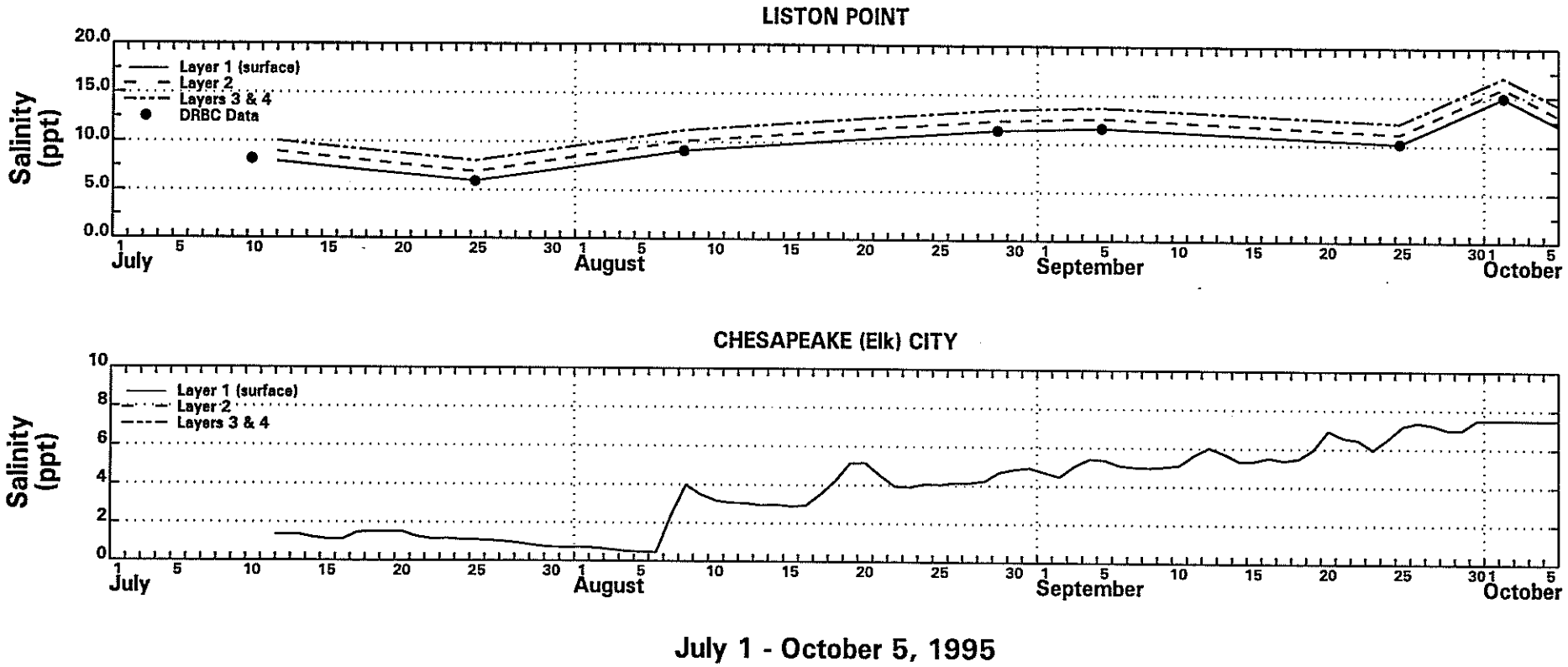

Figure 6-13. Salinity Boundary Conditions at Liston Point and Chesapeake City During 1995.

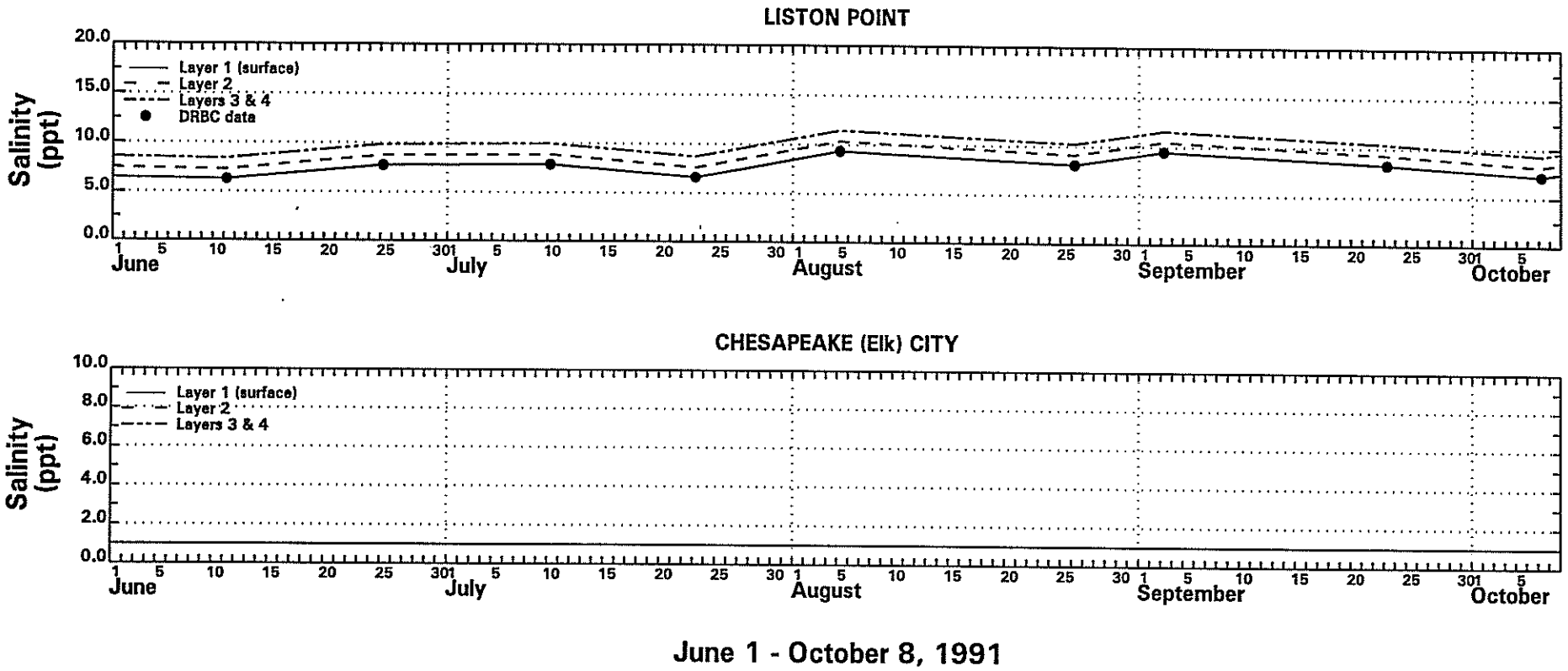

Figure 6-14. Salinity Boundary Conditions at Liston Point and Chesapeake City During 1991.

6.3 1984 CALIBRATION PERIOD

The hydrodynamic model was calibrated over a two-month period in 1984, from June 15 to August 15. The daily average flow rate of the Delaware River ranged between 7,000 and 60,000 cfs during this period. Salinity at the Liston Point boundary ranged between less than 1 and 16 ppt, with these values being estimated from available data as described in Section 6.2.

The parameters adjusted to calibrate the hydrodynamic model were the bottom roughness height (z_o) and k_1 in Equation 5-2. Best agreement between model and data was achieved with z_o = 0.5 mm and k_1 = 0.0028. The minimum value of the bottom friction coefficient was 0.0025, which is typically used in estuarine modeling studies. The horizontal eddy diffusivity (A_H) was set at 1 m^2/s and was not adjusted. A timestep of 45 seconds was used in all simulations.

Initial testing of the model using the above bottom friction coefficients did not produce satisfactory results in the C & D Canal. Gardner and Pritchard (1974) used a Manning's n value of 0.028 in their modeling work on the canal. This Manning's n value is equivalent to a bottom friction coefficient of 0.029 in the C & D Canal, which is the value that has been used in all simulations presented in this report.

Comparisons between predicted and measured tidal elevations at Reedy Point, Philadelphia and Trenton are shown on Figure 6-15. Only a 30-day period, from June 15 to July 15, is presented for clarity; similar results were obtained for the July 15 to August 15 period. Very good agreement at Reedy Point, for both amplitude and phase, indicates that the translation of tidal gauge data from Reedy Point to the Liston Point boundary, as described in Section 6.2, is a good approximation. Model-data agreement is seen to be nearly as good at Philadelphia, with the model slightly under predicting the tidal range. At Trenton, amplitudes are slightly under predicted and some phase differences occur. Further analysis of the model results was done by comparing predicted and observed values of the M_2 amplitudes and phases, see Table 6-3. The model under predicts the M_2 amplitude by approximately 0.05 to 0.10 m at the three gauging stations, which represents an error range of 6 to 10 percent.

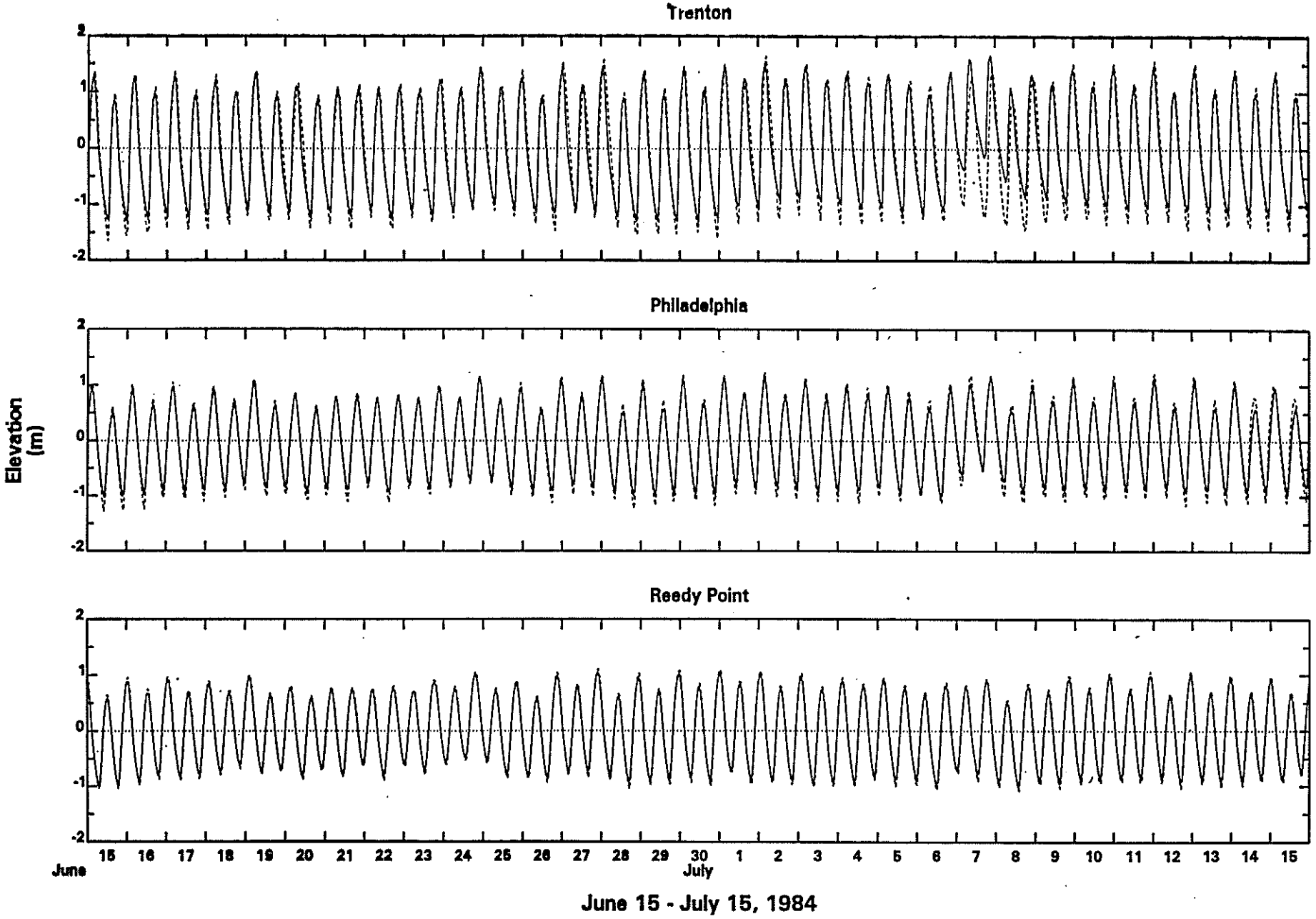

Figure 6-15. Comparison of Measured and Predicted Tidal Elevations at Trenton, Philadelphia and Reedy Point During 1984 Calibration Period.

Table 6-3. Comparison of Predicted and Observed M_2 Tidal Amplitudes and Phases

Location	Amplitude (meters)		Phase (degrees)	
	Measured	Predicted	Measured	Predicted
Trenton	1.17	1.07	47	39
Philadelphia	0.87	0.79	12	12
Reedy Point	0.83	0.78	292	290

Current meter and salinity data were available during the 60-day calibration period at six locations, see Figure 6-16. These data were obtained at a single depth, ranging from 4.3 to 5.2 m, at each location during a 1984 study conducted by the National Ocean Service (NOS, 1986). Comparisons between measured and predicted current velocities and salinities at the six stations are shown on Figures 6-17 to 6-22. The 30-day period from June 15 to July 15 is presented on these figures because nearly all of the current meter data were obtained during this time. Comparisons between observed and predicted current velocities have been made by examining the longitudinal (upstream/downstream) and lateral (cross-channel) components of the total velocity. A significant effort was made to correctly orient the current meter data to the model velocities. However, some uncertainty still exists in these comparisons because of possible errors in data orientation.

An alternative method for comparing measured and predicted current velocities that eliminates the orientation problem is to construct a principal axis plot. This type of graphical presentation allows direct comparison of the longitudinal and lateral velocities that are predicted and observed at a particular location. Principal axis plots for the six current meter locations considered here are shown on Figures 6-23 to 6-25.

An examination of Figures 6-17 to 6-25 indicates that good agreement exists between observed and simulated current velocities. As shown by the temporal plots, the hydrodynamic model adequately predicts the phase of the tidal current at all locations. Generally, magnitudes of the longitudinal and lateral current velocities are satisfactorily predicted.

The flow in the C & D Canal is of particular interest because other investigators have found that the canal can have an effect on circulation in the Delaware River estuary (Wong, 1990). Figures 6-22 and 6-23 show that the model does a good job of reproducing tidal currents in the canal. To investigate net flow in the C & D Canal during the calibration period, a 34-hour

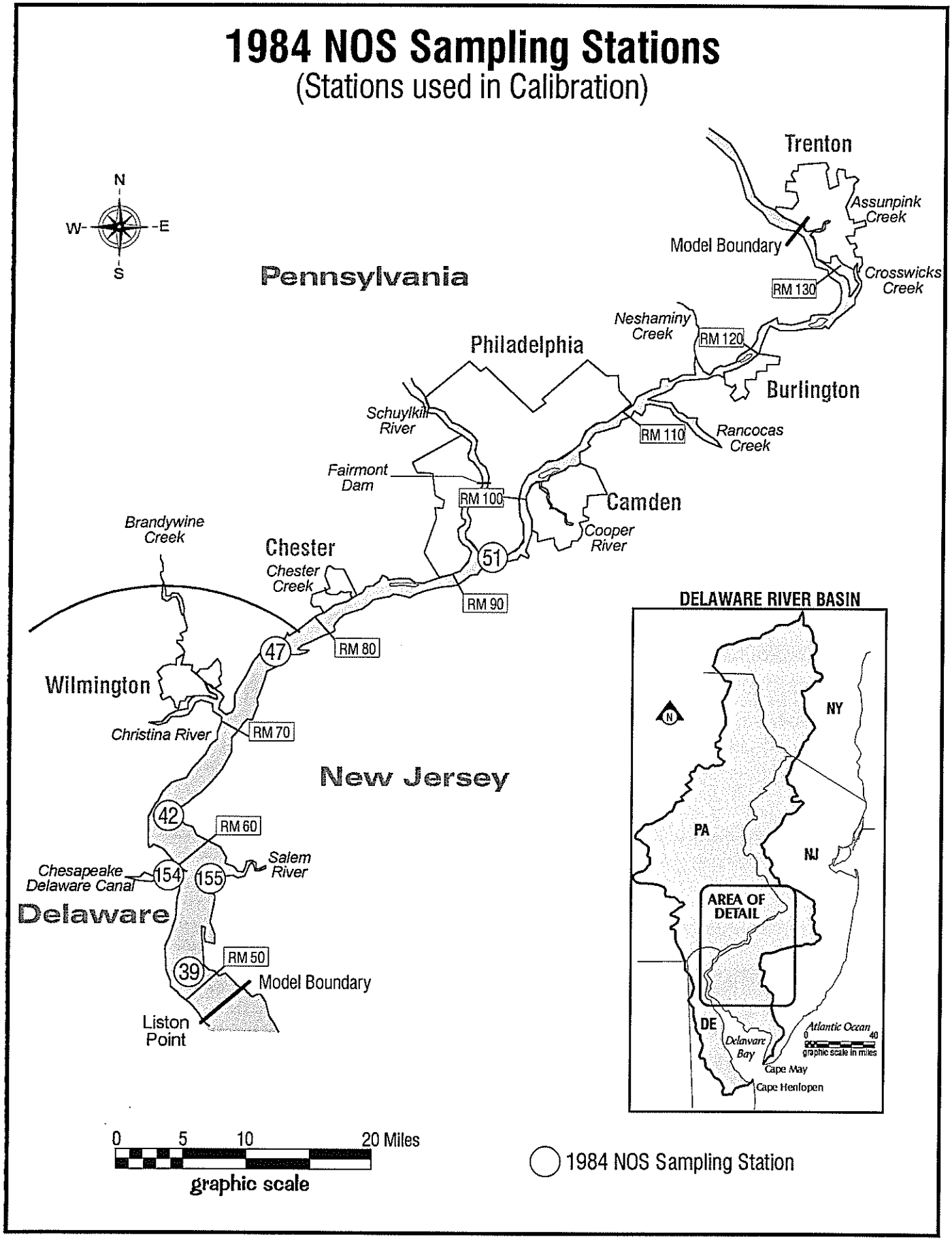

Figure 6-16. Locations of NOS Current Meter Stations in 1984.

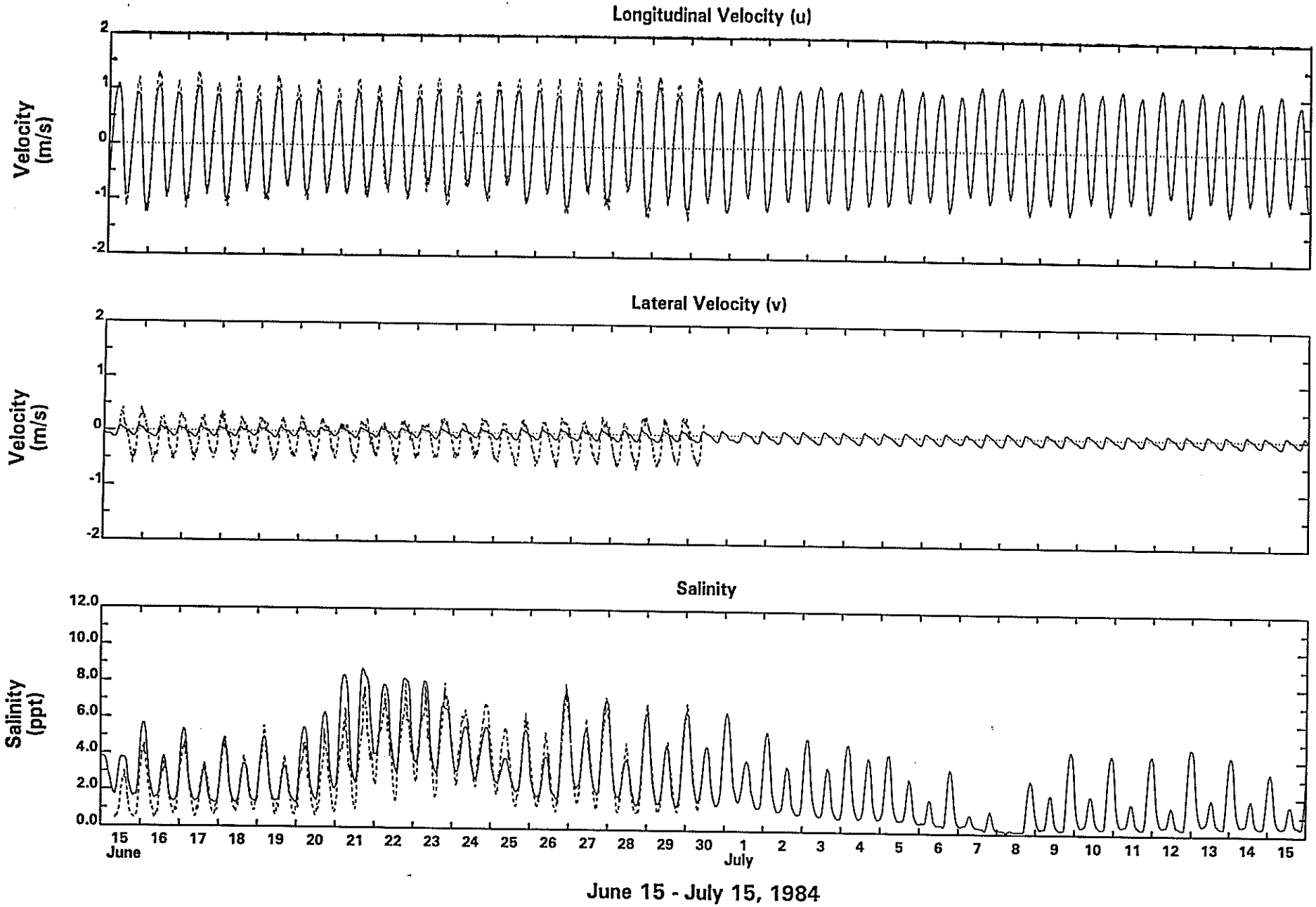

Figure 6-17. Comparison of Measured and Predicted Current Velocities and Salinities at Station 39 During 1984 Calibration Period.

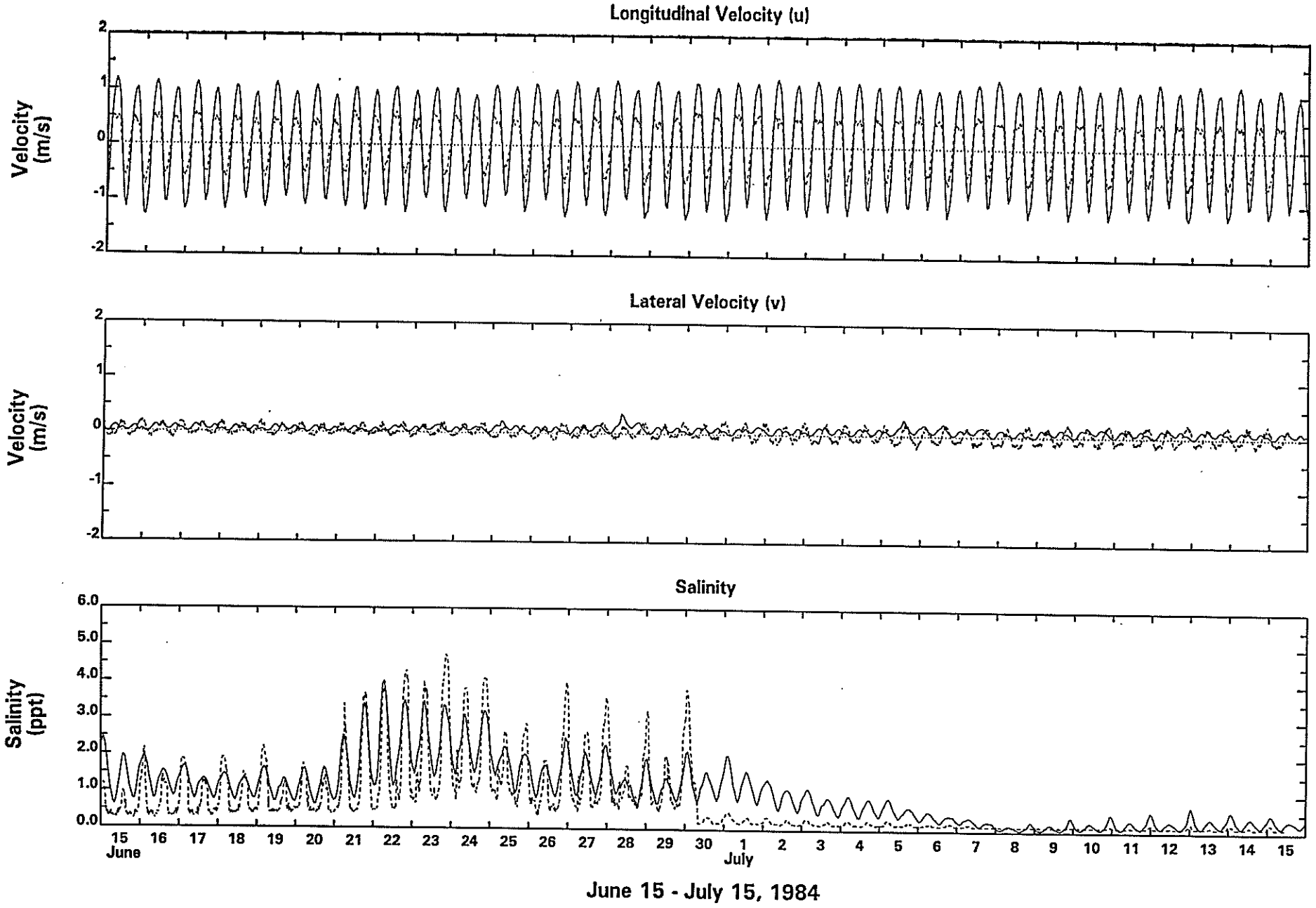

Figure 6-18. Comparison of Measured and Predicted Current Velocities and Salinities at Station 155 During 1984 Calibration Period.

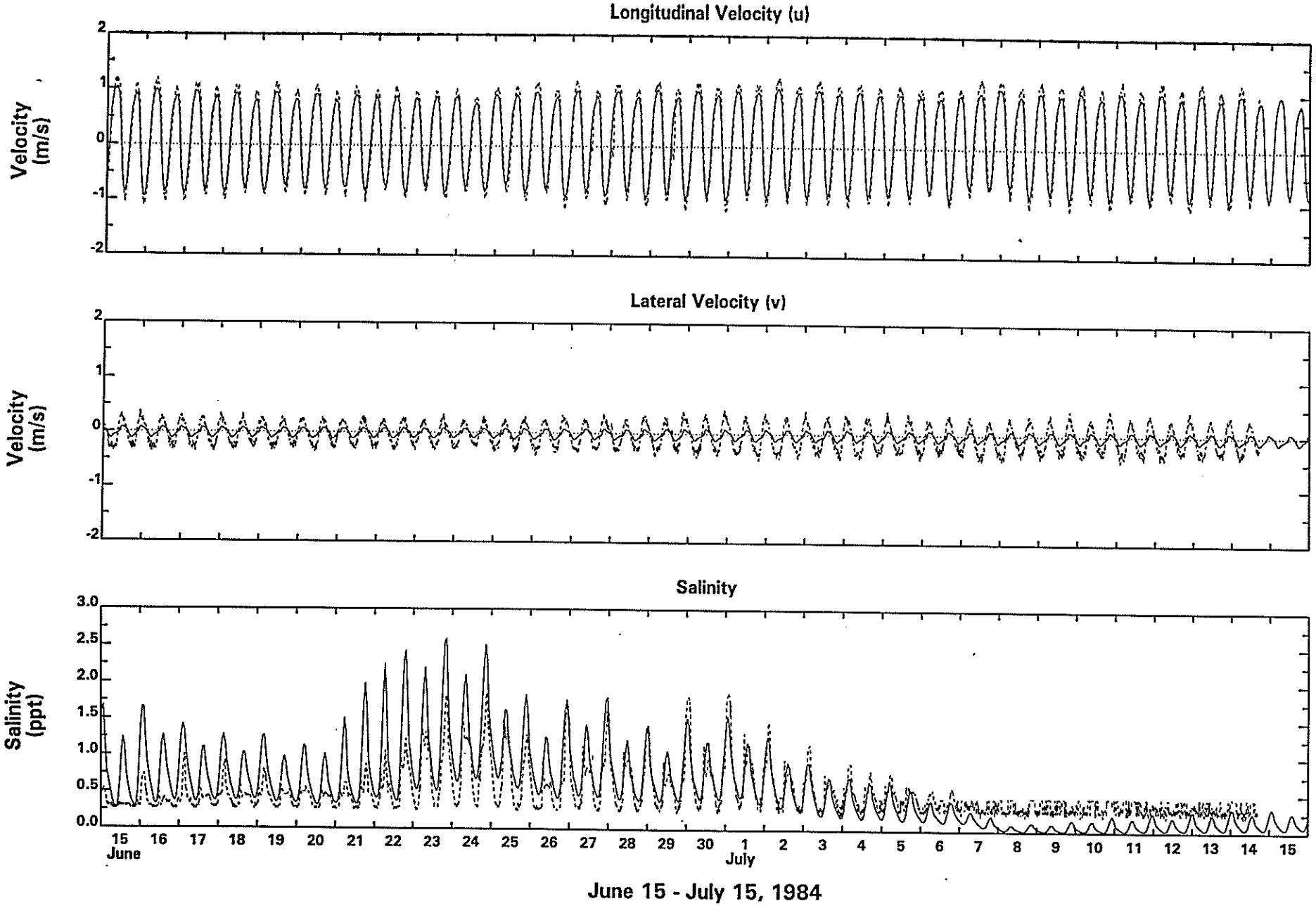

Figure 6-19. Comparison of Measured and Predicted Current Velocities and Salinities at Station 42 During 1984 Calibration Period.

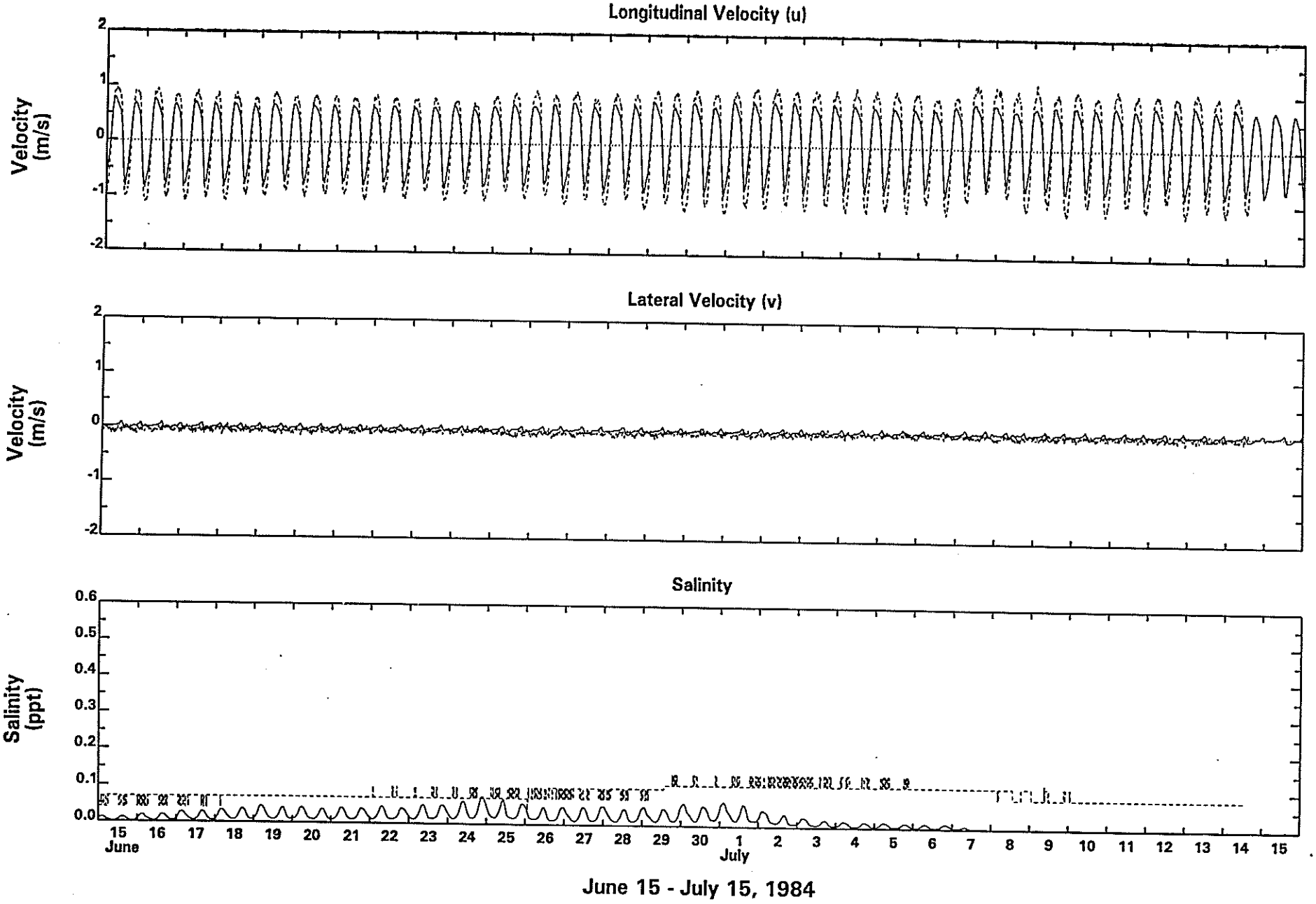

Figure 6-20. Comparison of Measured and Predicted Current Velocities and Salinities at Station 47 During 1984 Calibration Period.

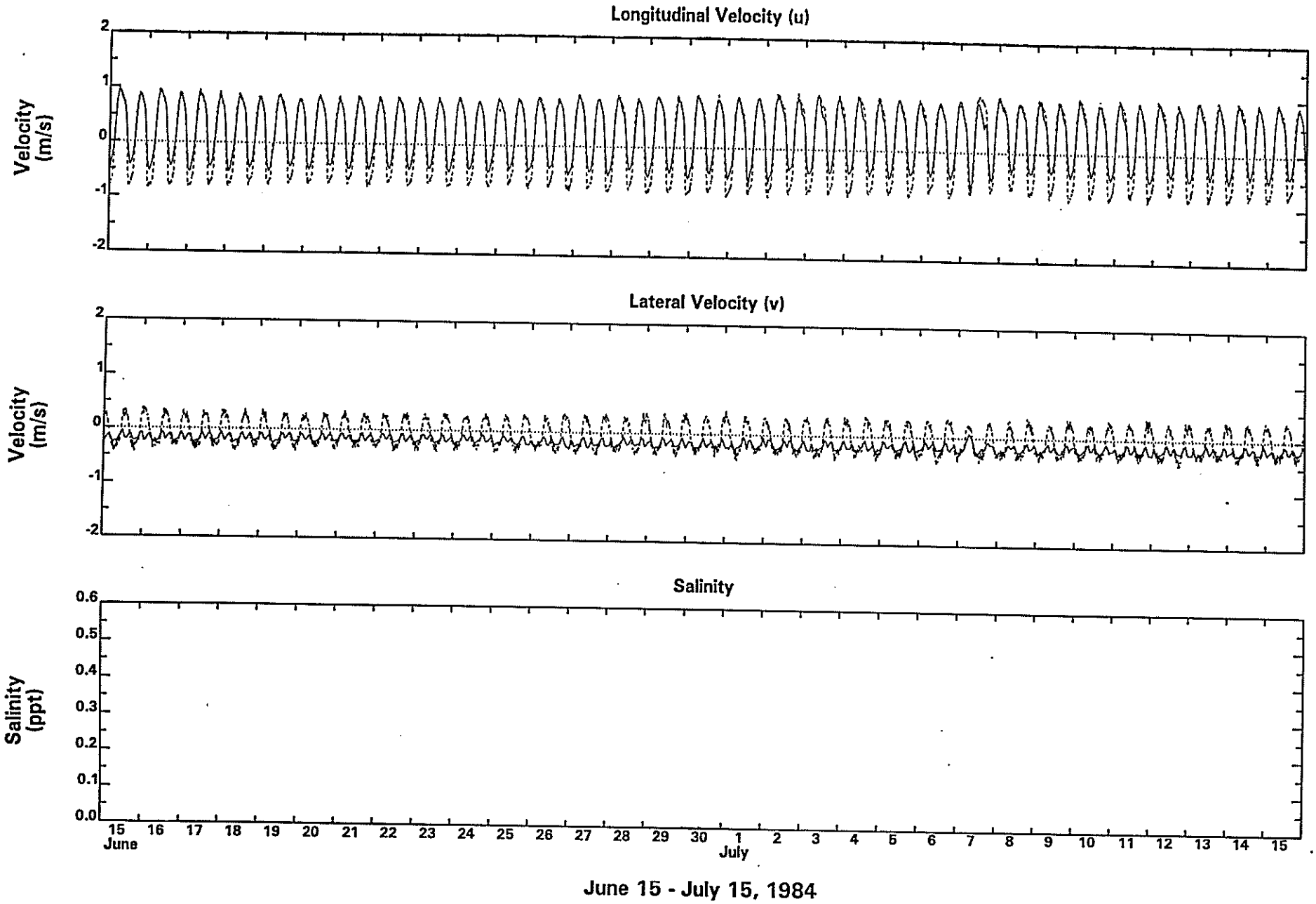

Figure 6-21. Comparison of Measured and Predicted Current Velocities and Salinities at Station 51 During 1984 Calibration Period.

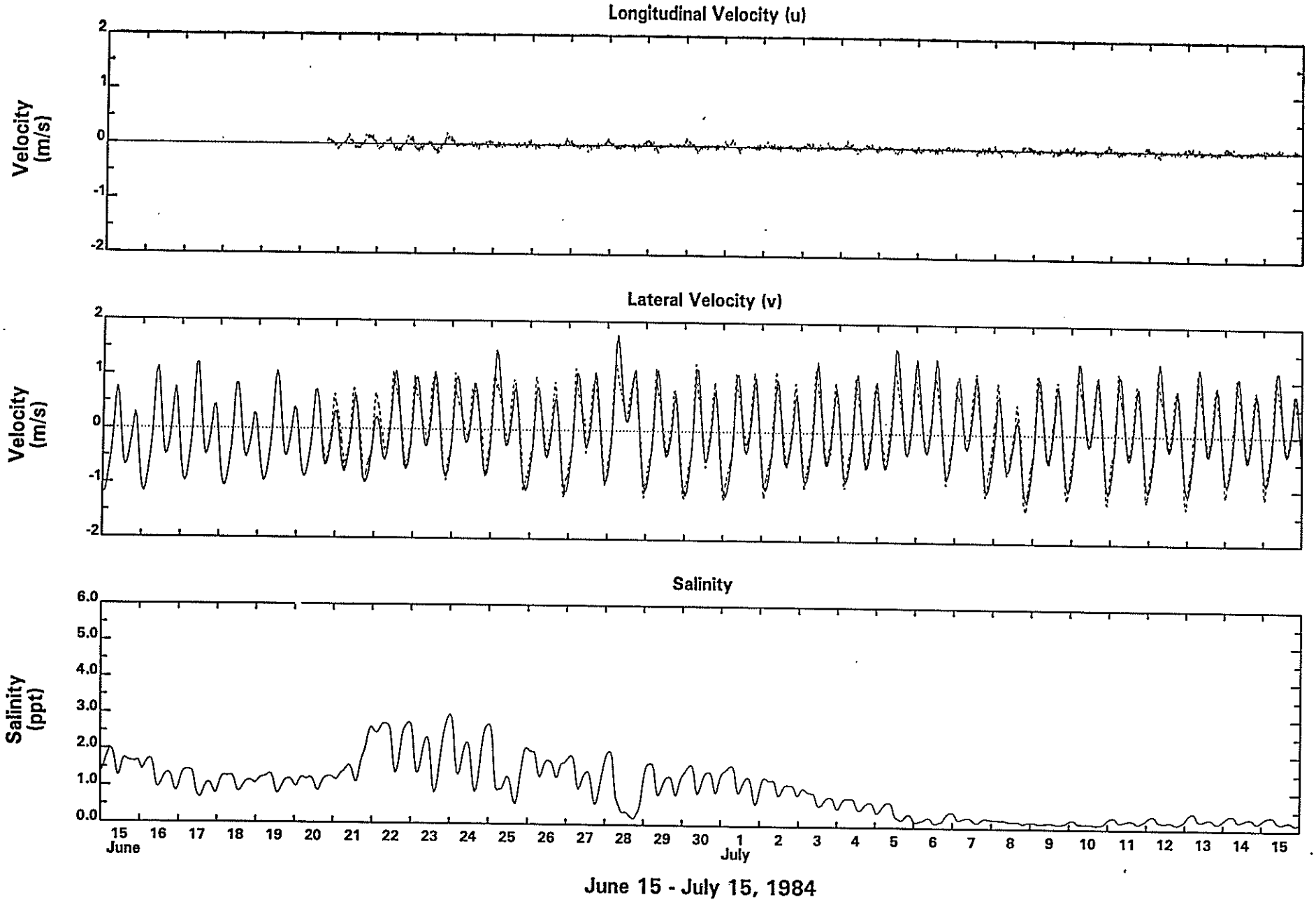

Figure 6-22. Comparison of Measured and Predicted Current Velocities and Salinities at Station 154 (C&D Canal) During 1984 Calibration Period.

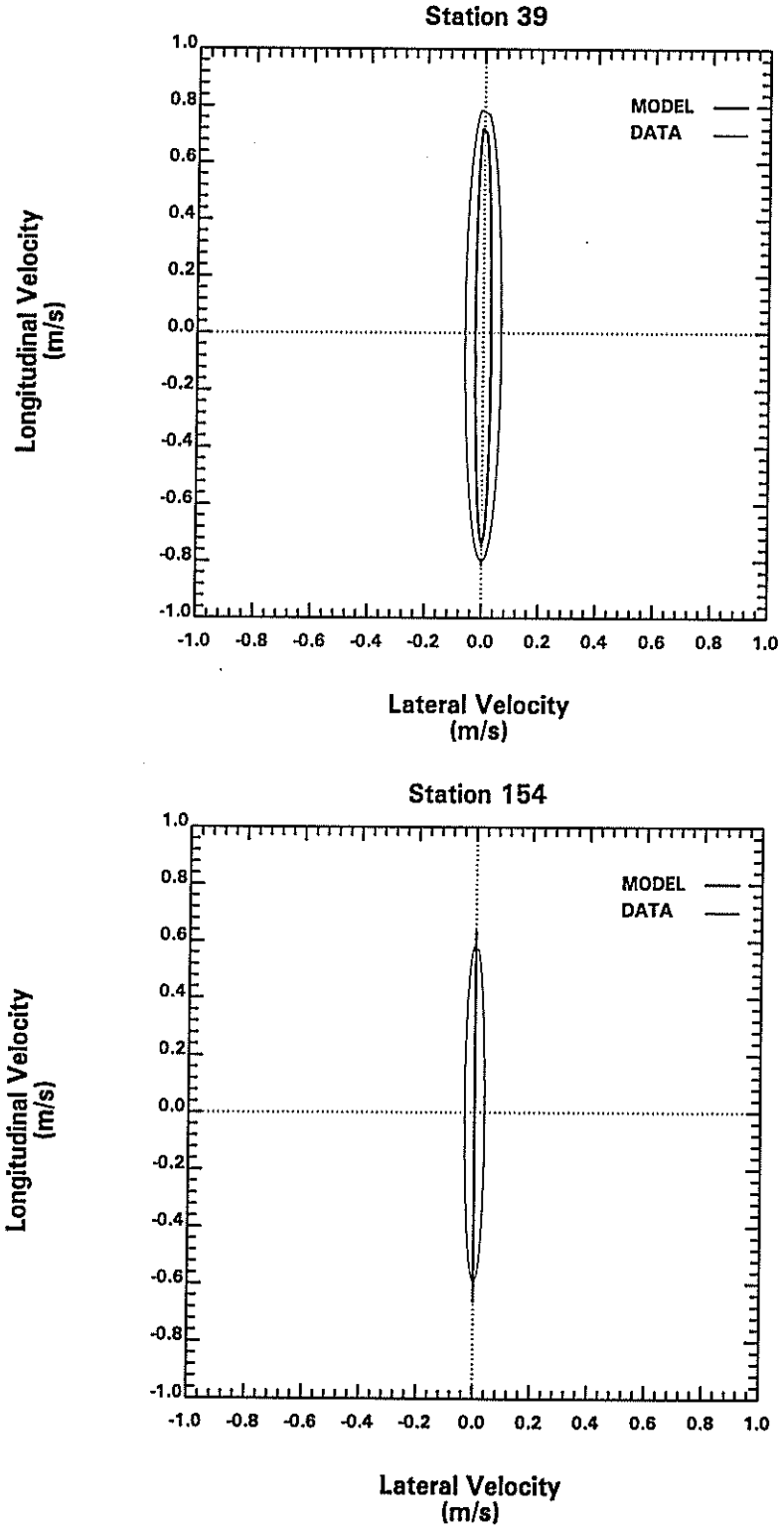

Figure 6-23. Comparison of Measured and Predicted Principal Axis Plots for Current Velocities at Stations 39 and 154 During 1984 Calibration Period.

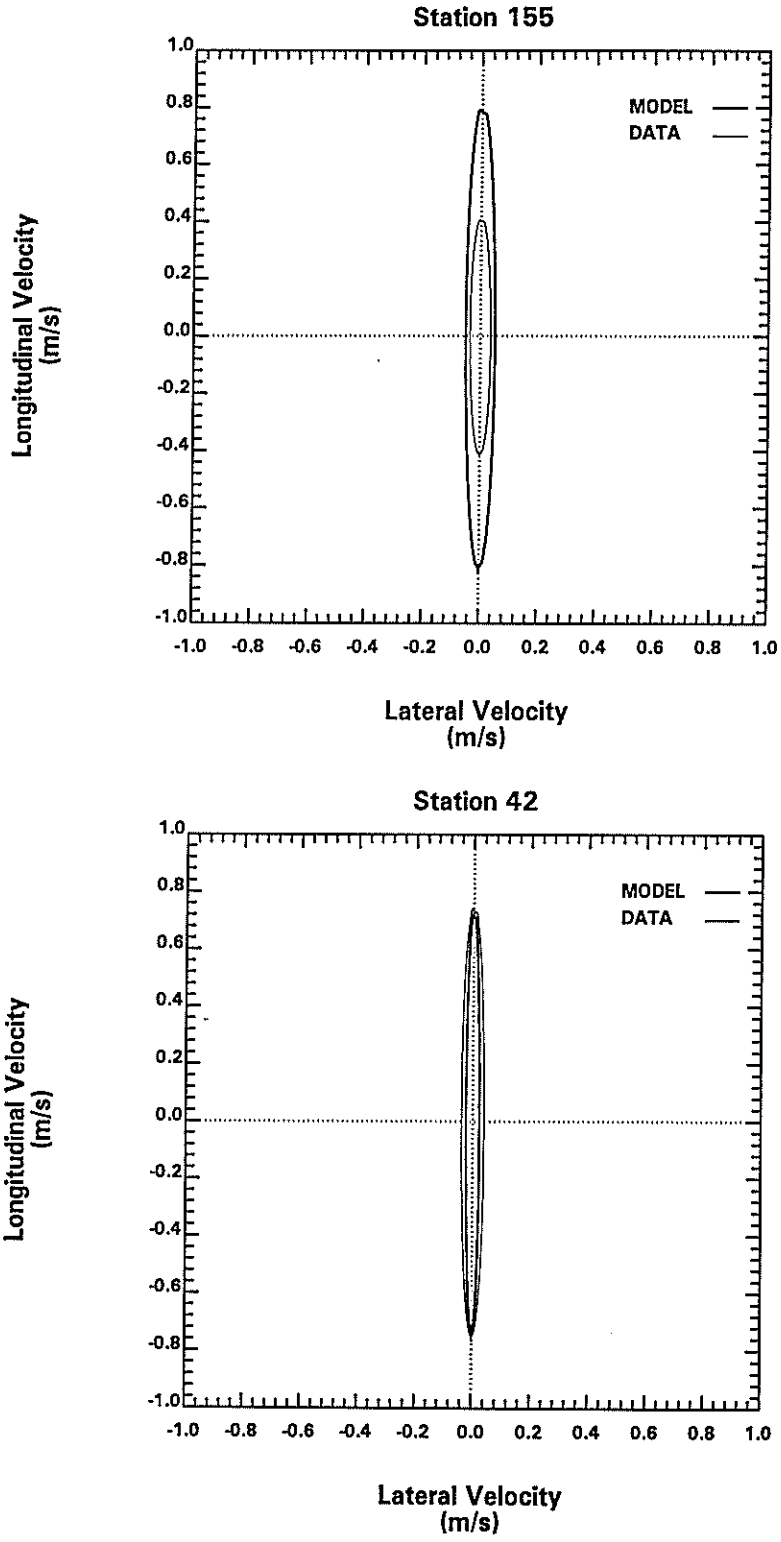

Figure 6-24. Comparison of Measured and Predicted Principal Axis Plots for Current Velocities at Stations 155 and 42 During 1984 Calibration Period.

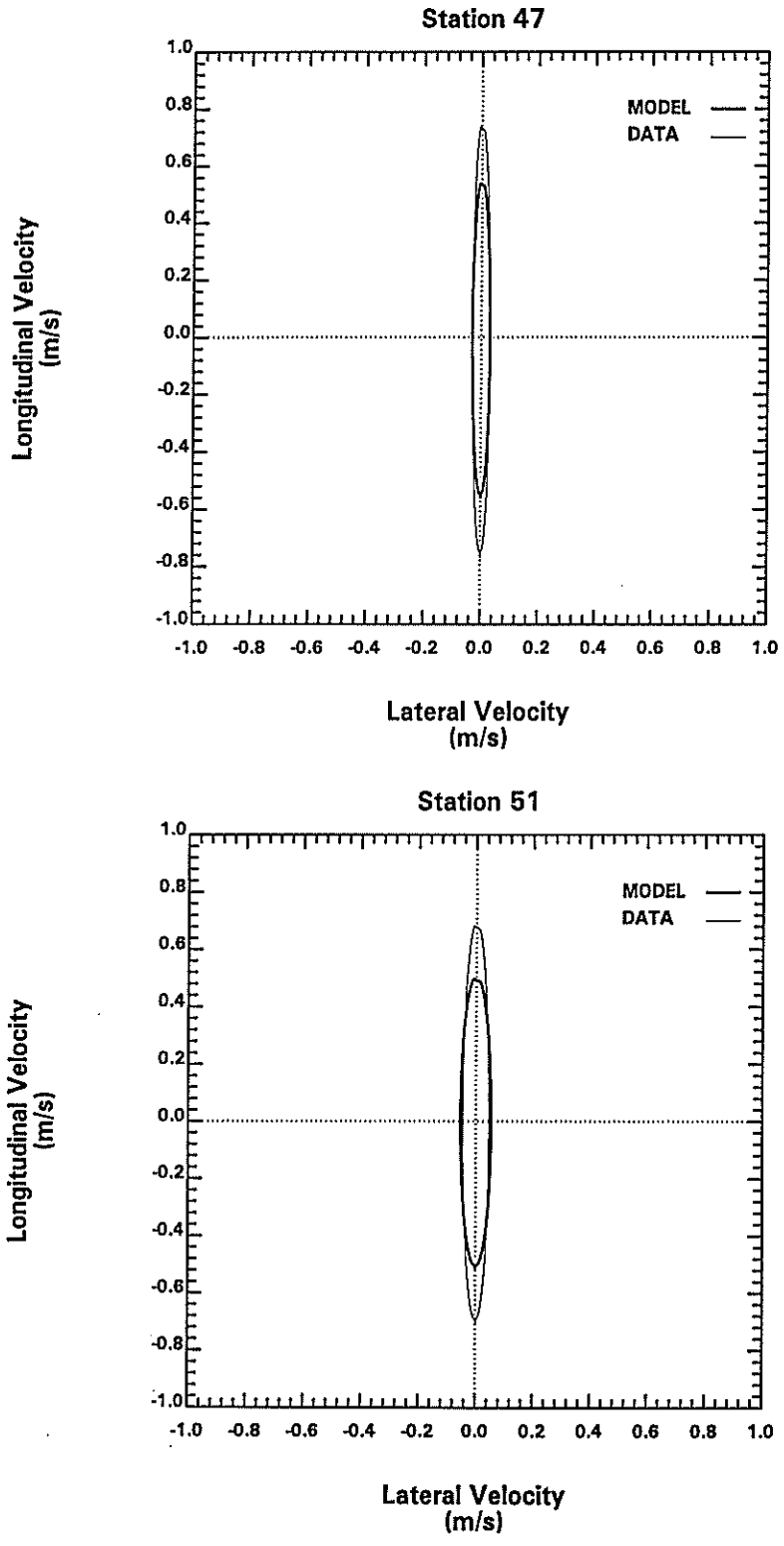

Figure 6-25. Comparison of Measured and Predicted Principal Axis Plots for Current Velocities at Stations 47 and 51 During 1984 Calibration Period.

low-pass filter, which removes the tidal component of the flow, was applied to the model output at the eastern end of the canal. The resulting time history of net flow in the C & D Canal is illustrated on Figure 6-26. The average net flow rate in the canal for the 60-day simulation period is 1,100 cfs and it is directed westward. Previous studies have found the mean net flow in the canal to be variable and it can be either westward or eastward (Pritchard and Gardner, 1974; Najarian et al., 1980).

Predicted and measured salinity at the current meter stations are presented on the lower panels of Figures 6-17 to 6-20. Simulated salinities are seen to be in phase with the observed values. The model tends to overpredict salinity somewhat at each location, but the extent of salinity intrusion is generally predicted satisfactorily.

6.4 1995 VALIDATION PERIOD

Validation of the hydrodynamic model was accomplished through simulation of a 97-day period in 1995, from July 1 to October 5. This timeframe was chosen because the water quality model of the Delaware River estuary was calibrated using data collected during this low flow period. Model parameter values determined during calibration, as discussed in the previous section, were not adjusted in the validation simulation. Daily average flow rates in the Delaware River, as measured at Trenton, ranged from 2,500 to 11,000 cfs during this 97-day period. Salinity at the downstream boundary, at Liston Point, ranged between 8 and 15 ppt and the boundary values were estimated as described in Section 6.2.

Predicted and measured tidal elevations at Reedy Point, Philadelphia and Trenton are compared on Figure 6-27. Note that no data were available at Trenton for this period. Only the month of August is presented for clarity. As would be expected, similar agreement between model and data was obtained during the validation period as was found for the calibration period. Current meter data were not available during this validation period.

Salinity data were collected about once every two weeks as part of the routine water quality sampling program in the estuary. Because this data set was generated from infrequent surface grab samples, its usefulness for model validation is somewhat limited. Of particular concern is specification of salinity at the downstream boundary, which involved temporal interpolation over long time periods (about two weeks). Also, only surface data were collected, making it necessary

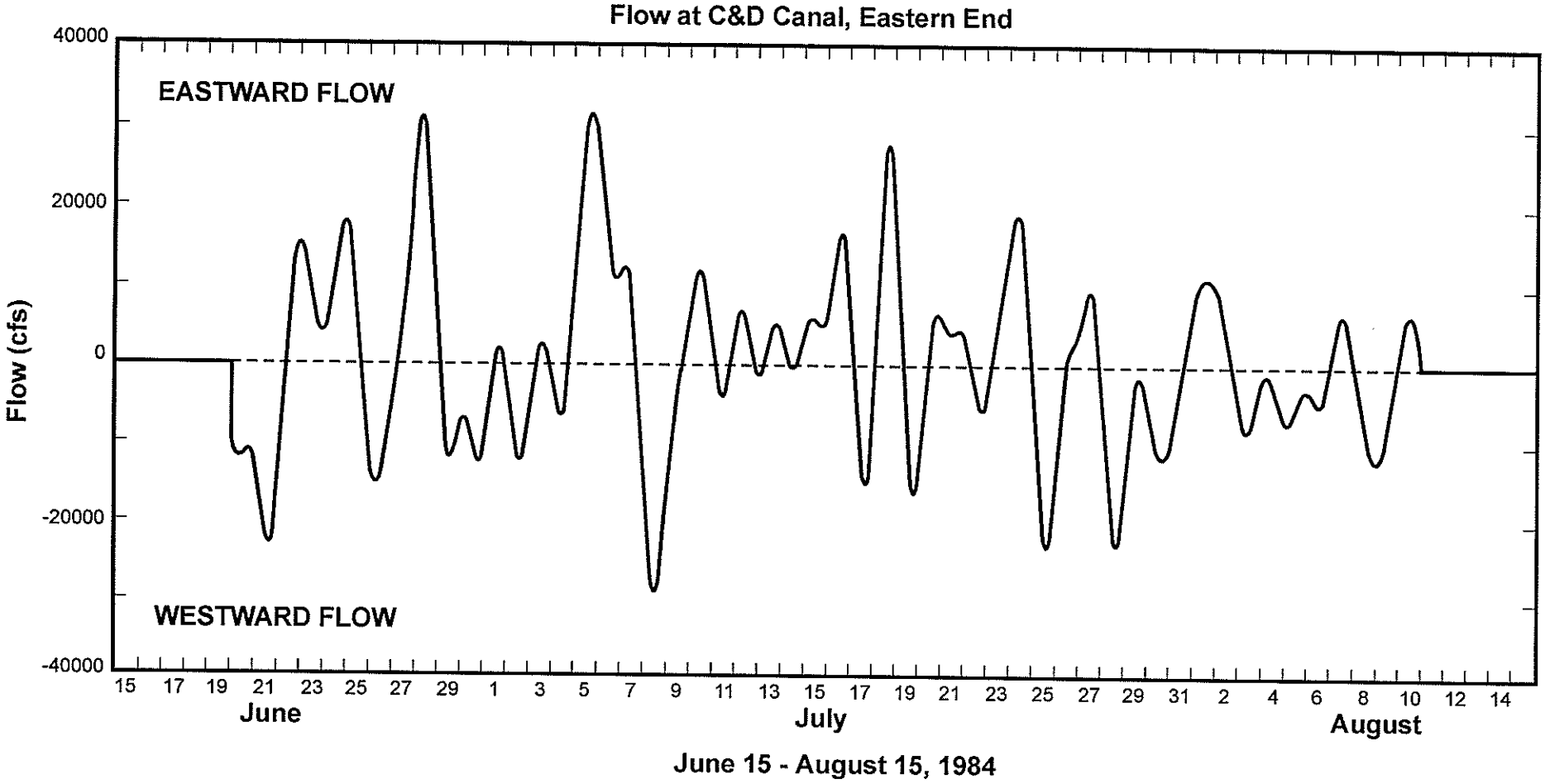

Figure 6-26. Predicted Residual Flow Rate at Eastern End of C&D Canal During 1984 Calibration Period.

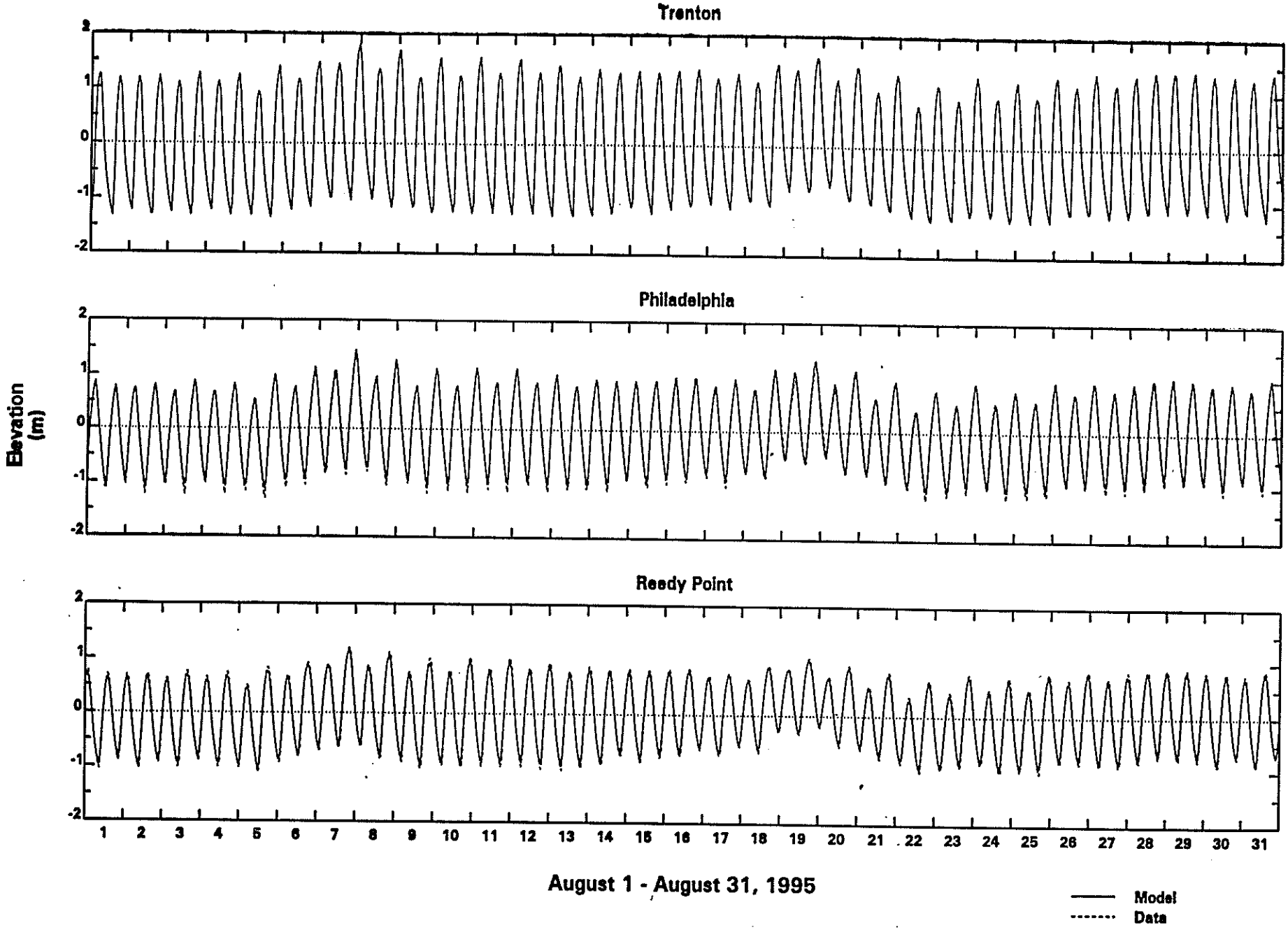

Figure 6-27. Comparison of Measured and Predicted Tidal Elevations at Trenton, Philadelphia and Reedy Point During 1995 Validation Period.

to make assumptions about the vertical distribution of salinity at the boundary, see Section 6.2 for a description. Thus, some uncertainty in the validation results exists due to uncertainty in specification of the downstream boundary condition.

Comparisons of predicted and observed spatial distributions of surface salinity in the Delaware River Estuary during this period are presented on Figure 6-28. The six days shown on that figure correspond to DRBC sampling runs on the river that were conducted approximately once every two weeks. Model output is presented as a daily average (solid line) and a range (shaded area) because the data were not collected synaptically. Generally, the model satisfactorily reproduces the longitudinal distribution of surface salinity in the estuary with the upstream limit of the salinity intrusion being predicted quite well. Cross-plots of predicted and measured salinities are shown on Figure 6-29. The model appears to adequately simulate the transport of salt in the Delaware River Estuary.

6.5 1991 VALIDATION PERIOD

Simulation of a 130-day period in 1991, from June 1 to October 8, provides further validation of the hydrodynamic model. This period was used for validation of the water quality model and it is quite similar hydrologically to the 1995 validation period. Daily average flow rates ranged from 2,300 to 7,800 cfs and salinity values at the Liston Point boundary were between 6.5 and 11.5 ppt. As was found in the 1984 and 1995 simulations, good agreement between measured and predicted tidal elevations at Reedy Point, Philadelphia and Trenton was achieved, see Figure 6-30.

Similar to the 1995 validation period, calculated longitudinal distributions of salinity were compared to data collected during the 1991 validation period. Similar to the 1995 validation results, model predictions agreed reasonably well with observed salinity distributions, see Figures 6-31a and 6-31b. Cross plots of predicted and observed salinities during the 1991 simulation period are presented on Figures 6-32a and 6-32b.

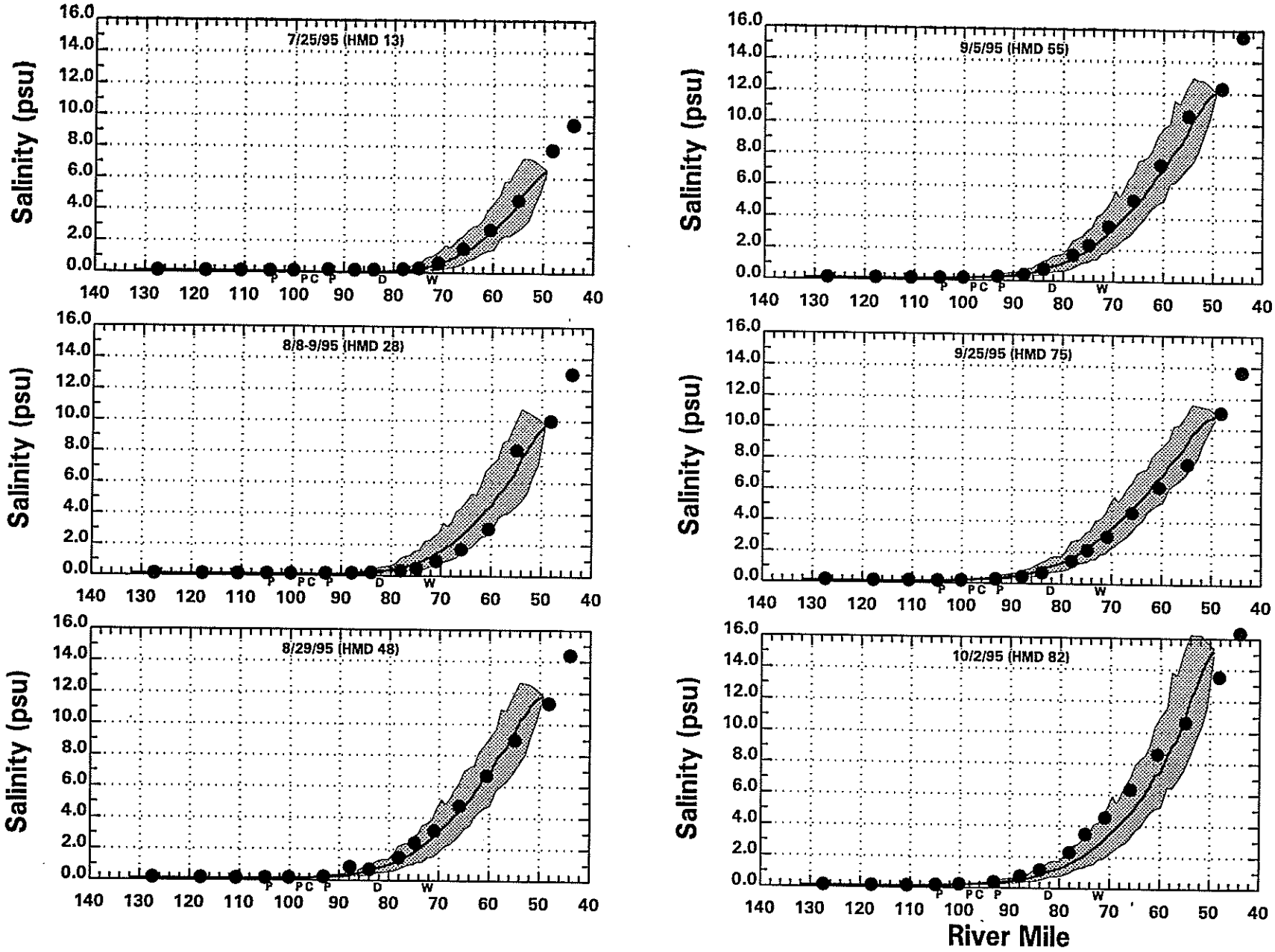

Figure 6-28. Comparison of Observed and Predicted Longitudinal Distributions of Surface Salinity on Six Days During 1995 Validation Period.

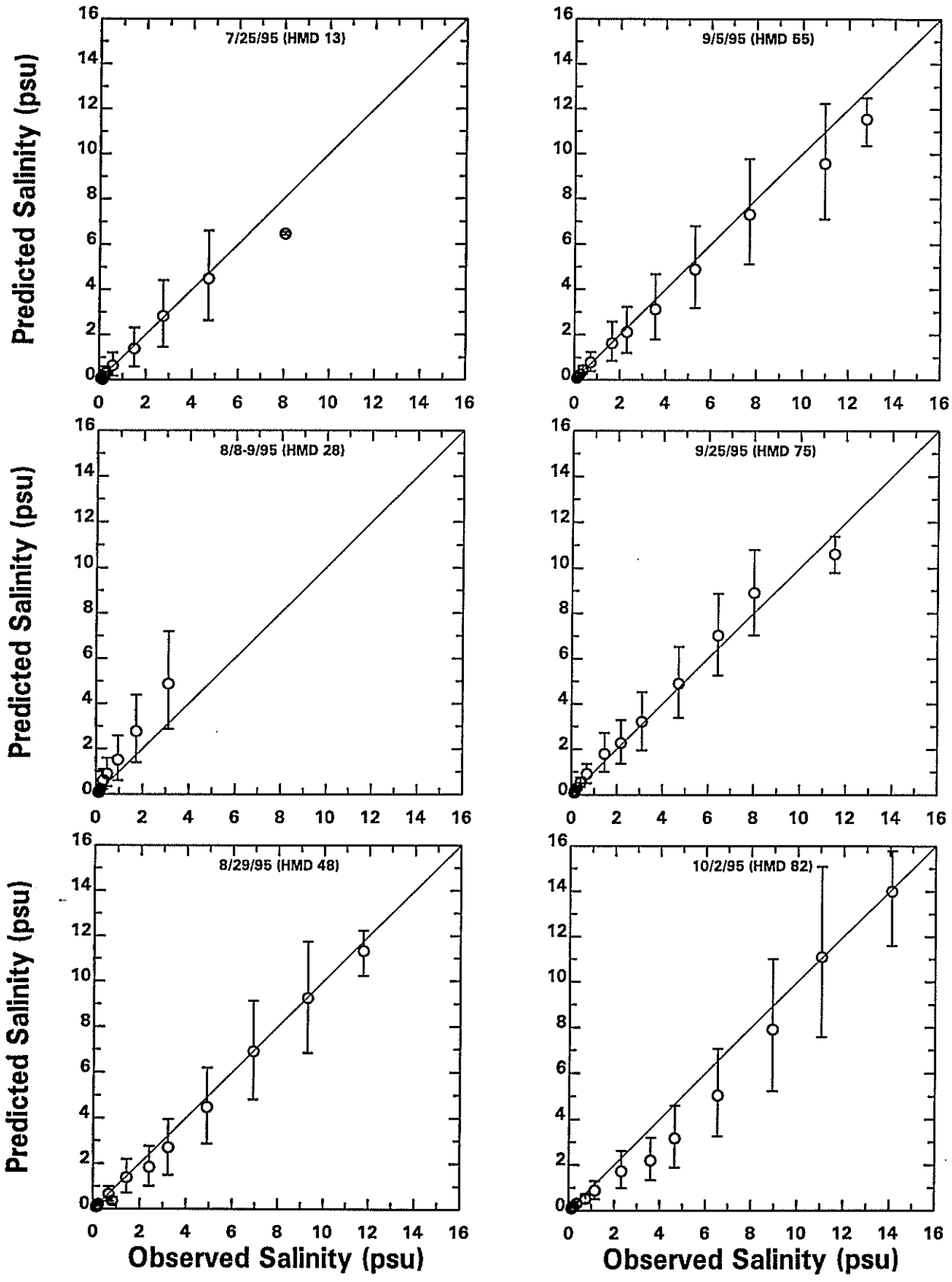

Figure 6-29. Cross-plots of Predicted and Measured Surface Salinities on Six Days During 1995 Validation Period.

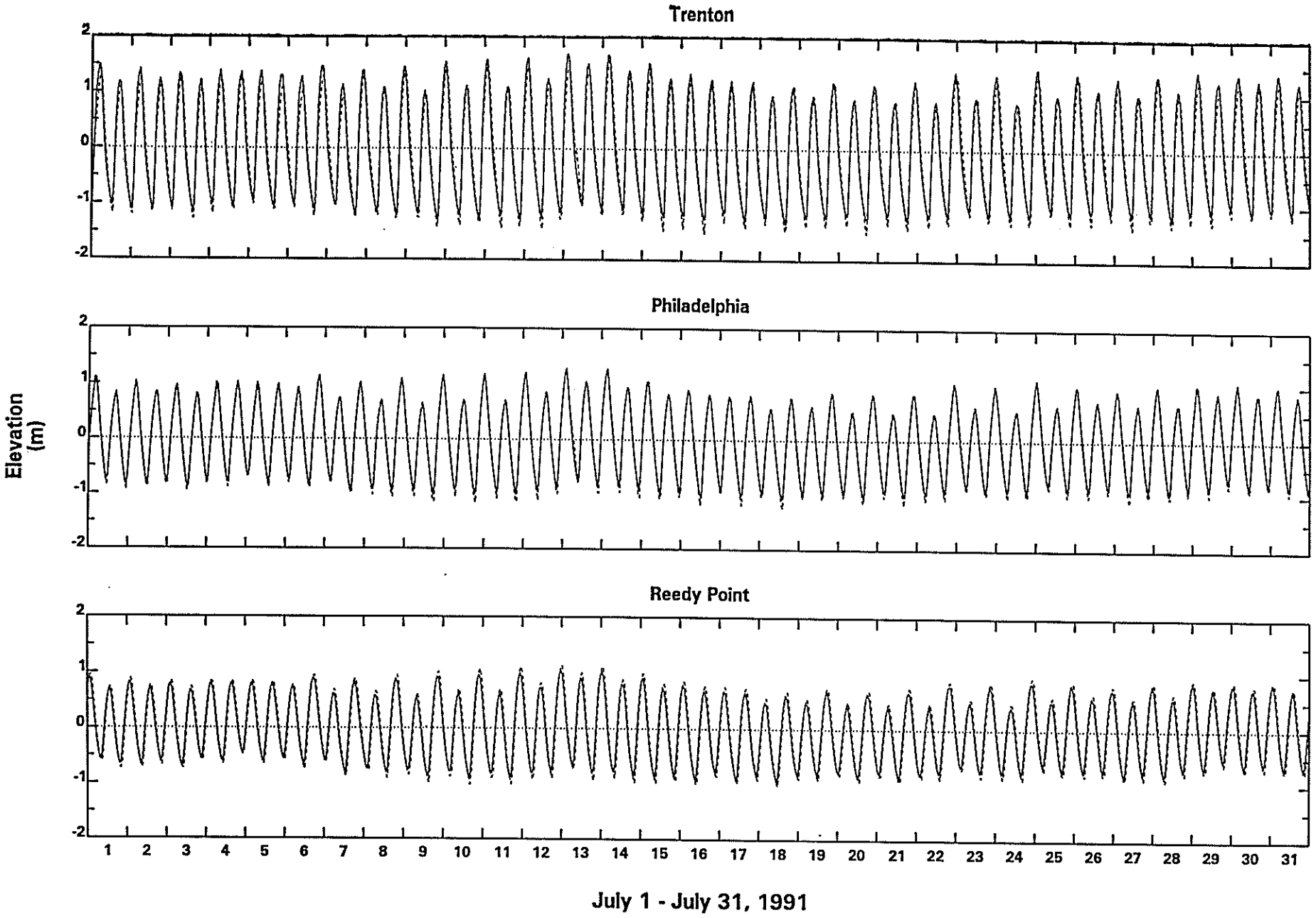

Figure 6-30. Comparison of Measured and Predicted Tidal Elevations at Trenton, Philadelphia and Reedy Point During 1991 Validation Period.

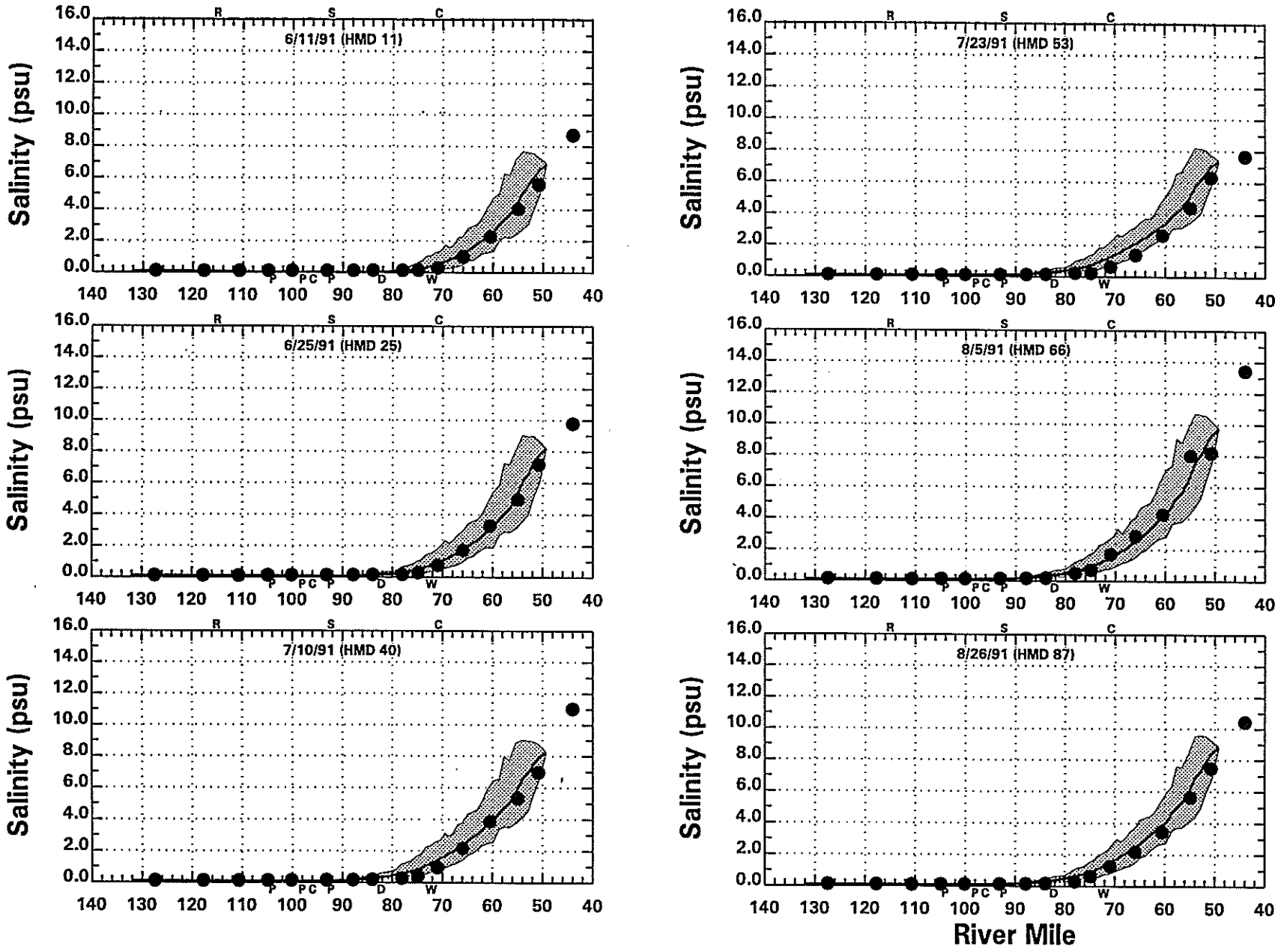

Figure 6-31a. Comparison of Observed and Predicted Longitudinal Distributions of Surface Salinity on Six Days During 1991 Validation Period.

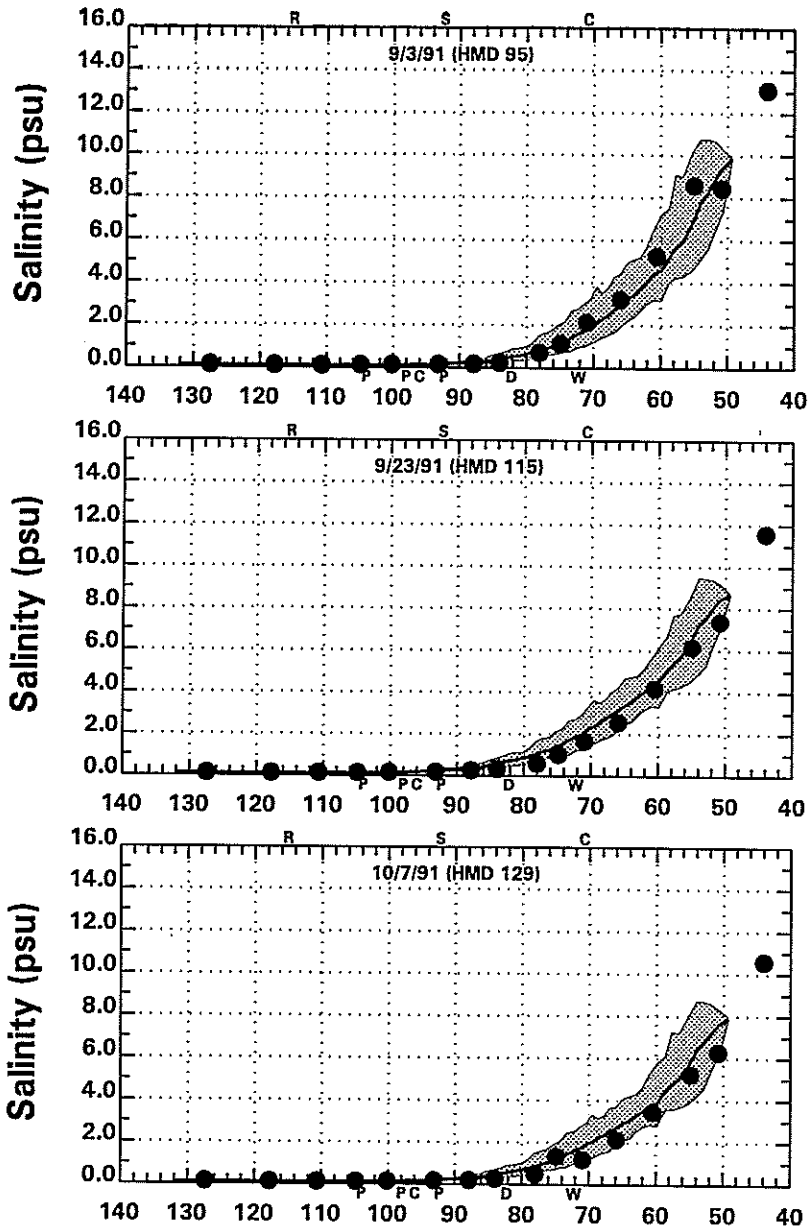

Figure 6-31b. Comparison of Observed and Predicted Longitudinal Distributions of Surface Salinity on Six Days During 1991 Validation Period.

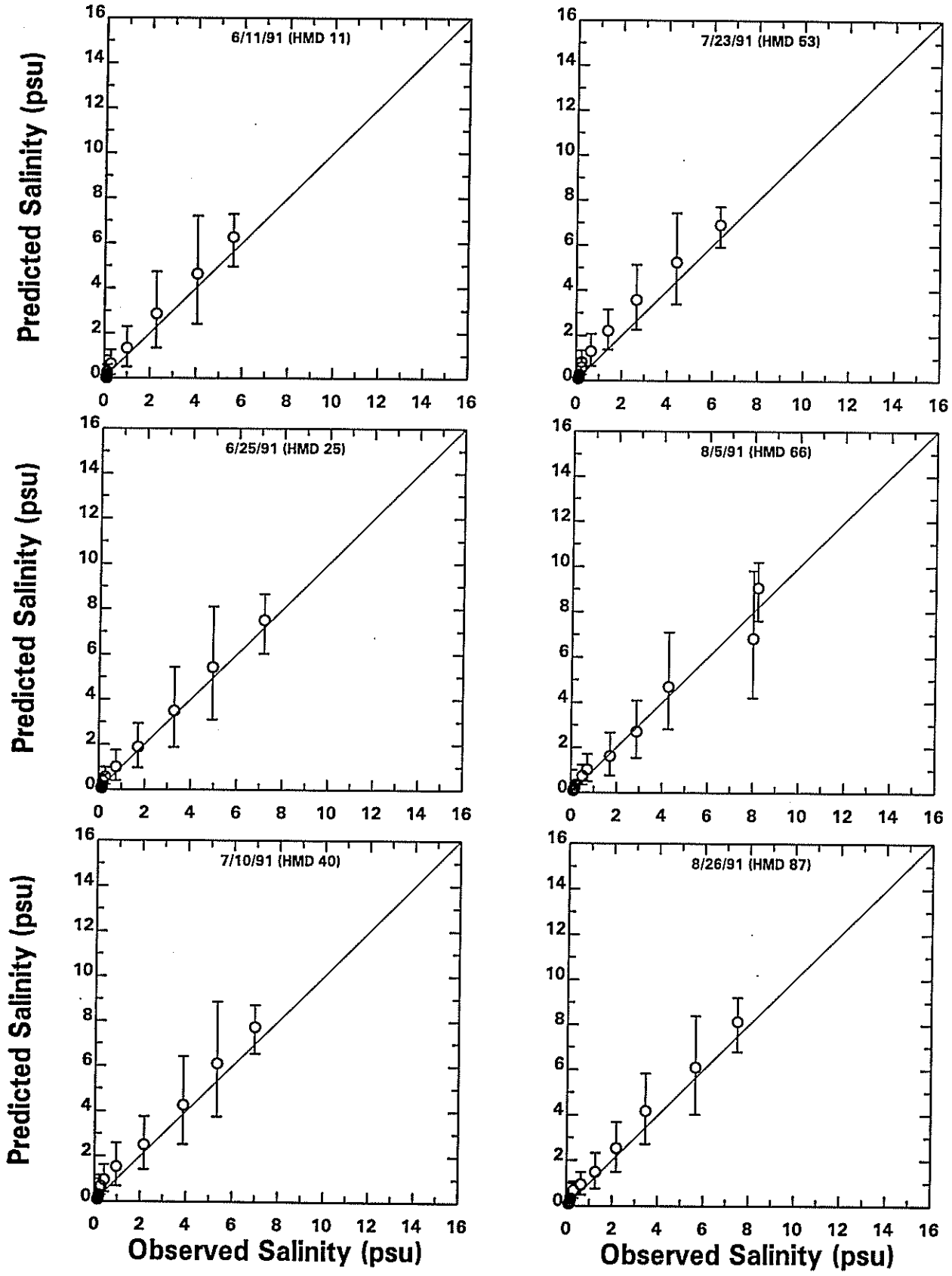

Figure 6-32a. Cross-plots of Predicted and Measured Surface Salinities on Six Days During 1991 Validation Period.

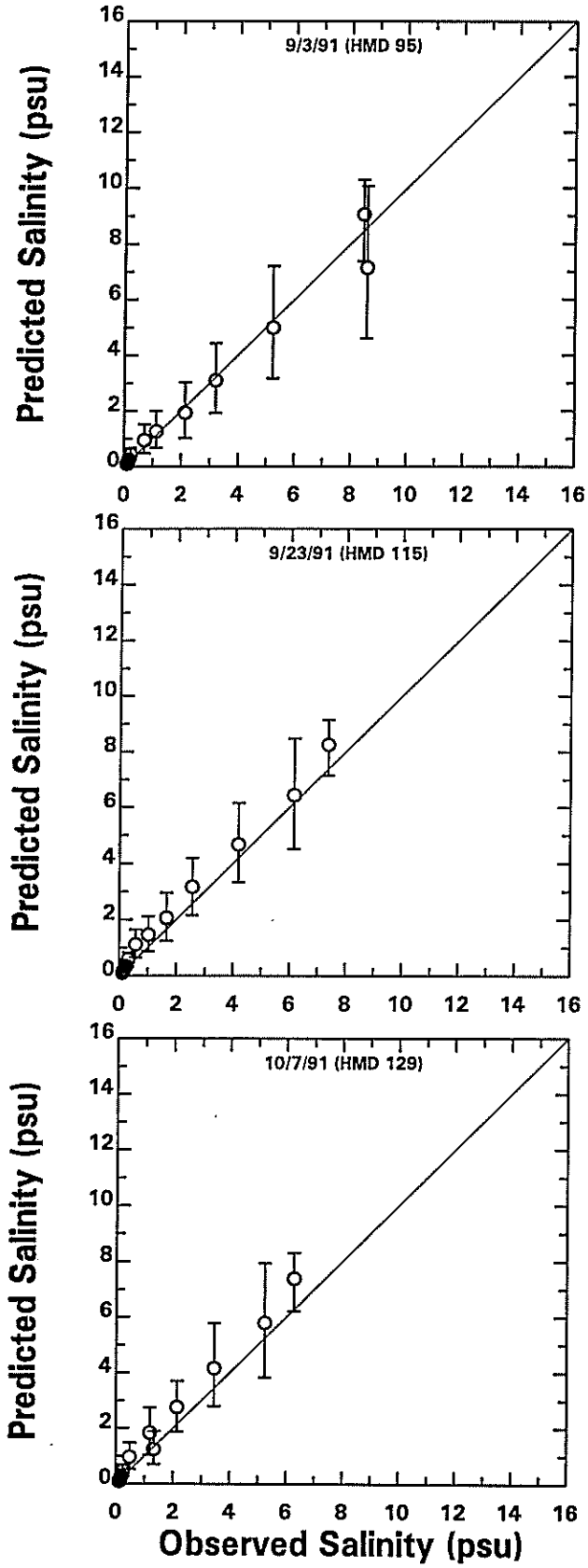

Figure 6-32b. Cross-plots of Predicted and Measured Surface Salinities on Three Days During 1991 Validation Period.

SECTION 7

WATER QUALITY MODEL CALIBRATION

This section describes the development, calibration and validation of the Delaware River water quality model. This section is divided into four subsections. Section 7.1 discusses the model inputs and forcing functions, which include boundary conditions, water temperature, meteorological conditions, light extinction coefficients, algal stoichiometry and kinetics, pollutant loadings, and reaction rates for BOD oxidation, nitrification, and reaeration. Next, Section 7.2 shows the model calibration to the 1995 data set followed by the model validation to the 1991 data set in Section 7.3. Finally, model sensitivity to reaction rates and loadings is presented in Section 7.4.

7.1 MODEL INPUTS AND FORCING FUNCTIONS

7.1.1 Boundary Conditions

A total of twelve boundary conditions are included in the model, ten are freshwater inputs which include the upstream Delaware River at Trenton and nine tributaries. These freshwater inputs are time variable freshwater discharges with no tidal exchange across the boundary interface. The other two boundary conditions are open water boundaries located at Liston Point and the Chesapeake side of the Chesapeake-Delaware Canal. Since these are open water boundaries, tidal exchange will occur across the boundary interface. Due to this tidal exchange, boundary concentrations are assigned only on the incoming tide.

The upstream boundary at Trenton (RM 133) was assigned the values of water quality measurements made at RM 127, which is the nearest DRBC sampling station. Since BOD concentrations are not typically measured by DRBC, the upstream ultimate carbonaceous BOD (CBODu) boundary value was assigned at 5.0 mg/l consistent with a special long term BOD River study done in August 1994.

For both 1995 and 1991, water quality data available for the nine freshwater tributaries and the C & D canal was limited and at best collected only once a month. With only limited data available, the data for each tributary and C & D Canal were averaged over the entire 1990 through 1995 period. These average values were then used as constant boundary concentrations for both the 1995 and 1991 modeling periods.

At the Liston Point boundary (RM 48.5), the assigned water quality boundary values for 1991 were interpolated from DRBC data at RM 44.0 and RM 50.8. In 1995, the sampling station at RM 50.8 was switched to RM 48.2. Since this is almost the same location as the model boundary at RM 48.5, data collected at RM 48.2 was used as the downstream boundary in 1995. As mentioned above, DRBC does not routinely measure BOD and, therefore, the downstream CBODu was assigned at 1.8 mg/l consistent with the 1994 long term BOD study.

The modeling framework requires that the organic material be assigned in either the dissolved or particulate form. Total CBODu, total organic nitrogen and total organic phosphorus were, therefore, assigned as 50% dissolved and 50% particulate.

The average BOD5 and ammonia tributary loadings for the 1991 and 1995 modeling periods are presented on Figure 7-1. Due to its high flow relative to the other tributaries, the Schuylkill's BOD5 load of 13,000 pounds per day is more than double the next highest BOD5 load. The tributary ammonia loads are small, ranging between 100 and 1000 pounds per day. In Figure 7-2, the same loads from Figure 7-1 are presented as CBODu and ultimate nitrogenous BOD (NBODu). In terms of oxygen demand, the tributary CBOD loads are over a factor of ten greater than the tributary ammonia loads.

7.1.2 Water Temperature and Meteorological Conditions

Water temperature and meteorological conditions affecting algal growth are presented in Figure 7-3 for 1995 and Figure 7-4 for 1991. The June through October data is plotted with the period modeled for each year indicated by the shaded area. The first panel shows the average water temperature and range. During the 1995 modeling period, the average water temperature ranged from 28.5°C in late July to 20.5°C in early October. During the August 8-9, 1995 survey, three water temperatures of approximately 18°C were measured. These low values are highly suspect given historical August water temperature and were not included as model input.

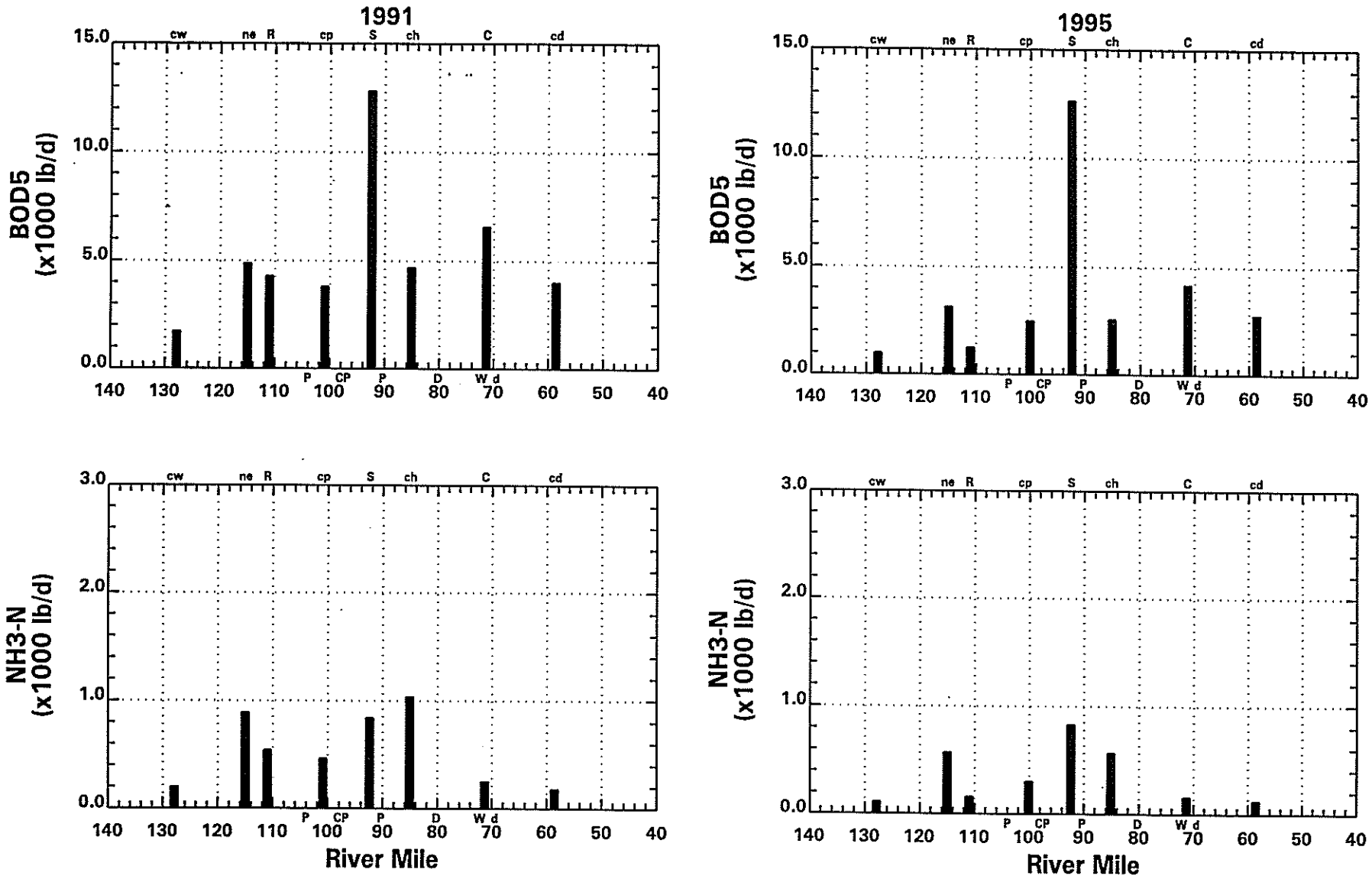

Figure 7-1. Average BOD5 and NH3 Loads from Major Tributaries for 1991 and 1995.

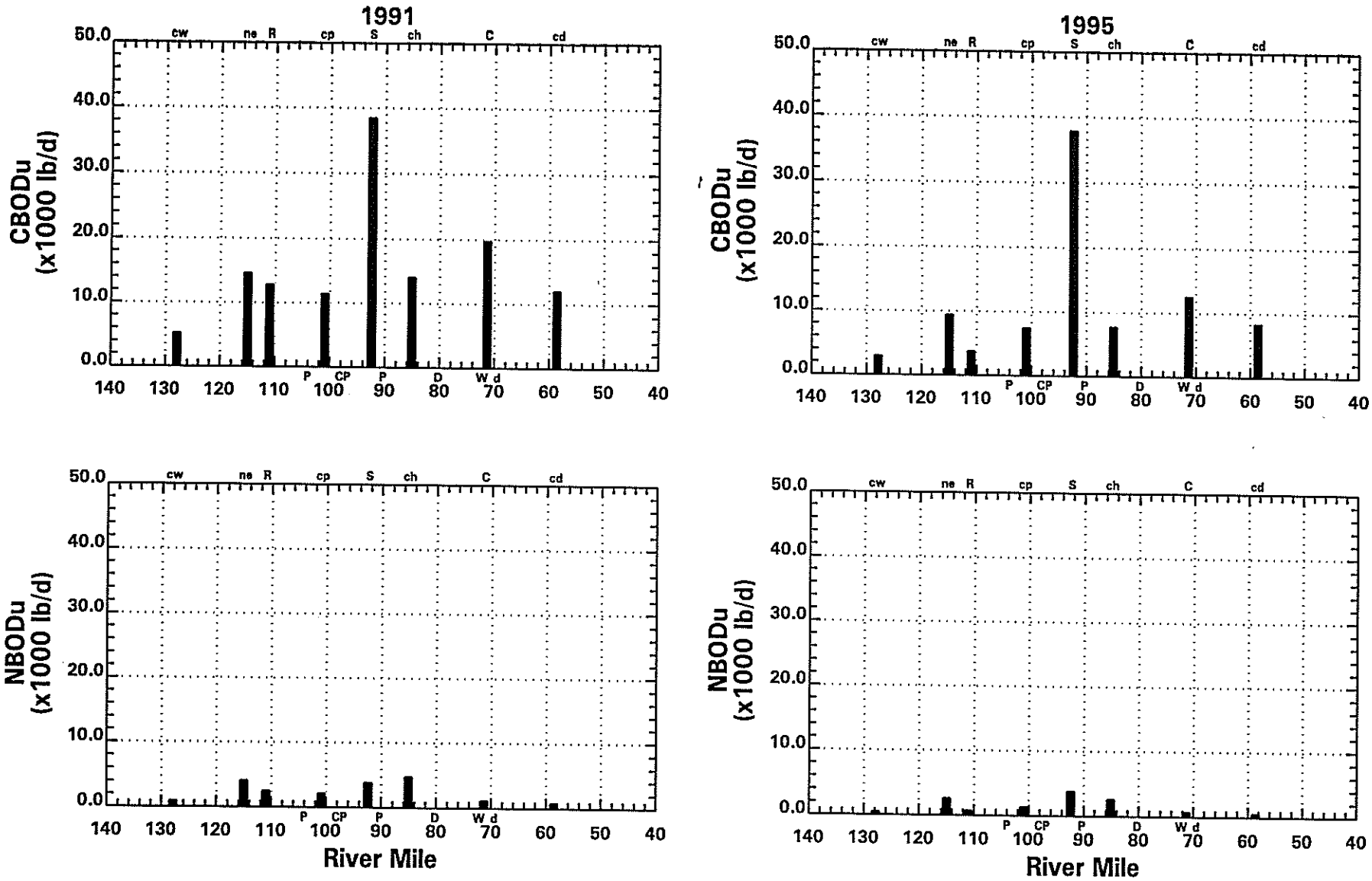

Figure 7-2. Average CBODu and NBODu Loads from Major Tributaries for 1991 and 1995.

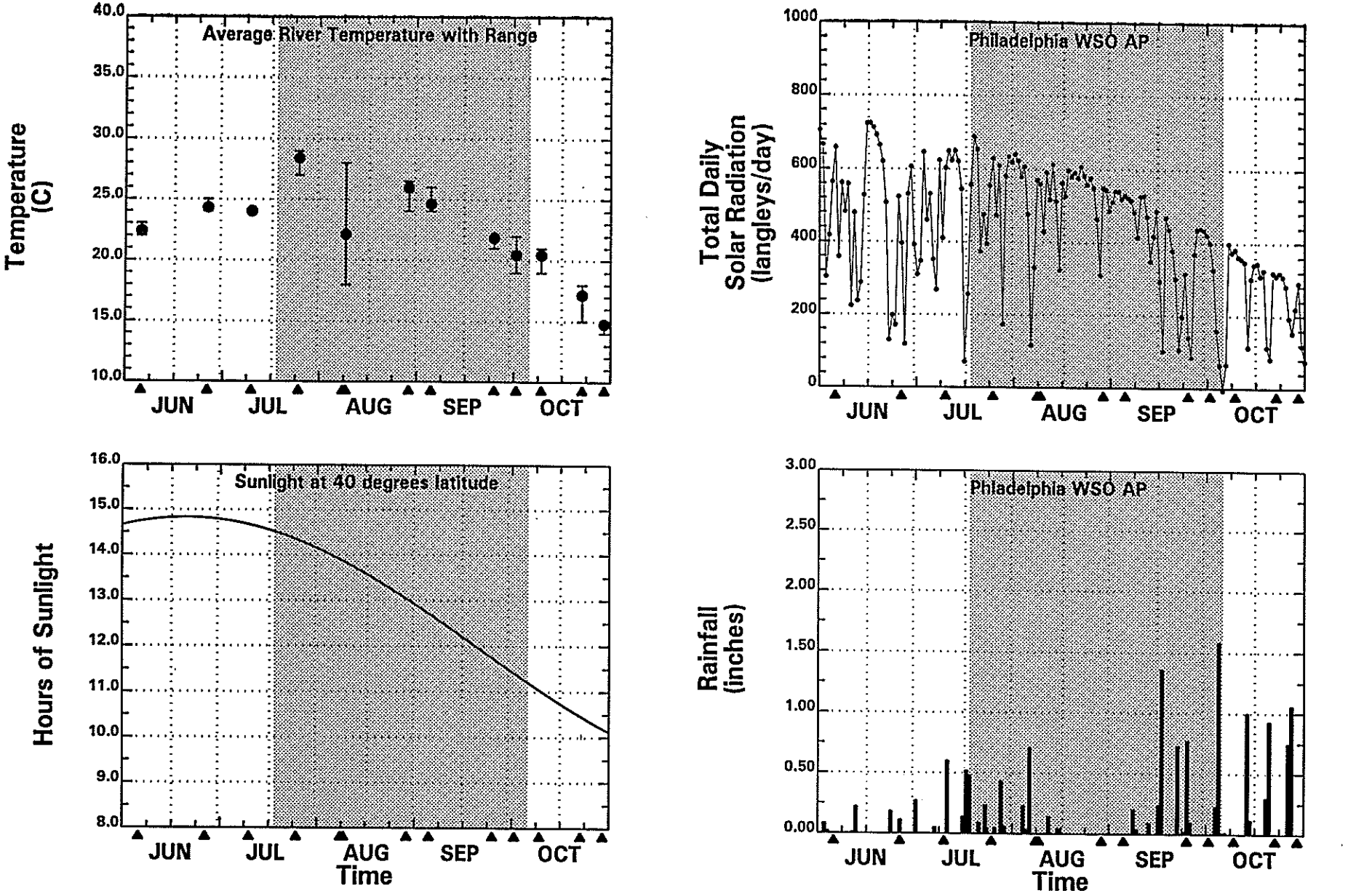

Figure 7-3. Water Temperature and Meteorological Conditions for June through October 1995.

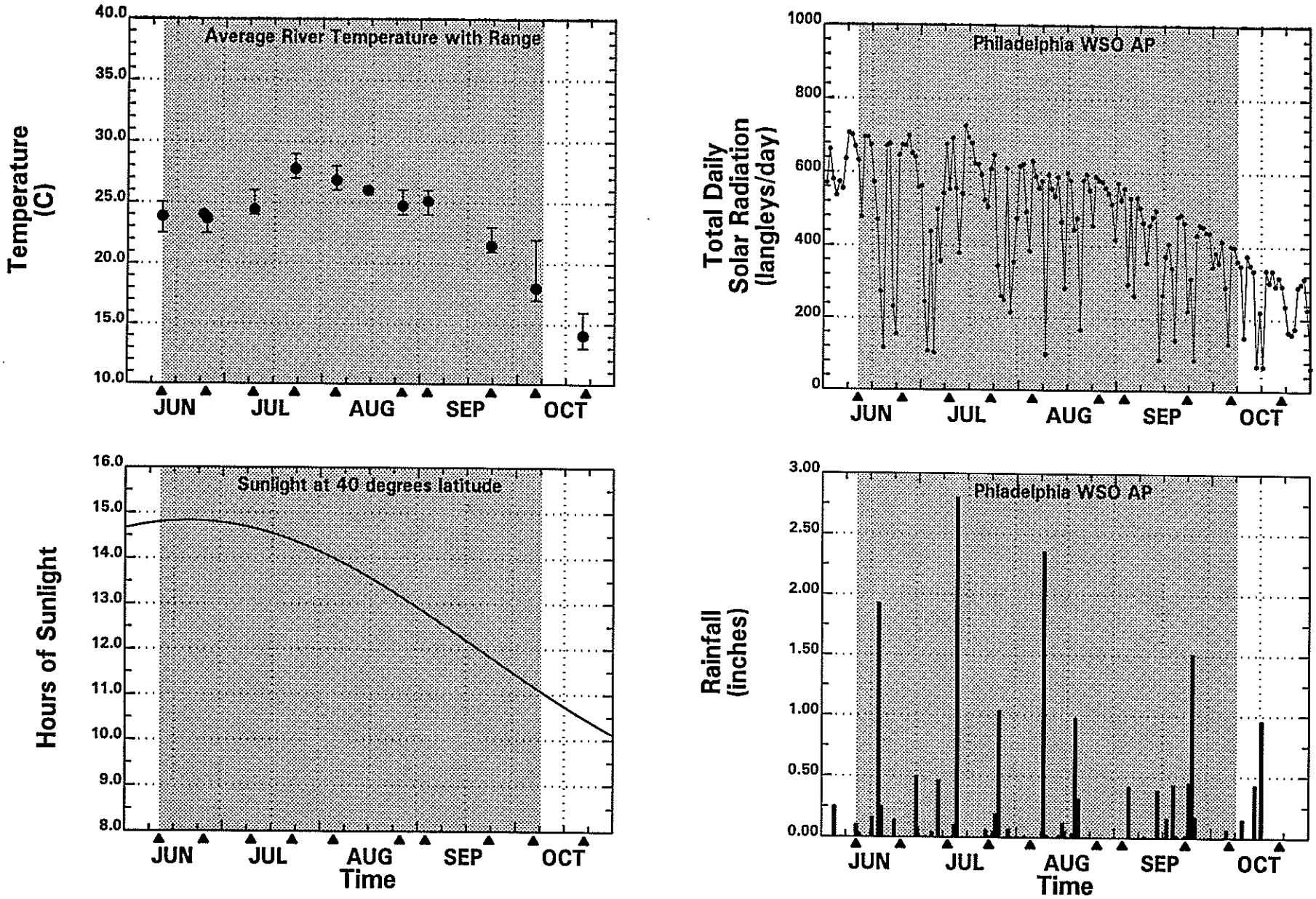

Figure 7-4. Water Temperature and Meteorological Conditions for June through October 1991.

For the 1991 period, the water temperature started at 24°C in mid June, increased to 28°C by late July and dropped to 18°C by early October. Water temperature affects the biological rates in the model with rates generally increasing with an increase in water temperature.

In the second panel, hours of sunlight are shown. For both years, the modeling period generally begins at 14.5 hours of daylight and steadily decreases to 11.0 hours by early October. Since algal growth only occurs during the day, the duration of sunlight within a day is required for the algal growth calculation.

Solar radiation is estimated by the Northeast Regional Climatic Data Center based on daily cloud cover at Philadelphia Airport and is summarized in panel three. Solar radiation is a measure of the energy available for algal growth and drives the algal growth calculation. Greater solar radiation allows a higher potential for algal growth. The total daily solar radiation ranged from a maximum of 700 langleys/day in June/July to 400 langleys/day in early October for both 1995 and 1991. Although this trend in solar radiation is the same for both years, there are two noticeable differences between the 1995 and 1991 data. First, the peak solar radiation values for June and the first half of July are higher in 1991. Second, the period being modeled in 1995 has fewer dips in solar radiation than in 1991 indicating that 1995 was consistently sunnier than 1991.

The rainfall pattern is presented in panel four. While not a direct model input, the model wet weather CSO loads are a function of rainfall. The rainfall pattern also offers some insight into the dynamics of the Delaware River system. The peaks in daily rainfall correlate inversely with the dips in solar radiation indicating rainy/cloudy days. In general, the 1995 modeling period had much less rain than 1991. In particular, there was no rain during the three week stretch from mid August to early September in 1995.

7.1.3 Light Extinction Coefficients

The solar radiation that is available for algal growth is at a maximum at the surface and decreases with depth in the water column. This decrease of solar radiation with depth is estimated by an exponential decay function and the light extinction coefficient, k_e. Typically direct measurements of k_e are not available, but are calculated from secchi depth measurements using the following equation (Thomann and Mueller, 1987):

$$k_e = 1.7/Z_s \quad (7\text{-}1)$$

where:

k_e = light extinction (1/m), [1/L]
z_s = secchi depth (m), [L]

Secchi depth, however, was not routinely measured by the DRBC monitoring program, but special surveys were done in August-September 1994 and October-November 1995. Using these secchi depth measurements, k_e values were calculated with Equation 7-1. These calculated k_e values were then regressed vs total suspended solids (TSS) data to relate light extinction to TSS data. Since TSS data are available for all the surveys being modeled, estimates of k_e were calculated from TSS data using the relationship below:

$$k_{e_{BASE}} = 1.17 + 0.044 * TSS\ (mg/L) \quad (7\text{-}2)$$

The Delaware River was divided into two zones at RM 85; an upstream zone of low solids and high phytoplankton and a downstream zone of high solids and low phytoplankton. In the downstream zone, k_{eBASE} was determined from Equation 7-2. Since TSS data were only available once every two weeks, the calculated k_{eBASE} values were held constant over the two week period between sampling runs.

While the downstream zone was consistently characterized by low phytoplankton productivity, the upstream zone was more dynamic and characterized by periods of both high and low productivity. Basing $k_{e\,BASE}$ values on TSS measurement made once every two weeks proved insufficient to reproduce the dynamics of the upstream phytoplankton system. Therefore, daily turbidity measurements made at Philadelphia's Baxter drinking water intake (RM 110) were used to characterize the upstream zone. Delaware River turbidity was related to TSS values using DRBC survey data producing the following relationship:

$$TSS\ (mg/L) = 2.08 * Turbidity\ (FTU) + 0.04 \quad (7\text{-}3)$$

The calculated TSS values were then used in Pennock's equation to calculate an upstream $k_{e\,BASE}$ as described below (Pennock, 1987):

$$k_{e\,BASE} = 0.095 + 0.075 * TSS\ (mg/L) \qquad (7\text{-}4)$$

The 0.095 value represents the natural background light extinction of Delaware River water. At times, the turbidity measurements at this one upstream location (RM 110) did not appear to represent general conditions in the upstream zone based on differences in calculated and observed chlorophyll-a data. Given the lack of light extinction data in the river and the importance of phytoplankton concentration in the dissolved oxygen balance, turbidity was used to control phytoplankton growth. The turbidity used in the upstream TSS calculation was slightly adjusted to achieve reasonable agreement between calculated and measured chlorophyll-a levels.

After $k_{e\,BASE}$ was determined in the upstream and downstream zones, the self shading effect of phytoplankton was then added to the $k_{e\,BASE}$ to determine the effective k_e. The following relationship was used.

$$k_e = k_{eBASE} + 0.017 * chlorophyll\text{-}a\ (ug/L) \qquad (7\text{-}5)$$

The chlorophyll-a values used in Equation 7-5 were the values calculated by the model.

7.1.4 Algal Stoichiometry and Kinetics

In the water quality model, the phytoplankton system is based in carbon units. This phytoplankton system is then linked to other model systems by ratios between phytoplankton carbon, nitrogen, and phosphorus. Lacking measurements to calculate these ratios, the phytoplankton cells were assumed to be comprised of carbon and nutrients according to the Redfield ratios of 106 Carbon:16 Nitrogen:1 Phosphorus. Studies have found this ratio can change under stressed conditions resulting from low nutrients, but nitrogen and phosphorus concentrations never decrease to levels limiting algal growth in the Delaware River. The Redfield ratio was, therefore, held constant throughout the two modeling periods.

Since model phytoplankton is expressed as carbon and actual field measurements are expressed as chlorophyll-a, a carbon to chlorophyll ratio (C/Chl) is required to convert field data to model input and model output back to chlorophyll-a. Since field measured C/Chl ratios are not available, a C/Chl equal to 40 was used. A C/Chl ratio of 40 is reasonable for light limited systems, such as the Delaware River, and falls within the range suggested in "Rates, Constants and Kinetics Formulation in Surface Water Quality Modeling", (Tetra Tech, 1985).

The factors affecting algal production and loss rates are presented on Figures 7-5 and 7-6. The light extinction coefficient, the growth reduction factors due to light, nutrient concentration, and salinity, the algal growth and loss rates and the net algal increase rate are shown. These values are averaged over the 1995 and 1991 modeling periods respectively and represent typical depth averaged conditions. The light extinction coefficient, k_e, is low upstream until RM 85 and then drastically increases following the same pattern as river TSS concentrations. The growth reduction factors for light, nutrients and salinity are presented in panels 2 and 3. These growth reduction factors reduce the optimum growth rate to reflect actual conditions. The growth reduction factor for light, $G_I(I)$, is calculated from the k_e values. Inversely proportional to k_e, $G_I(I)$ averages approximately 0.4 upstream of RM 85 and falls below 0.1 downstream of RM 85. Since the Delaware system is nutrient saturated, the growth reduction factor for nutrients, $G_N(N)$, equals 1.0 and, therefore, does not change the growth rate. The growth reduction factor for salinity, $G_s(S)$, is 1.0 upstream and gradually drops to 0.05 as salinity increases going downstream.

The gross algal growth and loss rates are presented in panel 4. The algal growth rate is set equal to the maximum growth rate under optimum conditions (2.0/day), which is then reduced by the growth reduction factors for temperature, light, nutrient concentration and salinity. The growth reduction factors account for the suboptimum growth conditions which typically exist. Since the system is light limited, the algal growth rate closely reflects the pattern of the growth reduction factor for light presented in panel 2. In general, all phytoplankton growth takes place upstream of RM 85. The loss rates represent algal respiration, grazing by predators, and settling to the sediment. The largest loss rate is respiration, which is set equal to a basal rate of 0.04/day plus 38% of the actual growth rate. Grazing was set equal to 0.15 per day upstream of RM 110 and 0.025 per day downstream. The high grazing rate upstream was required to reproduce the observed phytoplankton data in this region and may possibly represent the effect of bivalve filtering. The algal settling velocity was set to 0.1 meter/day and was converted to a loss rate

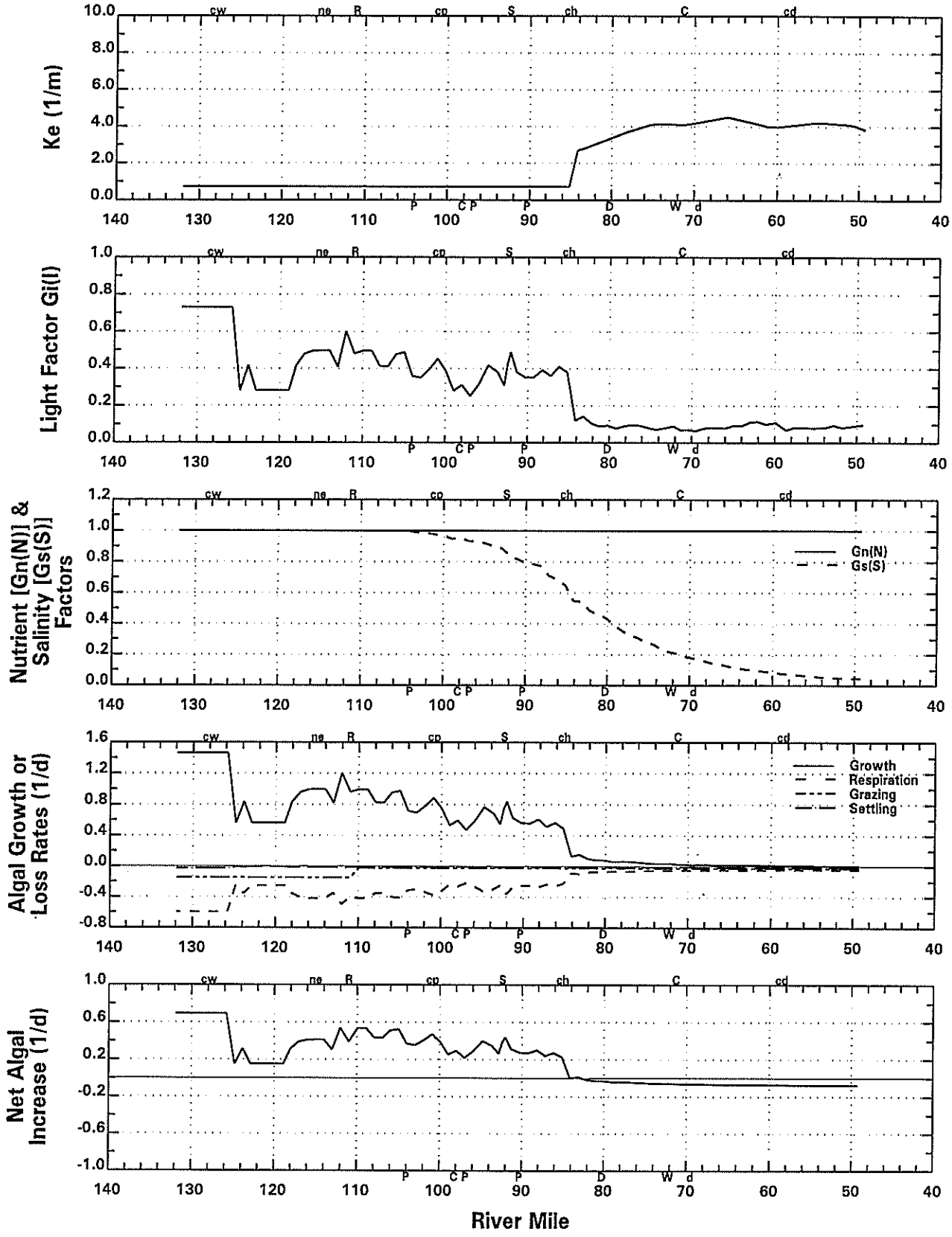

Figure 7-5. Model Algal Growth Rate and the Factors Affecting Algal Growth for 1995 (Values Averaged Over the Modeling Period).

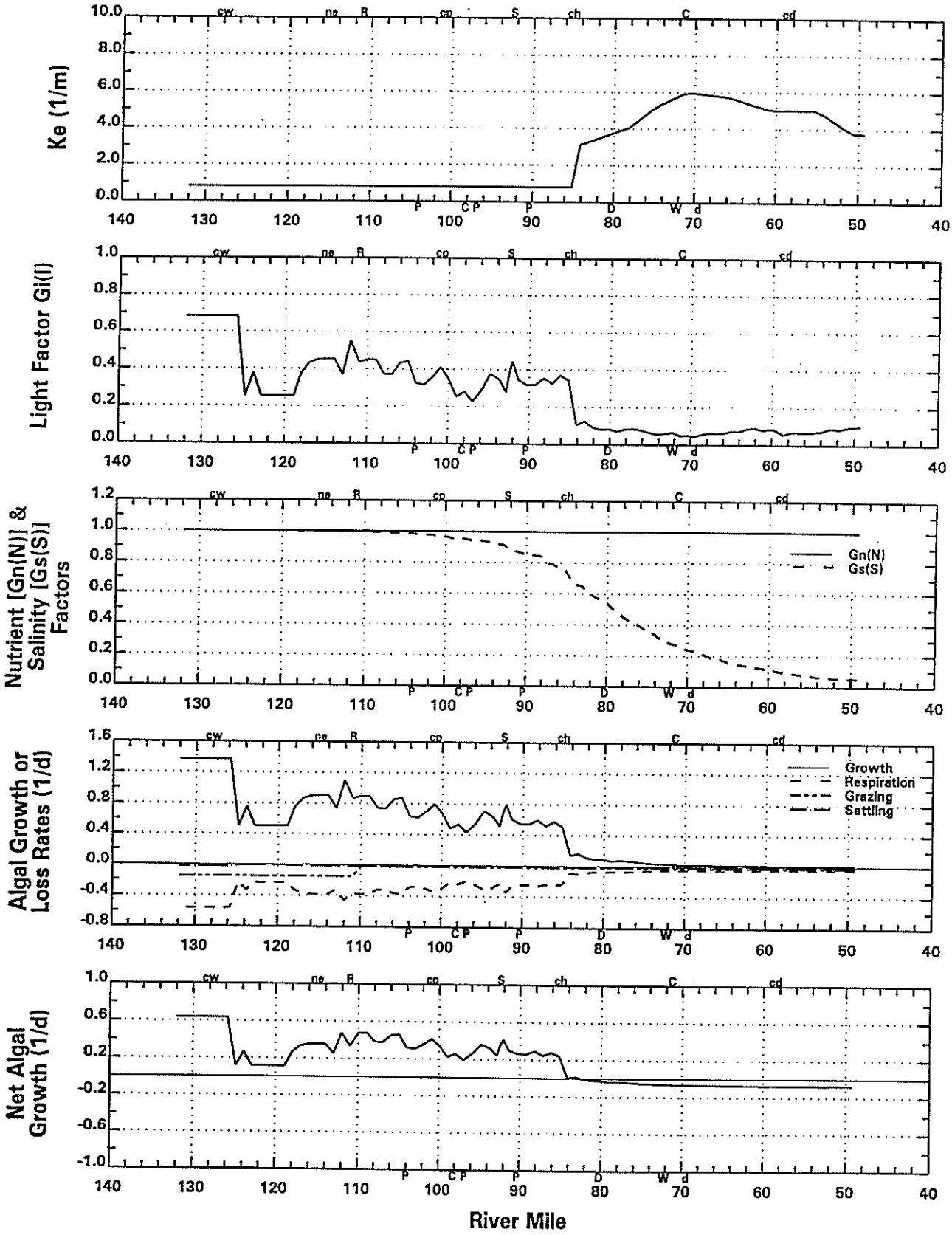

Figure 7-6. Model Algal Growth Rate and the Factors Affecting Algal Growth for 1991 (Values Averaged Over the Modeling Period).

(1/day) by dividing the settling velocity by the water column depth. Algal biomass loss by settling is small relative to respiration and grazing.

The net rate of algal increase is equal to the gross algal growth minus the total loss due to the combined effect of respiration, grazing and settling and is presented in panel 5. Above RM 85, there is typically a net increase in phytoplankton, which gradually decreases. While downstream of RM 85, there is typically a small constant net loss of phytoplankton.

7.1.5 Rates Affecting Oxygen: BOD Oxidation, Nitrification and Reaeration

The spatial patterns for the BOD oxidation, nitrification and reaeration rates used for the 1995 and 1991 modeling periods are presented in Figure 7-7. These rates did not vary temporally. BOD oxidation was also spatially constant and set to 0.05/day. The nitrification rate, K_N, varied spatially with the River divided into three nitrification zones: zone 1(RM 133 to 110) with K_N = 0.1/day, zone 2 (RM 110-83) with K_N = 1.0/day and zone 3 (RM 83-48.5) with K_N = 0.5/day. The assignment of the nitrification rate to each zone was guided by the fit of the model to the ammonia and nitrite+nitrate data. The same rates for BOD oxidation and nitrification were used for both the 1995 and the 1991 modeling periods. Presented in panel 3, reaeration rates were calculated using the O'Connor-Dobbins equation as follows:

$$k_a = \frac{12.9U^{1/2}}{H^{3/2}} \qquad (7\text{-}6)$$

where:

U = the average river velocity (fps), [L/T]
H = the average depth (ft), [L]

The average river velocities where determined from the hydrodynamic model and the average depth was calculated as the ratio of the volume to surface area for each model segment.

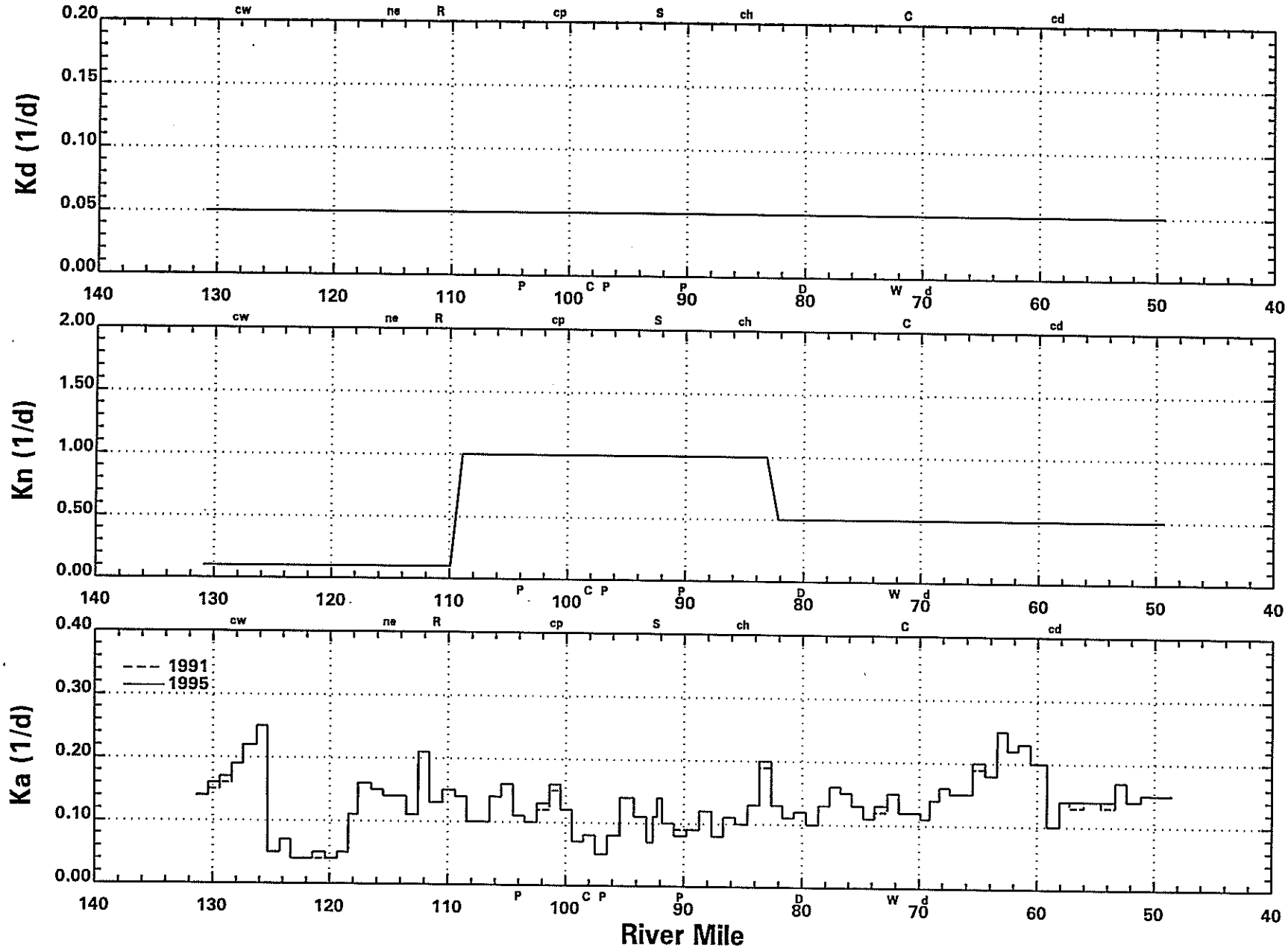

Figure 7-7. Model BOD Oxidation, Nitrification and Reaeration Rates for 1991 and 1995.

7.1.6 Pollutant Loading

7.1.6.1 Municipal and Industrial Point Sources

As discussed in Section 3.0, the Delaware River basin has a heavy concentration of municipal and industrial dischargers. The major municipal point sources on the river are shown in Figure 7-8 and include Philadelphia's Northeast, Southeast and Southwest, CCMUA (Camden), DELCORA (Chester) and Wilmington wastewater treatment plants. For these six municipal point sources, their discharges were input into the model in as much detail as was available. The discharge data available for each discharger are outlined in Table 7-1. Parameters were typically measured on either a daily or weekly basis. If a particular parameter was not measured during the given modeling period, historical values were used. In some cases no measurements for a particular parameter were available and values were estimated.

Table 7-1. Data Available for Major Municipal Dischargers

Point Source	Flow	BOD	NH_3	NO_2+NO_3	Organic Nitrogen	PO_4	Organic Phosphorus
Philadelphia, NE	■	■	X	X	X	/[a]	/[a]
Philadelphia, SE	■	■	X	X	X	/[a]	/[a]
Philadelphia, SW	■	■	X	X	X	/[a]	/[a]
CCMUA	■	■	X	/[b]	□	□	□
DELCORA	■	■	X	X	X	/[a]	/[a]
Wilmington	■	■[c]	/[d]	/[d]	/[d]	/[d]	/[d]

■ = Daily Measurements
X = Weekly Measurements
/ = Based on Measurements Outside Modeling Time Periods
□ = No Data → Values Estimated

a = Based on Total P & PO_4 measurements made October 1996
b = 1991 measurements only
c = Only average monthly values in 1991
d = Based on measurements made June - October 1988 - 1990

One industrial load, the DuPont Chamber Works facility (RM 69), is also noted on Figure 7-8 due to its significant ammonia load. The DuPont effluent ammonia concentrations were assigned based on weekly values and CBOD concentrations were assigned based on monthly Discharge Monitoring Report (DMR) values.

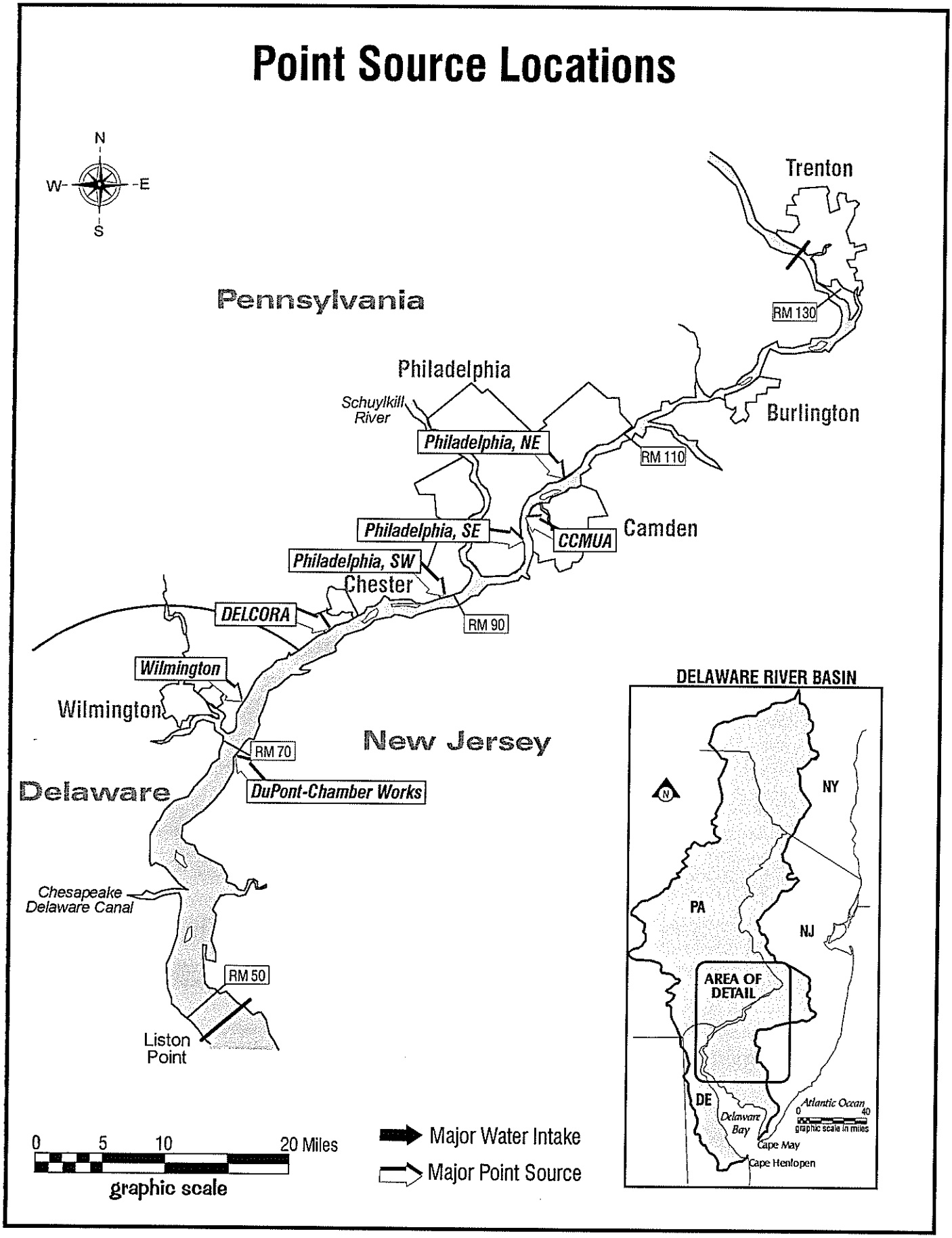

Figure 7-8. Point Source Location Map.

The average BOD5 and ammonia loadings for the 1995 and 1991 modeling periods are presented in Figure 7-9. These same loads are also presented in Figure 7-10 as CBODu and NBODu. In terms of oxygen demand, the NBODu loads from the Philadelphia Southwest plant in 1995 and the Southwest and Northeast plants in 1991 are the most significant loads for each modeling period respectively. These NBODu loads are more than double the next largest NBODu or CBODu load.

Most of the remaining industrial and smaller municipal point sources included in the model are listed in Table 7-2. This Table indicates whether BOD_5 and/or ammonia loading data were available for a particular discharger during the 1991 and 1995 modeling periods. The available data was extracted from EPA's Permit Compliance System (PCS) Database which is a compilation of DMR data. Dischargers routinely submit DMRs to regulatory agencies as part of National Pollutant Discharge Elimination System (NDEPS) permits. In general, only average monthly BOD_5 and ammonia loading data were available. While individually these smaller loads do not have significant impact on the River, their cumulative effect is important in the dissolved oxygen balance. The larger points sources described above are also included in Table 7-2 as reference.

7.1.6.2 Combined Sewer Overflows (CSO): Wet and Dry Weather

The CSO values used in the model were based on information from two DRBC CSO reports released in 1988 (DRBC, 1988) and 1994 (NJDEP, 1994), respectively. For wet weather discharges, an average of 8.3 million pounds of BOD5 per year was used as a typical combined CSO load from Philadelphia and Camden. This typical year was also assumed to have 40 inches of rain. The yearly BOD5 load was then divided by the 40 inches of yearly rainfall and multiplied by a 2.5 CBODu/BOD5 ratio. The result is an average wet weather loading rate of 518,750 lb CBODu/inch of rain. In a similar fashion, the average wet weather loading rate for ammonia was calculated as 3745 lb NH3/inch of rain. This load was based on an average CSO ammonia concentration of 1.0 mg/l and average wet weather flow rates determined from the 1994 DRBC CSO report. The same wet weather loading rates were used in both 1995 and 1991 modeling periods. During rain events, the wet weather CSO loads were put into the model at one location in the Philadelphia-Camden area, RM 93.7. The daily BOD5 and ammonia CSO loadings for 1991 and 1995 are presented in Figure 7-11. The June through October data is plotted with the period modeled for each year indicated by the shaded area. The CSO events in 1991 were more

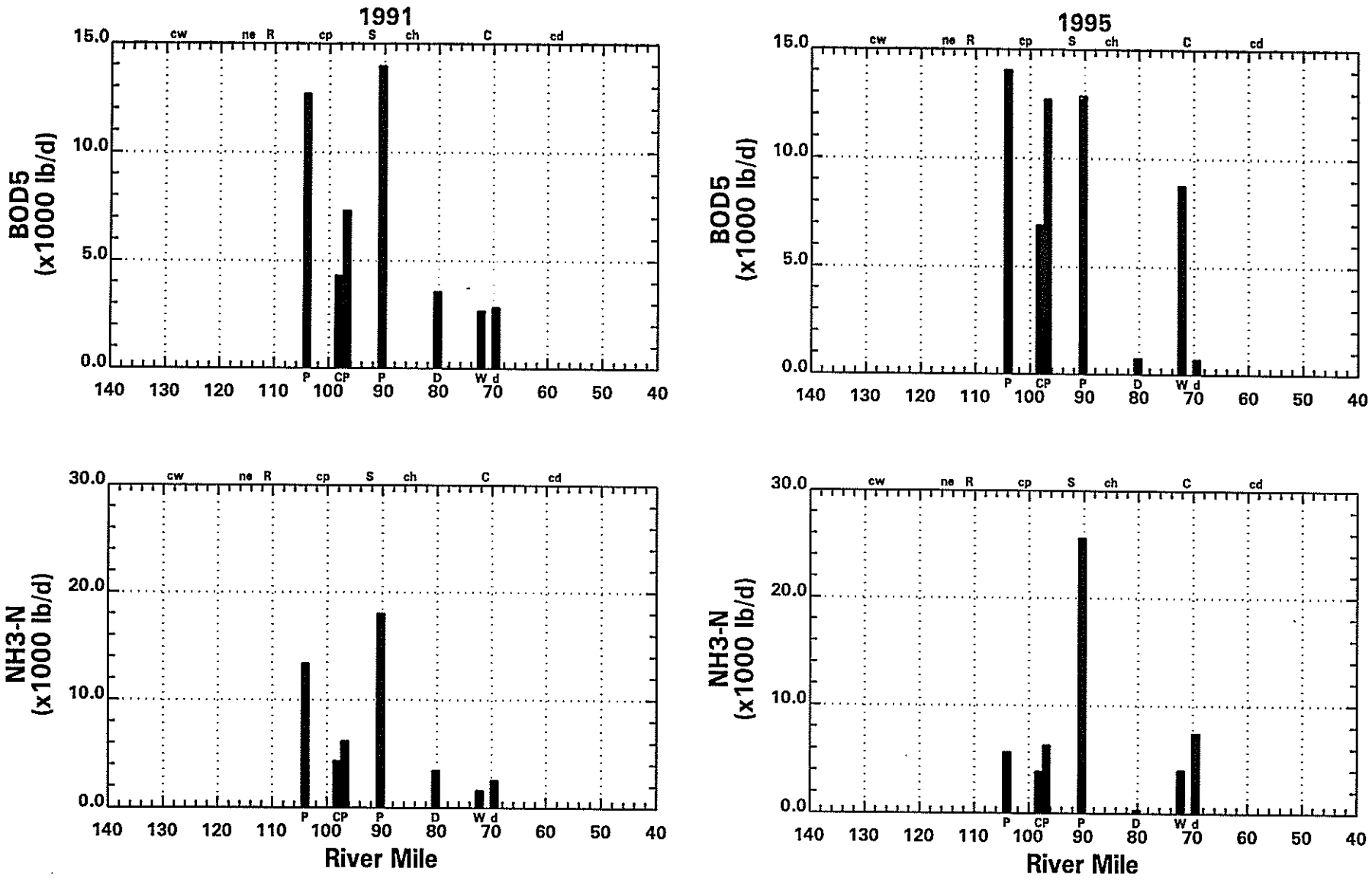

Figure 7-9. Average BOD5 and NH3 Loads from Major Dischargers for 1991 and 1995.

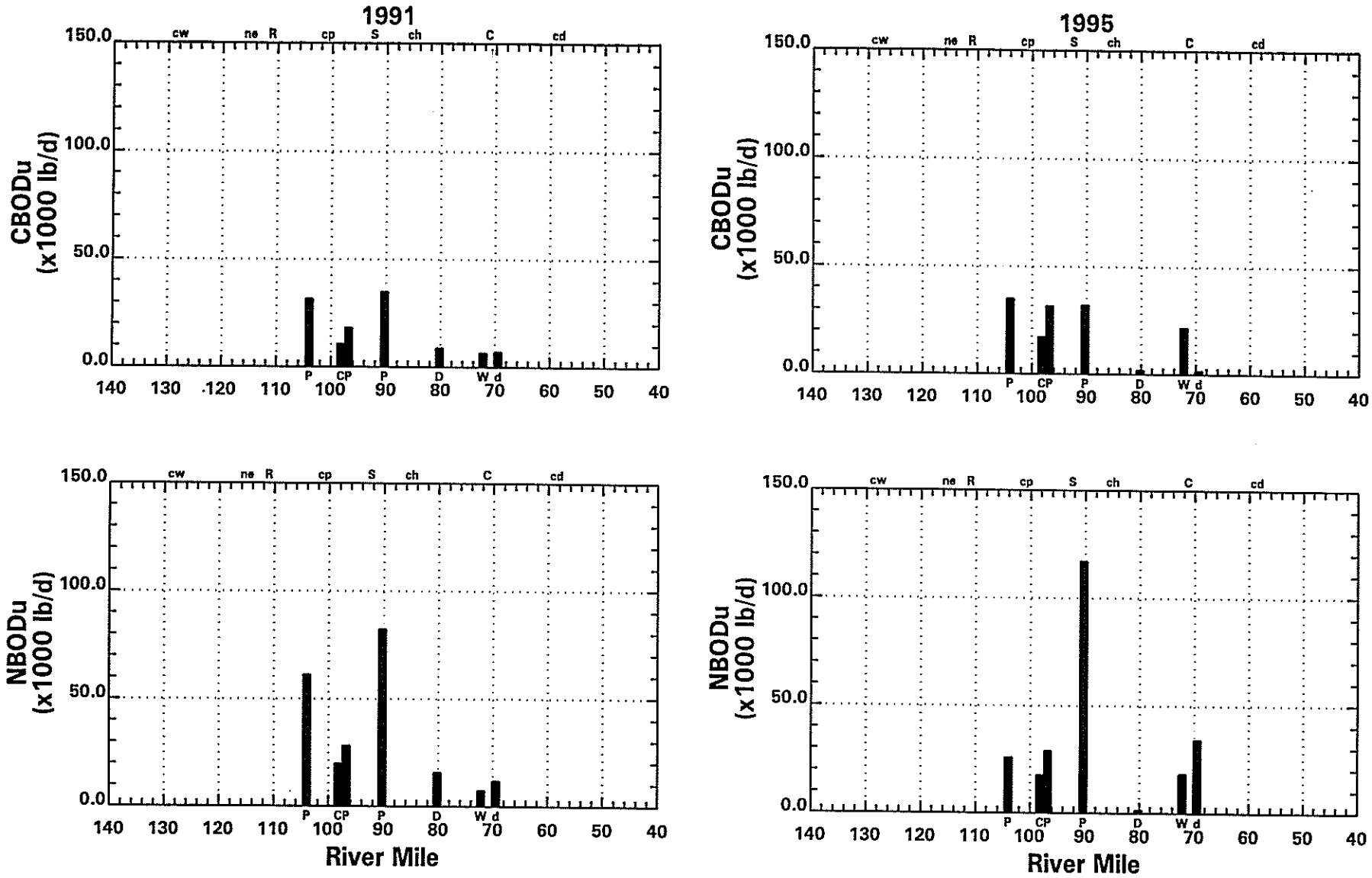

Figure 7-10. Average CBODu and NBODu Loads from Major Dischargers for 1991 and 1995.

Table 7-2. List of Discharges to the Delaware River Between RM 134 and RM 48.

State	Permit #	Outfall #	Mile Point	Description	Loads			
					BOD_5		NH3	
					1991	1995	1991	1995
PA	0026701	1	133.00	Morrisville Boro Mun. Auth-STP	X	X	X	X
NJ	0020923	1	131.80	Trenton Sewer Utility	X	X	X	X
NJ	0026301	1	128.41	Hamilton Township WPCF	X	X	X	X
NJ	0024678	1	128.22	Black's Creek WWTP	X	X		X
PA	0013463	2	127.97	United States Steel Group USX	X			
PA	0013463	5	127.97	United States Steel Group USX	X			
PA	0013463	103	127.97	United States Steel Group USX	X	X		
PA	0013463	203	127.97	United States Steel Group USX	X	X		
PA	0013463	303	127.97	United States Steel Group USX	X			
NJ	0031810	1	127.00	Fieldsboro, Borough of	X	X		
NJ	0023701	1	123.10	Florence Township STP	X	X		X
PA	0026468	1	122.10	Lower Bucks County Joint M.A.	X	X	X	X
PA	0027294	1	118.87	Bristol Boro Wat. & Sew. Auth.	X	X		
PA	0012769	9	118.70	Rohm & Haas Company	X	X		
NJ	0024660	1	117.12	Burlington City STP	X	X		X
NJ	0004391	1	117.10	Colorite Polymers Company			X	X
PA	0026450	1	116.91	Bristol TWP	X	X	X	X
NJ	0027481	1	114.70	Beverly Sewerage Authority	X	X	X	X
NJ	0025178	1	111.06	Mt. Laurel TWP MUA	X	X	X	X
NJ	0022519	1	111.06	Riverside STP	X	X	X	X
NJ	0023361	1	111.06	Willingboro Water PCP	X	X	X	X
NJ	0023507	1	111.00	Delran Sewerage Authority	X	X	X	X
NJ	0024007	1	108.82	Cinnaminson STP	X	X	X	X
NJ	0021610	1	108.76	Riverton Sewage Treatment	X	X	X	X
NJ	0024449	1	107.66	Palmyra STP	X	X	X	X
NJ	0004669	1	104.40	Georgia Pacific Corporation		X		
PA	**0026689**	**1**	**104.2**	**Philadelphia - Northeast WPCP**	**X**	**X**	**X**	**X**
NJ	**0026182**	**1**	**97.93**	**CCMUA - Delaware No. 1 (Camden)**	**X**	**X**	**X**	**X**
PA	**0026662**	**1**	**96.7**	**Philadelphia - Southeast WPCP**	**X**	**X**	**X**	**X**
NJ	0005401	1	94.50	Coastal Eagle Point Oil Co.		X		X
PA	0011533	15	92.47	Sun Co., Inc., R & M		X		X
PA	0026671	1	90.7	Philadelphia - Southwest WPCP	X	X	X	X
NJ	0024686	1	89.70	Gloucester Co. Util Auth.	X		X	X
NJ	0005134	1	87.20	Hercules, Inc.			X	X
NJ	0004278	1	86.88	Air Products & Chemicals, Inc.	X			
NJ	0030333	1	86.66	Greenwich Township STP	X	X		X

Table 7-2. List of Discharges to the Delaware River Between RM 134 and RM 48.

State	Permit #	Outfall #	Mile Point	Description	Loads			
					BOD_5		NH3	
					1991	1995	1991	1995
NJ	0004219	1	86.00	E I DuPont De Nemours & Co.	X	X	X	X
PA	0028380	1	85.28	Tinicum TWP Delaware Co. Sew. Auth.		X		
PA	**0027103**	**1**	**80.70**	**DELCORA**	**X**	**X**	**X**	**X**
NJ	0005240	1	80.66	Rollins Environmental Services	X	X		
PA	0012637	201	80.20	BP Oil, Inc.		X		X
NJ	0005045	1	79.00	Monsanto Chemical Co.	X	X	X	X
NJ	0027545	1	79.00	Logan Township MUA	X	X	X	X
DE	0000655	1	78.20	General Chemical Corp.	X	X	X	X
NJ	0004286	1	76.97	The Geon Co.	X	X		
DE	0000051	1	73.40	DuPont Pigments Dept.	X	X		
DE	0000051	2	73.40	E.I. DuPont De Nemours & Comp.		X		
DE	0000051	3	73.40	E.I. DuPont De Nemours & Comp.		X		
NJ	0024023	1	72.00	Penns Grove Sewerage Authority	X	X		X
DE	**0020320**	**1**	**71.76**	**Wilmington City**	**X**	**X**	**X**	**X**
NJ	0021601	1	70.80	Carneys Point Sewage Plant	X	X		X
NJ	**0005100**	**1**	**69.75**	**DuPont - Chamber Works**	**X**	**X**	**X**	**X**
DE	0000621	1	68.58	ICI America, Inc. Atlas Point	X			
DE	0000621	2	68.58	ICI America, Inc. Atlas Point	X	X		
DE	0000621	3	68.58	ICI America Inc. Atlas Point	X	X		
DE	0000621	4	68.58	ICI America, Inc. Atlas Point		X		
DE	0000621	5	68.58	ICI America, Inc. Atlas Point	X	X		
DE	0000621	6	68.58	ICI America, Inc. Atlas Point		X		
DE	0000621	555	68.58	ICI America, Inc. Atlas Point		X		
NJ	0021598	1	67.00	Pennsville Sewerage Authority	X	X	X	X
DE	0050911	1	62.66	Occidental Chemicals	X	X		
DE	0000647	1	62.66	GeorgiaGulf Corp.	X	X		
DE	0020001	1	62.65	Std. Chlorine of Delaware	X	X		
DE	0000256	601	61.70	Star Enterprises	X	X	X	X
DE	0000612	1	61.70	Formosa Plastics Corp.	X	X		
DE	0021555	1	60.80	Delaware City Sewage Treatment	X	X		
NJ	0024856	1	58.37	Salem Wastewater Treatment Plt.	X	X		X
DE	0021539	1	54.59	Port Penn Sewage Treatment Plt.	X	X		
NJ	0050423	1	54.45	Hancock's Bridge STP	X	X		
NJ	0034282	1	54.45	Leisure Arms		X		
NJ	0025411	461	51.51	PSE&G Hope Creek Generating St.			X	X
NJ	0025411	463	51.51	PSE&G Hope Creek Generating St.	X	X		

X = Monthly DMR

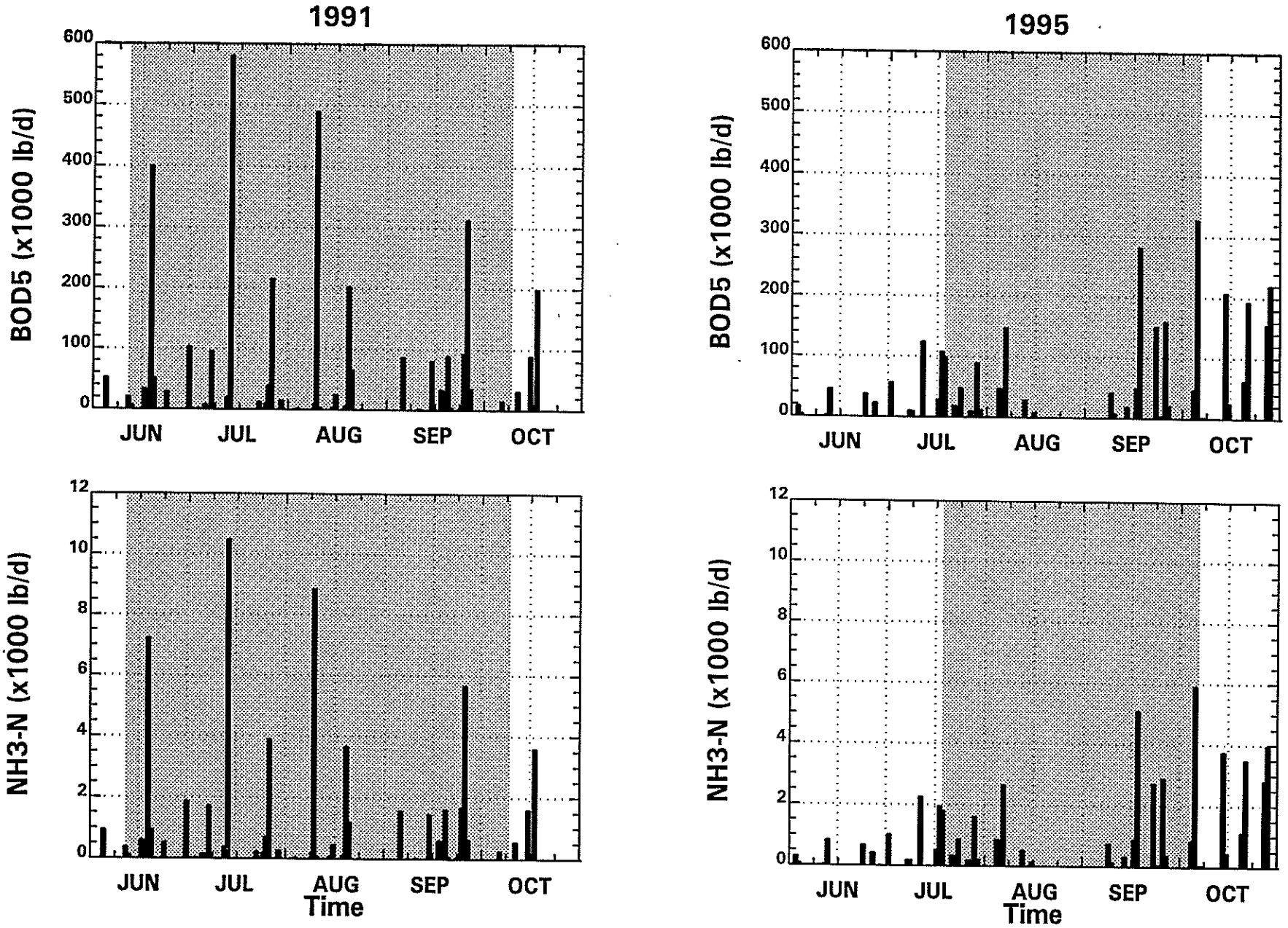

Figure 7-11. Model Wet Weather BOD5 and NH3 CSO Loads from Philadelphia and Camden for June through October 1991 and 1995.

frequent and greater in magnitude than in 1995. In terms of oxygen demand, the daily CBODu and NBODu CSO loadings for 1991 and 1995 are presented on Figure 7-12. For both years, the CBODu loads are more than a factor of ten greater than the NBODu loads.

During the 1990s, a large effort was made to eliminate dry weather CSOs. Based on the success of this effort, the dry weather CSO loads described in the 1988 CSO report were assumed to be reduced 50% by 1991 and eliminated by 1995. Dry weather CSO loads were put into the model at two locations: for Philadelphia at RM 93.7 and for Camden at RM 97. The loadings for BOD5 and ammonia are given in the Table 7-3 below.

Table 7-3. 1991 Dry Weather CSO Loads

	BOD5 [lb/day]	NH_3 [lb/day]
Philadelphia	11,830	1,390
Camden	4,880	575

The CBOD oxidation rate for the wet weather load was spatially constant and set to 0.05/day. This rate is the same value used for the oxidation of point source and non-point source (upstream and tributaries) CBOD. Although the model is set up to accommodate different reaction rates for CSO inputs, no data on the rate of oxidation for CSO CBOD was available. Given this lack of data, the same rates were used for both the dry and wet weather CBOD inputs.

7.1.6.3 Summary of CBODu and NBODu Loading

The distribution of the total pounds of CBODu and NBODu input into the model during the 1991 and 1995 modeling periods is presented in Figure 7-13. The CBODu and NBODu inputs were grouped into five categories: the major municipal discharges (Philadelphia, Camden, Chester, and Wilmington) and DuPont's Chamber Works facility, other minor municipal and industrial discharges, CSOs, upstream Delaware River at Trenton and tributaries. For CBODu, the major dischargers (~40%) and tributaries (~30%) are the two largest sources, combining for approximately 70% of the CBODu input. Upstream and CSO sources contribute roughly 15% each and the minor dischargers contribute less than 10%. For NBODu, the major dischargers account for approximately 85% of the NBODu entering the Delaware River and each of the other

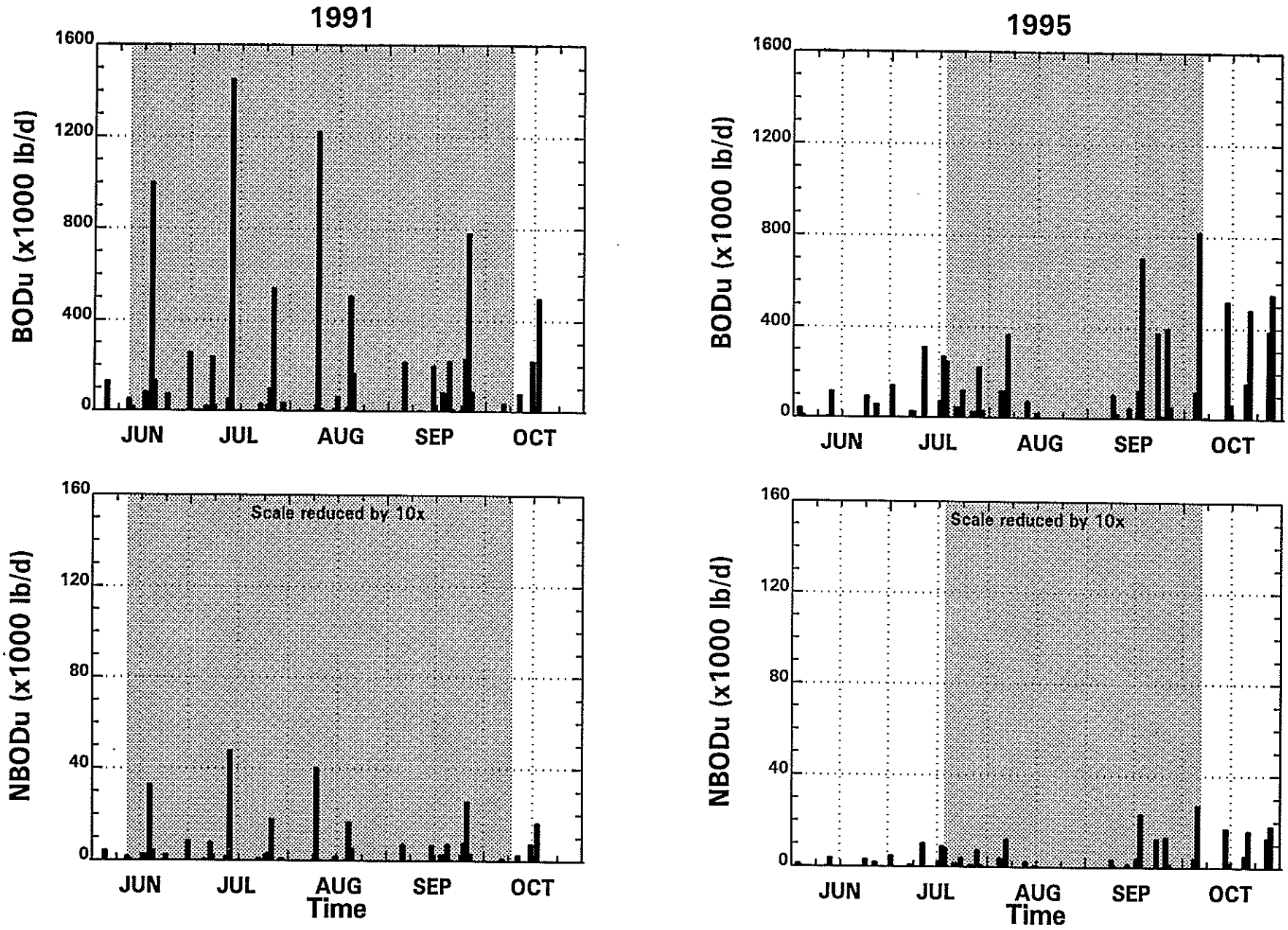

Figure 7-12. Model Wet Weather CBODu and NBODu CSO Loads from Philadelphia and Camden for June Through October 1991 and 1995.

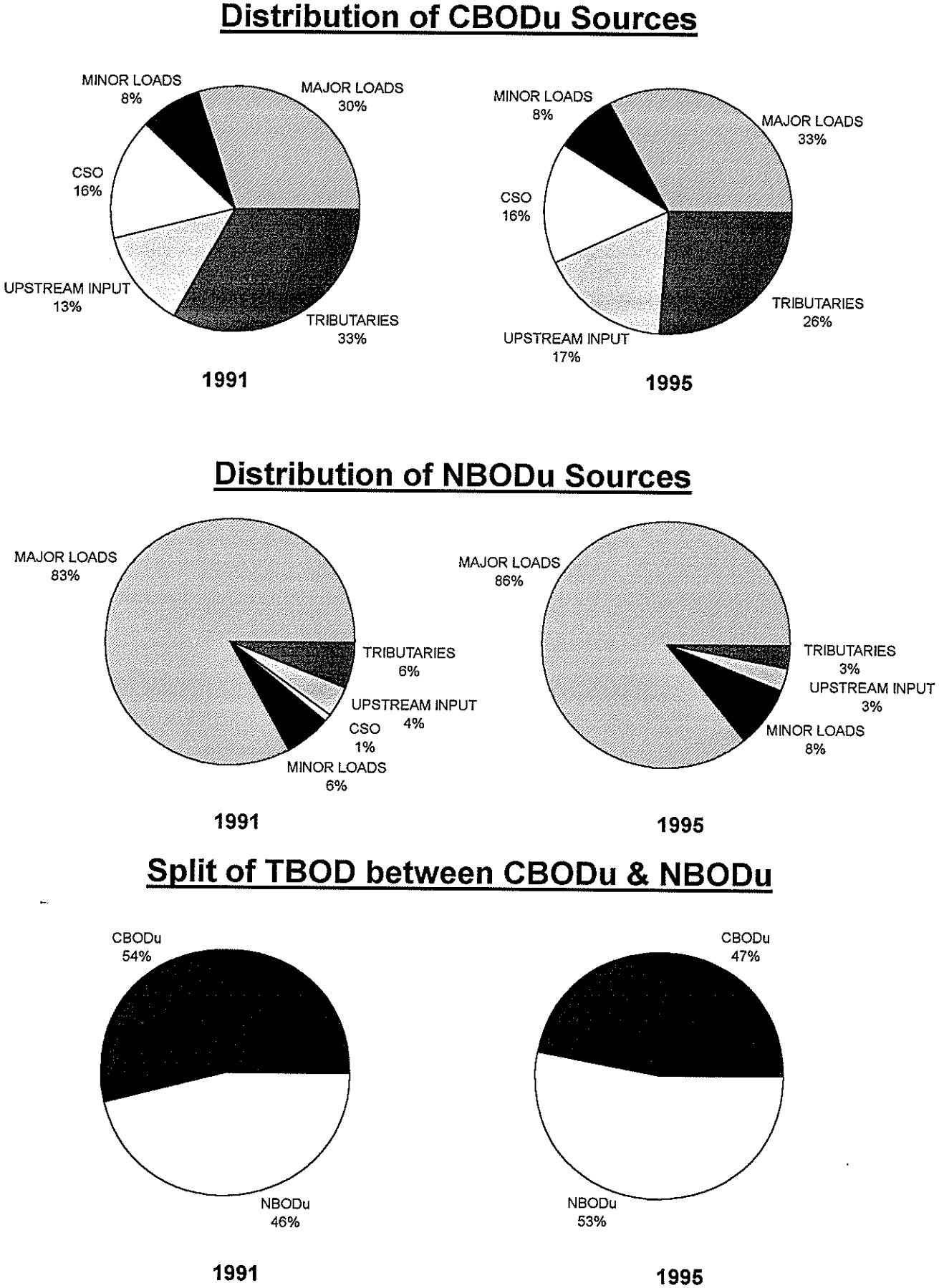

Figure 7-13. Summary of the Sources of CBODu and NBODu Input into the Model During the 1991 and 1995 Modeling Periods.

sources are each less than 10%. The split of the total BODu between CBODu and NBODu input into the River is approximately equal at roughly 50% each for both 1991 and 1995.

7.1.7 Sediment Fluxes: Sediment Oxygen Demand (SOD) and Nitrate

A spatially constant SOD of 0.5 $g/m^2.d$ was assigned during both the 1995 and 1991 modeling periods. This value agrees with the values typically measured during the 1996 sediment flux study on the Delaware River (Cornwell, 1997).

Data from the 1996 sediment flux study indicate a nitrate flux from the water column to the sediment. This nitrate flux from the sediment is necessary to explain observed water column nitrate concentrations if a mass balance is done for all known nitrate sources and sinks. This flux was represented in the model as a mass transfer coefficient multiplied by the water column nitrate concentration:

$$J_{NO3} = K_{L_{NO3}} * NO_3 \qquad (7\text{-}7)$$

where

J_{NO3} = Nitrate Sediment Flux Rate (g/m2-d), $[M/L^2\text{-}T]$
$K_{L_{NO3}}$ = Mass transfer coefficient (m/day), $[L/T]$
NO_3 = Water Column Nitrate Concentration (mg/1), $[M/L^3]$

The sediment nitrate concentration is much smaller than the water column concentration because nitrate can only exist in the relatively thin surface aerobic layer of the sediment. In the relatively thick anaerobic layer just below the aerobic layer, nitrate concentrations are 0.0. A combined sediment sample of the aerobic and anaerobic layers will, therefore, have very low nitrate concentrations.

Typically a sediment-water column flux rate is equal to the product of the mass transfer coefficient and the difference of the sediment and water column concentrations, $J_{NO3}=K_{L_{NO3}}*(NO_{3WATER}-NO_{3SEDIMENT})$. For the nitrate sediment flux calculation, the sediment nitrate concentration is assumed to be much smaller than the water column concentration, $NO_{3SEDIMENT} << NO_{3WATER}$, and drops out of the equation.

The model's fit of the water column nitrate data was used as a guide in assigning the transfer coefficient, $K_{L_{NO3}}$. An estimate of the K_{LNO3} values was calculated and then calibrated based on the fit of the model to the observed water column nitrate concentrations. Based on that model fit, $K_{L_{NO3}}$ was assigned at 0.5 meters/day.

7.2 MODEL CALIBRATION OF 1995 WATER QUALITY DATA

The model calibration results are compared to both spatial profiles of data from specific surveys and also to temporal profiles of data from individual stations sampled over the model calibration period. A comparison of algal productivity measured during the summer of 1987 and algal productivity computed during the summer surveys of 1995 is also presented. Providing insight into the significance of the factors affecting the dissolved oxygen balance in the Delaware River, the specific effects of carbonaceous BOD oxidation, ammonia nitrification, algal photosynthesis and respiration, and sediment oxygen demand are presented individually as component responses. Finally, probability plots of dissolved oxygen at different river mile points are used to compare data to model results.

7.2.1 1995 Calibration: Spatial Plots

The spatial plots for the 1995 calibration are presented on Figures 7-14 through 7-16 for the August 8th (Model Day 23), August 25th (Model Day 43) and September 25th (Model Day 70) surveys. These calibration figures have a similar format to the water quality data plots presented in section 4.0. The data are shown as symbols and the model results are presented as a line for the daily average and as a shaded area for the range over the day. Comparisons of data and model results are presented for dissolved oxygen, chlorophyll-a, orthophosphate, nitrite+nitrate and ammonia. Calculated ultimate carbonaceous BOD (CBODu) profiles are also shown even though there are no data for comparison.

Overall, the model does a good job reproducing the data. The calculated dissolved oxygen profiles agree reasonably well for August 8th and September 25th. On August 29th, however, there is a noticeable discrepancy between calculated dissolved oxygen and data, especially near RM 85. The model under predicts the dissolved oxygen data by almost 1.5 mg/l. The reason for the increase in river dissolved oxygen levels in this region is not known. One hypothesis is that oxygen produced by aquatic vegetation in this section of the Delaware River may be the cause.

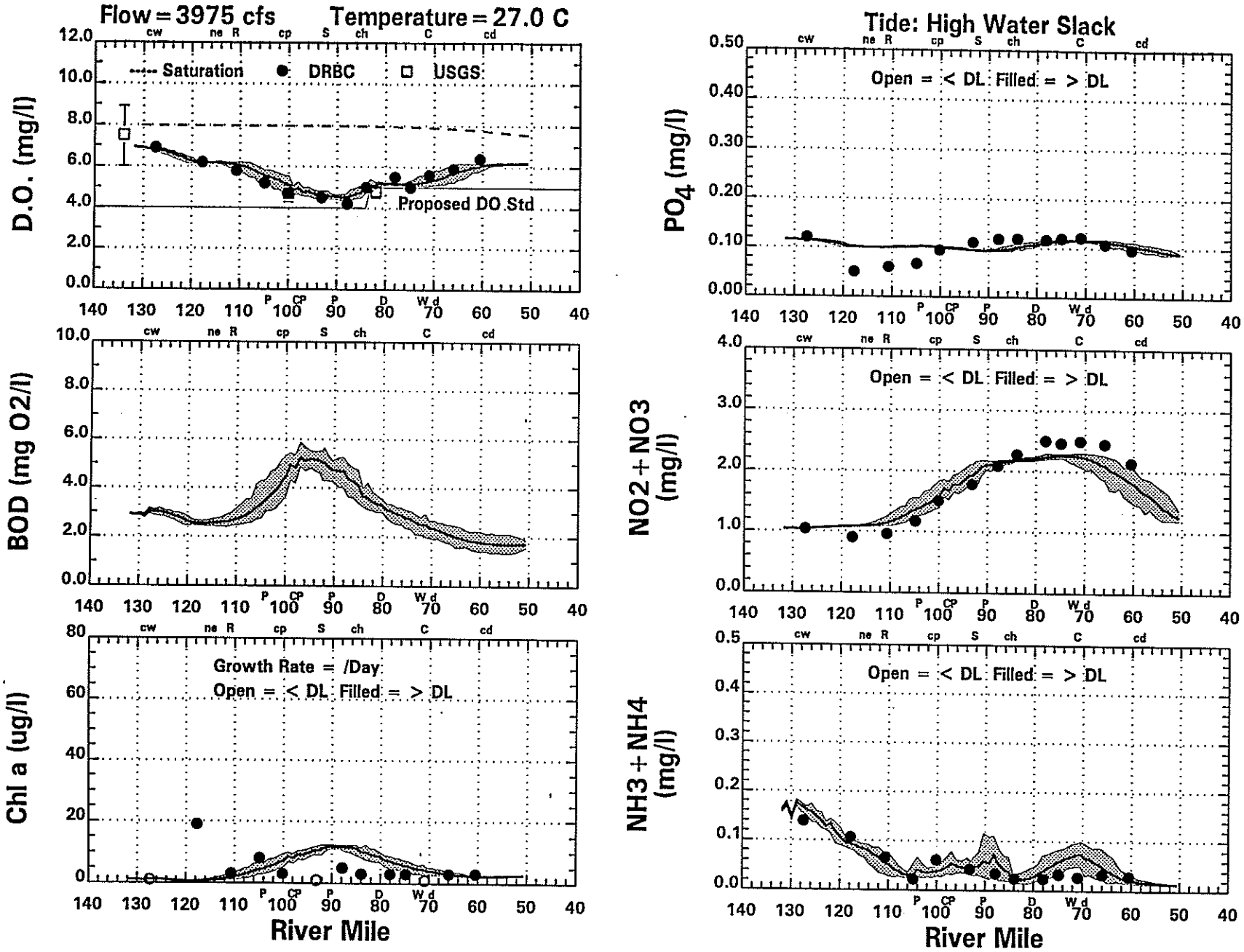

Figure 7-14. 1995 Water Quality Model Spatial Calibration for August 8-9.

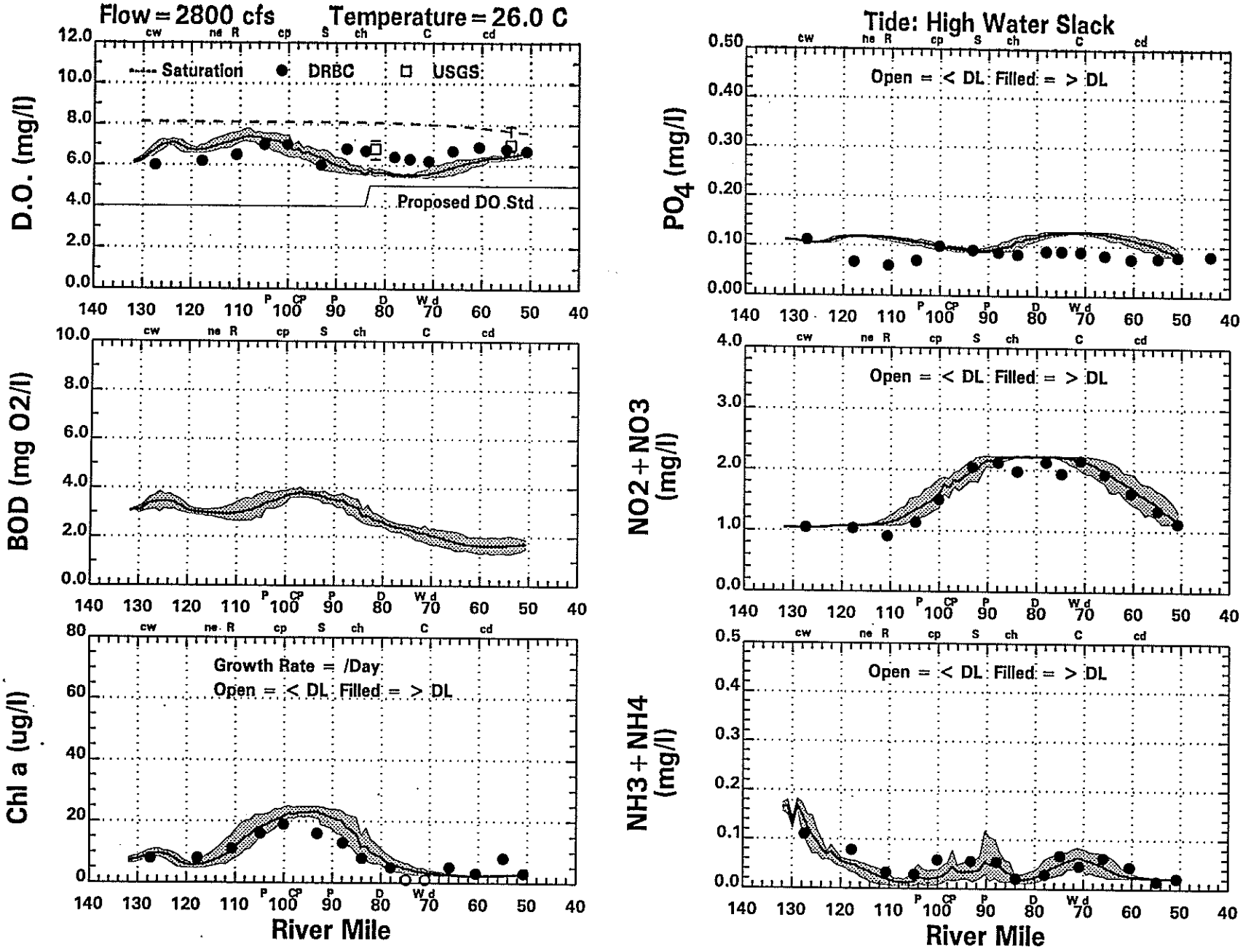

Figure 7-15. 1995 Water Quality Model Spatial Calibration for August 29.

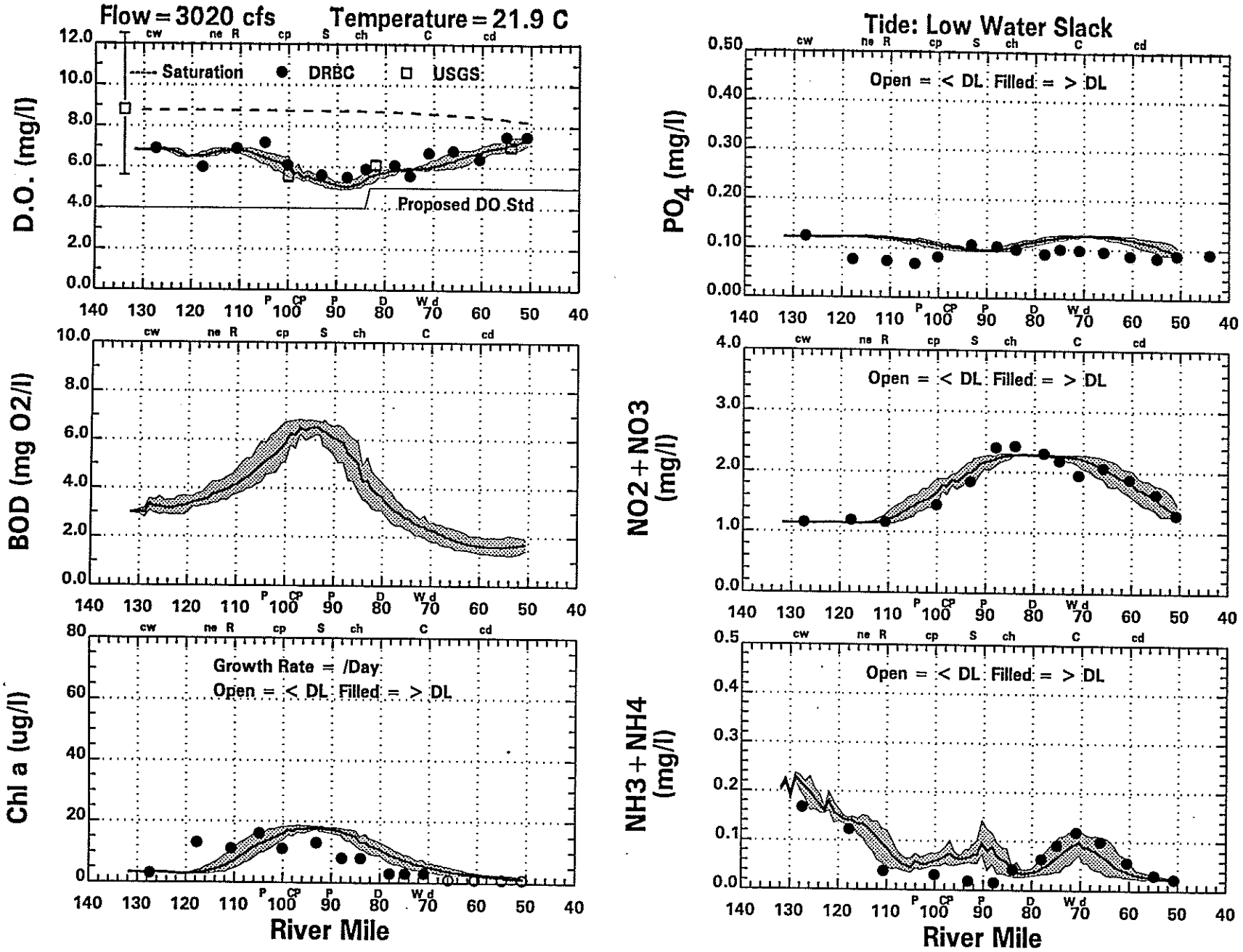

Figure 7-16. 1995 Water Quality Model Spatial Calibration for September 25.

While no 1995 BOD data are available to judge the model calculated CBODu values, the model results fall within the range of CBODu values measured during the 1994 long term BOD study.

Algal growth occurs primarily upstream of RM 85 with chlorophyll-a levels generally ranging between 5 μg/L and 20 μg/L. The patterns of river algal concentration are assumed to be related to variations in algal growth associated with temporal and spatial changes in light extinction. Upstream of RM 85, the light extinction was made a function of turbidity data measured at Baxter (RM 110). While the Baxter data was the best available information for estimating temporal variation in the river light extinction, it does not necessarily always represent river conditions between RM 127 and RM 85. The light extinction was, therefore, adjusted within reasonable bounds to generally represent measured chlorophyll-a levels. The comparison of measured and computed chlorophyll-a levels are shown in the lower left panel of Figures 7-14 through 7-16.

A grazing rate of 0.15/day between RM 133 and 110 was assigned to reproduce observed algal levels in the upper River. Without this relatively high grazing rate, calculated chlorophyll-a levels would greatly exceed measured values. Reasonable adjustments to other model coefficients were not sufficient to achieve the same effect as the assigned grazing rate. There is some support for a high grazing rate in this section of the river based on previous studies that indicates elevated levels of the benthic filter feeder, Corbicula fluminea.

The calculated orthophosphorous profiles generally agree with the observed orthophosphorous values, but the model overpredicts the upstream data. From RM 133 to RM 110, the orthophosphorous data typically decreases and then increases downstream of RM 110. The reason for this upstream decline in orthophosphorous values is unclear. One hypothesis for this decrease is uptake by adjacent tidal marshes. Since little tributary and no wastewater treatment plant data exists for orthophosphorous loadings in 1995, a large degree of uncertainty is associated with model calculated orthophosphorous values. However, reproducing measured orthophosphorous values is not critical to the overall model calculation because algae growth in the Delaware River is not phosphorus limited.

The measured river ammonia and nitrite+nitrate profiles are reasonably well represented by the water quality model. The low river ammonia levels and the increase in nitrite+nitrate concentrations from approximately 1.0 μg/l upstream to over 2.0 μg/l downstream are the result

of relatively high rates of nitrification in the river. Differences between model and data values for ammonia and nitrate+nitrate may reflect inaccuracies in the assigned effluent values. The major wastewater discharges typically only measure ammonia and nitrite+nitrate one time per week, which does not necessarily represent the concentrations on the days immediately preceding or following the sampling day.

7.2.2 1995 Calibration: Temporal Plots

For the 1995 calibration temporal plots, river miles 104.9, 87.9 and 60.6 were selected for presentation. These three river mile location were picked as representative of the upstream zone of low solids and high phytoplankton, the dissolved oxygen sag point, and the downstream zone of high solids and low phytoplankton respectively.

The temporal calibration plots for RM 104.9, 87.9 and 60.6 are presented in Figures 7-17 through 7-19. At all three locations, the model does a good job of reproducing the data. Upstream at RM 104.9, the model reproduces the temporal trends in both the dissolved oxygen and chlorophyll-a data. Temporal changes in model and data for phosphorus, nitrite+nitrate, and ammonia are small. At the dissolved oxygen sag point (RM 87.9), the model matches the general trend in the dissolved oxygen and chlorophyll data, but under predicts the dissolved oxygen values after day 40. In this section of the Delaware River there may be oxygen production by aquatic vegetation which is not represented in the model. Downstream at RM 60.55, the model and data agree with both exhibiting relatively flat profiles.

7.2.3 1995 Calibration: Primary Productivity Plots

The model calculated gross primary productivity and productivity data from 1987 are presented in Figure 7-20. The model calculated productivity values are shown spatially with one panel for each of the four summer water quality surveys performed during the 1995 modeling period. The 1987 data are shown on a separate panel. The calculated productivity for the four summer surveys generally brackets the measured 1987 summer average productivity upstream of RM 85. However, downstream of RM 85, the gross algal productivity computed by the model is much less than the productivity measured in 1987.

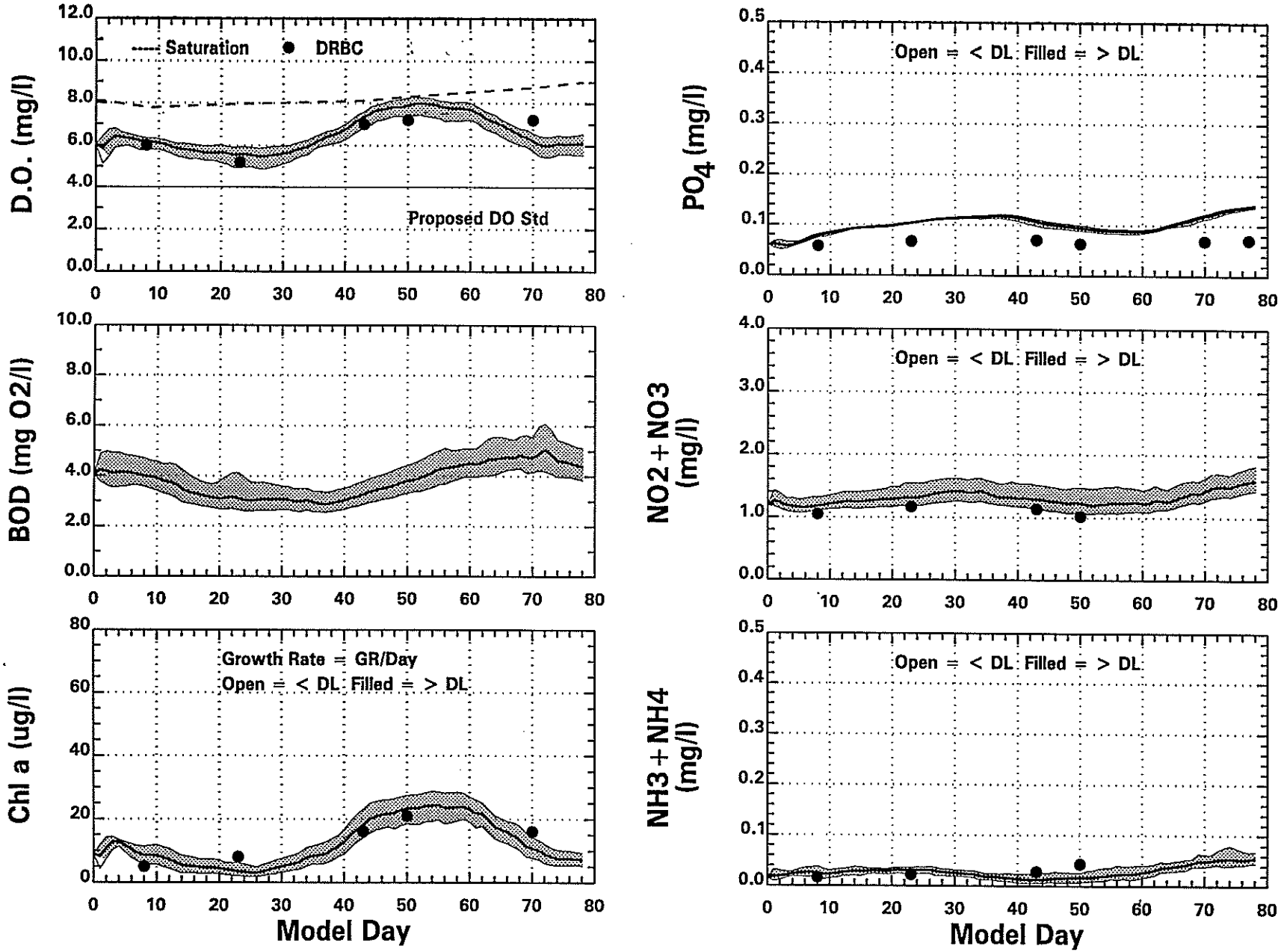

Figure 7-17. 1995 Water Quality Model Temporal Calibration at RM 104.9.

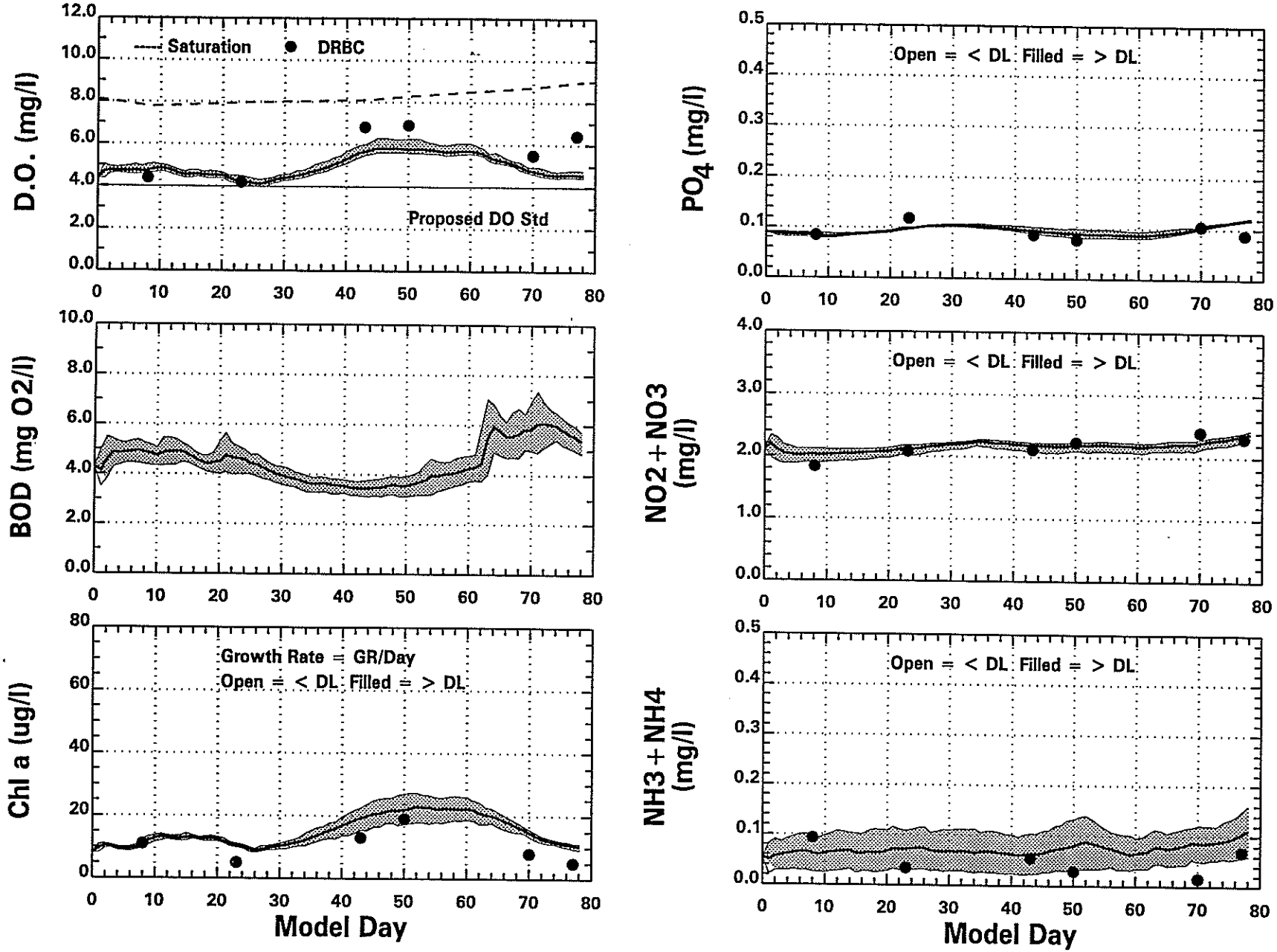

Figure 7-18. 1995 Water Quality Model Temporal Calibration at RM 87.9.

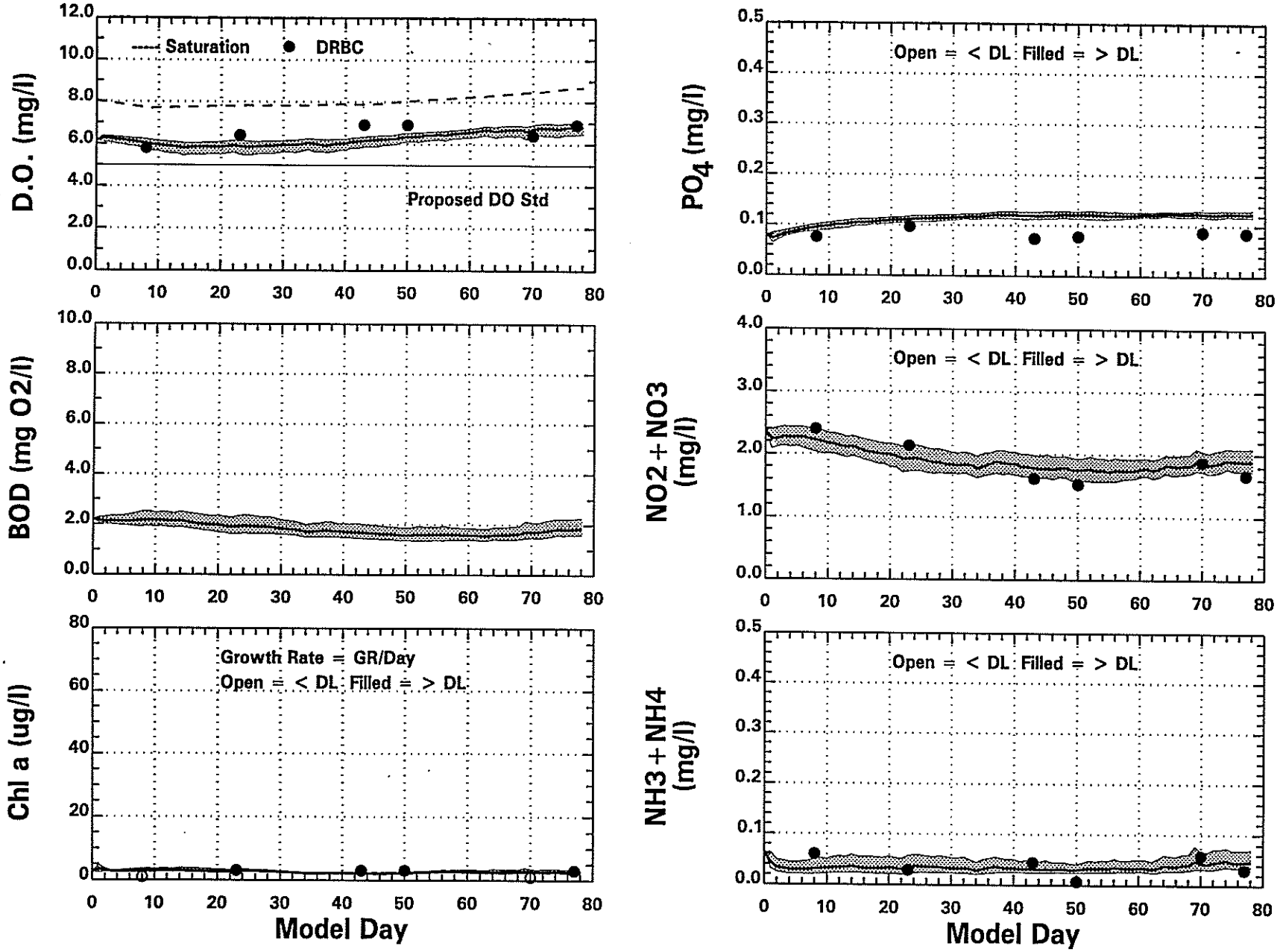

Figure 7-19. 1995 Water Quality Model Temporal Calibration at RM 60.6.

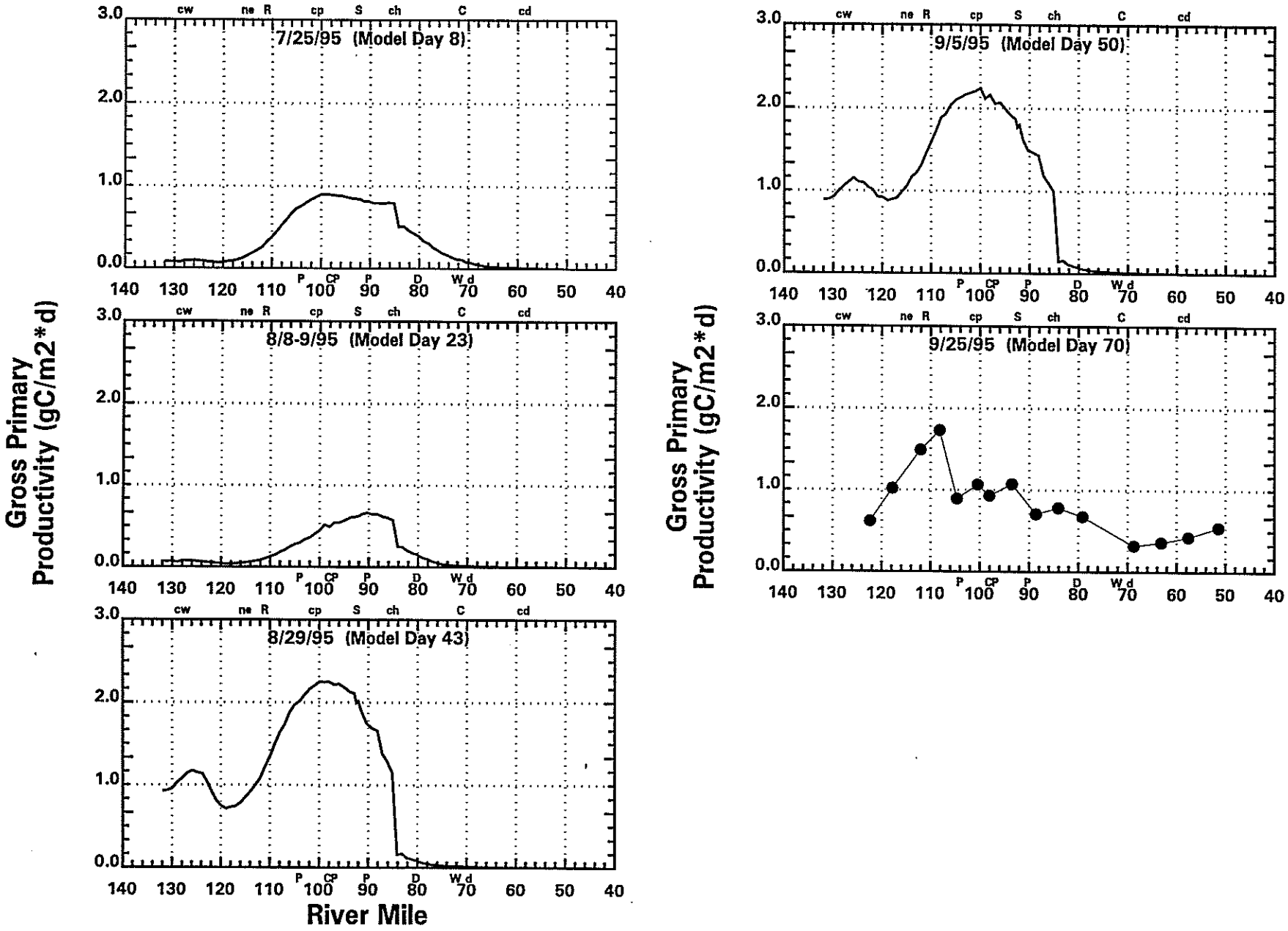

Figure 7-20. 1995 Gross Primary Productivity vs. River Mile and 1987 Summer Average Productivity Data.

7.2.4 1995 Calibration: DO Deficit Component Response

The total dissolved oxygen deficit and the deficit due to the individual processes affecting the dissolved oxygen balance are presented in Figures 7-21 through 7-23 for the August 8th (Model Day 23), August 25th (Model Day 43) and September 25th (Model Day 70) surveys. The processes affecting the dissolved oxygen balance are carbonaceous BOD oxidation, nitrification, SOD and the net phytoplankton effect including photosynthesis, respiration and decomposition of algal BOD. The deficit due to carbonaceous BOD oxidation reaches a maximum of 1.2 mg/l at RM 90. The most significant factor impacting dissolved oxygen in the Delaware River is the oxidation of ammonia which accounts for a dissolved oxygen deficit of approximately 2.0 mg/l at RM 90. The deficit due to SOD typically averages 0.6 mg/l and is constant from RM 120 through RM 70. These three oxygen consuming processes show little survey to survey variability and combine to account for a total oxygen demand of 3.8 mg/l at RM 90. The temporal differences in dissolved oxygen are primarily due to variability in algal photosynthesis and respiration. On August 8th and September 25th, algae produce a net increase in dissolved oxygen (shown as a negative deficit) of 0.5 mg/L. On these two days the maximum total deficit is between 3.8 and 4.0 mg/l at RM 90. On August 25th, however, algae produce a net dissolved oxygen increase of 1.8 mg/l and the maximum total deficit is only 2.6 mg/l. The zone of maximum dissolved oxygen deficit is also shifted farther downstream with the sag point moving from RM 90 to RM 80. While the net effect of algae may not always have the largest impact on the dissolved oxygen balance, algae dynamics account for most of the temporal variability in dissolved oxygen concentrations.

7.2.5 1995 Calibration: DO Probability Plots

The dissolved oxygen probability plot for the 1995 calibration period is presented in Figure 7-24. Dissolved oxygen data measured by DRBC and the daily average values calculated by the model are shown for RM 127.48, 104.90, 87.90, 83.98, 70.96 and 60.55. In general, the model does a adequate job reproducing the observed distributions in the dissolved oxygen data. At RM 87.90 and 83.98, however, the model consistently under predicts the measured dissolved oxygen values. As mentioned in the discussion of the spatial plots, this may be due to oxygen productivity by aquatic vegetation in this section of the Delaware River. At all locations to varying degrees, the model does not reproduce the variability observed in the measured data. The probability distributions for the model values is much flatter than the data. Given the model is

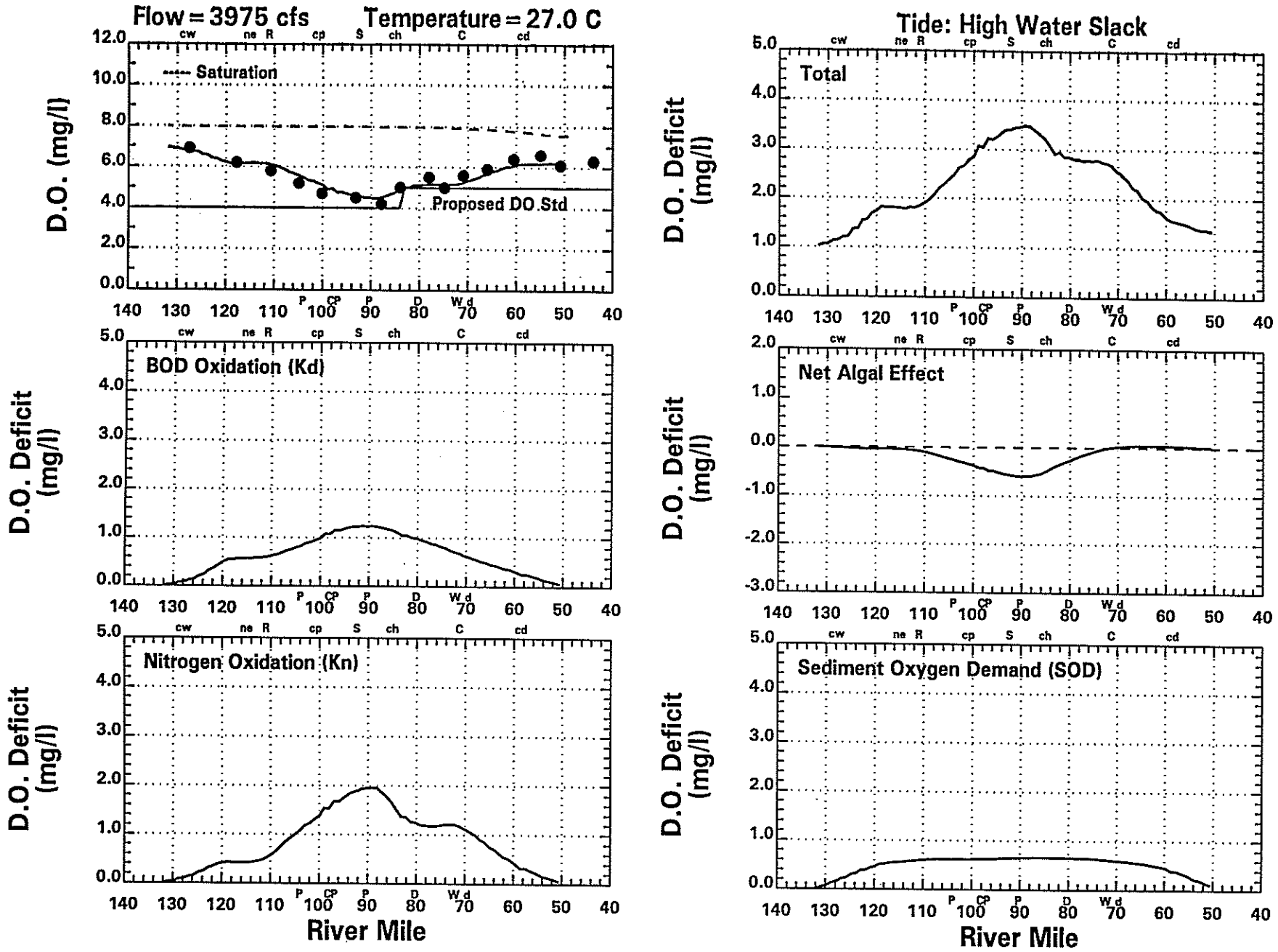

Figure 7-21. 1995 Dissolved Oxygen Deficit Component Response for August 8-9.

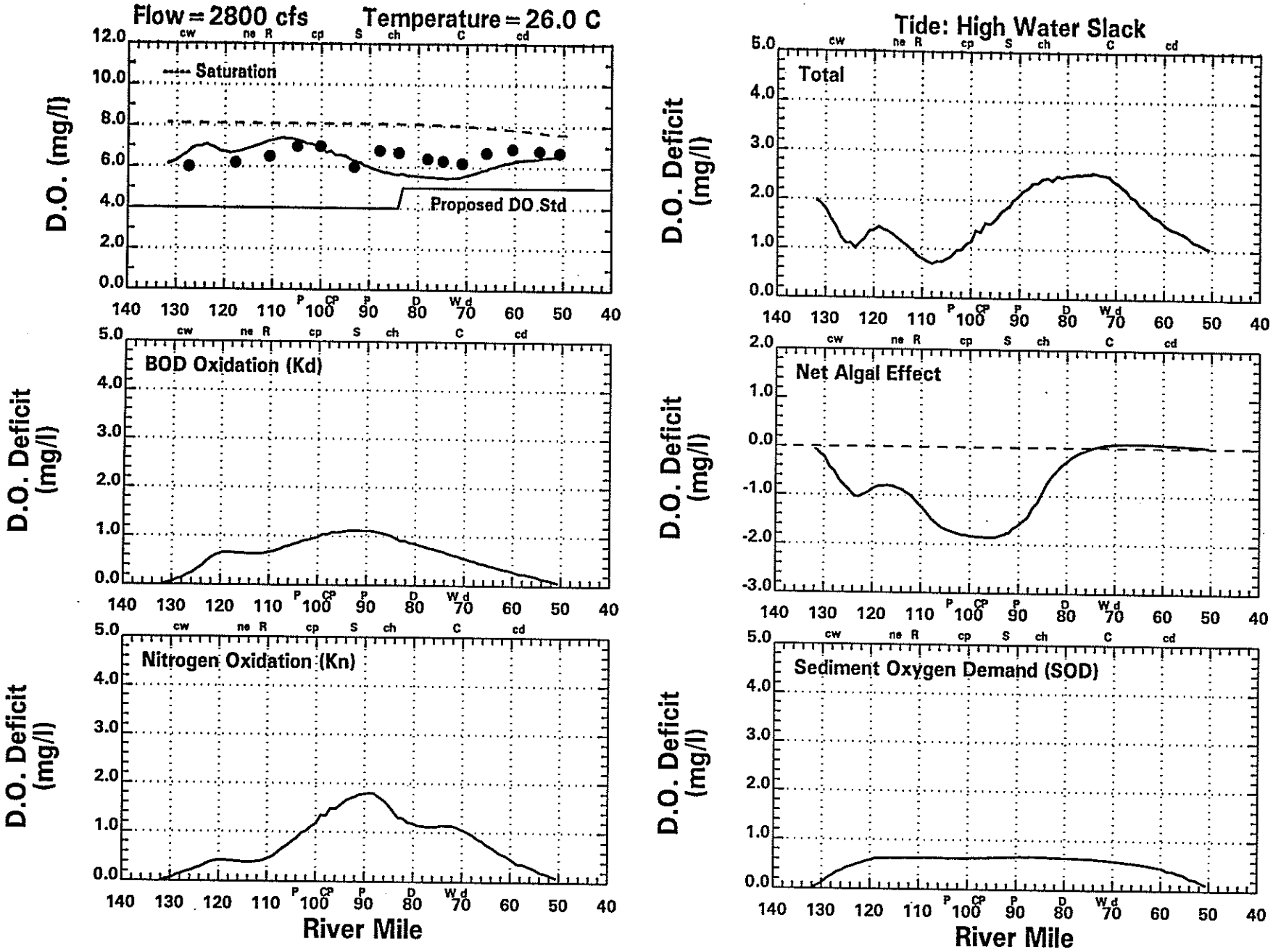

Figure 7-22. 1995 Dissolved Oxygen Deficit Component Response for August 29.

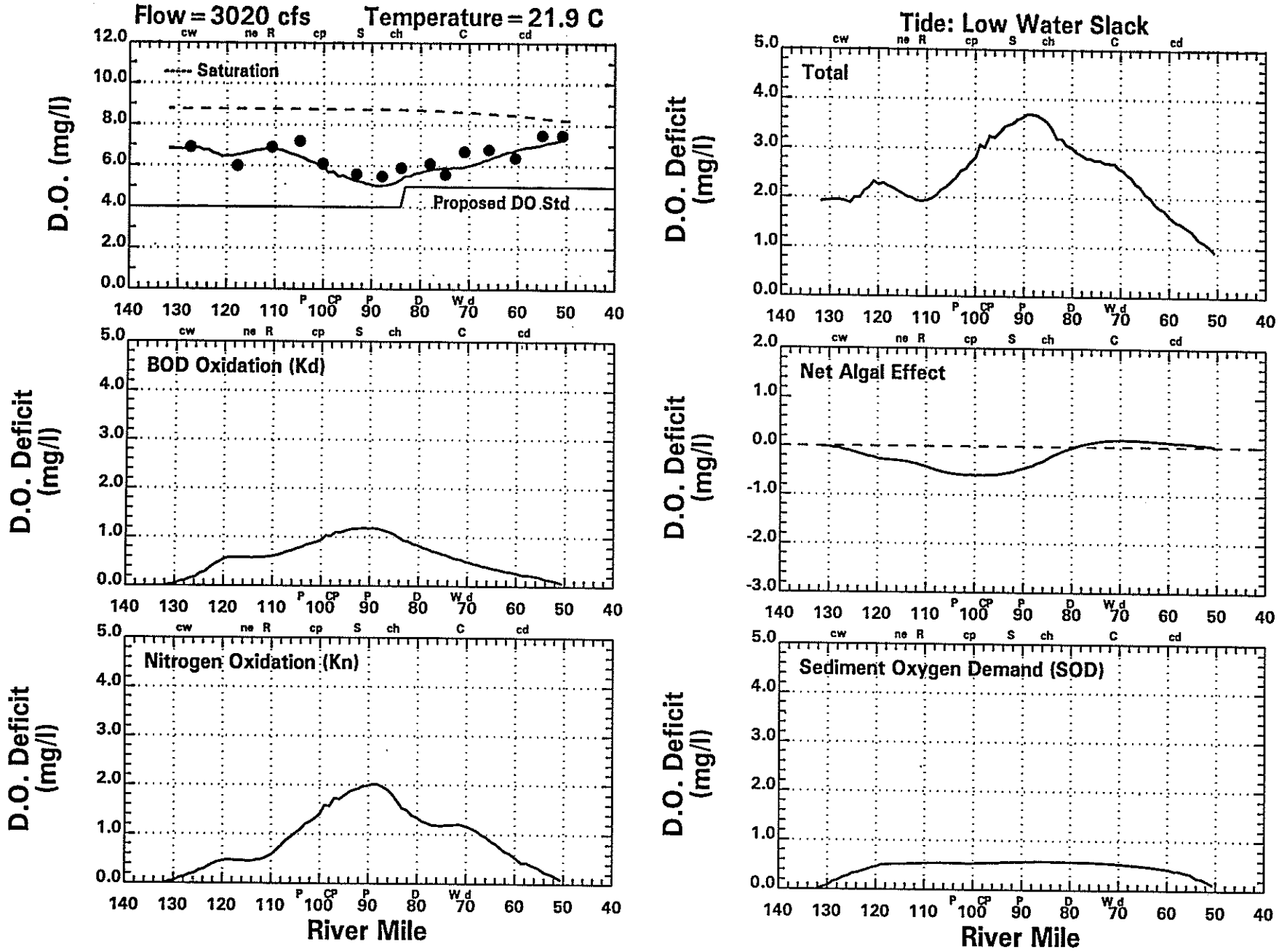

Figure 7-23. 1995 Dissolved Oxygen Deficit Component Response for September 25.

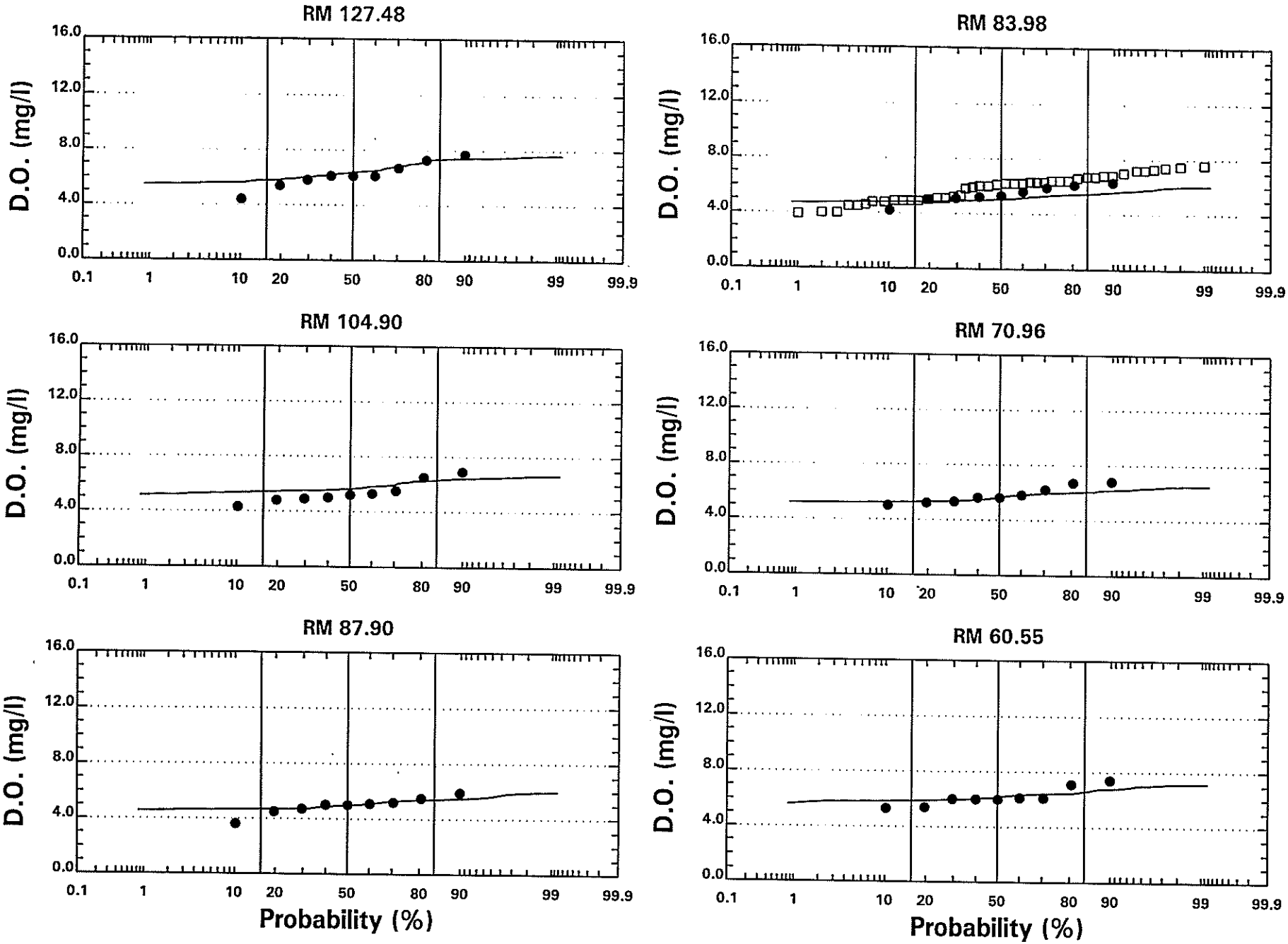

Figure 7-24. Probability Distributions of Observed and Modeled Dissolved Oxygen for 1995 Calibration. (● DRBC Data; □ USGS Data; — Model Daily Averages).

a simplistic representative of the actual conditions in the Delaware River, more variability in the measured data would be expected.

7.3 1991 VALIDATION

In this section, the validation results are presented in the same format as the calibration results from the previous section. For 1991, June 25th (model day 15), July 23rd (model day 43), August 26th (model day 77) and September 23rd (model day 105) were selected for presentation. The temporal plots for river miles 104.9, 87.9 and 60.6 are again shown. Gross primary productivity data from 1987 is presented as before with the 1991 productivity calculations. The dissolved oxygen component responses are then shown for the 1991 validation. Finally, the dissolved oxygen probability distribution of model and data are shown for 1991.

7.3.1 1991 Validation: Spatial Plots

The spatial plots for the 1991 validation are presented in Figures 7-25 through Figure 7-28. As with the calibration results, the modeling results generally agree with 1991 data. While over predicting dissolved oxygen concentration above RM 80 on June 25th, the model generally reproduces the dissolved oxygen data on July 23rd, August 26th and September 23rd. Similar to the 1995 calibration analysis, there is more variability in the data than is computed with the model.

7.3.2 1991 Validation: Temporal Plots

The temporal validation plots for RM 104.9, RM 87.9 and RM 60.6 are presented on Figures 7-29 through 7-30. The ability of the model to reproduce the 1991 data is similar to the 1995 calibration. The model generally matches the trend in the data while sometimes missing the survey to survey variability. The large increases in the BOD concentrations shown on Figure 7-30 correspond to wet weather CSO events, which temporarily increase River BOD concentrations.

7.3.3 1991 Validation Primary Productivity Plots

The model calculated gross primary productivity and the 1987 data are shown on Figure 7-32. The range of the model calculated values and the 1987 data are consistent. The model results for 1991 and 1995 showed similar patterns of calculated gross primary productivity.

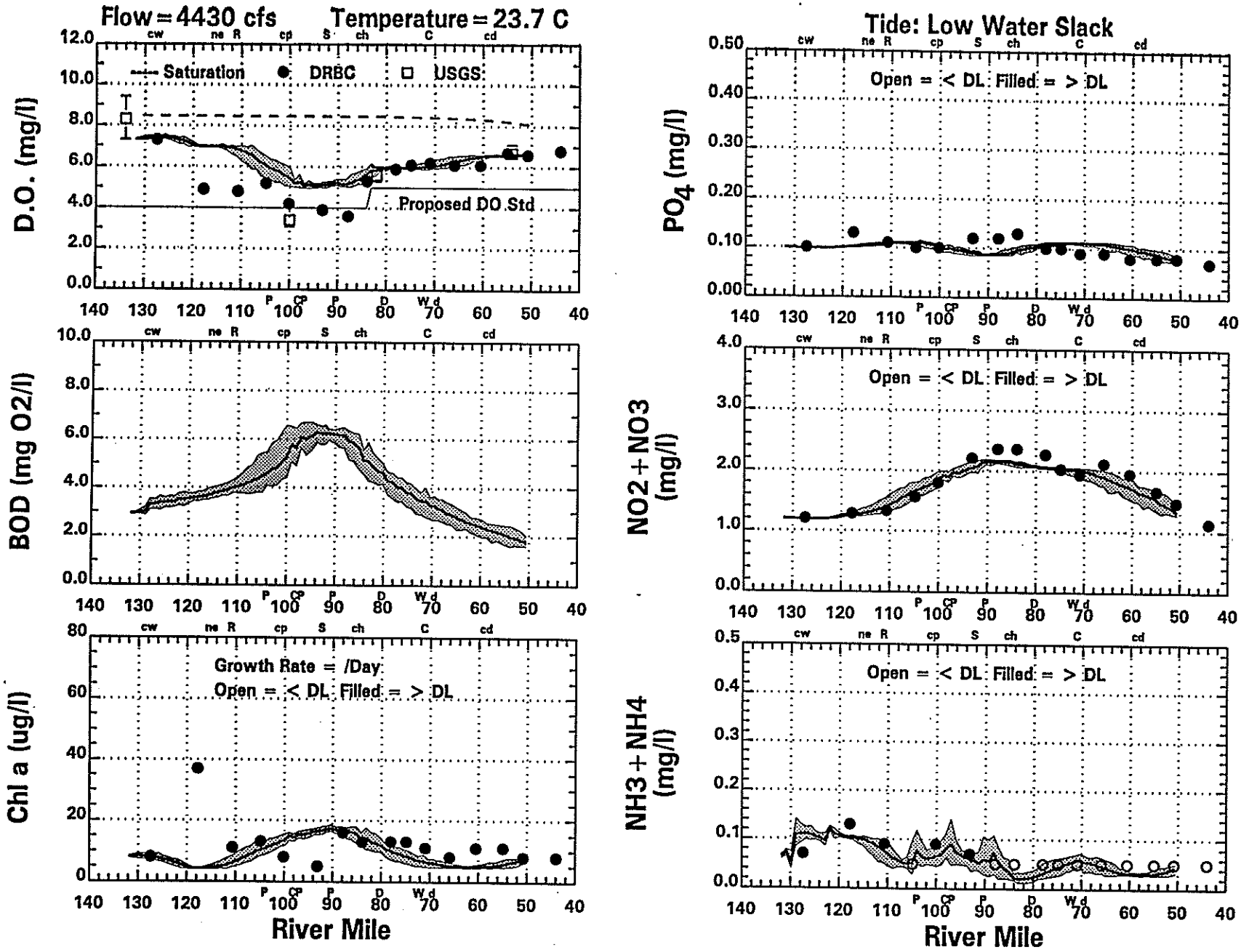

Figure 7-25. 1991 Water Quality Model Spatial Calibration for June 25.

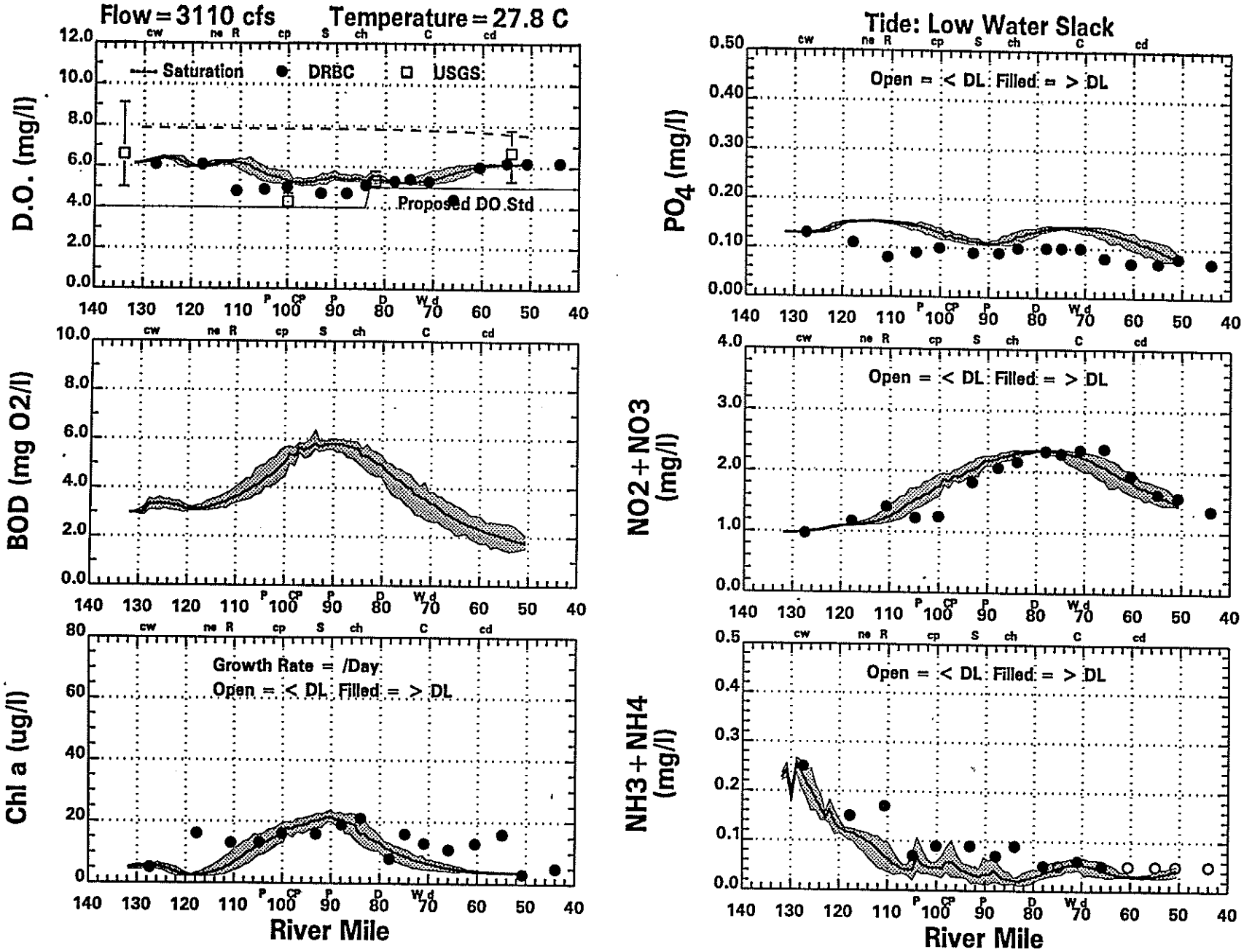

Figure 7-26. 1991 Water Quality Model Spatial Calibration for July 23.

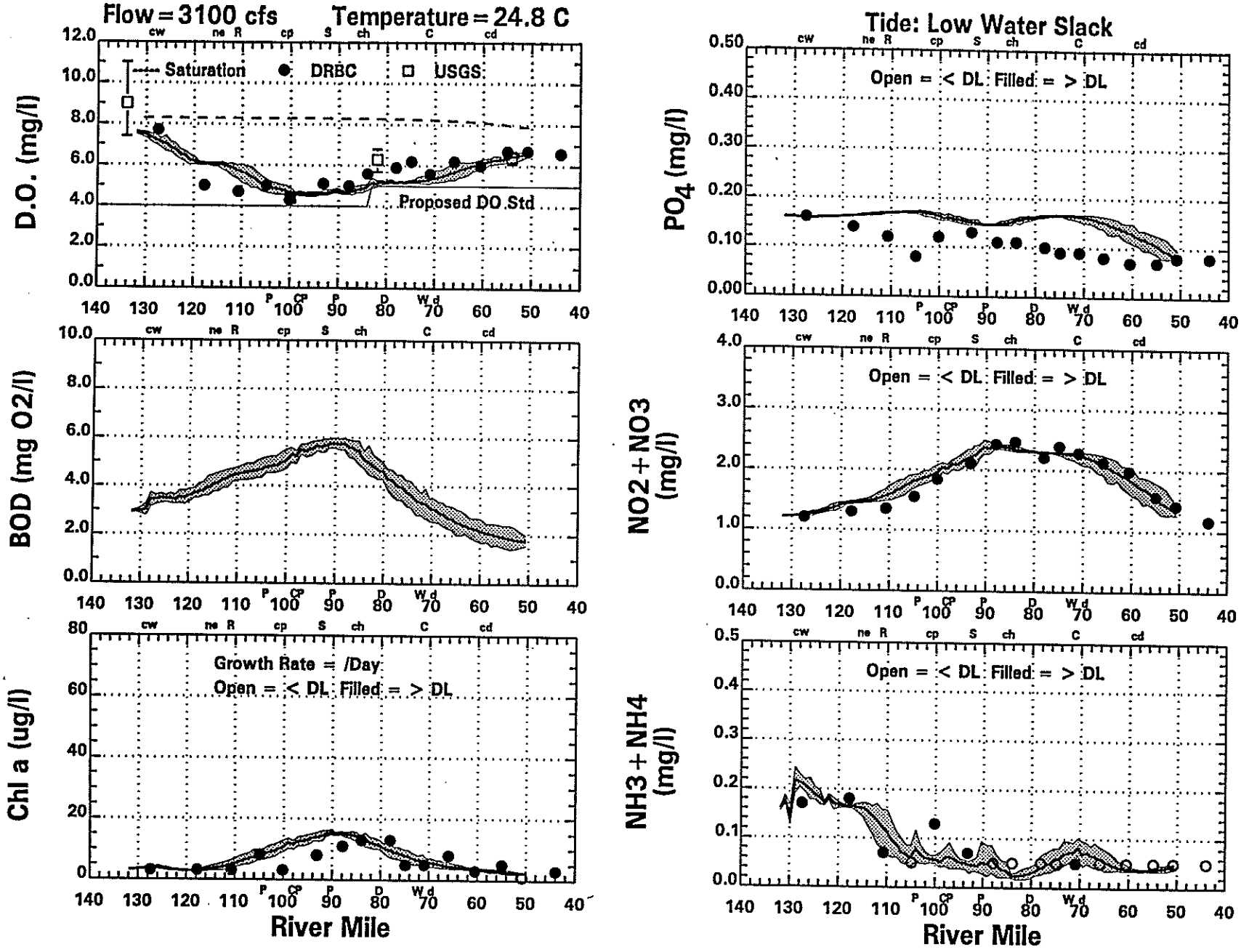

Figure 7-27. 1991 Water Quality Model Spatial Calibration for August 26.

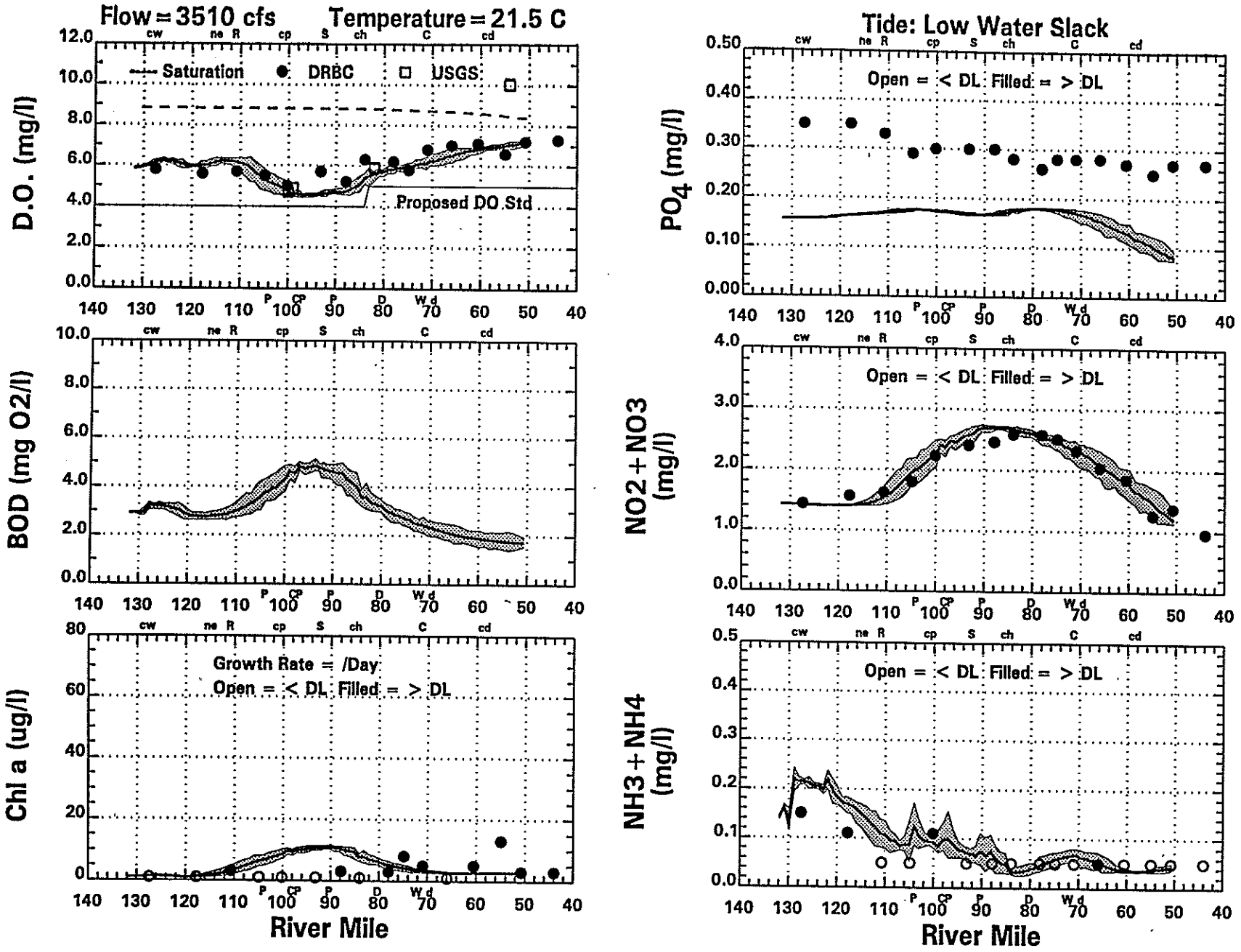

Figure 7-28. 1991 Water Quality Model Spatial Calibration for September 23.

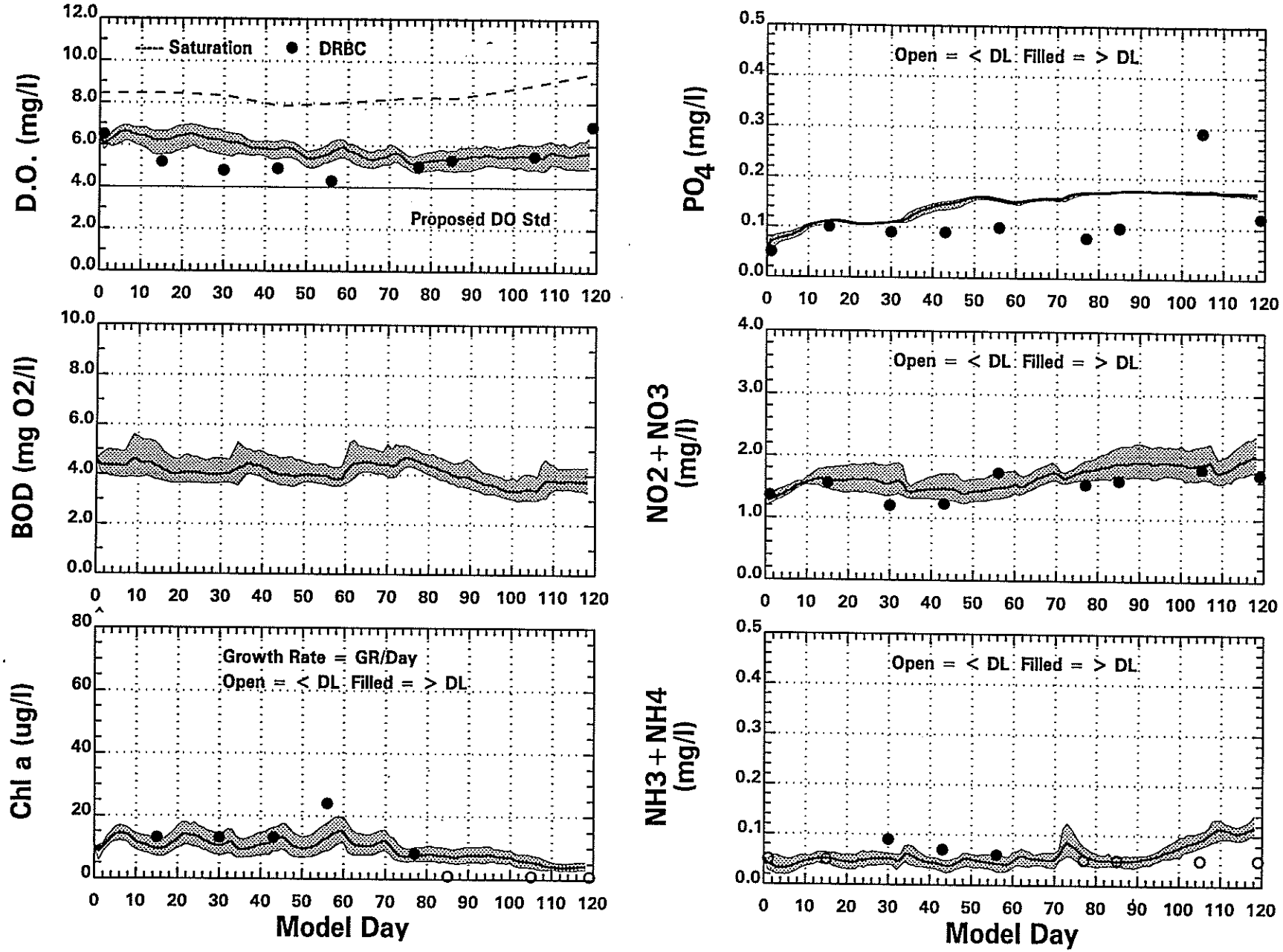

Figure 7-29. 1991 Water Quality Model Temporal Calibration at RM 104.9.

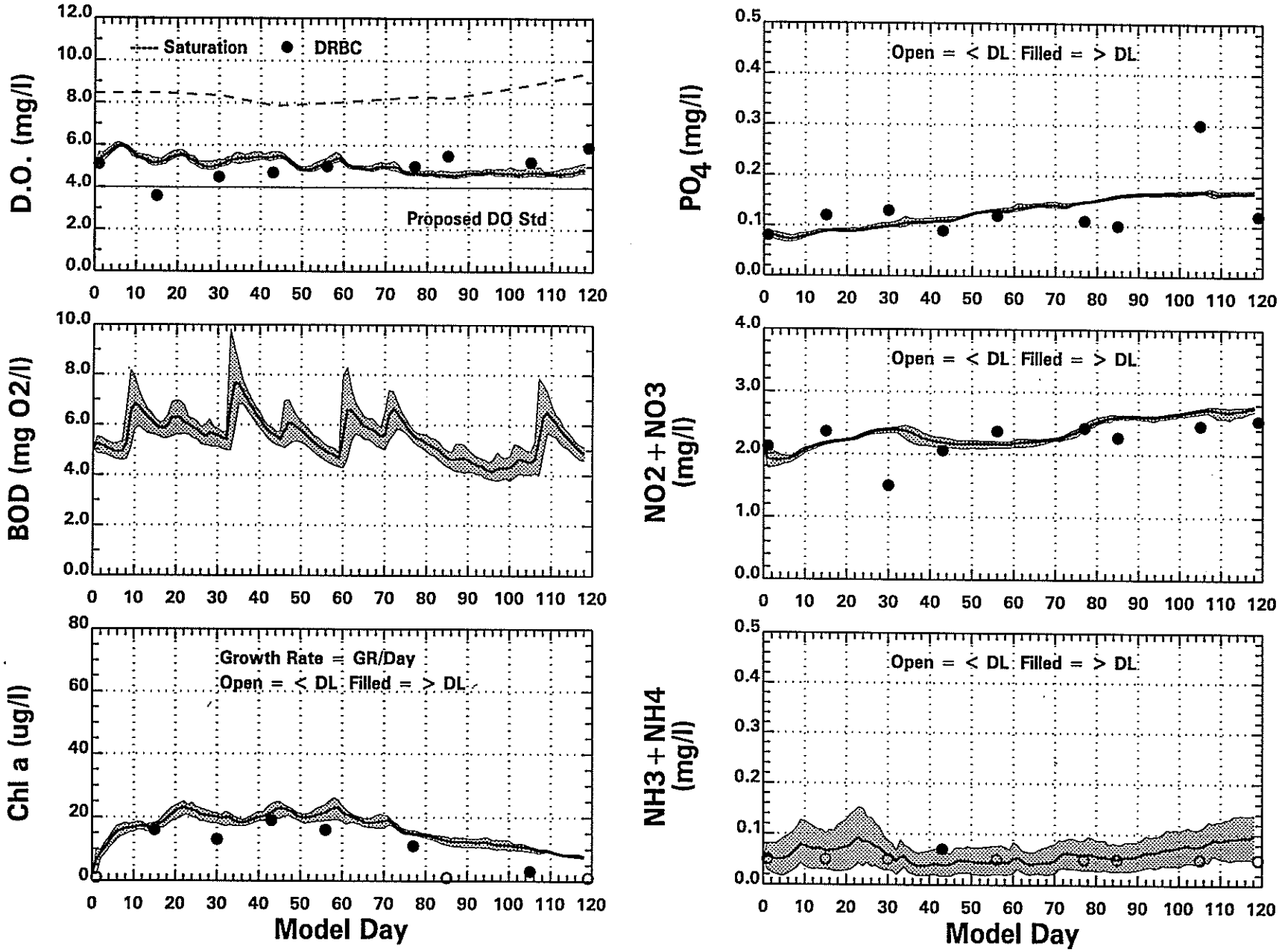

Figure 7-30. 1991 Water Quality Model Temporal Calibration at RM 87.9.

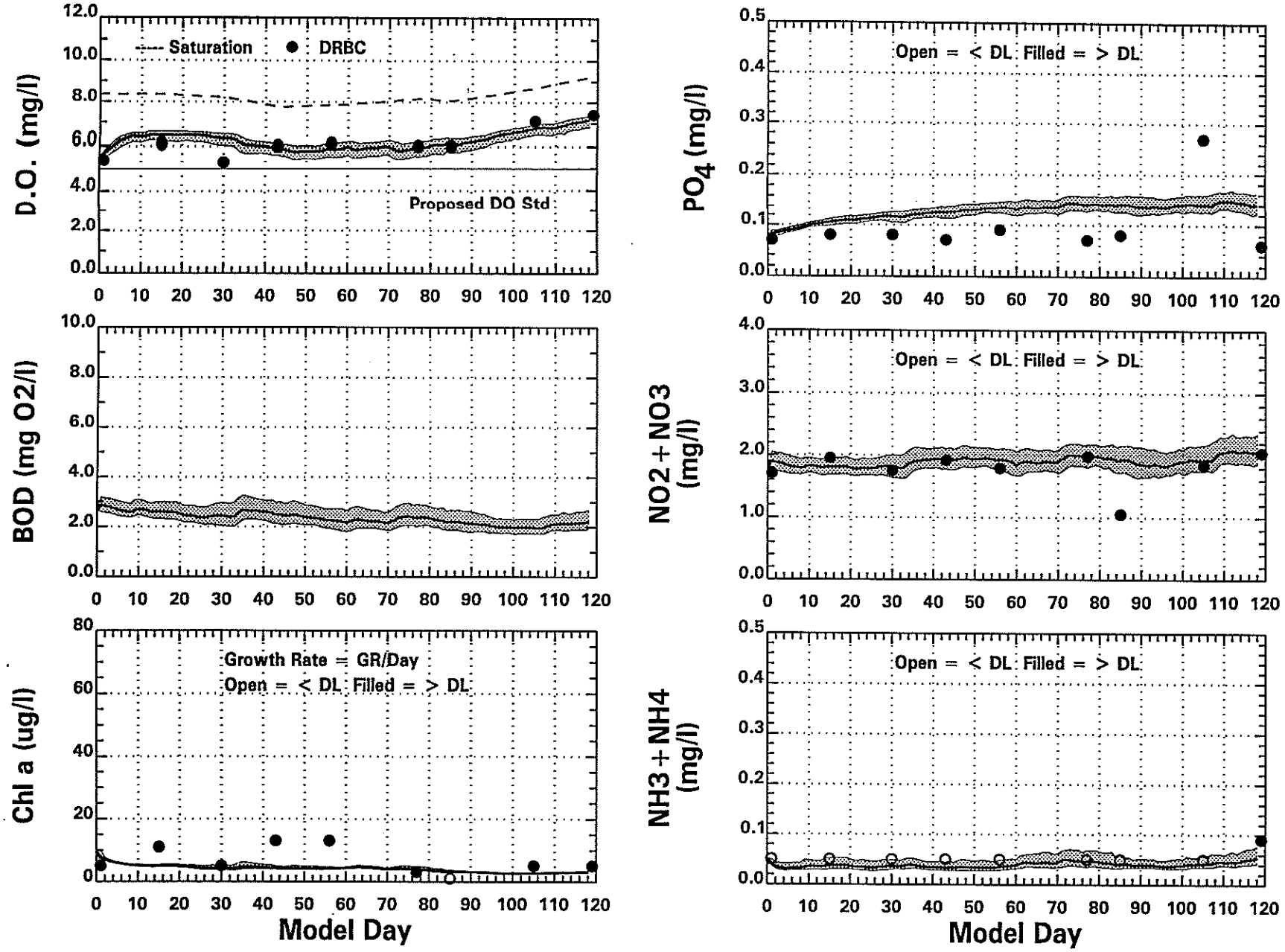

Figure 7-31. 1991 Water Quality Model Temporal Calibration at RM 60.6.

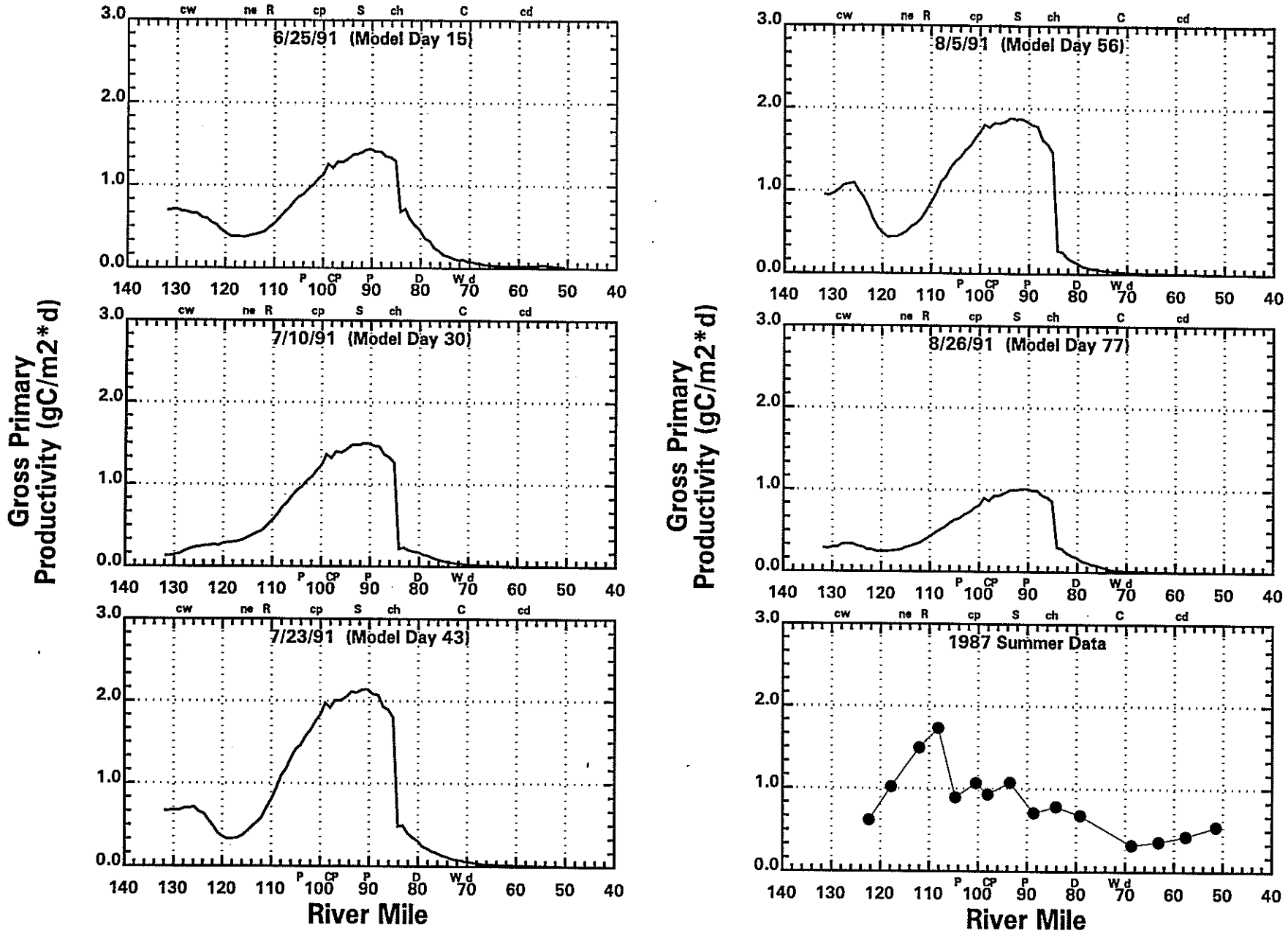

Figure 7-32. 1991 Gross Primary Productivity vs River Mile and 1987 Summer Average Productivity Data.

7.3.4 1991 Validation: DO Deficit Component Response

The 1991 DO deficit component response for June 25 (model day 15), July 23 (model day 43), August 26 (model day 77), and September 23 (model day 105) are presented on Figures 7-33 through 7-36. The patterns in the 1991 component responses are very similar to those seen in the 1995 component responses. The dissolved oxygen deficit due to BOD oxidation, nitrogen oxidation and SOD is consistent from survey to survey. As in 1995, the survey to survey variability seen in dissolved oxygen is due primarily to the net algal effect which typically reduces the deficit from 0.5 to 1.5 mg/l.

7.3.5 1991 Validation: DO Probability Plots

The dissolved oxygen probability plots for the 1991 validation period is presented in Figure 7-37. The dissolved oxygen data measured by DRBC and the daily average values calculated by the model are again shown for RM 127.48, 104.90, 87.90, 83.98, 70.96 and 60.55. The 1991 model calculation fits the observed dissolved oxygen distribution better than the 1995 calibration. The model generally goes through the median of the observed data but, as expected, does not reproduce the degree of variability seen in the data.

7.4 SENSITIVITY ANALYSIS

In order to better understand the model's performance, a number of model runs were preformed to test the water quality model's sensitivity to different processes described by the model. Sensitivity runs were preformed to investigate the impact of the following factors:

a. Nitrification
b. Sediment Nitrate Flux
c. Salinity Growth Reduction Factor
d. Algal Predation (Grazing Rate)
e. Upstream CBOD, Nitrogen and Phosphorus Loading
f. Tributary CBOD, Nitrogen and Phosphorus Loading
g. Point Source CBOD, Nitrogen and Phosphorus Loading
h. Wet Weather CSO CBOD and Ammonia Loading

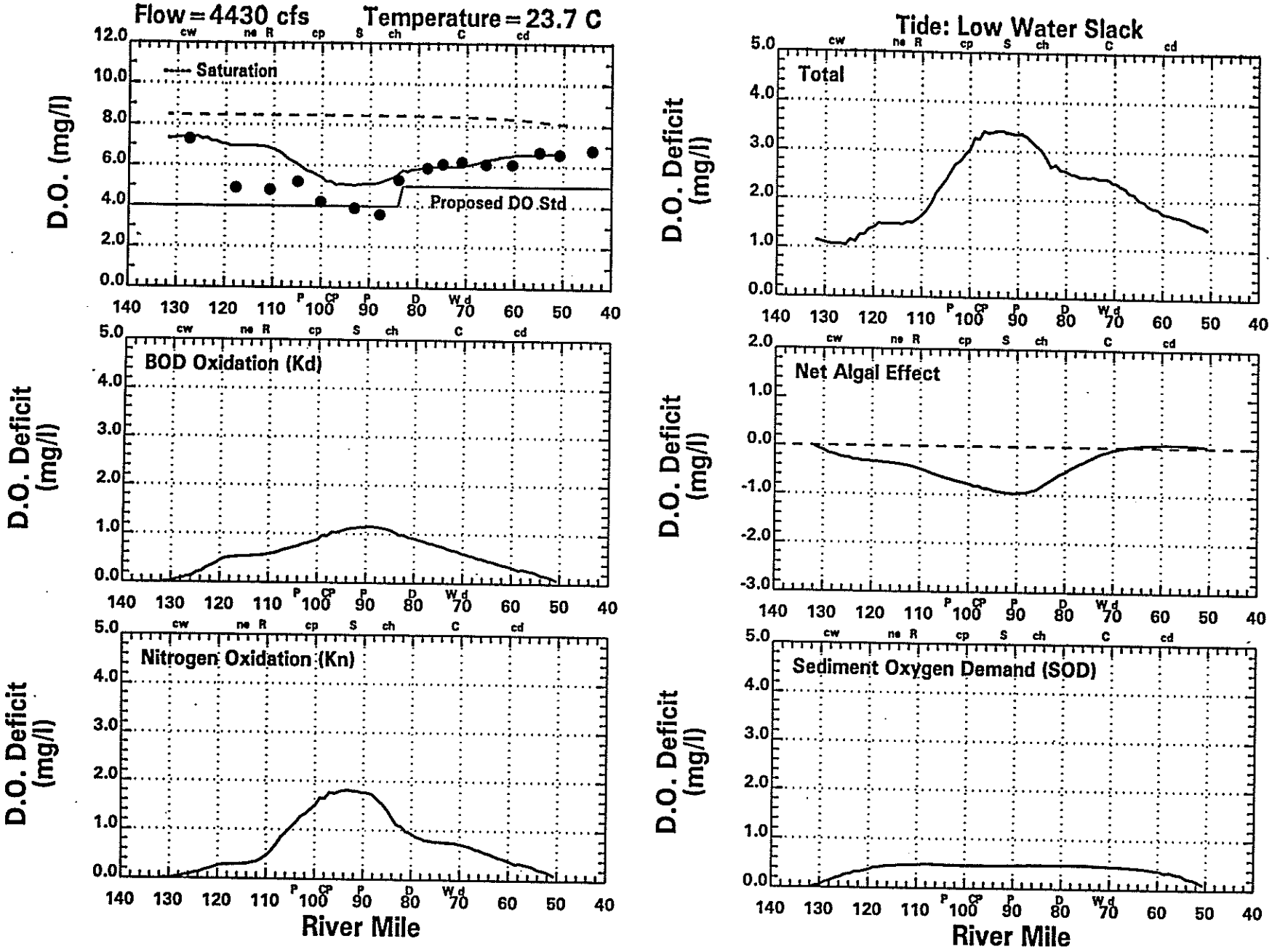

Figure 7-33. 1991 Dissolved Oxygen Deficit Component Response for June 25.

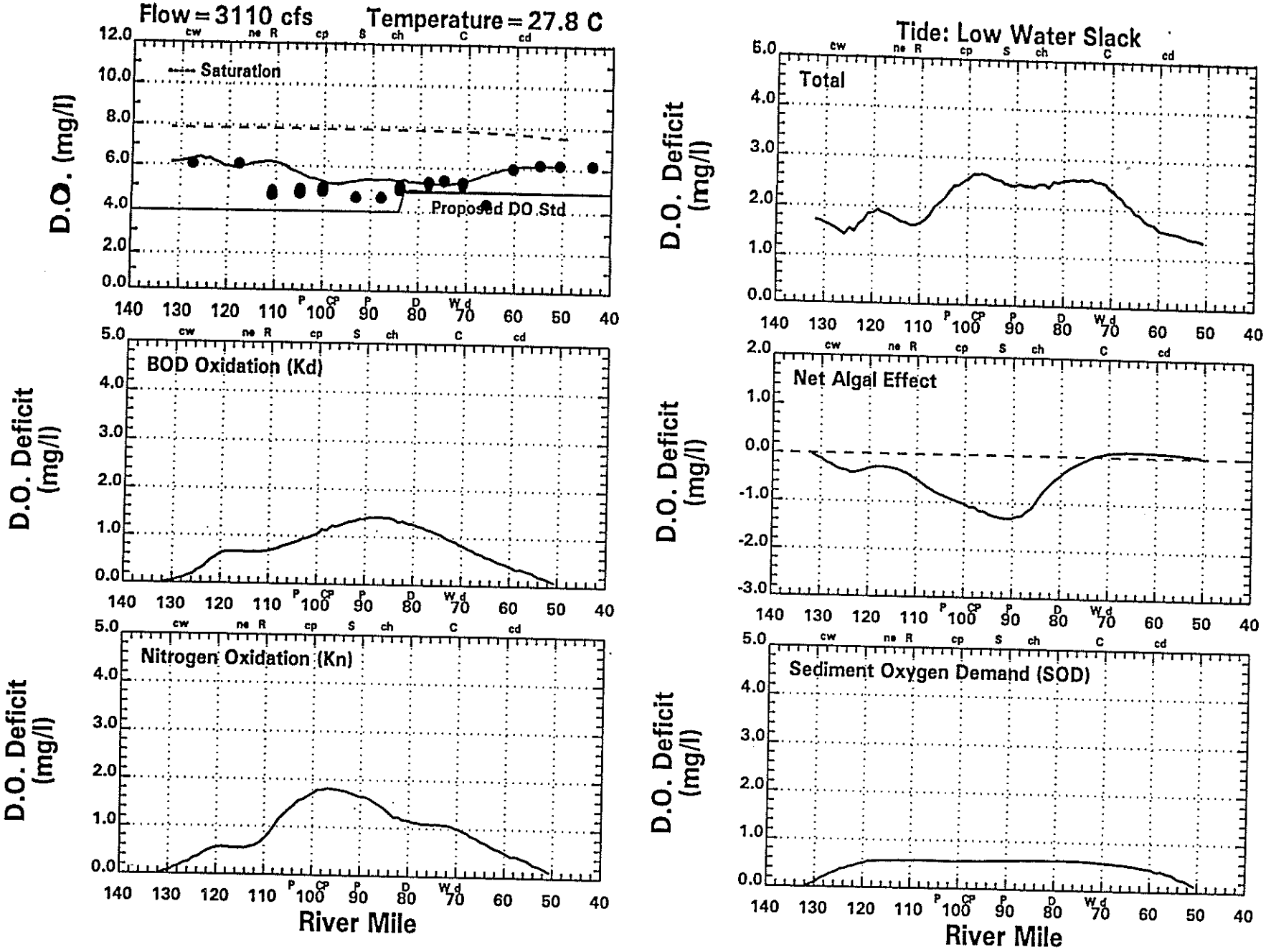

Figure 7-34. 1991 Dissolved Oxygen Deficit Component Response for July 23.

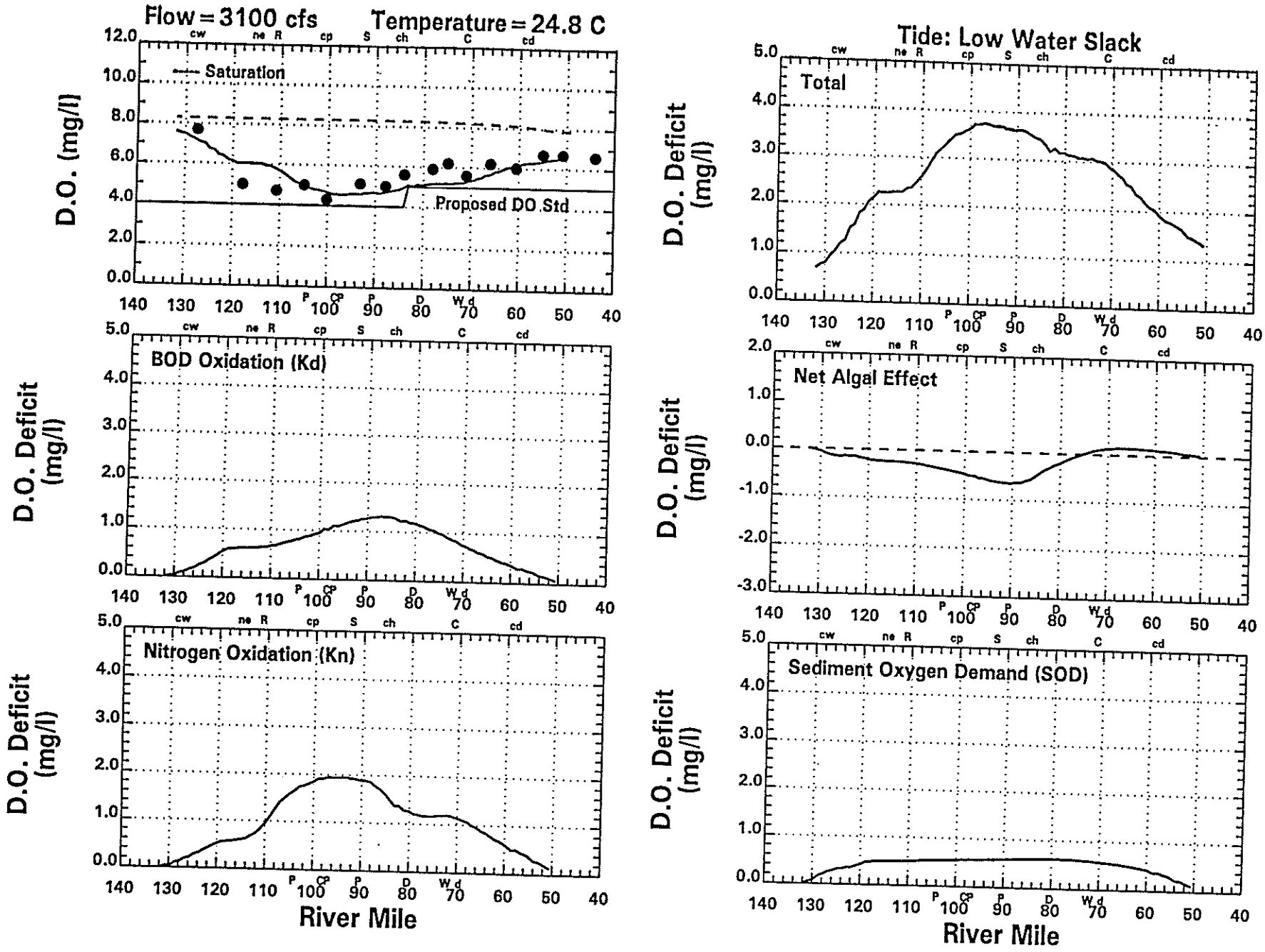

Figure 7-35. 1991 Dissolved Oxygen Deficit Component Response for August 26.

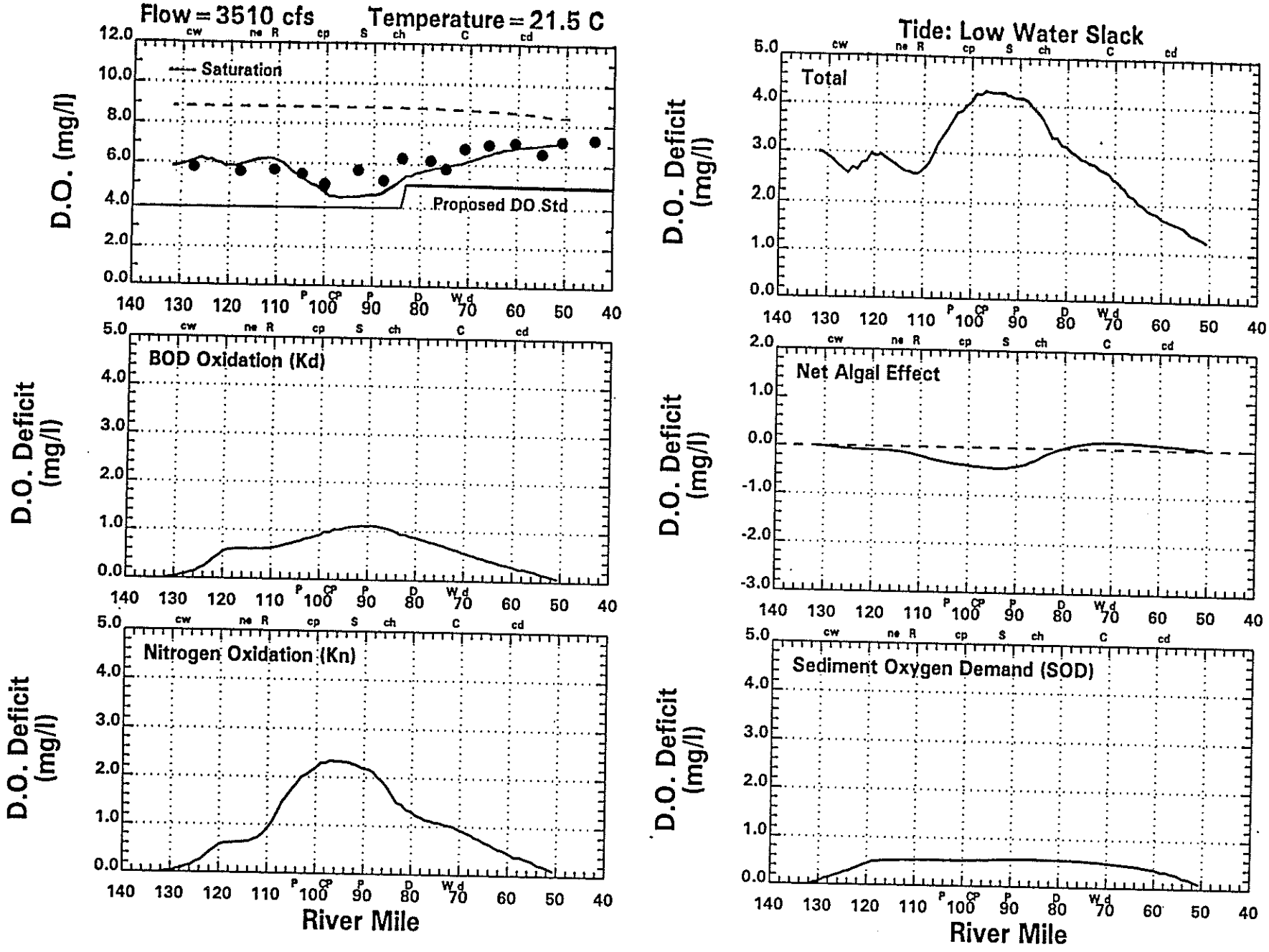

Figure 7-36. 1991 Dissolved Oxygen Deficit Component Response for September 23.

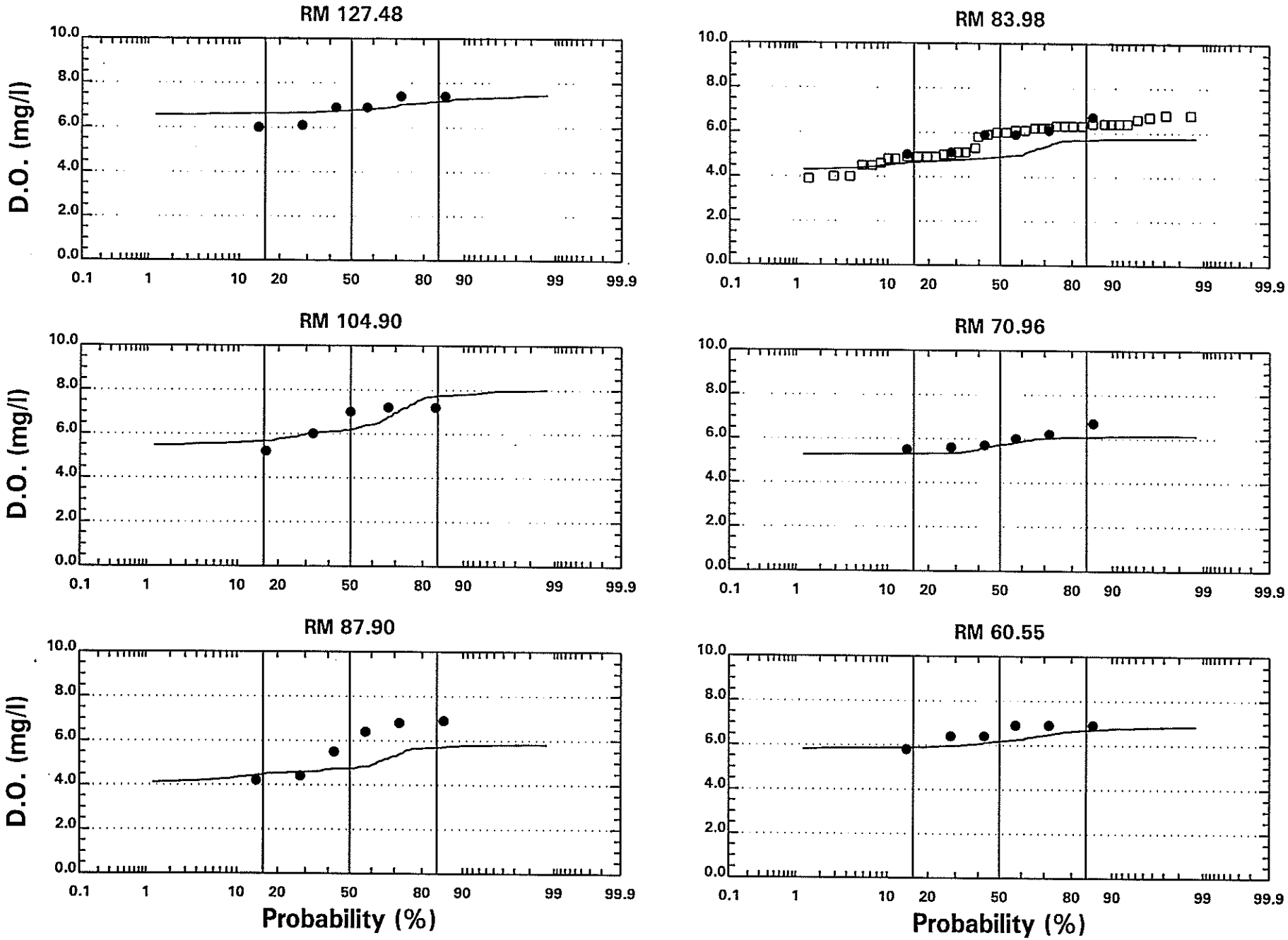

Figure 7-37. Probability Distributions of Observed and Modeled Dissolved Oxygen for 1991 Validation. (● DRBC Data; □ USGS Data; — Model Daily Averages).

The impact of each factor was determined by rerunning the model calibration with the appropriate rate or loading set to zero. Since river conditions in 1991 and 1995 were similar, the results of the sensitivity runs are only shown for September 25th (model day 70) of the 1995 calibration. The results of the sensitivity analyses are presented in Figures 7-38 through 7-45.

For the nitrification sensitivity run, the nitrification rate was set equal to zero and the results are presented in Figure 7-38. With no nitrification, the nitrite+nitrate concentrations remain constant and do not increase to the measured values of over 2 mg/l. The ammonia concentrations conversely increase from less than 0.2 mg/l with nitrification to approximately 1.5 mg/l with no nitrification. Because dissolved oxygen is consumed during the nitrification process, the dissolved oxygen concentrations increase almost 2 mg/l at RM 90 when nitrification does not occur. The changes in nitrite+nitrate, and ammonia highlight the necessity of the high nitrification rate used in the Philadelphia area to match the low observed ammonia concentrations and the high nitrite+nitrate concentrations. The almost 2 mg/l change in dissolved oxygen demonstrates the large role nitrification plays in the dissolved oxygen balance in the Delaware River.

For the sensitivity run assessing the sediment nitrate flux, the flux of nitrate from the water column to the sediment was set equal to zero. The result of this sensitivity run is presented in Figure 7-39. With the loss of nitrate to the sediment shut off, the water column nitrite+nitrate concentrations reach over 3 mg/l and over predict measured nitrite+nitrate values by almost 1 mg/l. Given the high nitrification rate assigned in the model for the Philadelphia area, an argument might be made for eliminating the nitrate flux to the sediment and reducing the nitrification rate. Two factors, however, prevent changing the current model parameterization. First, the high nitrification rate is necessary to match the low observed ammonia data. Second, field measurements of a nitrate flux to the sediment has been observed supporting the assignment of a nitrate flux to the sediment.

In Figure 7-40, the results of the sensitivity to changes in the salinity growth reduction factor are presented. For this sensitivity run, the salinity growth reduction factor is set equal to one which eliminates any inhibition of algal growth by salinity. Without salinity inhibition, the chlorophyll-a concentrations rise from 20 ug/l to almost 30 ug/l. Higher algal levels increase dissolved oxygen by 1 mg/l and slightly raises CBOD concentrations due to an increase in algal CBOD. Orthophosphorous, nitrite+nitrate and ammonia decrease due to an increased demand for

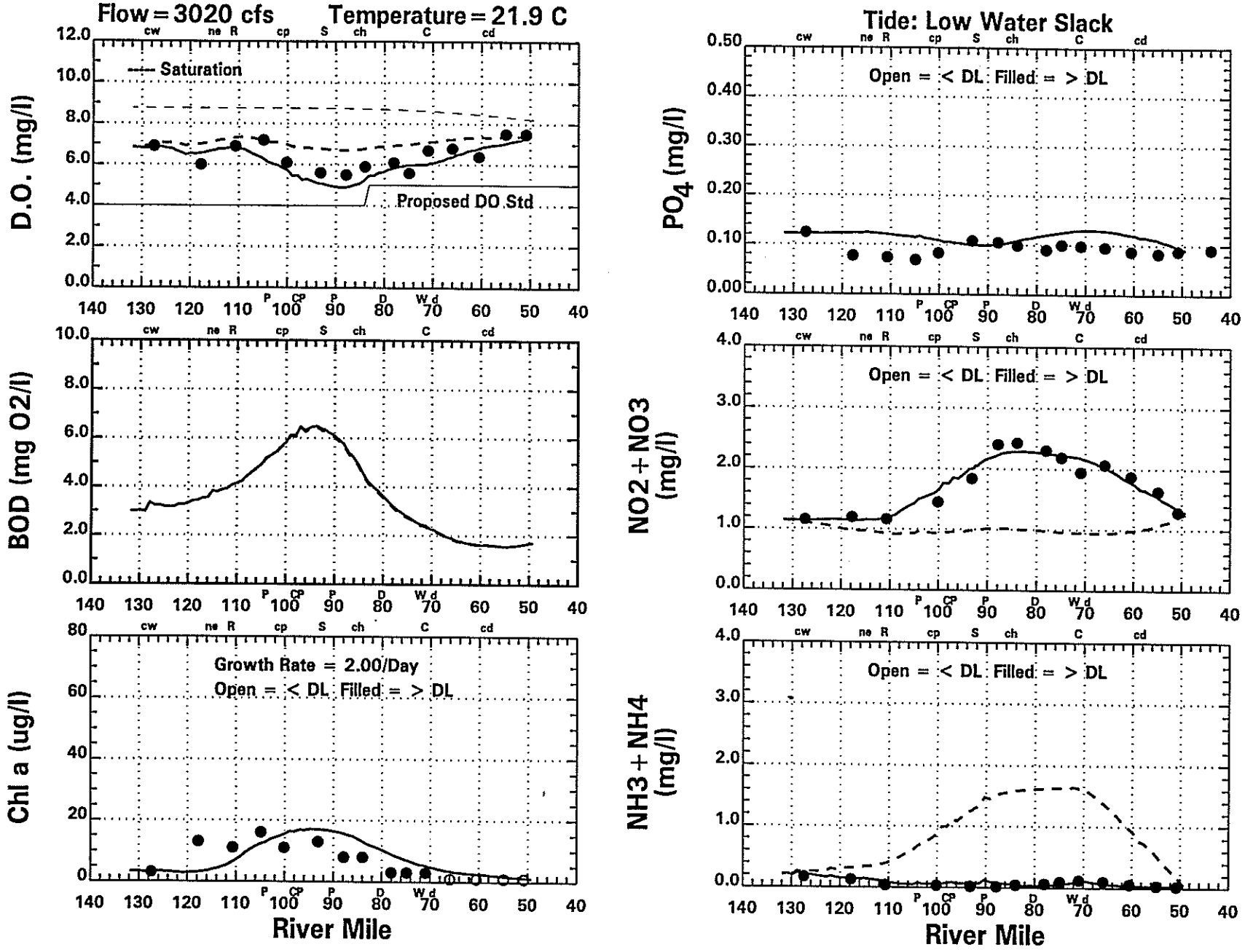

Figure 7-38. 1995 Sensitivity to Nitrification for September 25.

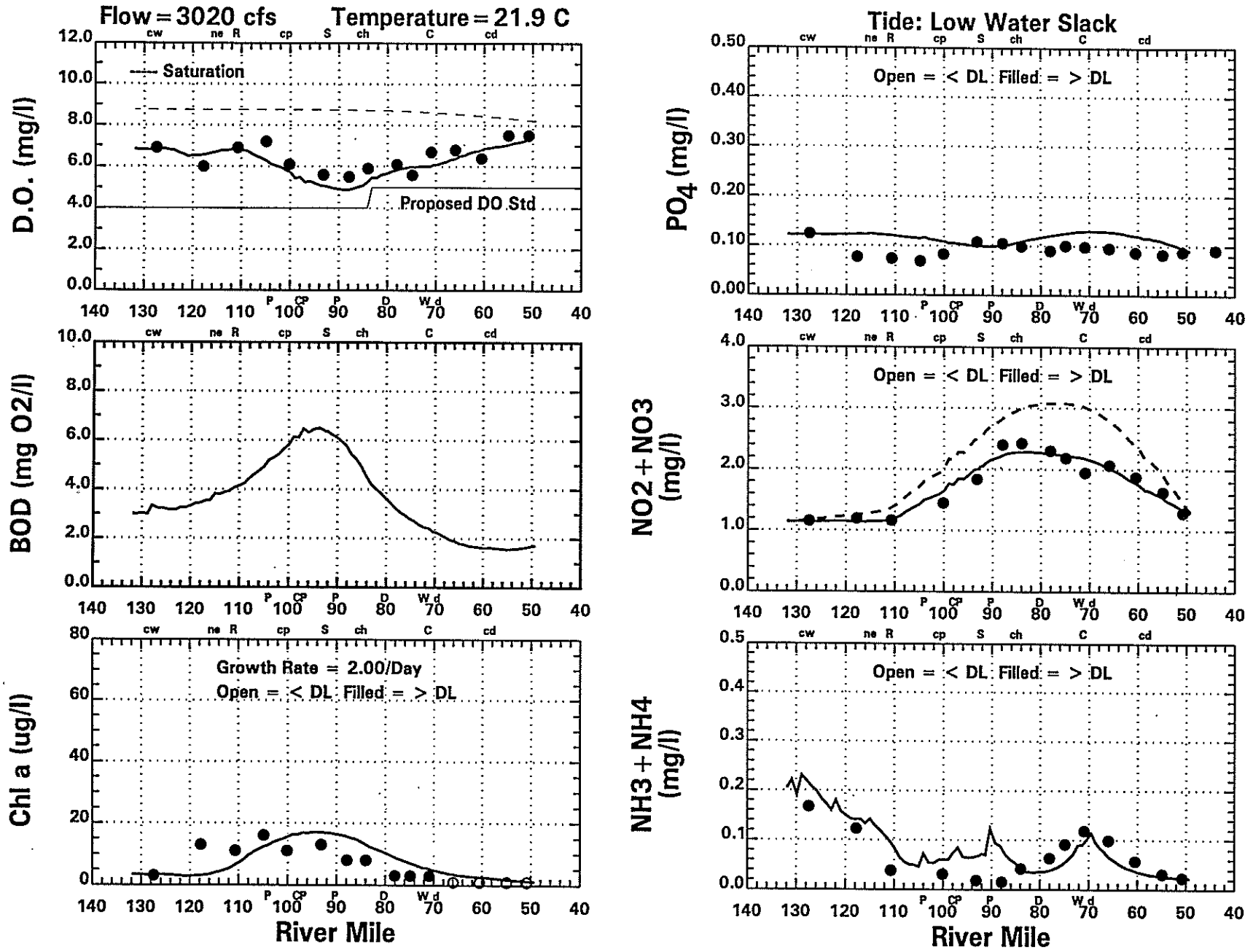

Figure 7-39. 1995 Sensitivity to Sediment Nitrate Flux for September 25.

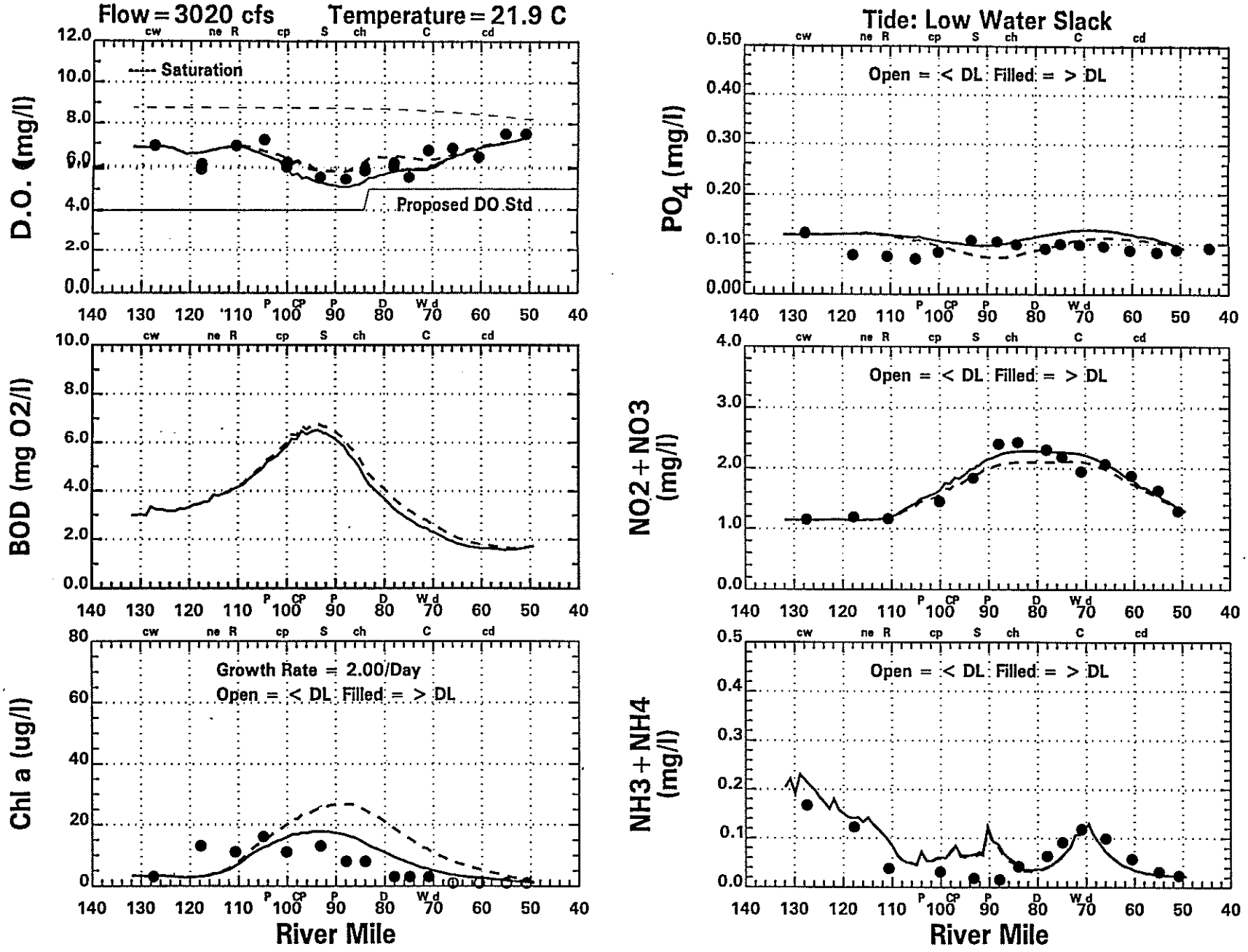

Figure 7-40. 1995 Sensitivity to Salinity Growth Reduction Factor for September 25.

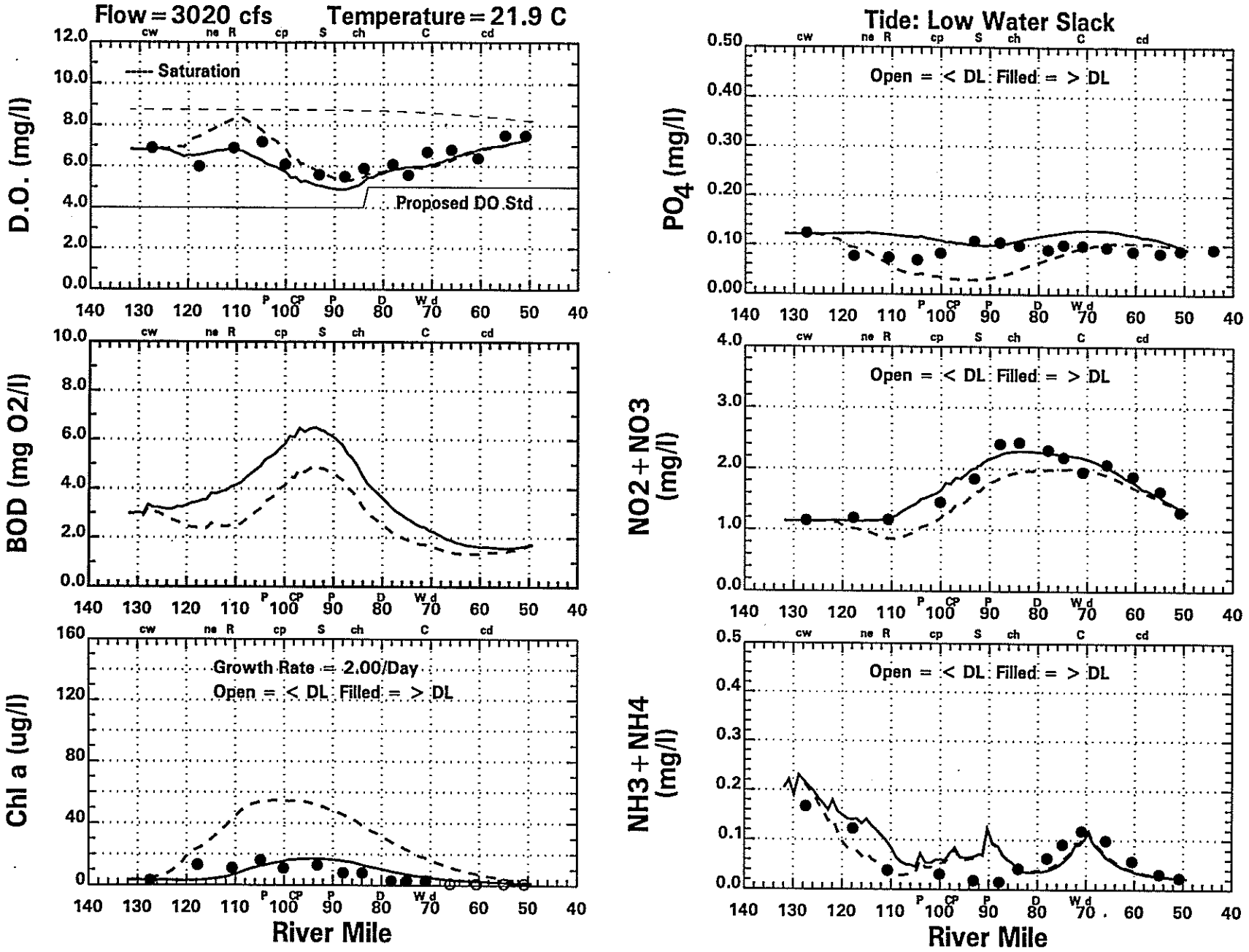

Figure 7-41. 1995 Sensitivity to Algal Predation for September 25.

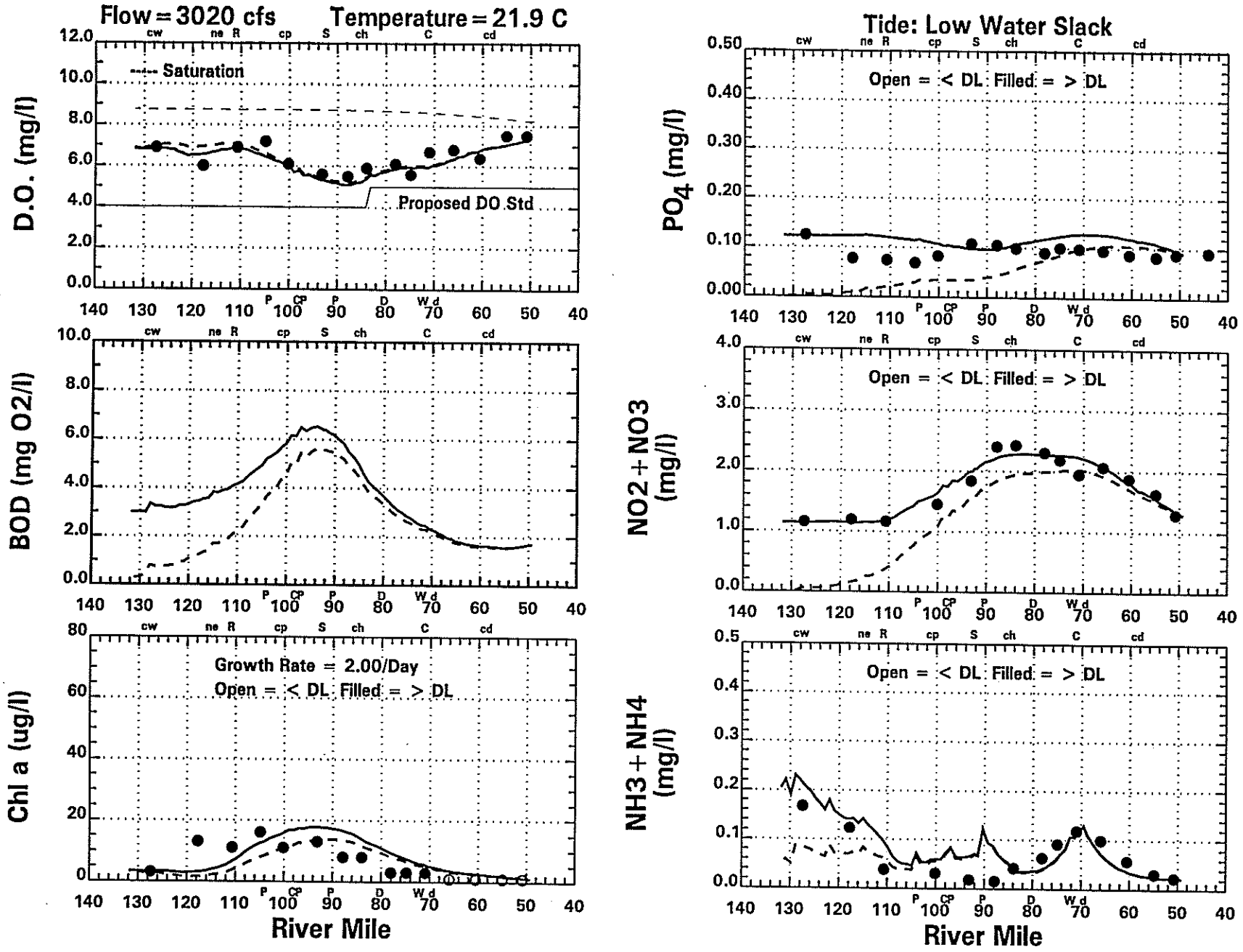

Figure 7-42. 1995 Sensitivity to Upstream CBOD, Nitrogen and Phosphorus Loading for September 25.

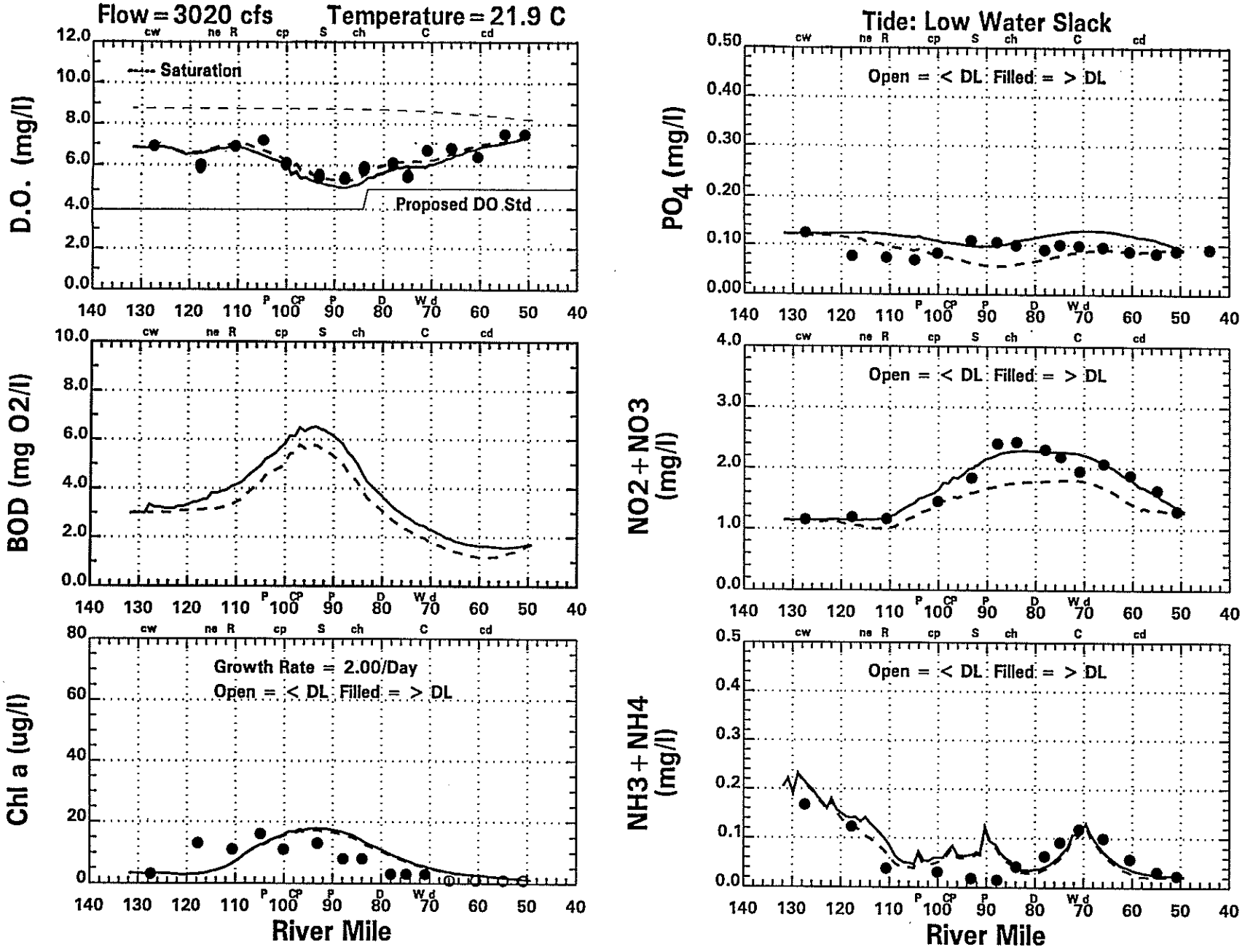

Figure 7-43. 1995 Sensitivity to Tributary CBOD, Nitrogen and Phosphorus Loading for September 25.

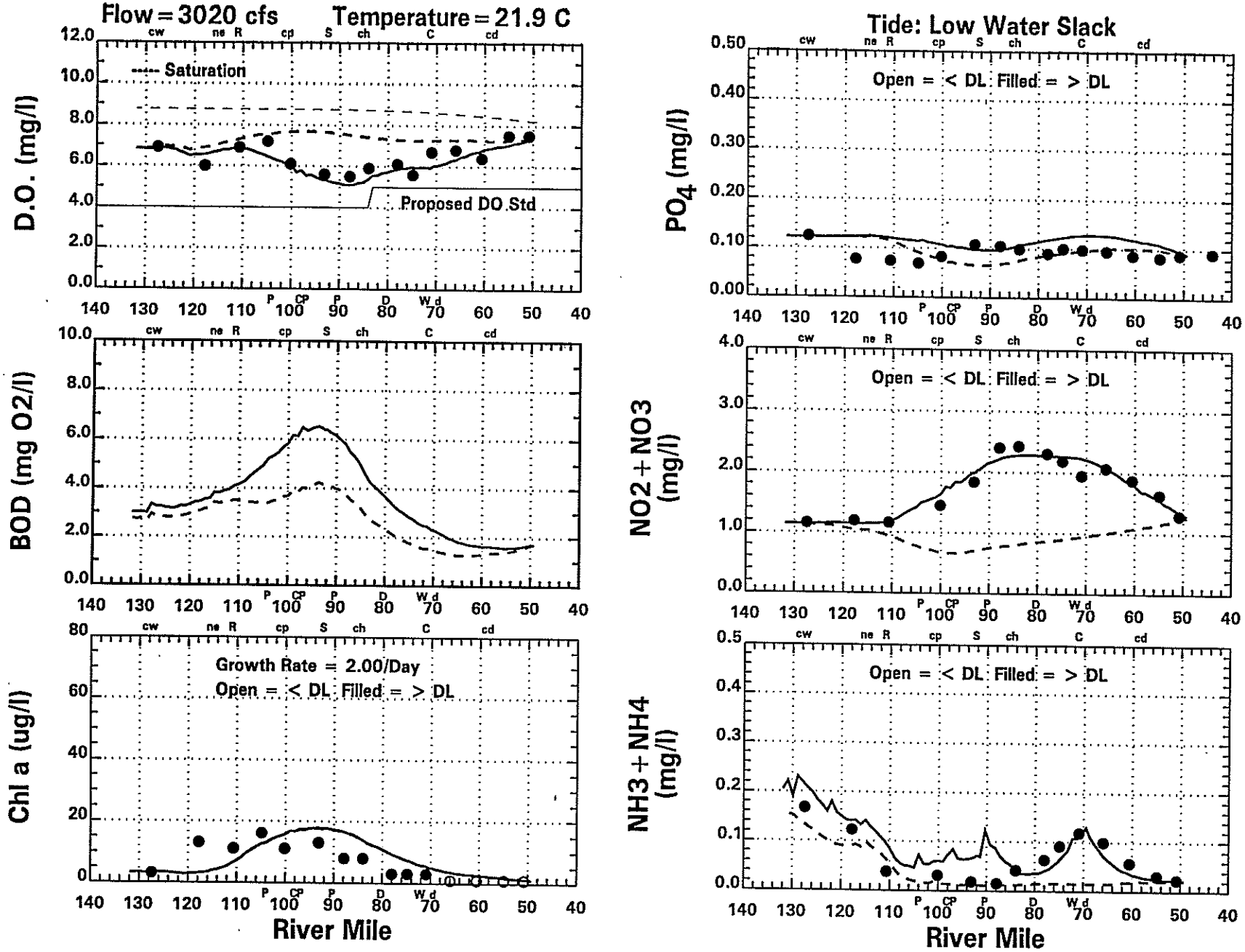

Figure 7-44. 1995 Sensitivity to Point Source CBOD Nitrogen and Phosphorus Loading for September 25.

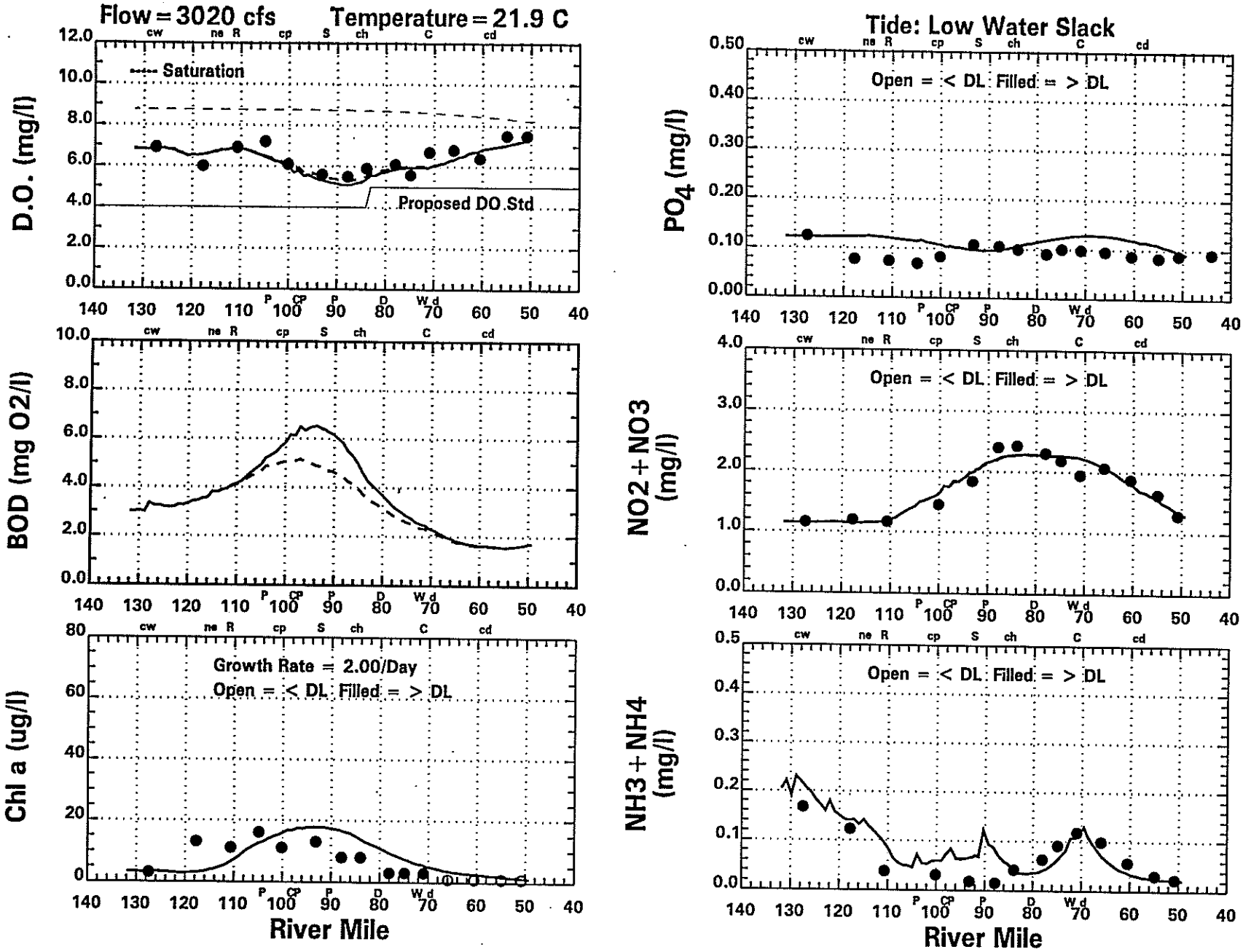

Figure 7-45. 1995 Sensitivity to Wet Weather CSO CBOD and Ammonia Loading for September 25.

nutrients by algal cells. While the use of a salinity growth reduction factor does effectively reproduce the chlorophyll-a profiles and salinity is known to inhibit growth of freshwater algae, the actual impact of salinity on phytoplankton growth in the River is unclear. Although the best estimate of the light regime in the lower Delaware River was used in the model, a large amount of uncertainty in the light actually available for phytoplankton growth remains. Given this uncertainty, the degree to which salinity vs available light is limiting phytoplankton growth in the lower Delaware River is not clear.

For the algal predation sensitivity run, algal grazing is set equal to zero. The results of this sensitivity run are presented in Figure 7-41. With no algal cells lost to grazing, the chlorophyll-a concentrations triple from 20 ug/l to almost 60 ug/l. With high grazing rates primarily assigned upstream of RM 100, the high chlorophyll-a concentrations downstream at RM 100 are due to a larger algal "seed" population being transported down stream. Higher algal levels raise the dissolved oxygen and slightly lower the CBOD because less algae are dying and being converted to CBOD. Orthophosphorous, nitrite+nitrate and ammonia decrease due to an increased demand for nutrients by algal cells. These results show the importance of grazing on algae by predators is important in reproducing the chlorophyll-a profile. As mentioned with the salinity growth reduction factor, the degree to which grazing vs available light is limiting phytoplankton growth in the upper Delaware River is not clear given the uncertainty in the grazing rate and the available photosynthetically active light.

For the sensitivity run to upstream loading, the upstream boundary for CBOD, nitrogen and phosphorus are set equal to zero. The results of this sensitivity run are presented in Figure 7-42. As a result of eliminating the upstream loads, the chlorophyll-a concentration drops from a maximum of 20 ug/l to 15 ug/l due to a drop in upstream phosphorus and upstream dissolved oxygen concentrations slightly increase due to a reduction in CBOD and ammonia levels. Orthophosphorous, nitrite+nitrate and ammonia decrease very significantly due to the upstream load reductions.

For the sensitivity run to tributary loading, all the tributary boundaries for CBOD, nitrogen and phosphorus are set equal to zero. The results of this sensitivity run are presented in Figure 7-43. As a result of eliminating the tributary loads, the dissolved oxygen slightly increases between RM 110 and RM 60 due primarily to the reduction in CBOD. No change is seen in the

chlorophyll-a concentrations. Orthophosphorous, nitrite+nitrate and ammonia decrease by varying amounts due to the load reductions.

For the sensitivity run to point source loading, all the point source loads for CBOD, nitrogen and phosphorus are set equal to zero. The results of this sensitivity run are presented in Figure 7-44. As a result of eliminating the point source loads, the dissolved oxygen increases almost 3 mg/l between RM 110 and RM 60, due primarily to the large reductions in ammonia and CBOD loads. With less ammonia available for nitrification, the nitrite+nitrate concentrations drop below 1 mg/l. No change is seen in the chlorophyll-a concentrations and orthophosphorous concentration slightly decrease.

For the CSO sensitivity run, the CSO CBOD and ammonia loads were set equal to zero. The results of this sensitivity run are presented in Figure 7-45. The impact of eliminating the CSO loads can be seen on September 25, 1995 (model day 70) since a rain event took place on this day. The CBOD drops approximately 1 mg/l at RM 95 with an increase in the dissolved oxygen of 0.1 to 0.2 mg/l. While important locally, the wet weather CSO loading of CBOD is a small part of the overall dissolved oxygen balance. No change is observed in the ammonia concentrations.

Evaluating all the load reduction sensitivities runs in terms of the dissolved oxygen balance for the River, the elimination of the point source loads shows the most drastic effect, changing the dissolved oxygen almost 3 mg/l. The elimination of the CSO loading, on the other hand, shows almost no impact on dissolved oxygen concentrations. The impact of the upstream and tributary loads show only a slightly larger impact than the CSO loads. Given the different sources of CBOD and ammonia to the Delaware River, point source discharges have the largest impact on River dissolved oxygen concentrations.

SECTION 8

REFERENCES

Blumberg, A.F. and G.L. Mellor, 1987. "A Description of a Three-Dimensional Coastal Model," pp. 1-16. Coastal and Estuarine Sciences, Vol. 4. AGU, Washington, D.C.

Blumberg, A.F., 1977. "Numerical Model of Estuarine Circulation," ASCE J. Hydr. Div., 103:295-310.

Blumberg, A.F. and G.L. Mellor, "A Coastal Ocean Numerical Model," In: Mathematical Modelling of Estuarine Physics, Proceedings of an International Symposium, Hamburg, August 24-26, 1978. J. Sundermann and K.P. Holz, Eds., Springer-Verlag, Berlin, 1980.

Blumberg, A.F. and G.L. Mellor, "A Description of a Three-Dimensional Coastal Ocean Circulation Model," In: Three-Dimensional Coastal Ocean Models, N. Heaps, Ed., 1-16, American Geophys. Union, 1987.

Casulli, V., 1990. "Semi-implicit Finite Difference Methods for the Two-dimensional Shallow Water Equations," J Comput. Phy. 86,56-74.

Delaware River Basin Commission, (DRBC) 1998. Combined Sewer Overflow Report DEL USA Project Element 8.

Gardner, G.B. and D.W. Pritchard, 1974. "Verification and Use of a Numerical Model of the Chesapeake & Delaware Canal," Chesapeake Bay Institute, Technical Report 87, Reference 74-7.

Hendry, G.S., 1977. "Relationships Between Bacterial Levels and Other Characteristics of Recreational Lakes in the District of Muskoka," Interim Microbiology Report, Laboratory Service Branch, Ontario Ministry of the Environment.

HydroQual, Inc., 1991. "Water Quality Modeling Analysis of Hypoxia in Long Island Sound,"

Prepared for Management Committee Long Island Sound Estuary Study and New England Interstate Water Pollution Control Commission.

HydroQual, Inc., 1993. "A Water Quality Model for Massachusetts Bay and Cape Cod Bay: Model Design and Initial Calibration." MWRA Environmental Quality Department. Technical Report No. 93-5.

Hyer, P.V., C.S. Fang, E.P. Ruzeck, and W.J. Hargis, 1971. "Hydrography and Hydrodynamics of Virginia Estuaries, Studies of the Distribution of Salinity and Dissolved Oxygen in the Upper York System," Virginia Institute of Marine Science.

Jewell, W.J. and P.L. McCarty, 1971. "Aerobic Decomposition of Algae," Environ. Sci. Technol. 1971, 5(10), p. 1023.

Kawabe, M., J.H. Sharp, K.C. Wong and M.E. Lebo, 1990. "Oceanographic Data Report Number 8: Density Profiles from the Delaware Estuary," October 1986 - September 1988, Delaware Sea Grant College Program, DEL-SG-07-90.

Laws, E.A. and T.T. Bannister, 1980. "Nutrient and Light-limited Growth of Thalassissira fluviatillis in Continuous Culture with Implications for Phytoplankton Growth in the Oceans," Limnol. Oceanogr. 25: 457-473.

Lebo, M.E., L.A. Cifuentes and Other, 1990. "Oceanographic Data Report Number 7: Data from the Delaware Estuary SCENIC Cruises, April 1986 - September 1988," Delaware Sea Grant College Program, DEL-SG-06-90.

Lowe, W.E., 1976. Personal Communication. Canada Centre for Inland Waters, Burlington, Canada.

Mellor, G.L. and T. Yamada, 1982. "Development of a Turbulence Closure Model for Geophysical Fluid Problems," Rev. Geophys. Space Phys., 20, 851-875.

Munk, W.H. and Anderson, E.R., 1948. "Notes on a Theory of the Thermocline," J. Mar. Res., 1:276-295.

Menon, A.S., W.A. Gloschenko and N.M. Burns, 1972. "Bacteria-Phytoplankton Relationships in Lake Erie," Proc. 15th Conf. Great Lakes Res., 94, Inter. Assoc. Great Lakes Res., 101.

Morel, F.M., 1983. Principles of Aquatic Chemistry, John Wiley and Sons, New York, New York.

Najarian, T.O., Thatcher, M.L. and Harleman, D.R.F., 1980. "C&D Canal Effect on Salinity of Delaware Estuary," ASCE J. Water. Port Coast. Div., Feb. 1980, p.1-17.

New Jersey Department of Environmental Protection, 1994. Projected Storm Water Generated Pollutant Loadings to the Delaware Estuary - A Modeling Study for the Delaware River Basin Commission (DRBC).

Pritchard, D.W. and Gardner, G.B., 1974. "Hydrography of the Chesapeake and Delaware Canal," Chesapeake Bay Institute, Ref. 74-1, Tech. Rep. 85.

Rives, S.R. and D.W. Pritchard, 1978. "Adaptation of J.R. Hunter's One-Dimensional Model to the C & D Canal System," Chesapeake Bay Institute, Special Report 66, Reference 78-6, October 1978.

Steale, J.H., 1962. "Environmental Control of Photosynthesis in the Sea," Limnol. Oceanogr., 7, 13: 7-150.

Tetra Tech, Inc., 1985. "Rates, Constants and Kinetics Formulations in Surface Water Quality Modeling (second edition)," for the U.S. Environmental Protection Agency, Environmental Research Laboratory, Athens, GA, June 1985 EPA600/3-85-040.

Thomann, R.V. and J.A. Mueller, 1987. "Principals of Surface Water Quality Modeling and Control." Harper & Row, New York, NY, 422.

Wong, K.C., 1990. "The Current and Sea Level Variability in the Chesapeake and Delaware Canal," J. Geophys. Res., 95(C10): 18,343 - 18,352.